HIGHWAY RESEARCH BOARD

Special Report 66

AASHO Road Test
Technical Staff Papers

1961

National Academy of Sciences—
National Research Council

publication 933

HIGHWAY RESEARCH BOARD

Officers and Members of the Executive Committee

1961

OFFICERS

W. A. BUGGE, *Chairman* R. R. BARTLESMEYER, *First Vice Chairman*

C. D. CURTISS, *Second Vice Chairman*

FRED BURGGRAF, *Director* ELMER M. WARD, *Assistant Director*

Executive Committee

REX M. WHITTON, *Federal Highway Administrator, Bureau of Public Roads* (ex officio)

A. E. JOHNSON, *Executive Secretary, American Association of State Highway Officials* (ex officio)

LOUIS JORDAN, *Executive Secretary, Division of Engineering and Industrial Research, National Research Council* (ex officio)

HARMER E. DAVIS, *Director, Institute of Transportation and Traffic Engineering, University of California* (ex officio, Past Chairman 1959)

PYKE JOHNSON, *Consultant, Automotive Safety Foundation* (ex officio, Past Chairman 1960)

R. R. BARTELSMEYER, *Chief Highway Engineer, Illinois Division of Highways*

E. W. BAUMAN, *Director, National Slag Association, Washington, D. C.*

W. A. BUGGE, *Director of Highways, Washington State Highway Commission*

MASON A. BUTCHER, *County Manager, Montgomery County, Md.*

C. D. CURTISS, *Special Assistant to the Executive Vice President, American Road Builders' Association*

DUKE W. DUNBAR, *Attorney General of Colorado*

H. S. FAIRBANK, *Consultant, Baltimore, Md.*

MICHAEL FERENCE, JR., *Executive Director, Scientific Laboratory, Ford Motor Company.*

D. C. GREER, *State Highway Engineer, Texas State Highway Department.*

BURTON W. MARSH, *Director, Traffic Engineering and Safety Department, American Automobile Association*

J. B. MCMORRAN, *Superintendent of Public Works, New York State Department of Public Works, Albany*

CLIFFORD F. RASSWEILER, *Vice-President, Johns-Manville Corp., New York, N. Y.*

GLENN C. RICHARDS, *Commissioner, Detroit Department of Public Works*

C. H. SCHOLER, *Applied Mechanics Department, Kansas State University*

WILBUR S. SMITH, *Wilbur Smith and Associates, New Haven, Conn.*

K. B. WOODS, *Head, School of Civil Engineering, and Director, Joint Highway Research Project, Purdue University*

Editorial Staff

FRED BURGGRAF ELMER M. WARD HERBERT P. ORLAND

2101 Constitution Avenue Washington 25, D. C.

HIGHWAY RESEARCH BOARD

Special Report 66

AASHO Road Test

Technical Staff Papers

1961

Presented at the
40th ANNUAL MEETING
January 9-13, 1961

National Academy of Sciences—
National Research Council
Washington, D. C.
1961

Contents

A Rationale for Analysis of Pavement Performance

P. E. IRICK, W. N. CAREY, Jr., and R. C. HAIN, respectively, Chief, Data Analysis Branch; Chief Engineer for Research; and Assistant Chief, Data Analysis Branch; AASHO Road Test, Highway Research Board

A hypothetical road test quite similar to the AASHO Road Test is used to illustrate a rationale for determining an association of pavement performance with variables that describe pavement design and applied loads. The rationale used for the illustration is essentially that used in the analysis of performance data for the factorial experiments at the AASHO Road Test.

The performance of a pavement is defined by a curve that shows its serviceability trend as axle load applications are increased. A mathematical form or model is selected for the association, then procedures are defined for fitting the data to the model so that all constants in the model are evaluated. When pavement design is given, the evaluated model can be used either to predict serviceability after a given number of specified loads has been applied, or to predict the number of specified load applications required to produce a given serviceability loss.

Many details of the rationale are given as the example proceeds from hypothetical data to the performance equation. Limitations and alternatives for the rationale are discussed, a table of discrepancies between predicted and observed performance is given, and the illustrative analysis ends with curves that may be used in the practical application of the derived equation.

● THE FIRST OBJECTIVE for the AASHO Road Test is to find significant relationships between pavement performance and certain characteristics of pavement design and and applied loads. To carry out this objective detailed specifications are needed in three areas. First, pavement performance must be defined so that performance data can be obtained for every test section in the investigation. Second, there must be experimental designs that give details for pavement design and load characteristics of the sections. Finally, it is necessary to set out definite procedures that lead to the required relationships. Several papers and talks have described Road Test specifications in the first two areas, and it is the main purpose of this paper to discuss specifications in the third area. However, the three sets of specifications are interrelated in that analytical procedures are determined to a large extent by the nature of the experimental designs and by the nature of the performance data. For this reason pavement performance and experimental designs are discussed before turning to a rationale for analysis. Use is made of a numerical illustration that differs from the AASHO Road Test pavement performance studies in certain details but not in principle. As a consequence, rationale for the illustration is applicable to the Road Test, and unless specific reference is made to the illustration, the following discussion pertains to the Road Test.

It is evident that there are alternatives for virtually every specification that may be given in any of the three areas; thus there are many possibilities for the total set of

specifications. Because it may be supposed that a number of these possibilities are equally acceptable for meeting the first objective of the Road Test, it cannot be claimed that the rationale to be described represents the best, nor the only way to satisfy the objective, but it is assumed that any other acceptable rationale would produce essentially the same conclusions.

PAVEMENT PERFORMANCE DATA

Inasmuch as a rationale for analysis is rather meaningless unless the data that go into the anlayis are well defined, it is necessary to pin down the specific nature of performance data. The concepts and specifications to be described in this area have evolved after consideration of many alternatives.

It is supposed that the present serviceability history of a pavement section plays a very useful role in performance evaluation. At any particular time the section's present serviceability is a measure of its ability to serve high-speed, high-volume traffic, and in a previous paper (1) a system for the development of present serviceability index formulas was described. Separate formulas were presented for flexible pavements and for rigid pavements. When appropriate measurements of surface deformation and deterioration are made on day, t, substitution of the measurements into the index formula gives an index value, p_t', for the index day. The complete serviceability history of a pavement section consists of index values for a series of index days that begins when the section is first constructed and ends when serviceability loss is such that major maintenance or replacement is required. In both the illustration and the AASHO Road Test, serviceability index values are obtained for every section on bi-weekly index days, and the serviceability history of a section is considered to be completed if and when its index falls to 1.5 on a scale where maximum serviceability is 5.0. Although not all bi-weekly index values are plotted, Figure 1, which shows the serviceability histories of two sections used in the illustration, indicates a completed history for section 3212 after about 17 index days. As in the case of the AASHO Road Test, it is supposed that the illustrative road test is stopped after 55 index days with the expectation that at least some sections will still have high serviceability at the end of the test. One such section is shown in Figure 1, where section 3222 has a serviceability index of about 3.2 after 55 index days.

The general continuous pattern of a serviceability history is called a smoothed serviceability history. Smoothed histories for the two sections in Figure 1 are indicated by the solid lines. The smoothed history for a section is defined by a moving average that includes at least three (generally five) successive index values and that uses the end values for the history as end values for the smoothed history. Smoothed serviceability history values on index days are denoted by p_t.

A second element of performance for a pavement section is its history of load applications. Although theories (2) and procedures exist for dealing with mixtures of axle loads, reference in this paper to any particular number of applications implies that each application represents the same axle weight. For the illustration, Figure 2 gives both the number of axle load applications between successive index days and the accumulated number of applications for any index day. The respective notation for these two quantities is n_t and N_t. If more than one traffic lane is represented by n_t and N_t, it is assumed that lane-to-lane variation in n_t is negligible and n_t is averaged for all lanes before the accumulation, N_t. Whenever it is necessary to evaluate accumulated applications between index days, linear interpolation is performed between successive values of N_t.

Before specifications are given for performance data, one more history is discussed—a history that is associated with the general state of environmental conditions at any particular time. This history is called a seasonal weighting function. Relative to a specified norm, or base, it may be supposed that the conditions at any time or location are either normal, better than normal, or worse than normal. It is considered that the seasonal weighting function reflects serviceability loss potential, and that any particular section may or may not lose serviceability during a period when the weighting function is high. No specific formula for a weighting function is given in this paper,

but it is supposed that such a formula has been evolved to give values, v_t, for every index period as shown in Figure 3. This function presumably depends in general on changes in moisture-temperature states, and has the value $v_t = 1.0$ for normal conditions. A value of zero is considered to be a lower bound at which no serviceability-loss potential exists for any pavement-load combination.

The seasonal weighting function shown in Figure 3 averages to be about 1.0 so that environmental conditions for the two years average to be normal even though there is much seasonal variation. Relative to the selected location, this index might not average to be 1.0 at a second location, whether or not the same seasonal variation occurred at the two locations.

For any index period, let the product of the weighting function value with axle load application be w_t, the number of weighted applications for the period. Thus $w_t = v_t n_t$ can be obtained by multiplication of index day ordinates from Figures 2 and 3. Also let W_t be the accumulation of weighted axle load applications through any index day. Graphs for both w_t and W_t are shown in Figure 4. If the weighting function were taken to be 1.0 on every index day, the curve of Figure 3 would be horizontal at unit height, and Figure 4 would be identical with Figure 2. Thus, N_t is a special case of W_t if v_t is always 1.0. In all the discussion that follows accumulated axle load applications are

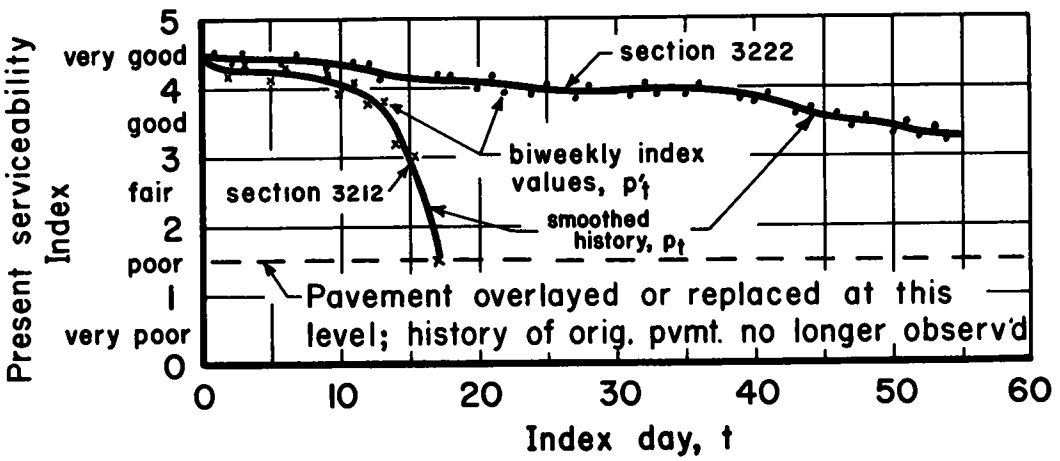

Figure 1. Present serviceability histories for two illustrative pavement sections.

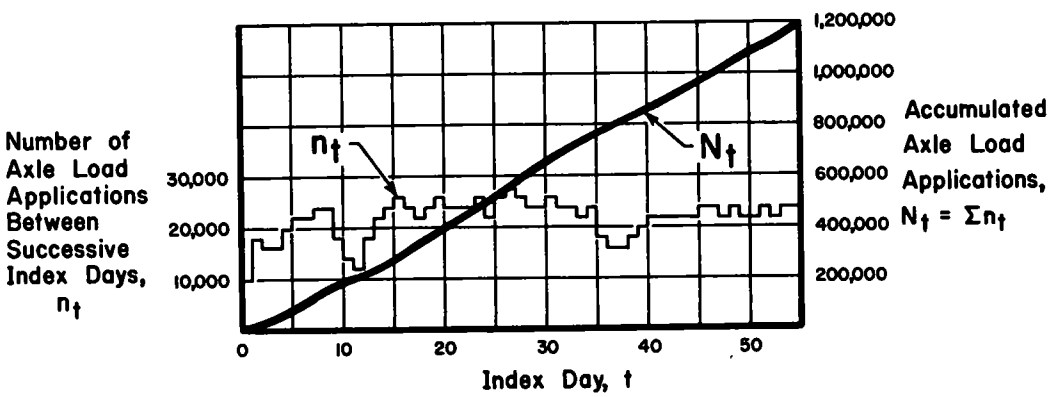

Figure 2. Axle load application history for the illustration.

represented by W, but it should be remembered that any difference between W and N depends on the values prescribed for v_t.

All of the variables just described have values that are observed and computed at points in time. If smoothed serviceability values for a pavement section are plotted against accumulated axle applications rather than against time, the resultant curve is called the section's serviceability trend. Coordinates of points on the serviceability trend are denoted by p and W, and the trend of p with W is defined to be the pavement's performance.

Trend plots for the two sections of Figure 1 are shown in Figure 5 for the case when applications are not weighted; that is, when $v_t = 1$. Coordinates for the trend curves in Figure 5 were obtained from ordinates of Figures 1 and 2 on common index days. Similarly, Figure 6 shows trend curves for the same sections when the seasonal weighting function of Figure 3 is used to obtain W. That is, coordinates for Figure 6 were obtained from ordinates of Figures 1 and 4 on common index days.

Summarizing the definitions of the various serviceability-time-applications relationships:

Serviceability history is the plot of observed values of serviceability, p_t', on a time scale;

Smoothed serviceability history is the plot of the five-point moving average of the serviceability history values on a time scale and smoothed history values are designated by p_t;

Serviceability trend is the plot of smoothed serviceability history values, p, on an

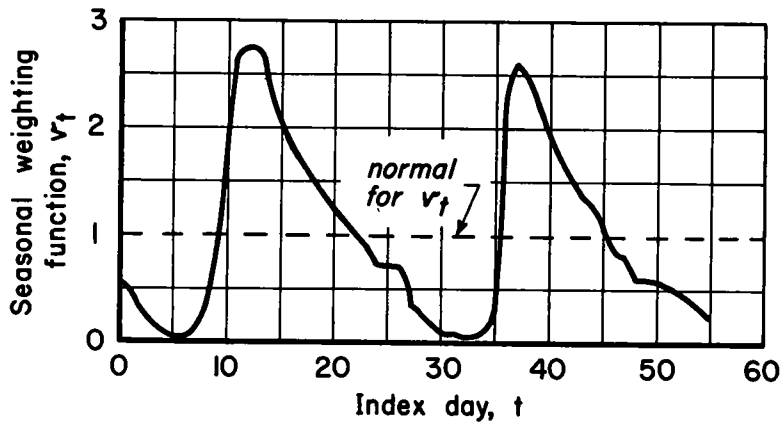

Figure 3. Seasonal weighting function for the illustration.

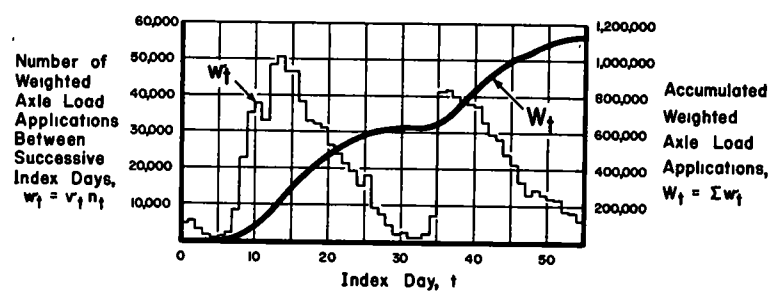

Figure 4. Weighted axle load applications for the illustration (seasonal weighting function from Fig. 3).

accumulated axle application scale, W, where axle applications may be weighted or unweighted; and the

Performance of a pavement is given by its serviceability trend

The final step in the specification of performance data is to suppose that for numerical analysis a small number of pairs of coordinates from any trend curve can be selected to represent the curve satisfactorily. In the Road Test rationale five pairs of coordinates were selected from every trend. If the trend was complete (that is, p had fallen to 1 5), the trend was represented by five values that spanned the range of p. Specifically, W was noted when p was 3.5, 3.0, 2.5, 2.0, and 1.5. In the case of incomplete serviceability trends (p at the end of the Road Test was greater than 1.5) the observations were spanned by noting pairs of W and p at specific times (at 11, 22, 33, 44 and 55 index days). In both cases it is more convenient to record and use all W values in logarithmic form so that recorded performance data appear in the form p, log W. Thus if p = 2.5 when W = 200,000 applications, the recorded performance data would be 2.5 and 5.30 for p and low W, respectively.

In the example only three pairs of coordinates are used to represent serviceability trends. For the complete curves W is noted when p = 3.5, 2.5 and 1.5, and for incomplete trends W and p are noted at 15, 35 and 55 index days. For the two sections shown in Figure 1, Table 1 gives performance data as just defined, using both weighted and unweighted applications.

EXPERIMENTAL DESIGNS FOR PAVEMENTS AND LOADS

As details are given in the second area of specification for the illustration, the reader who is familiar with experimental designs at the AASHO Road Test will recognize that the illustration parallels in principle the main factorial experiments of the Road Test.

Suppose that the illustrative road test involves three rigid pavement tangents, 1, 2, and 3, each having two 12-ft traffic lanes, 1 and 2, on either side of its center line. Axle load specifications for the six traffic lanes will be: tangent 1, 4-kip single in lane 1, 8-kip single in lane 2; tangent 2, 16-kip single in lane 1, 30-kip tandem in lane 2; tangent 3, 24-kip single in lane 1, and 36-kip tandem axle vehicles in lane 2. Figure 2 shows the illustrative specifications for frequency of axle load applications over a two-year period.

Suppose the objective for the illustration implies that differences in pavement design for test sections are determined by only two factors, thickness of portland cement

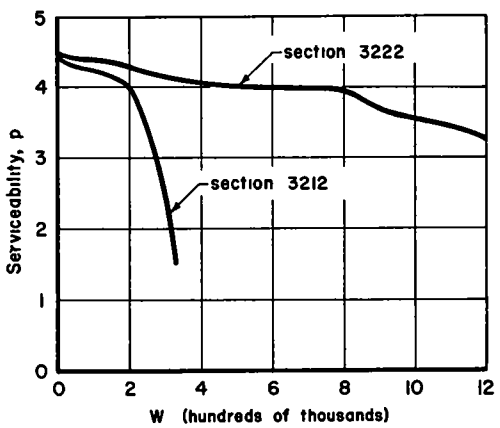

Figure 5. Performance curves for the two illustrative pavement sections of Figure 1 (v_t = 1).

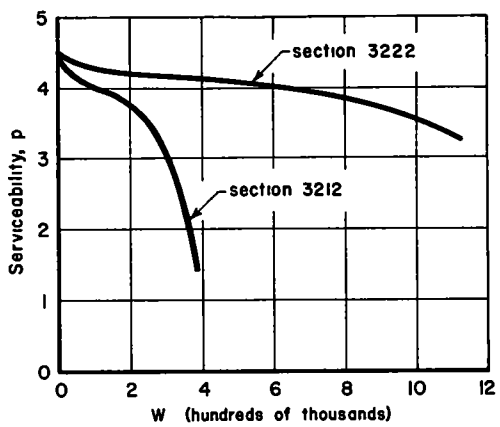

Figure 6. Performance curves for the two illustrative pavement sections of Figure 1 (seasonal weighting function from Fig. 3).

TABLE 1

PERFORMANCE DATA FOR TWO ILLUSTRATIVE SECTIONS OF FIGURE 1

Section No	History	t_p^a	Performance Data for $v_t = 1$ p	Performance Data for $v_t = 1$ log W	Performance Data for v_t from Figure 3 p	Performance Data for v_t from Figure 3 log W
3212	Complete	13 5	3 5	5 39	3 5	5 36
		16 0	2 5	5 49	2 5	5 54
		17 0	1 5	5 52	1 5	5 59
3222	Incomplete	15	4 2	5 45	4 2	5 48
		35	4 0	5 89	4 0	5 81
		55	3 2	6 08	3 2	6 05

[a] Index day at which smoothed serviceability history equals p

concrete surfacing and thickness of a granular subbase material. All other specifications for basement soil, pavement materials, and construction procedures are supposed to be identical for every test section.

Three fundamental principles of experimental design are balance, replication, randomization, and these principles are to be used in the design of the illustrative road test. The principle of balance is used to rule out undesired confusion among the effects of experimental factors on performance. By the effect of a factor is meant to change in performance that can be attributed to a change in the factor (for example, surface thickness effect is a change in performance that is clearly attributable to a change in surface thickness). It will be supposed that balance should be maintained in each test tangent for surface thickness and subbase thickness, so that the analysis can determine whether performance differences are due to one or the other of these factors or possibly to their interacting effect. In the absence of prior knowledge about their interacting effect, a sound experimental design for surface and subbase thickness is the complete factorial experiment that includes all possible combinations of levels selected for these two factors. In each tangent let each factor have three levels (that is, three values). Then the complete factorial experiment in each tangent requires 3 x 3, or nine, different pavement designs. As indicated in Table 2, levels for subbase thickness will be 3, 6, and 9 in. in each tangent, but levels for surface thickness are selected so that thicker pavements are used for heavier axle loads, there being one common surface thickness, 5.5 in., across all three tangents. Thus, although balance is maintained for surface and subbase thickness in each tangent and loads are balanced with subbase thickness across all tangents, load and surface thickness levels are unbalanced so that uninteresting surface thickness-load combinations will not occur. However, the load effect can be observed across the 5.5-in. surface thickness, and if there is no interaction between load and surface thickness effects, the load effect at 5.5-in. surface thickness could serve as the general effect of axle load on performance.

Replication (that is, repetition) of observations for controlled factor combinations provides a way to find how much the observations are influenced by residual variables that are uncontrolled. Replication can be performed in many categories. For example, the illustrative road test might be repeated in toto at a different location, or at a different time, or both. At a selected location and time, any tangent might be completely replicated by including a fourth tangent that has the same specifications as one of the tangents in Table 2. An axle load might be replicated in both lanes of the same tangent, or serviceability index values might be replicated for any index day. If there is sufficient replication in any category where conclusions are to be drawn about the effects of controlled factors within the category, it becomes possible to discern between per-

TABLE 2

LEVELS FOR THE EXPERIMENTAL FACTORS IN THE ILLUSTRATION

			Factorial Combinations			Replicated Combinations			
Tangent	Lane	Load[a] (kips)	Slab Thickness (in.)	Subbase Thickness (in.)	Number of Test Sections	Slab Thickness (in.)	Subbase Thickness (in.)	Number of Test Sections	Total Number of Test Sections
1	1	4S	2 5	3		2 5	6		
			4 0	6	9	4 0	6	2	11
			5 5	9					
	2	8S	2 5	3		2 5	6		
			4 0	6	9	4 0	6	2	11
			5 5	9					
2	1	16S	4 0	3		4 0	6		
			5 5	6	9	5 5	6	2	11
			7 0	9					
	2	30T	4 0	3		4 0	6		
			5 5	6	9	5 5	6	2	11
			7 0	9					
3	1	24S	5 5	3		5 5	6		
			7 0	6	9	7 0	6	2	11
			8 5	9					
	2	36T	5 5	3		5 5	6		
			7 0	6	9	7 0	6	2	11
			8 5	9					
Total					54			12	66

[a] S = single-axle load, T = tandem-axle load

formance changes that can be attributed to controlled effects and those changes that must be attributed solely to uncontrolled or residual effects. For the latter effects, replication provides estimates needed to assess the reliability of controlled effects.

In the illustration, as in the Road Test, replication is provided only for certain pavement designs within each tangent. Table 2 indicates that two different pavement designs are to be once replicated within each tangent; thus there are to be eleven test sections in each of the six traffic lanes, or 66 test sections in all. More replication might be required if the illustration were an actual road test, as the number of replicates should be sufficient to obtain reliable estimates of residual variation (within tangents).

The third principle, randomization, is closely associated with the principles of balance and replication. As was stated, balance is necessary to prevent confusion among controlled factor effects, but it is also important that there be no confusion between controlled effects and residual effects on performance. If, for example, the sections in each tangent were constructed so that surface thickness increased from thin to thick along the tangent, and if an uncontrolled construction variable that could affect pavement performance, say humidity, also increased as the tangent was paved from one end to the other, any conclusion about surface thickness effect would be confused to an unknown degree with effects attributable to humidity during paving. It is well known that systematic uncontrolled variables operate during almost any experimental investigation, so randomization is necessary in order to minimize the risk that residual effects will be mistaken for controlled effects. As in any sampling situation, randomization is also necessary for obtaining proper estimates of residual variation. For example, if each replicate were constructed adjacent to its companion section, it might be expected that an underestimate of residual variation in the tangent would be obtained.

In the example, the eleven sections in each tangent are assigned a random order of occurrence within the tangent. As a result it can be expected that conclusions about surface and subbase effects are not biased or confused by the presence of systematic residual variation within any tangent.

The major performance studies in the AASHO Road Test have experimental designs that involve balance, replication, and randomization, in much the same way as described for the illustration. In addition, still other experimental designs appear in the Road Test in order to provide for special studies whose objectives are somewhat different from the first Road Test objective.

Specifications have now been given for pavement performance data and for experimental designs within which the performance data are obtained. It is rather obvious that many alternatives were available for nearly every specification. Nevertheless, the net result of the selected specifications for the example is a set of performance data as given in Table 3. The performance data consist of three pairs of p and log W values for each of the 66 test sections when the weighting function of Figure 3 is used. Table 3 includes data previously given in Table 2 for sections 3212 and 3222. In this paper section numbers are codes for factor levels. Section 3212 appears in tangent 3, lane 2, at the first surface thickness level and the second subbase thickness level. Similarly, section 3222 is in the second lane of the third tangent and has the second level of thickness for both surface and subbase.

Any section whose serviceability history was complete has p values of 3.5, 2.5, and 1.5 in Table 3. All remaining sections had incomplete histories.

For the AASHO Road Test, tables that correspond to Table 3 cover five tangents and involve five pairs of p and log W values for each of 284 flexible pavement sections and 264 rigid pavement sections.

PROCEDURES FOR ANALYSIS

The analysis consists of procedures that produce an empirical formula wherein performance is associated with load and pavement design variables. In order to use mathematical procedures it is necessary to assume some algebraic form, or model, for the association. In addition to the experimental variables the model involves constants whose values are either to be specified or to be estimated from the data. Thus,

the analytical procedures are for the estimation of constants whose values are unspecified in the model—constants that indicate the effects of design and load variables on performance. The procedures also include methods for estimating the precision with which the data fit the assumed model.

In essence the model is an equation for serviceability trends as illustrated by Figure 5 or Figure 6. When pavement design and axle load are specified for a pavement section, the equation is supposed to predict the section's serviceability after a given number of applications. The equation should also be useful for predicting the number of applications the section will experience before reaching a pre-assigned serviceability level.

There are many different mathematical forms that could be used as models for serviceability trends, and a large number of these may fit the data with more or less the same precision. Only one of the numerous models investigated at the Road Test is used for the illustration in this paper. Further discussion of models is given after the illustration is completed.

Let p_o denote the initial serviceability trend values for a particular test section. Then $p_o - p$ is the serviceability loss experienced by the section when its trend value is at p. It will be assumed that p_o does not depend on pavement design variables in the range of interest, and that the best estimate for p_o is c_o, the average of all initial trend values for sections considered in the analysis. For the example, c_o will be 4.5.

The assumption to be used for the nature of serviceability trends is that serviceability loss is a power function of axle load applications; that is,

$$c_o - p = KW^{\beta} \qquad (1)$$

where β is a positive power and K and/or β may depend on load and design variables. Let $p = c_i$ be a serviceability level such that whenever p for a section falls to c_i, the section is "out of test" and no longer observed. Thus, the number of applications experienced by the section when $p = c_i$ may be called the experimental life of a section. For the example, as at the Road Test, $c_i = 1.5$. Let ρ be the

TABLE 3
PERFORMANCE DATA (ILLUSTRATION), WEIGHTED APPLICATIONS

Tangent 1										Tangent 2										Tangent 3									
Load[a] (kips)	Subbase Thickness (in.)	2 5-in Slab		4 0-in Slab		5 5-in Slab		7 0-in Slab		Load[a] (kips)	Subbase Thickness (in.)	4 0-in Slab		5 5-in Slab		7 0-in Slab		8 5-in Slab		Load[a] (kips)	Subbase Thickness (in.)	5 5-in Slab		7 0-in Slab		8 5-in Slab	
		p	log W	p	log W	p	log W	p	log W			p	log W	p	log W	p	log W	p	log W			p	log W	p	log W	p	log W
4S	3	4.4	5.48	4.5	5.48	4.5	5.48			18S	3	3.5	5.20	4.5	5.48	4.5	5.48			24S	3	3.5	5.28	3.5	5.82	4.5	5.48
		4.1	5.81	4.4	5.81	4.4	5.81					2.5	5.28	4.0	5.81	4.4	5.81					2.5	5.31	2.5	5.83	4.3	5.81
		3.9	6.05	4.3	6.05	4.4	6.05					1.5	5.30	1.8	6.05	4.0	6.05					1.5	5.33	1.5	5.90	3.9	6.05
	6	4.5	5.48	4.5	5.48	4.5	5.48				6	3.5	5.30	4.4	5.48	4.4	5.48				6	3.5	5.30	3.5	5.70	4.4	5.48
		4.3	5.81	4.6	5.81	4.5	5.81					2.5	5.31	4.3	5.81	4.3	5.81					2.5	5.33	2.5	5.85	4.2	5.81
		4.0	6.05	4.2	6.05	4.5	6.05					1.5	5.31	2.8	6.05	4.1	6.05					1.5	5.33	1.5	6.03	3.8	6.05
	6[b]	4.6	5.48	4.5	5.48						6[b]	3.5	5.48	4.5	5.48						6[b]	3.5	5.20	3.7	5.48		
		4.4	5.81	4.5	5.81							2.5	5.40	2.5	5.81							2.5	5.30	2.9	5.81		
	9	4.4	5.48	4.4	5.48	4.6	5.48				9	3.5	5.28	3.5	5.75	4.5	5.48				9	3.5	5.29	3.5	5.90	4.5	5.48
		4.4	5.81	4.4	5.81	4.4	5.81					2.5	5.30	2.5	5.81	4.2	5.81					2.5	5.31	2.5	5.95	4.4	5.81
		3.8	6.05	4.4	6.05	4.4	6.05					1.5	5.31	1.5	5.86	4.2	6.05					1.5	5.33	1.5	6.04	4.1	6.05
8S	3	3.5	5.57	4.5	5.48	4.5	5.48			30T	3	3.5	4.86	3.5	5.70	4.5	5.48			36T	3	3.5	5.47	3.5	6.00	4.6	5.48
		2.5	5.41	4.2	5.81	4.4	5.81					2.5	5.00	2.5	5.80	4.2	5.81					2.5	5.48	2.5	6.03	4.3	5.81
		1.5	5.41	3.6	6.05	4.5	6.05					1.5	5.02	1.5	5.90	3.7	6.05					1.5	5.49	1.5	6.03	4.1	6.05
	6	3.5	5.18	4.4	5.48	4.5	5.48				6	3.5	5.03	2.5	5.78	4.5	5.48				6	3.5	5.36	4.2	5.48	4.7	5.48
		2.5	5.41	4.4	5.81	4.5	5.81					2.5	5.04	1.5	5.80	4.3	5.81					2.5	5.54	4.0	5.81	4.4	5.81
	6[b]	1.5	5.44	4.0	6.05	4.4	6.05				6[b]	1.5	5.04	1.5	5.82	3.9	6.05				6[b]	1.5	5.59	3.2	6.05	4.3	6.05
		3.5	5.49	4.6	5.48							3.5	5.48	3.9	5.48							3.5	5.50	3.7	5.48		
		2.5	5.28	4.3	5.81							2.5	5.11	2.8	5.81							2.5	5.55	3.5	5.81		
		1.5	5.38	3.8	6.05							1.5	5.15	1.7	6.05							1.5	5.58	2.8	6.05		
	9	3.5	5.35	4.5	5.48	4.4	5.48				9	3.5	4.95	3.5	5.72	4.5	5.49				9	3.5	5.44	4.6	5.48	4.5	5.48
		2.5	5.55	4.3	5.81	4.4	5.81					2.5	5.01	2.5	5.78	4.3	5.81					2.5	5.46	4.4	5.81	4.3	5.81
		1.5	5.60	3.9	6.05	4.3	6.05					1.5	5.03	1.5	5.85	3.9	6.05					1.5	5.47	1.9	6.05	3.9	6.05

[a] S = single-axle load; T = tandem-axle load
[b] Replicate
Note: Section used in Figure 1 and others

value of W in Eq. 1 when $p = c_1$. Then $c_0 - c_1 = K\rho^{\beta}$, or $K = (c_0 - c_1)/\rho^{\beta}$, and Eq. 1 may be written in either of the forms.

$$c_0 - p = (c_0 - c_1) \left(\frac{W}{\rho}\right)^{\beta} \tag{2}$$

or

$$p = c_0 - (c_0 - c_1) \left(\frac{W}{\rho}\right)^{\beta}$$

where $c_1 \leq p \leq c_0$. (3)

For any particular section, β and ρ have fixed values, but it will be assumed that if β is not constant for all designs and loads, β decreases whenever ρ increases from one section to another. If $B > 1$, eq. 3 indicates that the serviceability trend will decline along a steeper and steeper curve as applications increase. If $\beta = 1$, the serviceability loss is linear with applications, and if $\beta < 1$, serviceability decreases along a curve that is concave upwards. Curves of Eqs. 2 or 3 are shown in Figure 7 for three different combinations of β and ρ. When $\beta = 2.0$ the trend is the right half of a parabola that opens downward, when $\beta = 1$ the trend is linear, and when $\beta = 0.5$ the trend is the lower half of a parabola that opens to the right.

In the first stage of the analysis, performance data for each section are used to obtain preliminary estimates of β and ρ for the section. If logarithms are taken on both sides of Eq. 2,

$$\log (c_0 - p) = \log (c_0 - c_1) + \beta (\log W - \log \rho) \tag{4}$$

or

$$\log\left[\frac{c_0 - p}{c_0 - c_1}\right] = \beta\left[\log W - \log \rho\right]$$

Calling the left side of Eq. 5 gives

$$G = \log\left[\frac{c_0 - p}{c_0 - c_1}\right] \tag{6}$$

where G is undefined unless $p < c_0$. G has a negative value whenever p is between c_0 and c_1, and G = 0 when $p = c_1$. Substituting Eq. 6 in Eq. 5 gives

$$G = \beta \left[\log W - \log \rho\right] \tag{7}$$

In G, log W coordinates, the graph of Eq. 7 is a straight line whose slope is β and whose intercept on the log W axis is $\log \rho$. Figure 8 shows curves of Eq. 7 for the β, ρ, combinations of Figure 7. Thus the curves in Figure 8 are linearizations of the performance curves shown in Figure 7. To show the connection between G and p, both scales are shown in Figure 8.

For each section, pairs of values for p and W are converted to corresponding values for G and log W, then a straight line is fitted to the G, log W points. Figure 9 shows transformed data and fitted lines for four sections whose data were given in Table 3. Sections 3212 and 3222 are the previously used illustrative sections, whereas sections 1133 and 1233 are included in Figure 9 in order to bring out certain rules used in the rationale. The fitted lines for sections 3212 and 3222 have slopes $\hat{\beta} = 1.97$ and $\hat{\beta} = 1.09$, respectively, and have log W intercepts $\log \hat{\rho} = 5.61$ and $\log \hat{\rho} = 6.44$. These estimates are determined by lines that minimize the sum of squared vertical deviations from the data for each section.

Section 1133 represents a case where not only is there no G value corresponding to the one p value that exceeds $c_0 = 4.5$ (Table 3), but the remaining two values also are the same, $p = 4.4$. Thus for this section $\hat{\beta} = 0$ and $\log \hat{\rho}$ is infinite. Section 1233 has p values 4.4, 4.4, and 4.3, so that little decrease in serviceability has been observed during the experiment. It is supposed that very little information about β and $\log \rho$ is given by data and graphs for sections whose serviceability loss is hardly outside the realm of measurement error. For such sections special rules are applied in order to obtain values of $\hat{\beta}$ and $\log \hat{\rho}$. After examining all $\hat{\beta}$ values for sections that experienced an appreciable serviceability loss, a minimum value is assumed for β, and if the data for any section give $\hat{\beta}$ less than the assumed minimum, the minimum β is assigned as the section's $\hat{\beta}$. For the example, minimum β is taken to be 1.0, and both sections 1133 and 1233 are given the value $\hat{\beta} = 1.0$. After this assignment, $\log \hat{\rho}$ is obtained by fitting a line whose slope is 1.0 to the observed points. Using this rule, $\log \hat{\rho}$ is 7.41 and 7.16, respectively, for sections 1133 and 1233, as indicated in Figure 9. If all p values for a section are equal to or greater than $c_0 = 4.5$, as for section 1132 in Table 3, not only is $\hat{\beta}$ assigned to be 1.0, but also $\log \hat{\rho}$ is set at the median $\log \hat{\rho}$ for all sections that differ only in subbase thickness from the section that has no G data. Table 4 gives $\hat{\beta}$ and $\log \hat{\rho}$ values.

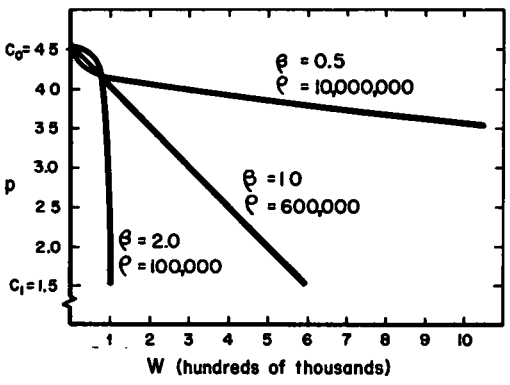

Figure 7. Graphs of $p = 4.5 - 3.0\left(\frac{W}{\rho}\right)^{\beta}$.

After $\hat{\beta}$ has been determined for each section, the $\hat{\beta}$ values are plotted against pavement design and load variables, and an analysis of variance is made in order to infer the nature and extent of any dependence of $\hat{\beta}$ on design and load variables. Neither the plots nor the analysis of variance are shown here, but both proceed from the assumption that β, is related to design and load variables according to the model

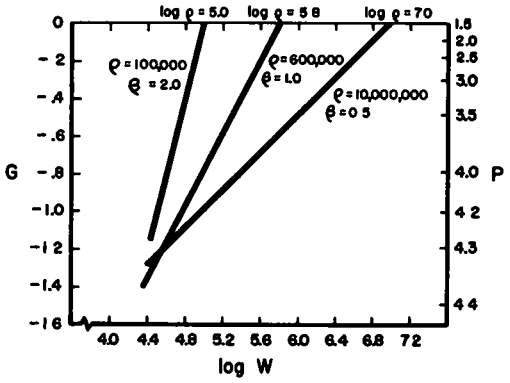

Figure 8. $G = \log\left(\frac{4.5-p}{3.0}\right) = \beta\left[\log W - \log \rho\right]$.

$$\beta = \beta_0 + \frac{B_0 (L_1 + L_2)^{B_2}}{(b_1 D_1 + b_2 D_2 + b_3)^{B_1} L_2^{B_3}} \qquad (8)$$

in which β_0 is a minimum value for β;
L_1 is the nominal load axle weight in kips
(that is, load values as given in Table 3); L_2 is one for single-axle vehicles, two for tandem-axle vehicles; D_1 is the first pavement design factor, slab thickness, in inches; and D_2 is the second pavement design factor, subbase thickness, in inches.

The remaining symbols on the right side of Eq. 8 are positive constants whose values are either to be assumed (as is done for β_0) or to be estimated from the $\hat{\beta}$ values.

In general Eq. 8 implies that β increases as axle load increases and that β decreases as pavement design increases for a fixed loading. If there were three pavement design factors, as at the Road Test, the third factor, D_3, would have been introduced in the combination $b_1D_1 + b_2D_2 + b_3D_3 + b_4$. The constant term in the design combination (b_3 in Eq. 8) appears so that β is not necessarily infinite when there is no thickness for D_1 and D_2, and L_2 has been added to L_1 so that β does not necessarily approach β_0 as L_1 approaches zero.

For the example, graphs and variance analysis for $\hat{\beta}$ show little or no dependence of $\hat{\beta}$ on subbase thickness, so b_2 is taken to be zero. With only one variable, D_1, in the design combination, the effect of D_1 can be relegated to the power B_1 by assigning values to b_1 and b_3. For the illustration, let $b_1 = b_3 = 1.0$. Then, as β_0 has already been assigned to be 1.0, Eq. 8 is reduced to

$$\beta = 1.0 + \frac{B_0 (L_1 + L_2)^{B_2}}{(D_1 + 1)^{B_1} L_2^{B_3}} \qquad (9)$$

in which only B_0, B_1, B_2 and B_3 remain to be estimated from the $\hat{\beta}$ data. Taking the logarithm of Eq. 9 gives

$$\log (\beta - 1.0) = \log B_0 + B_2 \log (L_1 + L_2) - B_3 \log L_2 - B_1 \log (D_1 + 1) \qquad (10)$$

For each lane, Eq. 10 represents a straight line when $\log (\hat{\beta} - 1.0)$ is plotted against $\log (D_1 + 1)$, and linear regressions of $\log (\hat{\beta} - 1.0)$ on $\log (D_1 + 1)$ give lane estimates for the slopes, B_1. Omitting lane 1 of tangent 1, because the majority of $\hat{\beta}$ values in this lane were 1.0 by assignment rather than values obtained from performance data, the regression slopes are averaged to give $\hat{B}_1$, the final estimate for B_1. The average slope for the remaining lanes is $\hat{B}_1 = 5.90$. Transposition of Eg. 10 gives

$$\log (\beta - 1.0) + B_1 \log (D_1 + 1) = \log B_0 + B_2 \log (L_1 + L_2) - B_3 \log L_2 \qquad (11)$$

where the left side of Eq. 11 is now estimated by $\log (\hat{\beta} - 1.0) + \hat{B}_1 \log (D_1 + 1)$ for every section. For any lane, average

TABLE 4
ESTIMATES OF β AND LOG β

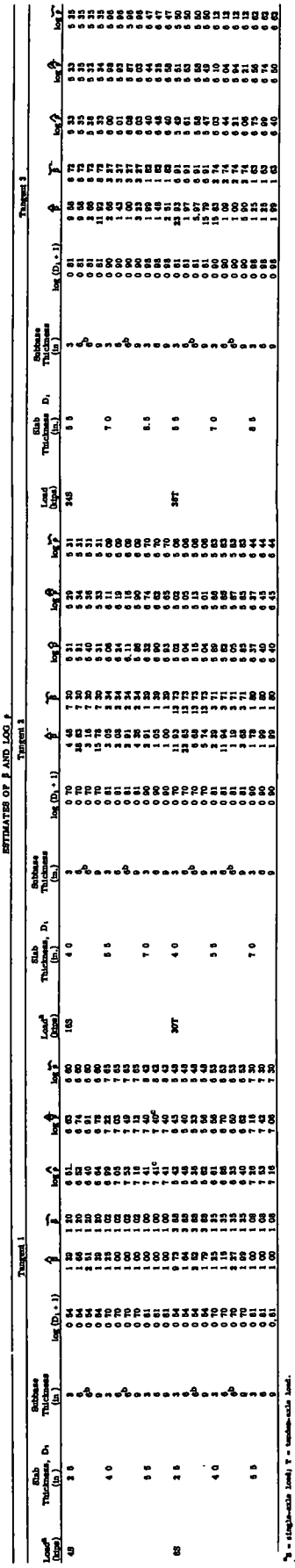

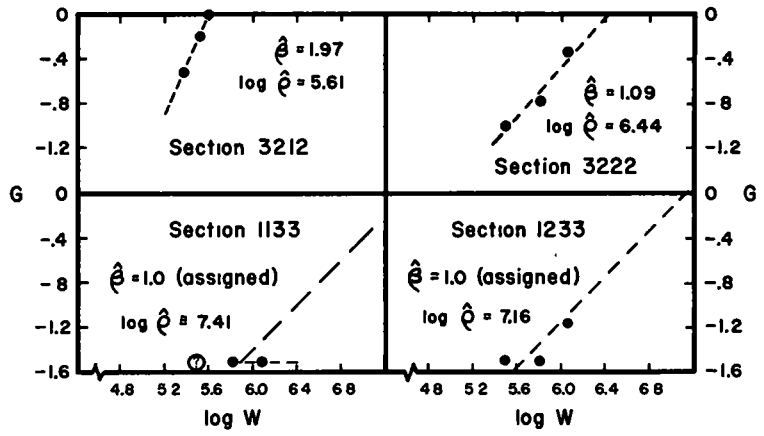

Figure 9. Illustrative estimates for β and log ρ from section data.

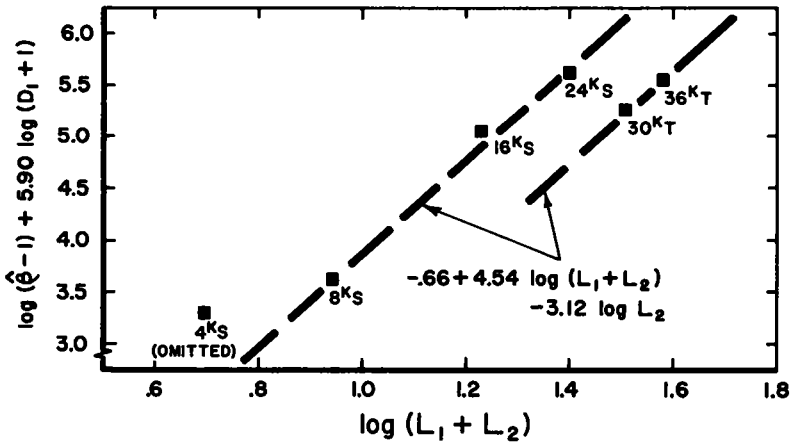

Figure 10. Adjusted mean log $(\hat{\beta}-1)$ vs log (L_1+L_2).

log $(\hat{\beta} - 1.0)$ + average $\hat{B}_1 \log(D_1 + 1)$ is called an adjusted lane mean, and according to Eq. 11 the adjusted lane means depend linearly on log $(L_1 + L_2)$ and log L_2. Figure 10 shows the six adjusted lane means for the example, and includes lines that are obtained from a linear regression analysis. The common slope of single- and tandem-axle lines is an estimate, $\hat{B}_2$, for B_2. The intercept of the single-axle line on the adjusted means axis is an estimate, log $\hat{B}_0$, for log B_0, and the difference between intercepts of the single-axle and tandem-axle lines produces an estimate, $\hat{B}_3$, for B_3. For the illustrative data, log $\hat{B}_0 = 0.66$ or $\hat{B}_0 = 0.22$, $\hat{B}_2 = 4.54$, and $\hat{B}_3 = 3.12$. Substitution of these values in Eq. 9 gives a new estimation formula for β,

$$\tilde{\beta} = 1.0 + \frac{0.22\,(L_1 + L_2)^{4.54}}{(D_1 + 1)^{5.90}\,L_2^{3.12}} \qquad (12)$$

Values for $\tilde{\beta}$ from Eq. 12 are given in Table 4.

The second phase of the analytical procedures begins by using $\tilde{\beta}$ values to obtain new estimates for log ρ from the data for each section. The first estimates for log ρ were denoted by log $\hat{\rho}$ and were obtained as log W intercepts (Fig. 9) for lines whose slopes were $\tilde{\beta}$. Using the same rules as for obtaining log $\hat{\rho}$, the new estimates, log

$\hat{\hat{\rho}}$, are obtained as log W intercepts for lines whose slopes are $\tilde{\beta}$. Table 4 gives values for log $\hat{\hat{\rho}}$ for each section in the illustration. In essence, the rationale supposes that estimates for β from Eq. 12 are better than estimates based only on individual section performance data, and that as a consequence, log $\hat{\hat{\rho}}$ values represent better estimates for log ρ than do the log $\hat{\rho}$ values.

As was done with the $\hat{\beta}$ values, log $\hat{\hat{\rho}}$ values are plotted against the design and load variables, and an analysis of variance is made to infer how and with what significance the log $\hat{\hat{\rho}}$ values depend on design and load variables. The algebraic form for the association of log ρ with design and load variables is assumed to be

$$\rho = \frac{A_0 (a_1 D_1 + a_2 D_2 + a_3)^{A_1} L_2^{A_3}}{(L_1 + L_2)^{A_2}} \qquad (13)$$

in which A_0, A_1, A_2, A_3, a_1, a_2, and a_3 are positive constants. Eq. 13 implies that ρ increases with pavement design and decreases with axle load. The constant a_3 is included so that ρ is not necessarily zero in the absence of surface and subbase, and L_2 is added to L_1 in the denominator so that ρ is not necessarily infinite when L_1 is zero.

For the illustrative data, even casual inspection of Table 4 indicates little or no association between log $\hat{\hat{\rho}}$ and subbase thickness, so a_2 is taken to be zero. As was done for b_1 and b_3 in Eq. 8, both a_1 and a_3 are set at 1.0. In logarithmic form, Eq. 13 thus becomes

$$\log \rho = \log A_0 - A_2 \log (L_1 + L_2) + A_3 \log L_2 + A_1 \log (D_1 + 1) \qquad (14)$$

Figure 11 shows how log $\hat{\hat{\rho}}$ values vary with corresponding values for log $(D_1 + 1)$ for two lanes. Linear regressions of log $\hat{\hat{\rho}}$ on log $(D_1 + 1)$ in each lane produce slopes that are estimates of A_1, and when the slopes are averaged for all but lane 1 of tangent 1, the estimate obtained for A_1 is $\hat{A}_1 = 6.79$.

Transposing $A_1 \log (D_1 + 1)$ in Eq. 14 adjusts log ρ for surface thickness, and for each lane, average log $\hat{\hat{\rho}}$ - average $\hat{A}_1 \log (D_1 + 1)$ is an adjusted lane mean that should depend on log $(L_1 + L_2)$ and log L_2. Figure 12 shows adjusted lane means versus log $(L_1 + L_2)$ for single and tandem axles, and shows the lines obtained from the regression analysis. As indicated in Figure 12, log $\hat{A}_0 = 5.98$, $\hat{A}_2 = 4.40$, and $\hat{A}_3 = 3.17$. Thus the procedures have produced a final estimation equation for log ρ,

$$\log \tilde{\rho} = 5.98 - 4.40 \log (L_1 + L_2) + 3.17 \log L_2 + 6.79 \log (D_1 + 1) \qquad (15a)$$

or

$$\tilde{\rho} = \frac{10^{5.98} (D_1 + 1)^{6.79} L_2^{3.17}}{(L_1 + L_2)^{4.40}} \qquad (15b)$$

Estimates for log ρ given by Eq. 15 are given in Table 4.

The results of the analysis can now be summarized. If it is desired to estimate p when W is given, Eqs. 3, 12 and 15 combine to give

$$\hat{p} = 4.5 - 3.0 \left(\frac{W}{\tilde{\rho}} \right)^{\tilde{\beta}} \qquad (16)$$

If it is desired to estimate log W when p is given, Eqs. 5, 12 and 15 combine to give

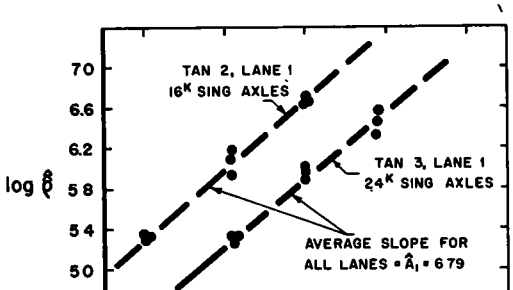

Figure 11. Log $\hat{\hat{\rho}}$ vs log (D_1+1) for two lanes.

$$\log \hat{W} = \log \tilde{\rho} + \frac{\log \left[\frac{4.5 - p}{3.0}\right]}{\tilde{\beta}} \qquad (17)$$

Eqs. 16 and 17 thus represent the first goal of the analysis—to associate the performance data with design and load variables.

The remainder of the rationale for analysis is concerned with summarizing the precision with which estimates can be made using Eq. 16 and 17 to estimate p and log W, respectively.

Values in parentheses in Table 5 are either serviceability estimates obtained from Eq. 16 for all sections whose serviceability did not fall to $c_1 = 1.5$, or are log W estimates obtained from Eq. 17 for all sections whose serviceability did reach 1.5. Estimates are given at 15, 35 and 55 index days in the first case and at p = 3.5, 2.5, and 1.5 for the second case. Differences between corresponding estimated values (Table 5) and observed values (Table 1) represent residuals that are not accounted for by Eqs. 16 and 17. Table 6 gives a summary of mean residuals and mean absolute residuals for both types of estimates, classified both by lane and by index day or serviceability level.

For all sections that were "in test" after 55 index days, the upper half of Table 6 gives the number of such sections in each lane, and the average residual $\hat{p} - p$, both algebraic and absolute. For the 31 sections involved, the average algebraic residual is shown to be 0.02, and the average absolute residual is 0.10. There does not appear to be any trend with respect to load, but in nearly all lanes the residuals increase with time or applications. However, even the largest mean residuals are only two or three tenths and it may be concluded that the p estimates are quite close to their respective observations.

In the lower half of Table 6, residuals in log W are summarized from differences obtained by subtracting log W values in Table 3 from corresponding log $\hat{W}$ values in Table 5 for all sections whose serviceability fell to p = 1.5. The mean algebraic residual in log W is nearly zero, while the mean absolute residual is about 0.04. These residuals appear to have about the same magnitude at each serviceability level and are not far from being equal in each lane. No log W residuals are shown for lane 1 of tangent 1 because no section was "out of test" in this lane.

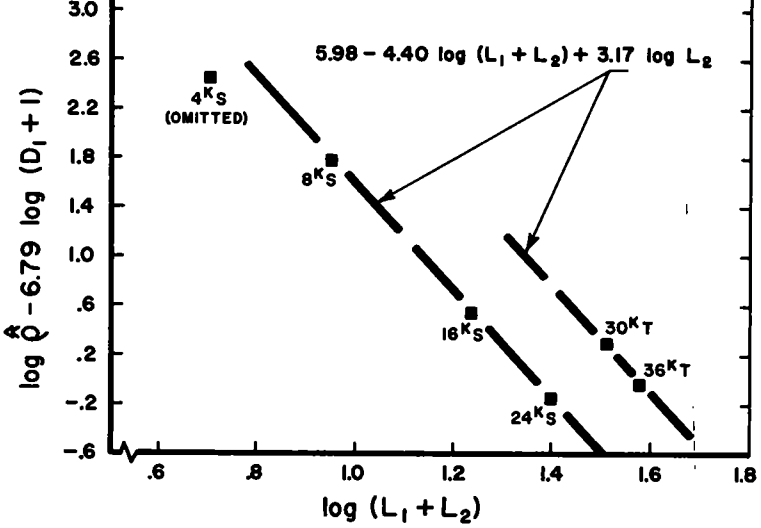

Figure 12. Adjusted mean log $\hat{\rho}$ vs log (L_1+L_2).

A particular log W residual can be converted to the ratio of estimated to observed applications. For example, if $\log \hat{W} - \log W = 0.10$, $\frac{\hat{W}}{W} = 10^{0.10}$, or $\hat{W} = 1.26W$. If the log W residual had been -0.10, then $\hat{W} = 0.79W$. Through such conversions, average Log W residuals may be used to obtain an indication of the agreement between predicted applications and observed applications. For the example, the average absolute residual represents about a 10 percent deviation from the observed value. In the Road Test performance analyses, the corresponding average residuals are about 0.2 for log W estimates.

For both the present example and for the Road Test data, residuals in log W predictions compare favorably with differences in log W between replicate sections. From Table 3, the average absolute difference in log W between replicate sections is about 0.09, so that the average deviation of two replicate sections from their own mean is about 0.045. Thus, the predicted log W from Eq. 17 deviates about the same distance from log W as does log W from the mean of log W values observed for the same design and load. For this reason it is unlikely that any appreciable decrease in log W residuals can be made by fitting the illustrative observations with another model or by using another set of procedures.

Both Eq. 16 and Eq. 17 are rather complex and difficult to use in the form given. However, graphs of these equations can be made for whatever conditions may be useful. Figure 13 shows the curves of Eq. 17 for every combination of surface thickness and loading used in the illustration—all for the case that p = 2.5. For a particular load, the plotted curves shows the number of applications expected for any surface thickness at the time when the serviceability level has dropped to 2.5. Applications beyond 10^6 represent extrapolations for all curves, and each load curve has been extended beyond the lower and upper surface thickness level used in the experiment. Corresponding curves, of course, could be plotted for other values of p.

To show how close the observations are to the curves of Figure 13, Figure 14 repeats three of the curves from

TABLE 5

ESTIMATED PERFORMANCE DATA[a] (ILLUSTRATION), WEIGHTED APPLICATIONS

Load[b] (kips)	Subbase Thickness (in.)	Tangent 1								Tangent 2								Tangent 3							
		2.5-in. Slab			4 0-in. Slab		5 5-in. Slab			4 0-in. Slab		5 5-in. Slab			7 0-in. Slab		8 5-in. Slab			5 5-in. Slab		7 0-in. Slab		8 5-in. Slab	
		p	or	(log Ŵ) log W	p	or	(log Ŵ) log W	p	or	Load[a] Target	Subbase Thickness (in.)	p	or	(log Ŵ) log W	p	or	(log Ŵ) log W	p	or	(log Ŵ) log W	Load[a] (kips)	Subbase Thickness (in.)	p	or	(log Ŵ) log W	p	or	(log Ŵ) log W	p	or	(log Ŵ) log W
18	3	(4.6)		5.48	(4.6)		5.48	(4.5)		18S	3	3.5		(5.25) 5.48	(4.5)		5.48	(4.5)		5.48	24S	3	3.5		(5.29) 5.48	3.5		(5.82) 5.48	(4.5)		5.48
		(4.4)		5.81	(4.5)		5.81	(4.5)				2.5		(5.29) 5.81	(4.1)		5.81	(4.4)		5.81			2.5		(5.33) 5.81	2.5		(5.91) 5.81	(4.4)		5.81
		(3.8)		6.05	(4.4)		6.05	(4.5)				1.5		(5.31) 6.05	(2.3)		6.05	(4.2)		6.05			1.5		(5.35) 6.05	1.5		(5.93) 6.05	(4.0)		6.05
	6	(4.5)		5.48	(4.5)		5.48	(4.5)			6	3.5		(5.25) 5.48	(4.5)		5.48	(4.5)		5.48		6	3.5		(5.33) 5.48	3.5		(5.82) 5.48	(4.5)		5.48
		(4.2)		5.81	(4.5)		5.81	(4.5)				2.5		(5.29) 5.81	(4.1)		5.81	(4.4)		5.81			2.5		(5.33) 5.81	2.5		(5.91) 5.81	(4.4)		5.81
		(3.8)		6.05	(4.4)		6.05	(4.5)				1.5		(5.31) 6.05	(2.3)		6.05	(4.1)		6.05			1.5		(5.35) 6.05	1.5		(5.96) 6.05	(4.0)		6.05
	9[c]	(4.5)		5.48	(4.5)		5.48	(4.5)			9[b]	3.5		(5.25) 5.48	(4.5)		5.48					9[b]	3.5		(5.29) 5.48	3.5		(5.82) 5.48			
		(4.2)		5.81	(4.5)		5.81	(4.5)				2.5		(5.29) 5.81	(4.1)		5.81						2.5		(5.33) 5.81	2.5		(5.91) 5.81			
		(3.8)		6.05	(4.4)		6.05	(4.5)				1.5		(5.31) 6.05	(2.3)		6.05						1.5		(5.35) 6.05	1.5		(5.96) 6.05			
	9	(4.5)		5.48	(4.5)		5.48	(4.5)			9	3.5		(5.25) 5.48	(4.5)		5.48	(4.5)		5.48		9	3.5		(5.29) 5.48	3.5		(5.82) 5.48	(4.5)		5.48
		(4.2)		5.81	(4.5)		5.81	(4.5)				2.5		(5.29) 5.81	(4.1)		5.81	(4.4)		5.81			2.5		(5.33) 5.81	2.5		(5.91) 5.81	(4.4)		5.81
		(3.8)		6.05	(4.4)		6.05	(4.5)				1.5		(5.31) 6.05	(2.3)		6.05	(4.1)		6.05			1.5		(5.35) 6.05	1.5		(5.96) 6.05	(4.0)		6.05
24S	3	(4.5)		5.48	(4.5)		5.48	(4.5)		30T	3	3.5		(5.25) 5.48	(4.5)		5.48	(4.5)		5.48	36T	3	3.5		(5.29) 5.48	3.5		(5.82) 5.48	(4.5)		5.48
		(4.2)		5.81	(4.5)		5.81	(4.5)				2.5		(5.29) 5.81	(4.1)		5.81	(4.4)		5.81			2.5		(5.33) 5.81	2.5		(5.91) 5.81	(4.4)		5.81
		(3.8)		6.05	(4.4)		6.05	(4.5)				1.5		(5.31) 6.05	(2.3)		6.05	(4.1)		6.05			1.5		(5.35) 6.05	1.5		(5.96) 6.05	(4.0)		6.05
	6	(4.5)		5.48	(4.5)		5.48	(4.5)			6	3.5		(5.25) 5.48	(4.5)		5.48	(4.5)		5.48		6	3.5		(5.29) 5.48	3.5		(5.82) 5.48	(4.5)		5.48
		(4.2)		5.81	(4.5)		5.81	(4.5)				2.5		(5.29) 5.81	(4.1)		5.81	(4.4)		5.81			2.5		(5.33) 5.81	2.5		(5.91) 5.81	(4.4)		5.81
		(3.8)		6.05	(4.4)		6.05	(4.5)				1.5		(5.31) 6.05	(2.3)		6.05	(4.1)		6.05			1.5		(5.35) 6.05	1.5		(5.96) 6.05	(4.0)		6.05
	9	(4.5)		5.48	(4.5)		5.48	(4.5)			9	3.5		(5.25) 5.48	(4.5)		5.48	(4.5)		5.48		9	3.5		(5.29) 5.48	3.5		(5.82) 5.48	(4.5)		5.48
		(4.2)		5.81	(4.5)		5.81	(4.5)				2.5		(5.29) 5.81	(4.1)		5.81	(4.4)		5.81			2.5		(5.33) 5.81	2.5		(5.91) 5.81	(4.4)		5.81
		(3.8)		6.05	(4.4)		6.05	(4.5)				1.5		(5.31) 6.05	(2.3)		6.05	(4.1)		6.05			1.5		(5.35) 6.05	1.5		(5.96) 6.05	(4.0)		6.05
30S	3	(4.5)		5.48	(4.5)		5.48	(4.5)		36T	3	3.5		(5.25) 5.48	(4.5)		5.48	(4.5)		5.48	42S	3	3.5		(5.29) 5.48	3.5		(5.82) 5.48	(4.5)		5.48
		(4.2)		5.81	(4.5)		5.81	(4.5)				2.5		(5.29) 5.81	(4.1)		5.81	(4.4)		5.81			2.5		(5.33) 5.81	2.5		(5.91) 5.81	(4.4)		5.81
		(3.8)		6.05	(4.4)		6.05	(4.5)				1.5		(5.31) 6.05	(2.3)		6.05	(4.1)		6.05			1.5		(5.35) 6.05	1.5		(5.96) 6.05	(4.0)		6.05
	6	(4.5)		5.48	(4.5)		5.48	(4.5)			6	3.5		(5.25) 5.48	(4.5)		5.48	(4.5)		5.48		6	3.5		(5.29) 5.48	3.5		(5.82) 5.48	(4.5)		5.48
		(4.2)		5.81	(4.5)		5.81	(4.5)				2.5		(5.29) 5.81	(4.1)		5.81	(4.4)		5.81			2.5		(5.33) 5.81	2.5		(5.91) 5.81	(4.4)		5.81
		(3.8)		6.05	(4.4)		6.05	(4.5)				1.5		(5.31) 6.05	(2.3)		6.05	(4.1)		6.05			1.5		(5.35) 6.05	1.5		(5.96) 6.05	(4.0)		6.05
	9[c]	(4.5)		5.48	(4.5)		5.48	(4.5)			9[b]	3.5		(5.25) 5.48	(4.5)		5.48					9[b]	3.5		(5.29) 5.48	3.5		(5.82) 5.48			
		(4.2)		5.81	(4.5)		5.81	(4.5)				2.5		(5.29) 5.81	(4.1)		5.81						2.5		(5.33) 5.81	2.5		(5.91) 5.81			
		(3.8)		6.05	(4.4)		6.05	(4.5)				1.5		(5.31) 6.05	(2.3)		6.05						1.5		(5.35) 6.05	1.5		(5.96) 6.05			
	9	(4.5)		5.48	(4.5)		5.48	(4.5)			9	3.5		(5.25) 5.48	(4.5)		5.48	(4.5)		5.48		9	3.5		(5.29) 5.48	3.5		(5.82) 5.48	(4.5)		5.48
		(4.2)		5.81	(4.5)		5.81	(4.5)				2.5		(5.29) 5.81	(4.1)		5.81	(4.4)		5.81			2.5		(5.33) 5.81	2.5		(5.91) 5.81	(4.4)		5.81
		(3.8)		6.05	(4.4)		6.05	(4.5)				1.5		(5.31) 6.05	(2.3)		6.05	(4.1)		6.05			1.5		(5.35) 6.05	1.5		(5.96) 6.05	(4.0)		6.05

[a]Numbers in parentheses for "out of test" sections are estimates of log W when p is given. Numbers in parentheses for "in test" sections are estimates of p when log W is given.

TABLE 6

SUMMARY OF RESIDUALS

	Item		Lane 11	12	21	22	31	32	Average All Sections
p residuals		No. Sect.	9	6	5	3	3	5	
	Avg. $(\hat{p} - p)$	t = 15	0.00	0.01	0.02	-0.01	0.02	-0.03	0.00
		t = 35	0.01	0.01	0.03	0.09	0.08	0.07	0.04
		t = 55	0.06	-0.05	-0.08	0.09	0.05	0.03	0.01
		All	0.02	-0.01	-0.01	0.06	0.05	0.03	0.02
	Avg. $\lvert\hat{p} - p\rvert$	t = 15	0.04	0.04	0.04	0.01	0.04	0.15	0.05
		t = 35	0.09	0.08	0.12	0.09	0.09	0.12	0.10
		t = 55	0.10	0.08	0.25	0.09	0.13	0.35	0.16
		All	0.08	0.07	0.13	0.06	0.09	0.21	0.10
log W residuals		No. Sect.	0	3	4	6	6	4	
	Avg. $(\log \hat{W} - \log W)$	p = 3.5	-	0.05	0.02	0.00	0.01	-0.01	0.01
		p = 2.5	-	-0.03	0.04	0.01	0.00	0.00	0.01
		p = 1.5	-	-0.01	0.06	0.00	-0.03	0.01	0.01
		All	-	0.01	0.04	0.00	0.00	0.00	0.01
	Avg. $\lvert\log \hat{W} - \log W\rvert$	p = 3.5	-	0.06	0.07	0.04	0.04	0.04	0.05
		p = 2.5	-	0.05	0.06	0.02	0.03	0.03	0.04
		p = 1.5	-	0.08	0.06	0.03	0.04	0.05	0.05
		All	-	0.06	0.06	0.03	0.03	0.04	0.04

Figure 13 and includes appropriate data given as observations in Table 3. Data for only those sections whose p reached 2.5 can be shown in Figure 14. The dotted curves represent the band formed by $\pm$ 0.08; that is, plus or minus twice the mean absolute residual in log W. If residual deviations have a normal frequency distribution about the curves as shown in Figure 14, then plus or minus two mean absolute deviations should include about 90 percent of all individual residuals.

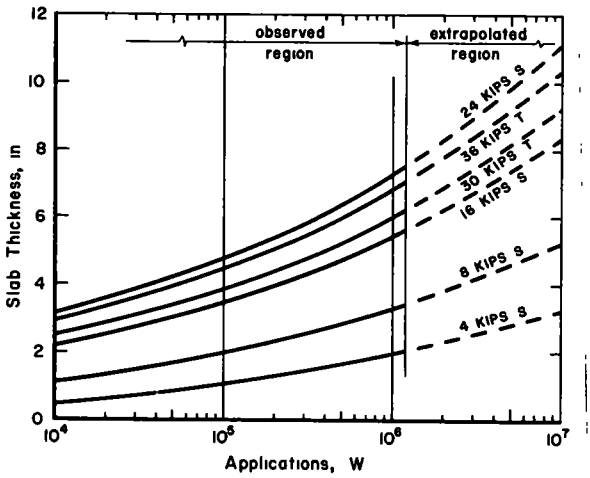

Figure 13. Performance equation (Eq. 17) for test loads (p = 2.5).

Another form of Figure 13 is given in Figure 15, which shows the associated surface thickness and load for selected applications expected when p = 2.5. Figure 15 serves to bring out the effect of load on surface thickness requirements.

When bands for residual variation are added to the graphs, either or both of Figures 13 and 15 constitute a summarization of the data given in Table 3, and presumably satisfy (for p = 2.5) the stated objective for the investigation.

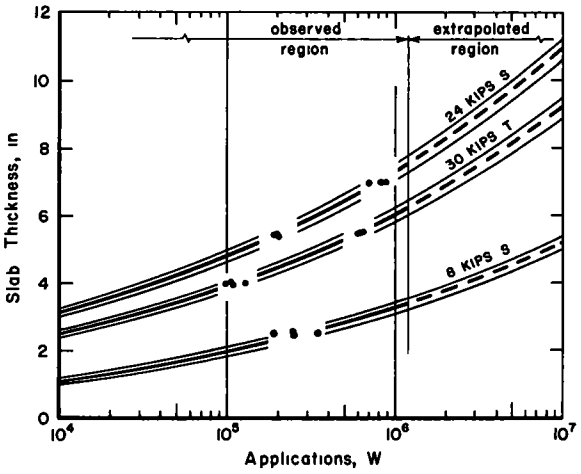

Figure 14. Performance equation (Eq. 17) for three selected loads (p = 2.5).

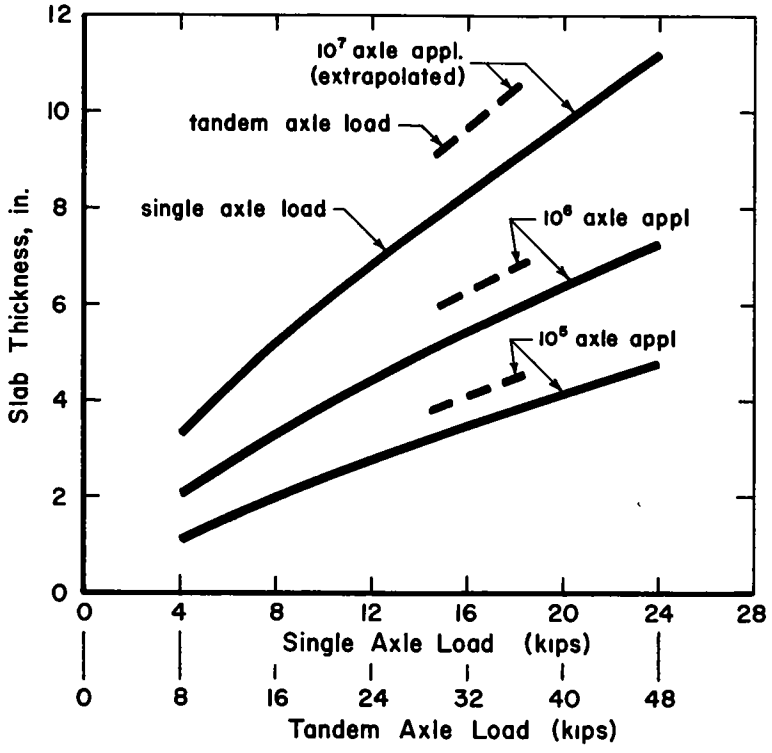

Figure 15. Performance equation (Eq. 17) for selected applications (p = 2.5).

SUMMARY AND DISCUSSION

The rationale just described defines both performance data and procedures for analyzing the data. The procedures included the selection of a general mathematical model for the association of experimental variables, the assignment of values to certain constants in the model, and rules for estimating values for all remaining constants in the model. The end result of the rationale was given by Eqs. 16 and 17, by a residual summary in Table 6, and by Figures 13, 14, and 15, which are meant to bring out the nature of the equations and their residuals.

If the experimental objectives are satisfied by curves such as in Figures 13 and 15, it is important to know how different the curves might be if the rationale were to be changed in one or more ways, say by the selection of a different model or by choosing different estimation rules.

Efforts to answer this question at the Road Test are represented by the investigation of many rationales, each of which produces a residual summary as illustrated by Table 6. A rationale is considered to produce an adequate fit to the data if mean algebraic residuals are near zero and if mean absolute residuals are of the same magnitude as deviations of replicate observations from their own mean. In terms of Figure 14, this criterion implies that the central curves should tend to pass through median observed points and that replicate observations should be scattered about the curves to the same degree as are unreplicated observations. If the first of these conditions is not met it may be supposed that the estimation rules have produced biased estimates for constants in the model, and if the second condition does not hold the model may not be appropriate. In either case the rationale can be modified until the criterion is met. It is noteworthy that existing theory for pavement performance gives little or no guidance in the area of model selection.

Changes in the rationale may also change the curves in the extrapolation regions of Figures 13, 14, and 15. Actual performance data for these regions would be necessary in order to appraise the validity of the extrapolations.

Calibration and Use of BPR Roughometer at the AASHO Road Test

W. RONALD HUDSON, Assistant Rigid Pavement Research Engineer, and
ROBERT C. HAIN, Assistant Chief, Data Processing and Analysis,
AASHO Road Test, Highway Research Board

The primary problem is using the Bureau of Public Roads roughometer at the AASHO Road Test has been the variability of the instrument. Frequent calibration has been found to be necessary. Using the Road Test profilometer as a standard, a method has been developed whereby the whole dynamic system of the roughometer can be calibrated. This paper describes the calibration technique for the roughometer and its use at the AASHO Road Test, including methods for making present serviceability determinations.

●THE PRIMARY PURPOSE of a highway or highway system is to serve the riding public. A pavement that provides a smooth ride is presumed to be serving better than one which offers a rough ride, other factors being equal. The importance of pavement roughness has long been recognized. Many devices, including single-wheel indicators and multiwheel profilometers, have been developed to measure roughness. One of the earliest of these instruments was developed for use on the Bates Road Test in 1923 (1). Numerous devices have followed (2, 3, 4, 5). In 1941 a relatively simple, standardizable instrument, the road roughness indicator, was introduced by the Bureau of Public Roads. For simplicity this instrument is referred to in this paper as the BPR roughometer (6). Since its conception, considerable development work has been done on this device by the Bureau of Public Roads, the University of California (7, 8), and Purdue University (9), among others; and many improvements have been made in its operation. At present the BPR roughometer is the most widely used type of road roughness indicator in the United States. Table 1 gives the agencies owning one of these instruments.

The basic roughometer used at the AASHO Road Test was constructed by the Bureau of Public Roads. The details of the device are those reported by Buchanan and Catudel (6) in 1941, with slight modifications. The complete plans are available from the Bureau of Public Roads (10). The roughometer consists of a single-wheel trailer towed by a light truck (Fig. 1). The wheel is suspended on two single-leaf springs (Fig. 2). A smooth tread 6.70 x 15, 4-ply tire is mounted on the wheel. Irregularities of a pavement surface are recorded as differential movement of the axle relative to the frame of the device. This movement is transmitted by a strong wire cable to a double-acting ball-clutch integrator that converts the upward vertical motion to unidirectional rotary motion. This rotary motion actuates a microswitch that records roughness in inches on a mechanical pulse counter in the towing vehicle. The dashpot dampers have ball-joint end connectors but do not employ "O" rings.

The Roughometer and the Present Serviceability Concept

The primary purpose of the AASHO Road Test was to determine significant relationships between a known number of specified axle loads and the performance of pavements

TABLE 1

ORGANIZATIONS PRESENTLY POSSESSING ROUGHOMETERS

1. AASHO Road Test
2. Illinois Toll Road
3. BPR Region 9
4. BPR Division of Research
5. Waterways Experiment Station
6. Alabama State Highway Department
7. Connecticut State Highway Department
8. California State Highway Department
9. Illinois State Highway Department
10. Indiana State Highway Department
11. Iowa State Highway Department
12. Kansas State Highway Department
13. Louisiana State Highway Department
14. Maryland State Highway Department
15. Michigan State Highway Department
16. Minnesota State Highway Department
17. Missouri State Highway Department
18. North Carolina State Highway Department
19. North Dakota State Highway Department
20. Oklahoma State Highway Department
21. Oregon State Highway Department
22. South Dakota State Highway Department
23. Virginia State Highway Department
24. Wisconsin State Highway Department

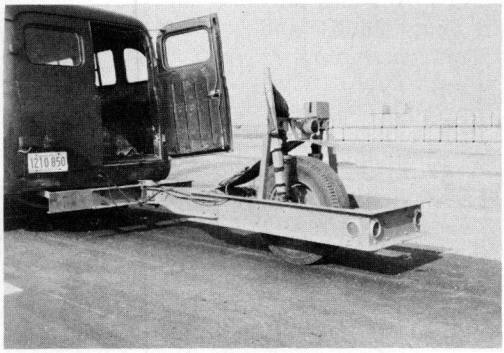

Figure 1. Standard BPR roughometer.

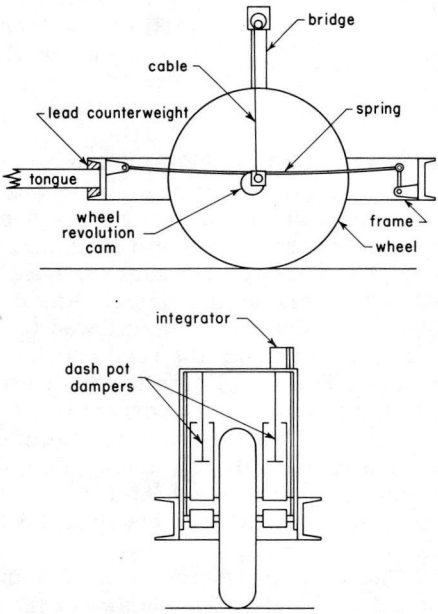

Figure 2. Schematic diagram of BPR roughometer.

of various designs. To help define performance, a broad term with several definitions, the concept of present serviceability was established. This concept is fully described elsewhere (11). Briefly, it consists of having a panel representing highway users subjectively rate a section of pavement usually ¼ mi long. The average panel rating of a section is defined as its present serviceability. The present serviceability ratings of several sections of pavement are regressed on physical measurements of these sections made coincidentally with the ratings. For any pavement, an estimate of mean panel serviceability rating can then be made at any time, using physical measurements alone.

The following definitions are taken from Carey and Irick (11):

Present Serviceability— The ability of a specific section of pavement to serve high-speed, high-volume, mixed (truck and automobile) traffic in its existing condition.

Present Serviceability Rating (PSR)—The mean of the individual ratings made by the members of a specific panel of men selected for this purpose by the Highway Research Board.

Present Serviceability Index (PSI) or Estimated Present Serviceability Rating—A mathematical combination of values, obtained from certain physical measurements of a large number of pavements, so formulated as to predict the PSR for those pavements within prescribed limits.

Slope Variance (SV)—A summary statistic which describes the variation in slope, sampled at 1-ft intervals, of a continuous slope record produced by the AASHO profilometer.

For clarity, other notations and definitions will be useful, as follows:

BR_S = Roughness reading, in inches per mile, of the standard BPR roughometer operated at a speed of s miles per hour.

AR_S = Roughness reading, in inches per mile, of the AASHO Road Test modified roughometer (AASHO roughometer) operated at a speed of s miles per hour.

PSI_{abc} = An estimated serviceability rating, where abc is a three-digit code which uniquely identifies the particular equation used to estimate PSR. This code is necessary to identify the estimation equation with regard to three factors:

a = type of pavement to which applicable; i.e., rigid or flexible;
b = data used to derive the equation. As the rating panel rated more sections new equations were developed from the additional data. As additional data were gathered to relate slope variance to AR_{10}, new equations were developed;
c = measuring instrument. There are equations involving each of the three methods used to measure roughness; i.e., the profilometer, the roughometer, and the rut depth gage.

C(rigid pavement) = Major cracking, in feet per 1,000 square feet of pavement area. Major cracks are sealed cracks and those cracks which are spalled to a width of ¼ in. for one-half their length on the slab surface. Measurement is made on the longitudinal or transverse projection of the crack, whichever is greater.

P(rigid pavement) = Bituminous patching, in square feet per 1,000 square feet of pavement area. Area cracking which is awaiting matinenance may also be included in this category.

C(flexible pavement) = Area cracking, in square feet per 1,000 square feet or surface area, which has progressed into a definite pattern joined in both directions.

P(flexible pavement) = Repair of the surface either by skin patching or deep patching, in square feet per 1,000 square feet of surface area.

$\overline{RD}$ = Average rut depth of both wheelpaths, in inches, measured at the center of a 5-ft span in the most deeply rutted part of the wheelpath. The measurements are made at 20-ft intervals on long sections (over 500 ft) and at 5-ft intervals on short sections.

The physical measurements useful in formulating a PSI have been as follows:

1. Mathematical functions of wheelpath profile.
2. Responses of vehicles to wheelpath roughness.
3. Pavement rutting.
4. Physical damage.

It should be noted that certain mathematical functions of these measured variables, combined in a multiple regression, satisfactorily predict PSR. However, these measured variables only approximate the over-all three-dimensional profile of a pavement. Other functions, or more complete three-dimensional profiles, might yield statistically better predicitions of PSR.

The roughometer essentially measures the response of a vehicle to wheelpath roughness. Therefore, as could be expected, its output is correlated with PSR. The serviceability rating sessions from which data were obtained to relate present serviceability to physical measurements are described by Carey and Irick (11). During two of the sessions the AASHO roughometer was used to obtain physical measurements. Figures 3, 4, 5 and 6 show the associations between average wheelpath slope variance ($\overline{SV}$), average wheelpath roughness ($\overline{AR}_{10}$), and present serviceability rating (PSR).

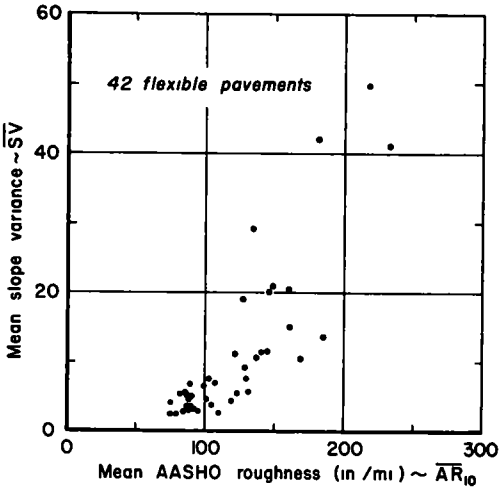

Figure 3. Slope variance vs roughness.

Analyses of these data show that there is a higher statistical association between PSR and log $(1 + \overline{SV})$ than there is between PSR and log $\overline{AR}_{10}$. However, although log $\overline{AR}_{10}$ does not explain as much of the variation in PSR as log $(1 + \overline{SV})$, it does explain a significant amount if the hypothesis of no association is used. Therefore, the roughometer is an instrument which can be used to predict serviceability.

USE OF ROUGHOMETER AT ROAD TEST

Modifications

Due to the widespread use of the roughometer, one was purchased for use at the Road Test. Ordinarily the BPR roughometer is not used on pavements as short as Road Test sections which vary in length from 100 ft to 240 ft. On a 100-ft section the standard counter, which counts in inches, has a resolution of (5280/100) R = 52.8R inches per mile, where R is the roughness of the section in inches. On a 240-ft section the resolution is 22R inches per mile. These increments are not small enough for measuring small changes in the roughness of a short section. Additional error is encountered on short sections because of the 20-mph speed. At this speed it is difficult to mark the beginning and end of a section. To alleviate this problem, the operating speed was reduced to 10 mph and a digital output counter was constructed to record roughness in tenths of inches. A discussion of these changes follows:

Speed. The dynamic characteristics of the roughometer vary with speed. This variation has been studied at the AASHO Road Test. The results (Fig. 7) show that the maximum recorded roughness occurs at approximately 8 mph. At slower speeds the

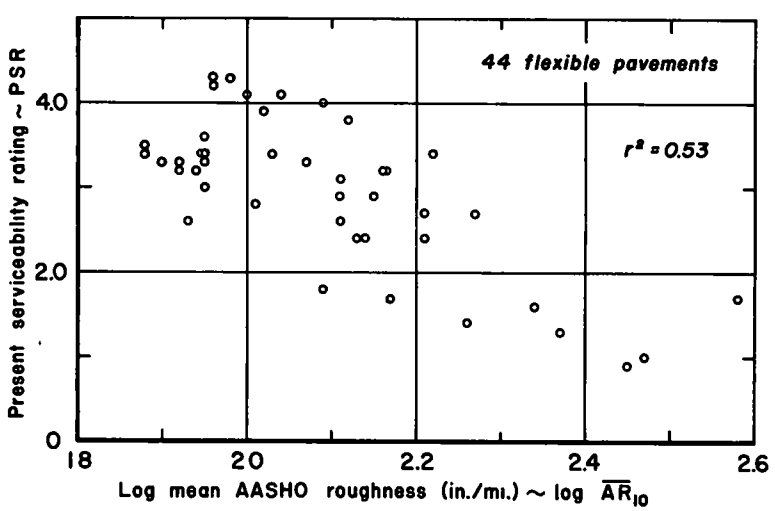

Figure 4. Present serviceability rating vs log mean AASHO roughness.

instrument shows less reaction and at faster speeds the frequency response of the indicator is slower than the input. Other research has shown this same type of relationship between speed and indicated roughness (9). Furthermore, the roughness recorded at 10 mph is highly correlated with the roughness recorded at 20 mph, as shown in Figure 8. Knowing of this correlation, the roughness of short sections can be predicted. Comparisons can then be made with other roughometers run at standard speed (20 mph). From these considerations the 10-mph travel speed was selected for use at the Road Test.

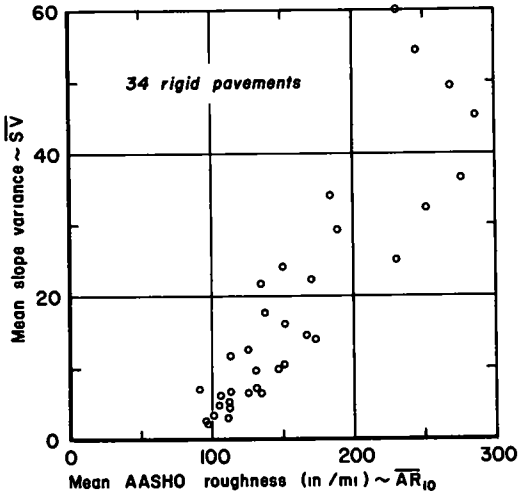

Figure 5. Mean slope variance vs mean AASHO roughness.

Counter System. Several methods were tested to record roughness in units smaller than 1 in. These methods included (a) decreasing the circumference of the input drum on the integrator from 6 in. to 1 in., thus increasing the counts on the six-lobe cam to six per inch; (b) magnifying the vertical displacement of the cable through a three-to-one pulley system, thus increasing the count to three per inch; and (c) replacing the cam and microswitch arrangement with a flexible shaft drive and a high-speed mechanical counter, thus increasing the count to ten per inch. All of these methods were unsatisfactory. The first two failed because the standard pulse counter has a maximum speed of about 600 counts per second. On rough pavements the increased count ratios often resulted in counts which exceeded the maximum speed of the counter. Method three failed because the force required to turn the shaft and the gears was excessive. Wear and slippage in the ball-clutch was inevitable.

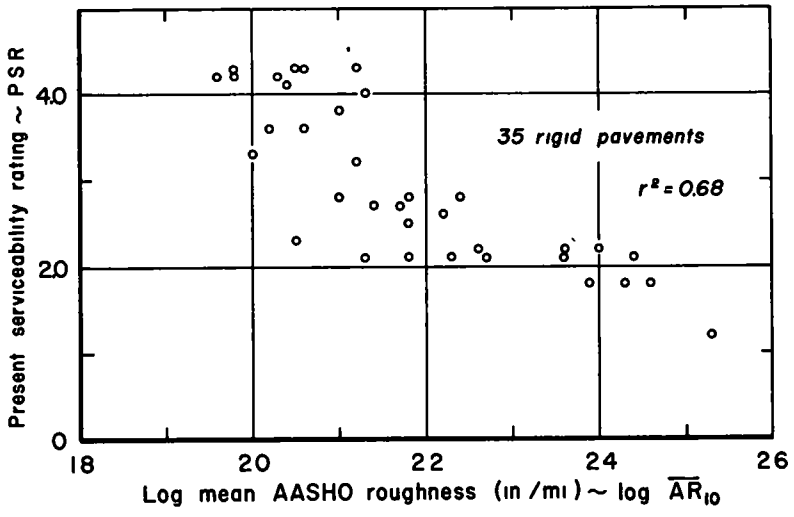

Figure 6. Present serviceability rating vs log mean AASHO roughness.

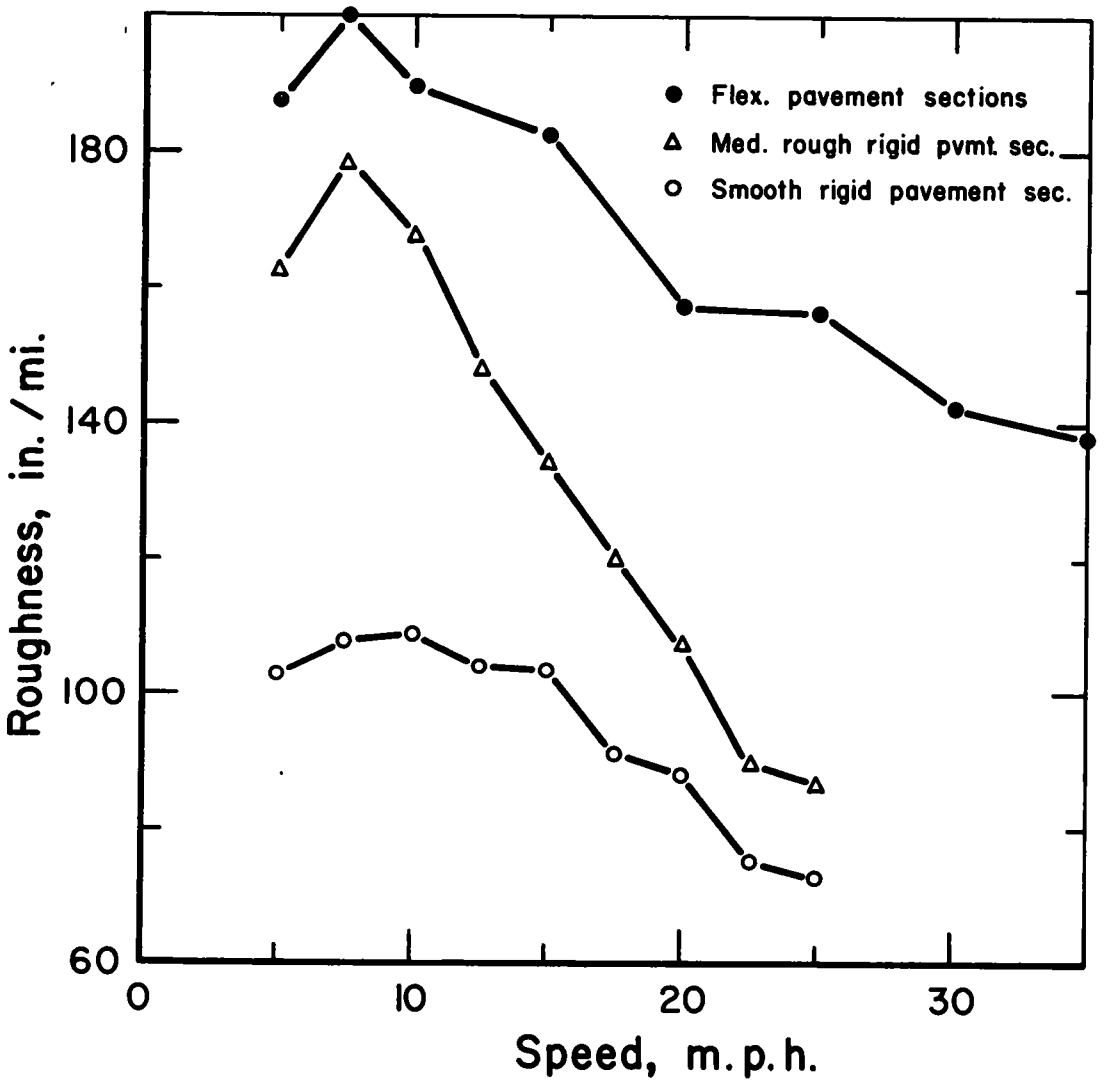

Figure 7. Indicated roughness vs speed.

To overcome the counter-speed deficiency, an electronic counter system was devised by Henry C. Huckins, Chief of the Instrumentation Branch at the Road Test. Two 5-in. diameter discs with 30 holes evenly spaced around their peripheries were attached to an extension of the integrator shaft (Fig. 9). The holes in one disc were offset an equal peripheral distance from the holes in the other disc. A fixed light source between the discs was used to impulse a pair of photocells as the light passed through the holes in the rotating discs. A flip-flop circuit was used to accept impulses from the two photocells alternately. This arrangement was necessary to prevent flutter in the impulse pickup if a hole stopped in line with the light source. The following relationship is true with this counter:

$$\frac{60 \text{ counts per rev.}}{6 \text{ in. per rev.}} = 10 \text{ counts per in.}$$

The counts are displayed on a visual decade counter and recorded by hand. Figure 10 shows the wiring diagrams for this counting system. This method proved to be the most satisfactory for the Road Test use. Automatic recording equipment should be considered for continuous operation over long periods of time.

With the exception of these two modifications, the AASHO roughometer (Fig. 11) and its method of operation at the Road Test were standard.

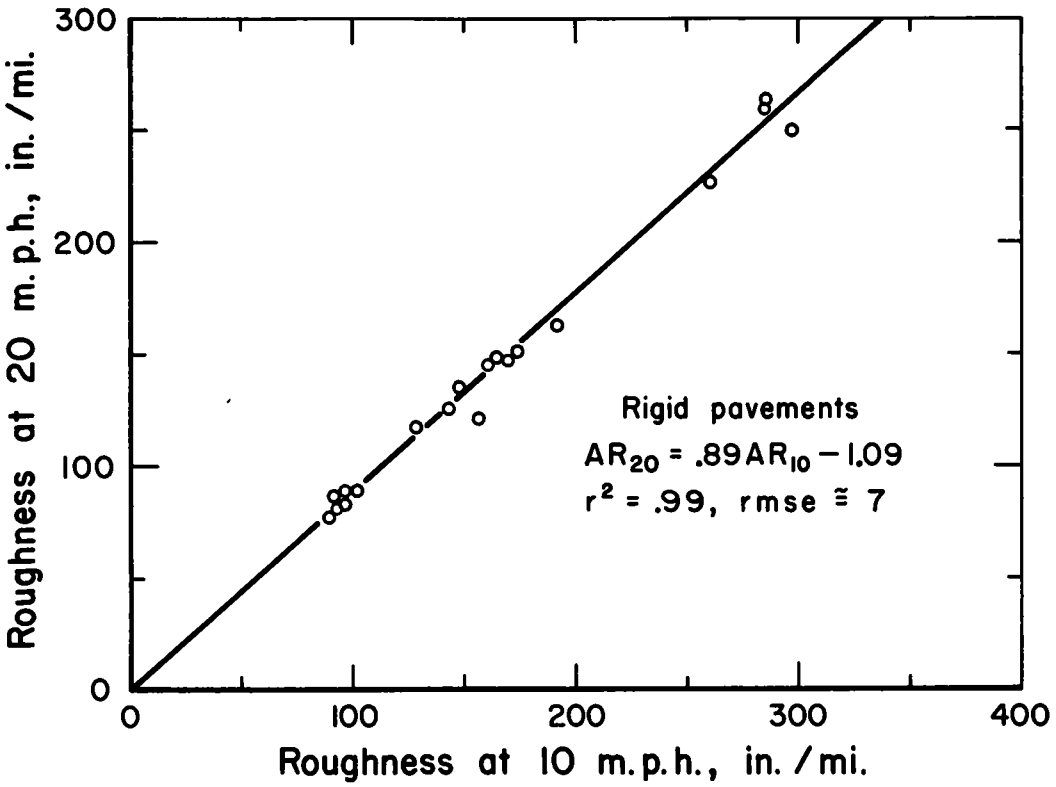

Figure 8. Roughometer speed correlation.

Roughness History of Test Section

The Road Test staff felt that it would be worthwhile to record the roughness of all test sections periodically with the roughometer in order to provide a record that could be used to compare the history of Road Test sections with pavements in service in the various States. Such comparisons could be helpful in adapting the results of the Road Test for future use. To fulfill this need, the roughometer was run over all sections on the Road Test every four to six weeks. The record of these runs will be made available along with other Road Test data for future comparison. Figures 12, 13, 14, and 15 show sample plots of AR_{10} vs axle applications for some failed and unfailed flexible and rigid test sections.

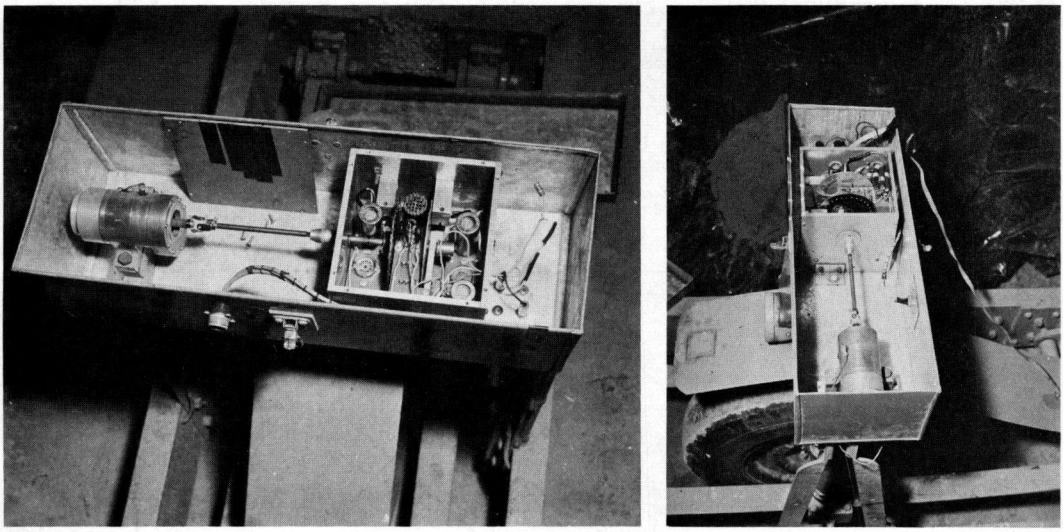

Figure 9. Side view (a) and top view (b) of electronic counter.

Rapid Determination of PSI

The main use of the roughometer at the Road Test was the rapid, efficient estimation of present serviceability. Normally the PSI was obtained biweekly using profilometer slope measurements. However, when a single section was in acute distress, it was easy to send the roughometer to make the measurements. It was primarily to provide this service that all development work was done on the roughometer.

At the beginning of the Road Test the following equations were used to rapidly estimate PSR:

$$PSI\ 113 = 11.92 - 3.95 \log \overline{AR}_{10} - 0.03\sqrt{C + P} \quad (1)$$

$$PSI\ 213 = 9.37 - 2.61 \log \overline{AR}_{10} - 0.12\sqrt{C + P} \quad (2)$$

It quickly became apparent that these equations were giving a biased estimate of serviceability and that a new correlation was necessary. The primary causes of this bias were (a) the development of the final electronic counter after the development of the serviceability equations, (b) the continual change of the dynamic response characteristics of the instrument as observed on a standard pavement, and (c) a discrepancy between log $(1 + \overline{SV})$ and log $\overline{AR}_{10}$ caused by the different numerical range of these variables. As two numbers become smaller the logarithm of their average moves closer to the logarithm of the larger number. Slope variance normally varied between 0 and 100, whereas AR_{10} varied between 70 and 400 in. per mile. Therefore, log $(1 + \overline{SV})$ reflected more the influence of a rougher wheelpath than did log $\overline{AR}_{10}$. This effect was most apparent and troublesome on sections where the two wheelpaths had widely different roughnesses.

These three characteristic differences between the profilometer and roughometer equations were remedied by, first of all, finding an equation

$$\hat{SV} = K_0 + K_1 AR_{10} \quad (3)$$

in which

$\hat{SV}$ = estimated slope variance;

AR_{10} = wheelpath roughness (inches per mile) of the AASHO roughometer at 10 mph; and

K_0, K_1 = constants determined by least squares regression analysis.

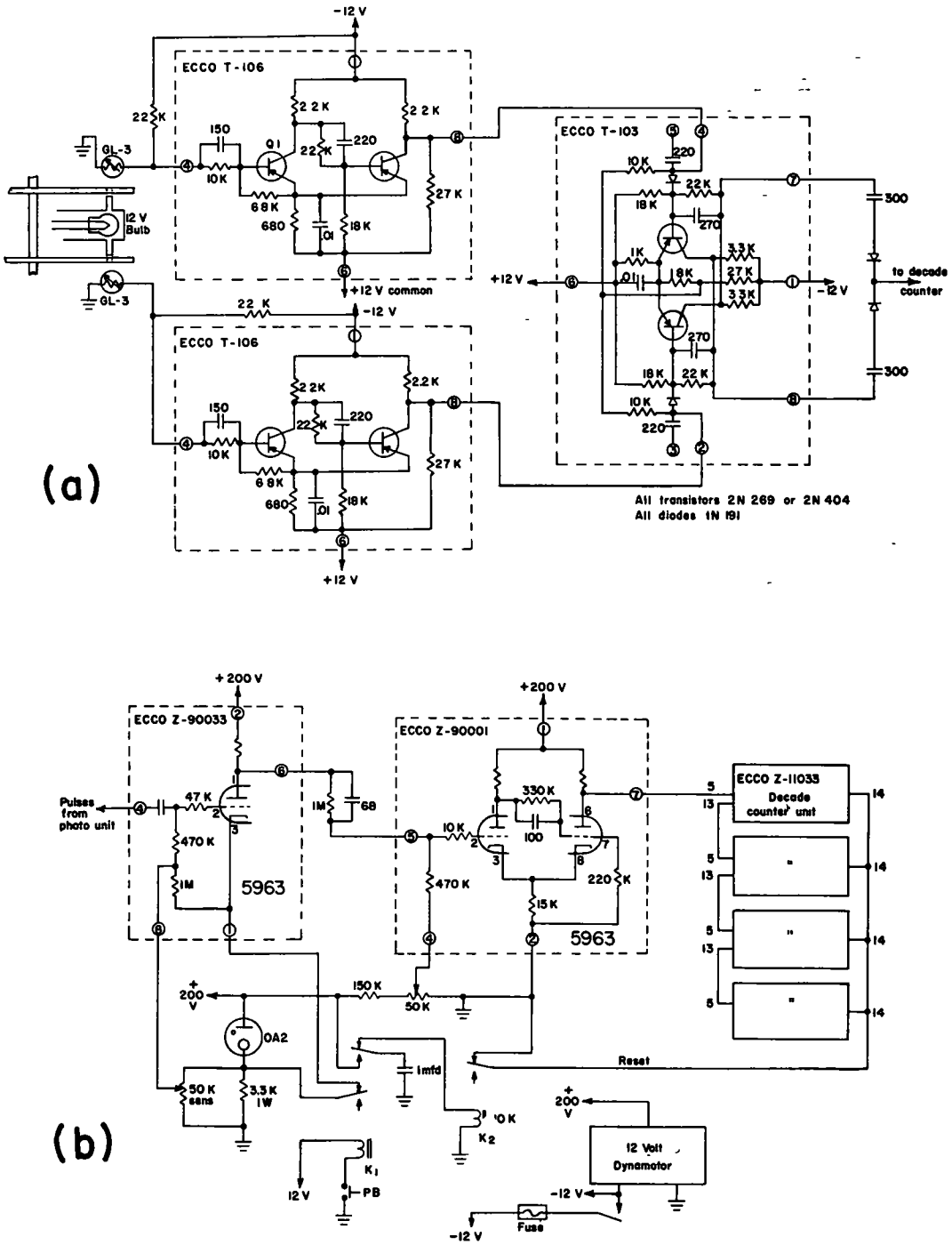

Figure 10. Wiring diagrams for roughometer (a) photo pickup and (b) counter chassis.

Eq. 3 was then substituted into the profilometer slope variance equation

$$PSI\ 211 = A_0 - A_1 \log (1 + \overline{SV}) - A_2 \sqrt{C + P} \quad (4)$$

to derive

$$PSI\ 214 = A_0 - A_1 \log (1 + K_0 + K_1 \overline{AR}_{10}) - A_2 \sqrt{C + P} \quad (5)$$

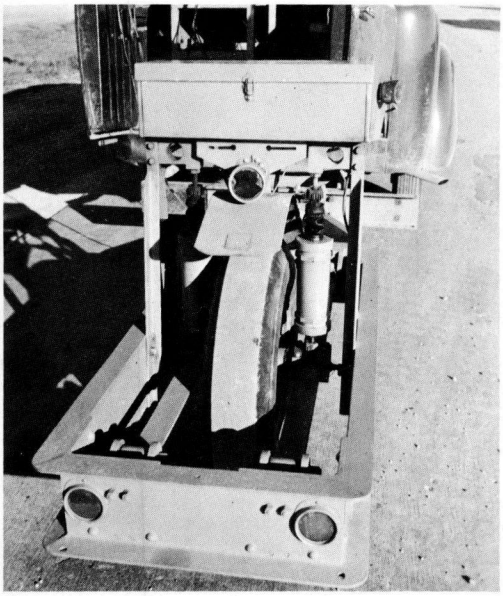

Figure 11. Rear view of AASHO roughometer.

To obtain estimates of K_0 and K_1 supplementary investigations were made. During a three-day period, in fact a normal period for taking pavement profiles, the profilometer and roughometer were run as coincidentally as possible over all Road Test sections. 210 rigid pavement and 150 flexible pavement sections were selected for this study. Wheelpath SV and AR_{10} were correlated for the 420 rigid and 300 flexible wheelpaths.

However, only about 5 percent of the rigid pavement wheelpaths were even moderately rough (i.e., had a slope variance larger than 10). A poor squared correlation coefficient ($r^2 = 0.47$) resulted, but the root mean square error (rmse = 13 slope units) was satisfactorily low. Because the resulting equation (PSI 214) better represented the correlations between PSR, $\overline{SV}$, and $\overline{AR}_{10}$ for short Road Test sections than did the rating session equation (PSI 213), it was used until more short, rough sections became available for correlation.

For flexible pavements the squared correlation coefficient was 0.31 and the root mean square error was 12 slope units. This correlation suffered from the same defect as the rigid correlation—there were relatively few rough sections available. Nothing more was done with a roughometer equation for flexible pavements because other methods of estimating PSR were available.

A more complete experiment was performed in the spring of 1960. Within a two-week period the profilometer and roughometer were run coincidentally on 20 rigid pavement sections. The sections were either 120 or 240 ft long. The roughness readings (AR_{10}) in inches per mile were corrected using the calibration concept explained in a later section. The corrected roughnesses and slope variances for the 40 wheelpaths are given in Table 2. The regression equation obtained is shown in Figure 16. It should be noted that both SV and AR_{10} were assumed to be measured with error. Therefore, there were two possible regression lines. Slope variance was regressed on AR_{10} inasmuch as this is the way the equation was used.

The equation,

$$\hat{SV} = 0.40\ AR_{10} - 34 \quad (6)$$

was substituted into the Road Test profilometer equation

$$PSI\ 221 = 5.41 - 1.80 \log(1 + \overline{SV}) - 0.09 \sqrt{C + P} \quad (7)$$

to obtain

$$PSI\ 225 = 5.41 - 1.80 \log(1 + 0.40\ \overline{AR}_{10} - 34) - 0.09 \sqrt{C + P} \quad (8)$$

or

$$PSI\ 225 = 5.41 - 1.80 \log(0.40\ \overline{AR}_{10} - 33) - 0.09 \sqrt{C + P} \quad (9)$$

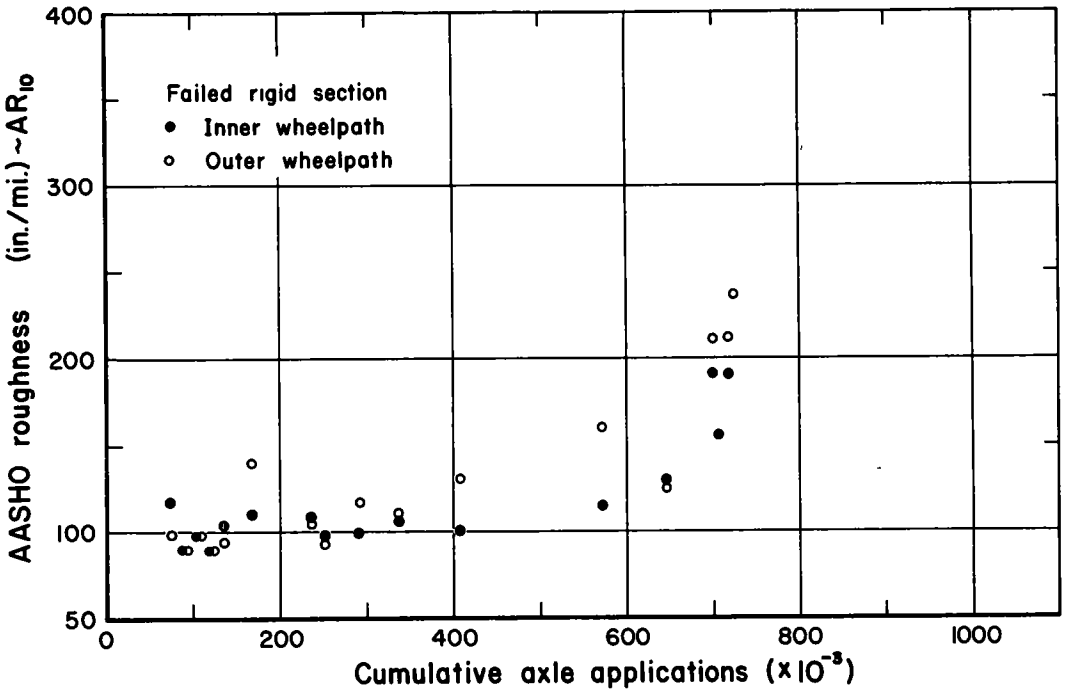

Figure 12. Roughness history, failed rigid section.

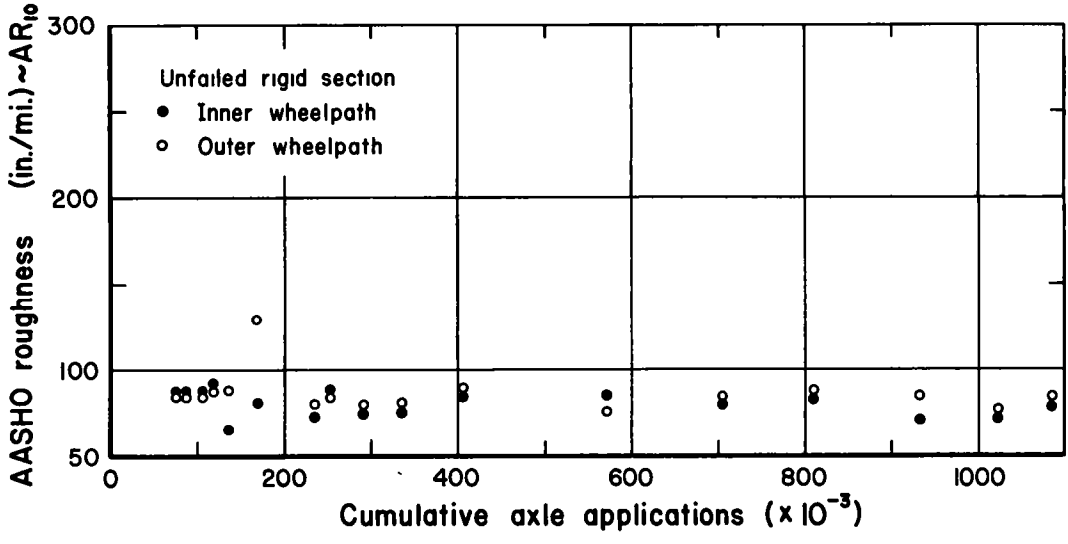

Figure 13. Roughness history, unfailed rigid section.

Eq. 9, which was used to determine serviceability indexes for sections as needed, has the advantage of giving, through use of the calibration concept, an unbiased estimate of serviceability—thus correcting all three discrepancies previously described.

This analysis assumes that the relationship between SV and corrected AR_{10} does not change significantly. However, this must be checked periodically. The results of several such checks on ¼-mi sections of highway pavements are given in Table 3.

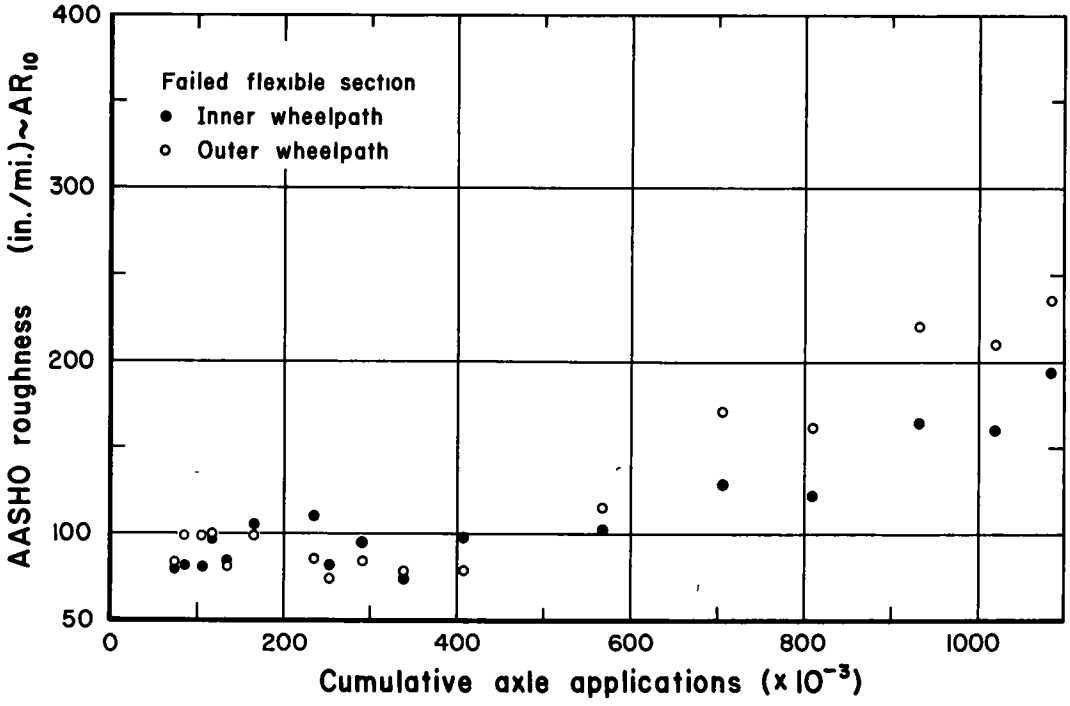

Figure 14. Roughness history, failed flexible section.

TABLE 2

DATA FOR 40 SELECTED RIGID PAVEMENT WHEELPATHS

Section Number	Section Length (ft)	Inner Wheelpath		Outer Wheelpath	
		Roughness (AR_{10})	Slope Variance	Roughness (AR_{10})	Slope Variance
226	120	106	4	114	14
384	120	97	1	99	5
402	120	117	15	154	26
490	120	136	17	224	56
506	120	96	4	141	31
643	120	123	24	134	31
Osage A	240	264	41	276	52
Osage B	240	286	87	262	85
490-a	120	158	22	229	100
494	120	132	17	174	39
506-a	120	95	3	161	26
226-a	120	117	4	180	28
234	240	109	3	183	28
643-a	120	117	25	132	24
650	120	139	21	152	20
704	120	108	4	200	87
Osage C	240	267	99	330	117
Osage D	240	262	45	237	46
Osage E	240	271	51	262	37
Osage F	240	267	99	266	82

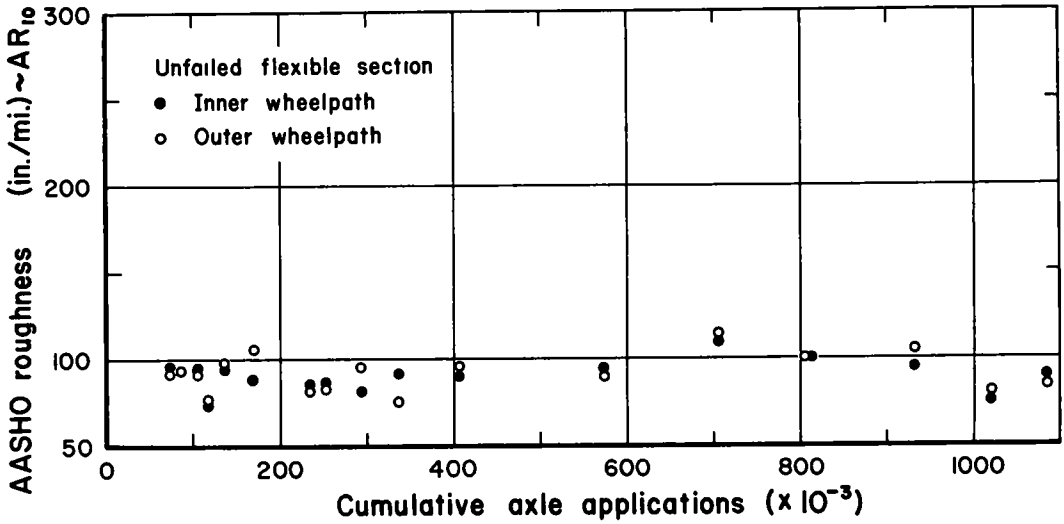

Figure 15. Roughness history, unfailed flexible section.

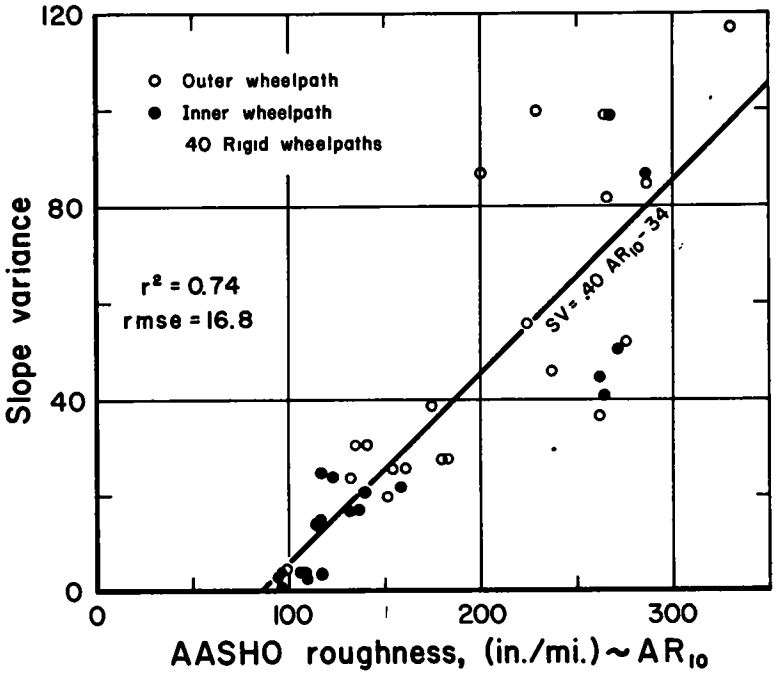

Figure 16. Slope variance vs AASHO roughness.

It should be noted that there are at least two reasons why slope variance and AR_{10} will never be perfectly correlated. These are:

1. The profilometer and roughometer probably do not measure the same elements of pavement roughness. The roughometer runs faster than the profilometer and has an entirely different tire and suspension system.

2. The instruments have different frequency response characteristics.

EVIDENCE OF VARIATION WITHIN THE ROUGHOMETER AND BETWEEN ROUGHOMETERS

Statistical Concepts

The roughometer may be used to estimate two variables—present serviceability rating and slope variance—associated with roughness. In such an estimating procedure two sources of variation, or effects, are encountered and estimated, as follows:

1. The amount of change in PSR or slope variance explained by or associated with a change in roughometer reading. In other words, this tells how well the rating of a pavement can be predicted with the roughometer.
2. Residual Variation. The amount of change in PSR or slope variance which cannot be explained by a change in roughometer reading. It can also be thought of as the deviations observed when a straight line is passed through a plot of PSR vs log $\overline{AR}_{10}$.

TABLE 3

EQUATIONS FOR UNCORRECTED AND CORRECTED ROUGHOMETER OUTPUT

Pavement Type	Date of Correlation	Uncorrected			Corrected		
		Equation	r^2	rmse	Equation	r^2	rmse
Rigid	May 5, 1960	$SV = 0\ 34\ UAR_{10} - 33\ 0$	0 97	6	$SV = 0\ 34\ AR_{10} - 33\ 0$	0.97	6
	Oct 13, 1960	$SV = 0\ 40\ UAR_{10} - 38\ 9$	0 91	8	$SV = 0\ 35\ AR_{10} - 33\ 2$	0 91	8
	Nov 16, 1960	$SV = 0.36\ UAR_{10} - 37\ 5$	0 92	7	$SV = 0\ 33\ AR_{10} - 32\ 5$	0 91	8

Residual variation, in addition, is made up of the following two different types of variation:

1. Inherent Variation. This variation is analogous to variation encountered when a coin is flipped and lands heads or tails. Inherent variation is caused by climatic conditions, chance physical changes in the instrument, and chance changes in the operation of the instrument. Chance errors in processing the data may also, for the current purposes, be classified as inherent variation.
2. Assignable Variation. That variation which is statistically significant compared to inherent variation. It may be caused by a physical change in the instrument (changing a tire, breaking a spring, etc.) or it may show up as an "out-of-control" point on a control chart with no detectable change in the instrument.

Inherent variation in indicated roughness may be estimated by measuring the roughness of an unchanging pavement. Assignable variation may also be detected with this technique. A control chart is a method of picturing these variations. A control chart uses the variation (e.g., range) between runs which are close together (15 min in this case) as a yardstick to discover excessive variation (out of control) between runs made hours or days apart. The control charts for four pavements of unchanging roughness are shown in Figure 17.

Physical Aspects

A major problem in estimating variation is to find an acceptable standard against which to check. At the Road Test two such "standards" were available: (a) mean panel rating and (b) output of the profilometer (SV). Through continuous comparison of the roughometer with these two "standards," it became apparent that the magnitude of the assignable variation in the roughometer could be great. For example, the early plots of roughometer history of some test sections might show wide fluctuation from smooth to rough and back to smooth in four to six weeks. In reality these changes did not occur, as was seen by comparison with the profilometer. This is best illustrated by the control charts in Figure 17, where out-of-control points occur many times.

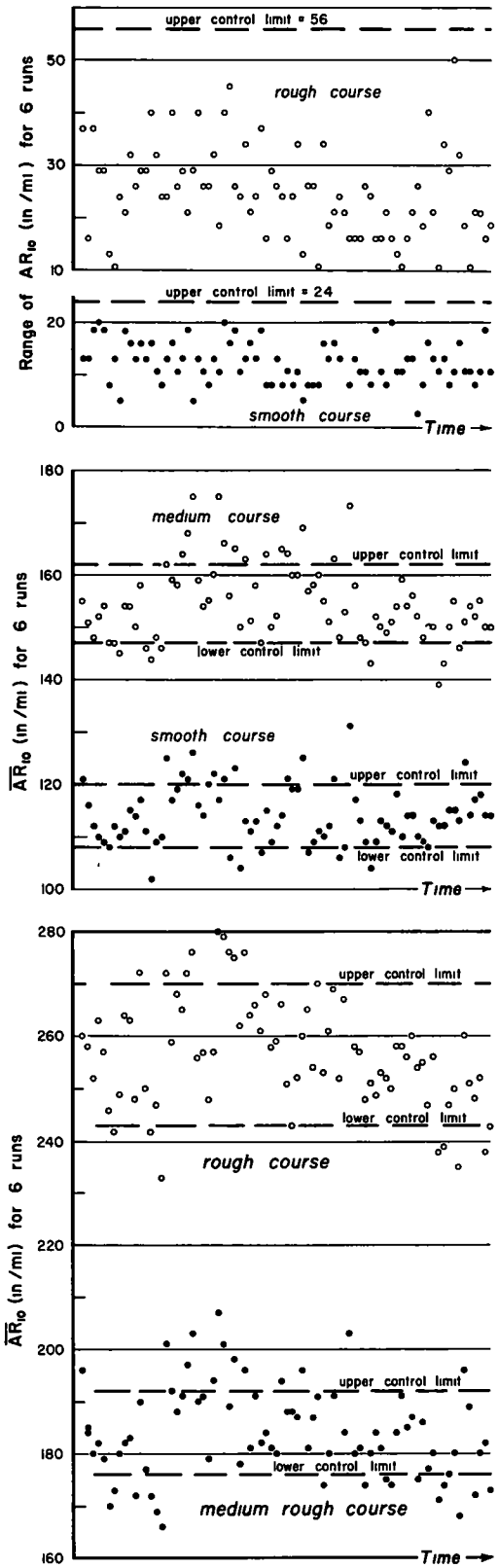

Figure 17. Showing (top) daily range chart for AR_{10}, (center) daily control chart for $\overline{AR}_{10}$, and (bottom) daily control chart for $\overline{AR}_{10}$.

In other words the apparent roughness of a section was significantly different from its true roughness.

Actual physical changes in the roughometer can result in radical changes in its output (e.g., the change from a treaded to a smooth tire resulted in a detectable change in indicated roughness, as did the introduction of the new counter system). General wear and tear on the instrument causes a gradual change in the output because the response of the instrument to roughness is an integral part of the output.

Variations Among Instruments

Standard plans for the BPR roughometer do exist (10); however, many organizations have made modifications, either major or minor, which affect the output of their device. Some example modifications include: (a) those made on the Road Test roughometer; (b) the Illinois Department of Highways transports and operates its device from a specially constructed trailer and records the results electrically through a potentiometer circuit; (c) Minnesota has made several modifications, including the addition of an electronic integrator (12). Comparison runs have been made with the AASHO, Illinois, Indiana, Michigan, and Missouri roughometers. These comparisons were run as part of correlation studies with the profilometer. In every case a formula was generated for determining the PSI with the various State instruments. A correlation equation was also generated comparing each instrument to the AASHO roughometer. These equations (Table 4) adequately illustrate the variation between roughometers.

CALIBRATION PROCEDURE TO MINIMIZE EFFECT OF ASSIGNABLE VARIATION IN THE ROUGHOMETER

Fundamental Calibration Concepts

One normally applied calibration procedure consists of checking a measuring device against a standard and then adjusting the device either mechanically or electrically until the output is equal to the standard by definition. A second common type of calibration is that applied to a device such as a proving ring. Several known loads are applied to the ring and the corresponding deflections are recorded. This procedure is repeated several times and the mean deflection for a given load is established. A best

fitting line is passed through the points and a calibration curve results. From this curve it is then possible to predict an unknown load from a known deflection of the ring. In this type of calibration, an accurate loading platen, such as a Universal testing machine, is used as the standard.

Dynamic Calibration

This applies to static measuring devices. Some instruments, however, are used to record dynamically, and their output depends not only on the accuracy of the static calibration, but also on the method and speed with which the devices react to dynamic excitation. For example, the leaf springs and the integrator of the roughometer can be calibrated separately for a known input of deflection or displacement. It is impossible from this static calibration, however, to predict the response under dynamic conditions. This situation is borne out by the variation in roughometers previously reported.

TABLE 4

EXAMPLES OF VARIATIONS BETWEEN ROUGHOMETERS

Instrument	Pav't Type	Date	Correlation with AR_{in} Equation	r^2	rmse	Correlation with AR_{so} Equation	r^2	rmse	Slope Variance Equation	r^2	rmse
Ind	Rigid	5/22/59	$AR_{in} = 1\ 59INR_{so} - 18\ 6$	0 95	17	$AR_{so} = 1\ 59INR_{so} - 39\ 7$	0 96	15	$SV = 0\ 44INR_{so} - 33$	0 87	7
	Flex		$AR_{in} = 1\ 73INR_{so} - 27\ 1$	0 92	22	$AR_{so} = 1\ 38INR_{so} - 23\ 3$	0 93	16	$SV = 0\ 54INR_{so} - 36$	0 76	13
Mo	Rigid	5/5/60	$AR_{in} = 1\ 45MR_{so} - 12\ 9$	0 99	13	$AR_{so} = 1\ 45MR_{so} - 35\ 0$	0 98	12	$SV = 0\ 48MR_{so} - 38$	0 92	8
	Flex		Insufficient data			$AR_{so} = 0\ 96MR_{so} + 11\ 9$	0 89	5	$SV = 0\ 44MR_{so} - 30$	0 70	4
Ill	Rigid	10/13/60	$AR_{in} = 1\ 43IR_{so} - 4\ 1$	0 98	12	$AR_{so} = 1\ 19IR_{so} + 2\ 2$	0 95	15	$SV = 0\ 50IR_{so} - 34$	0 88	10
	Flex		$AR_{in} = 1\ 45IR_{so} - 15\ 2$	0 92	28	$AR_{so} = 0\ 94IR_{so} + 17\ 7$	0 88	23	$SV = 0\ 18IR_{so} - 6$	0 70	8
Mich	Rigid	11/16/60	$AR_{in} = 0\ 90MiR_{so} - 9\ 4$	0 96	15	$AR_{so} = 0\ 67MiR_{so} + 6\ 1$	0 98	7	$SV = 0\ 29MiR_{so} - 36\ 0$	0 89	9
	Flex		$AR_{in} = 0\ 65MiR_{so} + 22\ 0$	0 77	26	$AR_{so} = 0\ 73MiR_{so} - 1\ 8$	0 90	18	$SV = 0\ 20MiR_{so} - 19\ 7$	0 82	7

Road Test Calibration

As the roughometer was used it became more apparent that the variability in indicated roughness made it impossible to record the actual roughness history of test sections with the desired degree of accuracy. It was clear that a method of dynamic calibration had to be developed if the roughometer was to become a useful tool at the Road Test.

Theoretically it is possible to calibrate the roughometer directly against the profilometer every day. This, however, would defeat the purpose of using the roughometer in the first place. It was decided instead to establish standard sections which presumably did not change during the two years of the Road Test. The true or "constant" roughness of these standard sections could be established through correlation between the roughometer, the profilometer and the rating panel. After that, it was possible to recalibrate the roughometer through another correlation on the standard section. Any time the results appeared questionable, a recorrelation with the profilometer could be run.

If the control charts show the roughometer to be out of control, the output must be adjusted to bring it into control. By trial and error, tire pressure, travel speed or mechanical parts can be adjusted until the roughometer reads the calibration course correctly. This would be a time consuming technique and concommitant changes in several parts would be unwise. In lieu of physical change, it is possible that mathematical correction of the output can be employed as in the case of the proving ring, which is calibrated periodically to insure against change due to material adjustment or fatigue. The principle is the same; the difference is merely one of time. The proving ring needs checking only every three or four months, whereas the roughometer should be checked daily.

Experimentation with the roughometer indicated that the variation on any one day might not be constant throughout the entire range of roughness. This indication, plus common sense, dictated that any calibration should investigate the entire range of interest (i.e., interpolation is normally more accurate than extrapolation). With this in mind, four calibration sections were set up: smooth (80 to 100 in. per mi), medium

(100 to 160 in. per mi), medium rough (180 to 200 in. per mi) and rough (230 to 250 in. per mi). The primary factor involved is that the course must remain constant in roughness. Secondly, the four sections should be adjacent for convenience. It was felt that these two conditions could not be met by utilizing naturally rough pavements with cracks, patches and faults. A pavement with bumps and potholes could be cast out of steel, but this is impractical. Instead a new, heavy-duty portland cement concrete pavement was chosen, over which no heavy traffic and minimum of light traffic was allowed to travel.

To simulate roughness, a series of artificial bumps were installed which could be standardized for use elsewhere. Bars of tempered aluminum were chosen as readily available and corrosion resistant. Bars of varying width and height were used to simulate various types and severity of bumps, and the proper number of bumps required to produce the range of roughness desired was installed (Figs. 18 and 19). A layout of the course as used is shown in Figure 20. It is understood that this type of course may not indicate the exact response of the roughometer to all types of roughness, particularly flexible pavements. However, the results thus far indicate that it does an acceptable job, because the amount of roughness is more critical than the character of the bumps. The mean or constant roughness for the calibration sections was established by averaging AR_{10} for 50 roughometer runs per section made within a period of five days. At the same time a correlation was made between AR_{10} and SV on 40 rigid pavement sections. Thus the constant values were obtained for a correlation between the profilometer and the roughometer.

Steps in Calibration Procedure:

1. Run the roughometer at least 1 mi to get the whole system warmed up and eliminate any flat spot developed in the tire.
2. Run the four calibration sections, which are laid out in random order, three times in each direction for a total of six readings on each course. (Using both directions is a convenience).
3. Average the six runs for each course and convert the four averages to AR_{10} (in. per mile).
4. Plot the average indicated roughness for each section against the constant roughness for that section (Fig. 21).
5. The least squares regression line for these points becomes a calibration or correction factor from which the output on any test section can be corrected to the standard (Fig. 21).

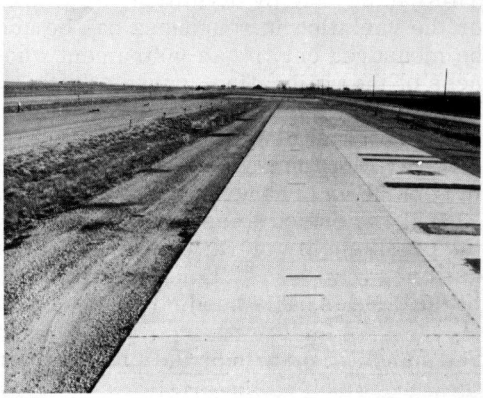

Figure 18. General view of calibration course.

Validity of the Calibration Procedure

The calibration procedure makes use of a well-known, well-defined statistical concept, regression analysis. This technique is such that the sum of squares of the observed points from the regression line is a minimum. Two assumptions are that the independent variable is fixed (that is, measured without error) and that the dependent variable is random (that is, measured with error). The slope variance and AR_{10} are both measured with error, so two regressions are possible.

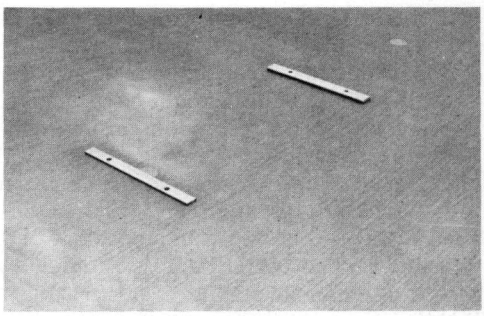

Figure 19. Aluminum Calibration Bar (1/2 x 2 x 24").

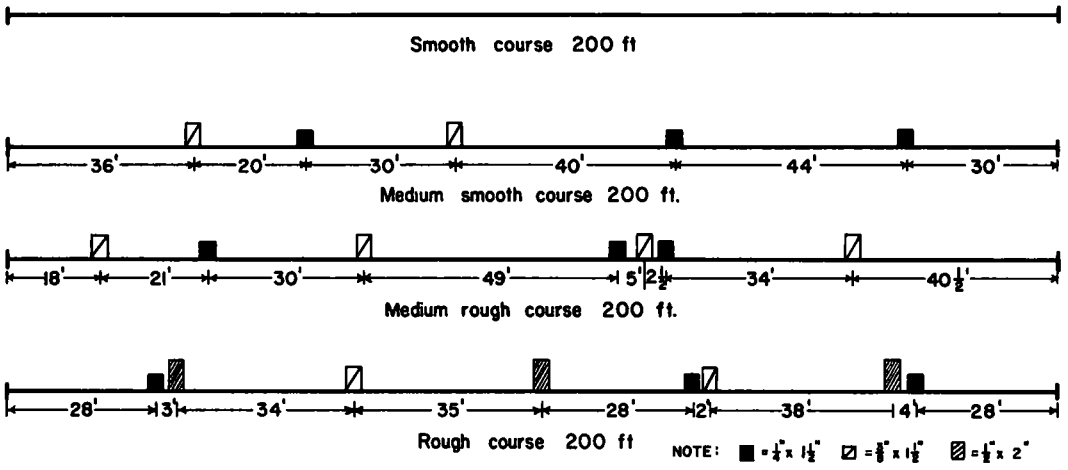

Figure 20. AASHO roughometer calibration course.

Only one was chosen, the regression of SV on AR_{10}, because this is the way the equation is used.

An assumption about the calibration course is that its roughness is not changing. This can be true by definition, as in the case of a meter bar in the Bureau of Standards, or the variation in roughness can be acceptably small. Any change in roughness could be measured only by an instrument whose variation is less than the variation in roughness of the calibration course. With a suitable calibration course, it should be possible over any period of years to correct any changes in the roughometer back to an initial condition when the actual roughness of the course was established. This technique gives a solid foundation for discriminating between changes in roughness of a pavement in service and changes in the roughometer.

If it is desired to estimate PSR or SV, the roughometer can be calibrated against the profilometer or rating panel each time it is run. However, as long as it can be assumed that the relationship between the original corrected roughness and PSR or SV still holds, this need not be done.

Setting up a Permanent Calibration Course

There are certain problems involved in setting up a calibration course for use outside the Road Test (e.g., the long life required). There is no previous experience to indicate exactly how to establish such a course. Possibly a continuously reinforced concrete pavement would do the job successfully. It would probably be helpful to locate the calibration course on a residential street, which would have some continuous traffic of low magnitude to serve as conditioning traffic. On the other hand, it may be that a specially constructed course not on any normal thoroughfare would best do the job. In any event, some detailed thought must be given to developing a permanent standard calibration course.

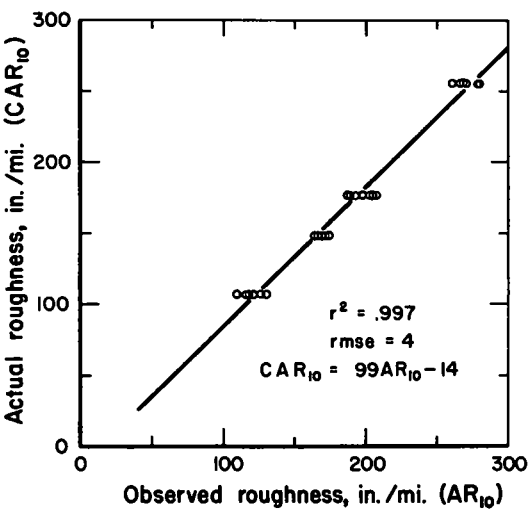

Figure 21. Sample roughometer calibration curve.

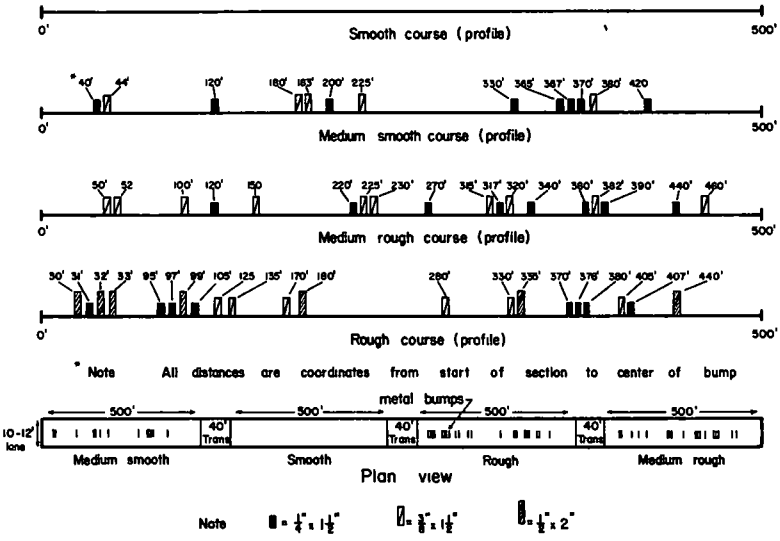

Figure 22. Proposed layout for permanent calibration course.

It would be necessary to check the roughness of the course periodically. A rod and level survey could be used to detect any general changes. Use of the present AASHO profilometer would be more precise. If the profilometer could be used every year or two to check the calibration course, the uniformity of the course could be assured or the calibration could be adjusted to the new level of roughness. A rating session could and should be held periodically to check the results of the roughometer output against an actual rating panel.

For setting up a calibration course, it is hoped that some standard set of bumps can be established in order to make it possible to standardize measurements between agencies without actually transporting the equipment. One possible layout for such a course is shown in Figure 22.

SUMMARY

Four roughometers have been used to establish PSI equations, either by direct correlation with the rating panel or by cross-correlation with the profilometer. These correlations all indicate a high degree of success in predicting PSI with reasonable accuracy, as shown in Table 4. The data were obtained in a relatively short time and thus were not affected greatly by long-term variation of the indicator. Table 3, however, shows the variation of the Road Test roughometer in predicting slope variance before and after application of the calibration-correction procedure. It can be seen that correcting AR_{10} results in more stable coefficients. Sufficient data are not available for a comparison on flexible pavements. More data will be obtained.

The roughometer is one answer to the problem of measuring roughness or performance. The Road Test profilometer, however, does a better job of predicting PSR as judged by correlation coefficients and residuals. This system is costly and requires detailed summary work. Other instruments are also being used, such as the California and Michigan profilographs. At present, development work is being done at the Road Test on a profilometer using a summary recording device which eliminates the necessity for reading charts. Such a development would greatly decrease the cost.

It is sincerely hoped that continued development will soon place at the disposal of the highway departments a more perfect means of measuring roughness. Until such devices become generally available, the BPR roughometer with a calibration procedure can do an acceptable job of estimating roughness or serviceability within a

reasonable budget. It is hoped that the roughometer will help expand the use of the pavement serviceability performance concept.

REFERENCES

1. Hogentogler, C. A., "Apparatus Used in Highway Research Projects." Bull. Nat. Research Council, 6:Pt 4, No. 35, 14-16 (Aug. 1923).
2. "An Instrument for the Measurement of Relative Road Roughness." Pub. Roads, 7:7, 144 (Sept. 1926).
3. Dana, H. J., "The Dana Automatic Recording Roughometer for Measuring Highway Roughness." Proc. HRB 12:Pt I, 362 (Dec. 1932).
4. Housel, W. S., and Stokstad, O. L., "Pavement Profile Surveys to Correlate Michigan Design Practice with Service Behavior." Transportation Inst., Univ. of Michigan, Ann Arbor.
5. Hveem, F. N., "Devices for Recording and Evaluating Pavement Roughness." HRB Bull. 264 (1960).
6. Buchanan, J. A., and Catudal, A. L., "Standardizable Equipment for Evaluating Road Surface Roughness." Proc. HRB, 29:621 (1940).
7. Moyer, R. A., and Shupe, J. W., "Roughness and Skid Resistance Measurements of Pavements in California." HRB Bull. 37 (1951).
8. Moyer, R. A., and Ahlborn, G., "New Developments in the BPR Roughness Indicator and Tests on California Pavements." HRB Bull. 139 (1956).
9. Holloway, F. M., "Road Roughness Measurements on Indiana Pavements." Thesis, Purdue Univ. (June 11, 1956).
10. "Manual of Information Regarding the Operation and Maintenance of the Public Roads Relative Road Roughness Indicator." Revised 1957, and Public Roads Dwgs. Nos. D413, D414, D415, D416, D417, D490, all as revised.
11. Carey, W. N., Jr., and Irick, P. E., "The Pavement Serviceability-Performance Concept." HRB Bull. 250 (1960).
12. Petrok, B. R., and Johnson, K. L., "Minnesota Modifications to BPR Roughness Indicator." HRB Bull. 139 (1956).

A Theory for Transforming AASHO Road Test Pavement Performance Equations to Equations Involving Mixed Traffic

F. H. SCRIVNER, Rigid Pavement Research Engineer, AASHO Road Test, Highway Research Board

The general equations to be developed at the AASHO Road Test relating pavement performance, pavement design and axle load will describe the behavior of these pavements when subjected to repeated applications of an axle load of a given type and weight. The theory proposed herein can be used to derive from each such equation a corresponding equation which, by hypothesis, will predict the behavior of these pavements if subjected to mixed traffic of any given composition. The theory may be of use in the application of Road Test results to the design of highway pavements to carry a known distribution of axle loads.

I. General Description, Application to Pavement Design

MIXED VS SINGLE-LOAD TRAFFIC

●INCLUDED in the official reports of the AASHO Road Test research will be two general pavement performance equations, one applying to flexible and the other to rigid pavements. Each equation will describe the performance of a pavement of a given design when subjected to repeated applications of an axle load of a given weight and type (single or tandem). Such an equation will be referred to hereafter as a "single-load" equation.

Neither of the two equations will directly yield information as to the behavior of pavements acted on by mixed traffic; that is, normal highway traffic composed of both single and tandem axles of a variety of weights.

Without question the usefulness of the forthcoming Road Test single-load equations will be enhanced if they can be transformed to multiload equations applicable to mixed traffic. A technique for accomplishing such a transformation is described herein so that interested highway engineers may, if they wish, apply the transformation procedure to the AASHO Road Test equations when they are published. In the interest of brevity, the procedure will be referred to hereafter as the "mixed-traffic theory."

DISCUSSION OF ASSUMPTIONS

Certain assumptions are being made in connection with the derivation of the AASHO Road Test single-load equations They may be stated as follows:

1. At the moment a new pavement is opened to traffic, damage to the pavement begins to accumulate, and continues to accumulate throughout the life of the pavement.
2. Accumulated damage can be measured, and the measurement expressed as a single number. (Occasionally the letter g will be used hereafter to represent this number.)
3. A mathematical relationship exists between accumulated damage on the one hand and pavement design, traffic and environment on the other.

The mixed-traffic theory rests on the preceding assumptions as well as two additional assumptions, the first of which is:

4. Two or more pavements with the same value of g will react to a given axle load in the same manner, if the pavements are of the same design and exist in the same environment.

Before stating the fifth assumption, certain implications of the first four will be illustrated by applying them to the graphical solution of a problem involving mixed traffic of a particularly simple kind. The problem may be stated as follows:

Two test pavements, designated Pavements 1 and 2, respectively, exist in the same environment and are of the same design. Pavement 1 has been extensively tested under an axle load, X, and Pavement 2 under an axle load, Y. Measurements of accumulated damage, g, have been made on both pavements at frequent intervals, and a curve of accumulated damage versus axle applications has been plotted for each pavement, as indicated by the solid lines in Figure 1.

A new pavement, designated as Pavement 3, is to be subjected to 1,000,000 applications of load X, followed by 1,000,000 applications of load Y. Pavement 3 is of the same design as Pavements 1 and 2, and exists in the same environment. Two questions bearing on the performance of Pavement 3 are to be answered by the use of the assumptions; namely, (a) how may a curve of g versus axle applications be plotted for Pavement 3, short of actually measuring the accumulated damage, and (b) what is the accumulated damage of Pavement 3 after the 2,000,000 applications?

For the first 1,000,000 applications, the required curve tracks the curve for Pavement 1, ending at point A (see Figure 1). From point A it parallels segment UV of the curve for Pavement 2 for the next 1,000,000 applications (AU and BV being parallel to the applications axis), and terminates at point B. The required curve is OAB and the accumulated damage is the g coordinate of point B. A comparison with the assumptions previously stated will show that the procedure followed in arriving at these answers is consistent with the assumptions.

But if the loads X and Y had been applied to Pavement 3 in the reverse order, curve OA'B' of Figure 1 would have resulted, and the total accumulated damage would have been the g corrdinate of point B' instead of B as in the previous case. It can be seen at once that both the shape and the terminal point of the damage-application curve for Pavement 3 depend upon the order in which the two loads are applied.

If, on the other hand, the curves of Pavements 1 and 2 had been straight lines, as shown in Figure 2, the curve for Pavement 3 would have been the connected line segments, OAB, if load X had been applied first, or OA'B, if load Y had been applied

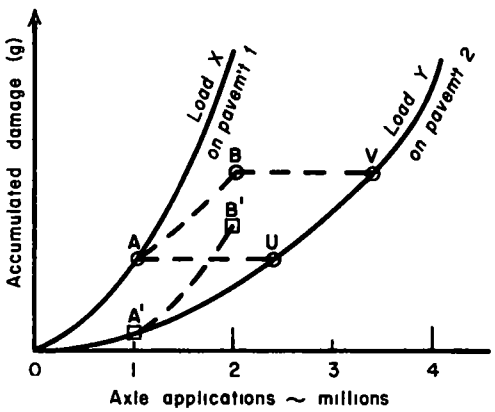

Figure 1. Accumulated damage as a curvilinear function of axle applications.

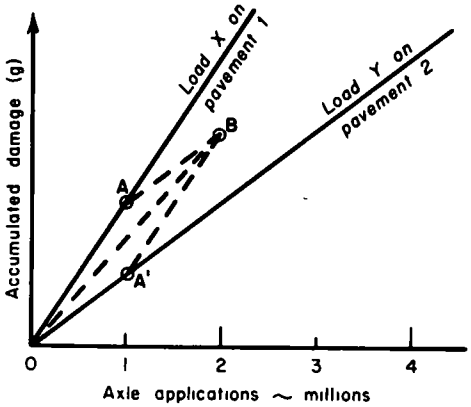

Figure 2. Accumulated damage as a linear function of axle applications.

first. For this case, then, the shape, but not the terminal point, of the damage-application curve depends upon the order in which the loads are applied.

One is forced to the intuitive conclusion that a complete and unique answer to a mixed-traffic problem cannot be obtained by a technique based on the first four assumptions alone; in addition, the order of application of the loads must be known or assumed. Rather than make such an assumption in solving practical problems, the issue is avoided by assuming, instead, that the traffic is well mixed. This, the fifth and last assumption may be stated as follows:

5. Whenever a pavement is subjected to more than one weight and/or type (single or tandem) of axle load, it is assumed that a representative sample of this traffic passes a fixed point in the pavement within a period of time so short, when compared to the life of the pavement, that this period may be treated as a differential quantity without excessive error, and the traffic is said to be "well mixed."

If the traffic applied to Pavement 3 had been well mixed, for the straight-line case illustrated in Figure 2 it can be shown that the curve of g versus applications for this pavement would have been the straight line OB. For a solution to the curved line case shown in Figure 1, it is necessary to turn to the calculus (see Part II).

All five assumptions may be summarized in a single equation which has proved to be useful in the development of the mixed-traffic theory. The equation is stated as:

The rate of change of accumulated damage, g, with respect to applications of an axle of a given weight and type = a mathematical function of pavement design, environment, axle weight, axle type, and g (1)

As will be shown later, any Road Test single-load equation can be reduced to the special differential form previously given. Given this differential relationship, development of the corresponding multiload equation is a matter of straight-forward mathematics (see Part II) which is deferred for the present, to pass, instead, directly to a discussion of the treatment of practical problems.

PRESENT SERVICEABILITY INDEX

A measure of pavement condition being extensively used at the AASHO Road Test is the present serviceability index, developed by the Road Test staff. This index has been described in detail elsewhere (1). For present purposes it is sufficient to report that its value depends primarily upon the relative smoothness of the pavement, and to a lesser extent upon the amount of visible damage — cracking, patching and rutting — present in the pavement. The index varies between a minimum value of zero for a very rough, badly damaged pavement to a maximum value of five for a perfectly smooth pavement with no visible damage.

The serviceability index, together with the design and load factors, will be the variables in the Road Test single-load equations now in the process of being derived. Some function of the serviceability index will be used as the measure of accumulated damages, g, required by the mixed-traffic theory, as illustrated in the following section.

A HYPOTHETICAL SINGLE-LOAD EQUATION

A hypothetical single-load equation applying to rigid pavement is given here, and its multiload version in the next section. These examples are given to illustrate, in one specific instance at least, the result of applying the mixed-traffic theory. The equations should not be construed as reflecting the results of the AASHO Road Test.

The single-load equation is

$$n = 10^{f}g \qquad (2)$$

in which n is the number of applications of an axle load of a specified type (single or tandem) and specified weight required to reduce the serviceability index of a given pavement from an initial value, P_0, to the value P; the accumulated damage, g, is

given by

$$g = \log_{10}(1 + P_o - P) \tag{3}$$

and f represents a function of slab thickness and axle load, and has separate forms for single and tandem axles. For single axles,

$$f = 7.0 + 0.5D - 0.8\sqrt{L} \tag{4a}$$

and for tandem axles,

$$f = 7.0 + 0.5D - 0.7\sqrt{L} \tag{4b}$$

In Eqs. 4a and 4b, D is the slab thickness in inches and L is the axle load in kips.

CORRESPONDING MULTILOAD EQUATION

Before writing the multiload version of the foregoing single-load equation (Eq. 2), it is necessary to provide an appropriate mechanism for characterizing the traffic. Accordingly, the following rules applying to the counting of tandem axles and steering axles are observed.

Tandem axles: The two closely-spaced axles forming a tandem unit are counted as a unit, and a tandem axle load is understood to be the total load carried by the two axles making up the unit.

Steering axles: Steering axles are counted on passenger cars, pick-ups, panel-bodied trucks, buses and empty trucks, but not on loaded trucks.

Except for those steering axles excluded under the rules, all the axles applied daily to one lane of a highway are divided into a specified number of categories, with each category containing a specified number of axles all of the same type (single or tandem) and approximately of the same weight.

Table 1 is an abbreviated example of such a subdivision of traffic. Here each category is given a sequential number, i, and it is presumed that every axle in the category can be represented by a specified load, L_i. The symbol, C_i, represents the proportion of all axles occurring in the ith category.[1] The total number of categories is represented by k and the number of single-axle categories by k'.

TABLE 1

EXAMPLE OF THE TRAFFIC PARAMETERS, L_i, C_i, k' and k

(Figures apply to one lane)

Axle Type	Category No., i	Load, L_i (kips)	No. Axles per Day	C_i
Single	1	6	300	0.30
	2	12	180	0.18
	3=k'	18	110	0.11
Tandem	4	24	230	0.23
	5=k	32	180	0.18
Total			1,000	1.00

With these definitions established and by application of the theory described in Part II, the multiload equation may be written as follows:

$$N = \frac{10^h g}{A + B} \tag{5}$$

in which g is defined by Eq. 3

$$h = 7.0 + 0.5D \tag{6}$$

$$A = \sum_{i=1}^{k'} C_i 10^{0.8\sqrt{L_i}} \tag{7}$$

$$B = \sum_{i=k'+1}^{k} C_i 10^{0.7\sqrt{L_i}} \tag{8}$$

and N represents the total number of applications of axles of all types and weights (excepting those steering axles excluded under the rules) required to reduce the present serviceability index from P_0 to P.

APPLICATION TO DESIGN OF PAVEMENTS

An illustration of the use of a multiload equation in pavement design is as follows:

Suppose that it is desired to compute, from Eq. 5, the thickness of concrete pavement required to carry the traffic given in Table 1 for a period of 20 years, the serviceability index meanwhile being permitted to drop from an initial value of 4.5 to a value of 2.5 (It being beyond the scope of this paper to discuss the effect of changes in environment or materials on pavement behavior, it is assumed that this pavement is to be constructed in the same environment and of the same materials as those existing at the Road Test.)

The computation is made as follows:

$$g = \log (1 + P_0 - P) = \log (1 + 4.5 - 2.5) = 0.47712$$

$$N = 20 \text{ years} \times 365 \text{ days} \times 1{,}000 = 7.3 \times 10^6 \text{ appl.}$$

$$A = 0.30 \times 10^{0.8\sqrt{6}} + 0.18 \times 10^{0.8\sqrt{12}} + 0.11 \times 10^{0.8\sqrt{18}} = 406$$

$$B = 0.23 \times 10^{0.7\sqrt{24}} + 0.18 \times 10^{0.7\sqrt{32}} = 2{,}259$$

$$7.3 \times 10^6 = \left(\frac{0.47712}{406 + 2259}\right) \times 10^h$$

Solving for h, and then for D (Eq. 6), one obtains D = 7.2 in.

LIMITATIONS ON APPLICATION

The general limitations on the application of AASHO Road Test single-load equations to pavement design have been discussed elsewhere (2). It need be added here only that these limitations apply also to the corresponding multiload equations. An additional limitation on the latter stems from the fact that they cannot be obtained directly from AASHO Road Test data, but arise instead from the indirect use of these data in the mathematical theory described in Part II. Thus predictions from the multiload equations can be checked directly only by comparing them with the observed behavior of highways subjected to mixed traffic of known composition.

Nevertheless, it is well known that practicing engineers find ways of overcoming the limitations both of theories and experiments and are able to turn the findings from both to practical advantage. Perhaps such will be the case in the present instance.

II. Mixed Traffic Theory

GENERAL MULTILOAD EQUATION

Consider a highway of design D, where D is some function of the pavement design parameters such as surface thickness, base thickness, etc. The design, materials

and environment are similar to those at the AASHO Road Test. The highway is subjected to mixed traffic.

The daily traffic in a selected lane of the highway is characterized by the parameters k, k', L_1 and C_1, defined in Part I under "Corresponding Multiload Equation." It is assumed that these parameters do not change with time; i.e., the traffic is well mixed.

Let N be the number of axles of all weights and types which have passed a fixed point in the lane from time t = O (taken as the time the highway was first opened to traffic) to time $t = t_1$. Let P be the present serviceability index at time $t = t_1$.

Let g(P) be any function, g, of P, continuous in the interval $O<P<P_O$, where P_O is the initial value of P (i.e., $P = P_O$ when N = O). As before, it is assumed that g is a measure of damage accumulated under traffic and therefore can be expressed as a function of the traffic passing over the pavement in the interval, t = O to $t = t_1$, and of the pavement design D, as follows:

$$g = \text{a function of the variables } N_1, N_2, \ldots, N_i, \ldots, N_k, \text{ and the constants } L_1, L_2, \ldots, L_i \ldots, L_k, \text{ and } D, \tag{9}$$

where $N_1 = C_1N$, $N_2 = C_2N$, ..., $N_i = C_iN$, ..., $N_k = C_kN$, and N_1 is the number of axles in in the ith category which have passed a fixed point in the lane from time t = O to $t = t_1$.

In the interval $t = t_1$ to $t = t_1 + dt$, there is a change, dg, in g, given by

$$dg = \frac{\partial g}{\partial N_1} dN_1 + \frac{\partial g}{\partial N_2} dN_2 + \ldots + \frac{\partial g}{\partial N_i} dN_i + \ldots + \frac{\partial g}{\partial N_k} dN_k \tag{10}$$

Because $N_i = C_iN$, it follows that $dN_1 = C_1dN$. Substitution of C_idN for dN_i in the ith term of Eq. 10, gives

$$dg = \sum_1^k C_i \frac{\partial g}{\partial N_i} dN \tag{11}$$

According to the differential equation given in Part I (Eq. 1), each partial derivative, $\partial g/\partial N_1$, appearing in Eq. 11 can be expressed as a function of L_1, D and g. Let this function be Y_1. Then

$$\frac{\partial g}{\partial N_1} = Y_1 = \text{a function of the constants } L_i \text{ and D, and the variable g} \tag{12}$$

It follows from Eq. 12 that the variables g and N of Eq. 11 can be separated. Consequently,

$$N = \int \frac{dg}{\sum_1^k C_1 Y_1} + \text{constant of integration} \tag{13}$$

in which each Y_i is to be derived from the appropriate Road Test single-load equation, and the constant of integration is to be found from the initial condition that $P = P_O$ when N = O.

DERIVATION OF THE RATE FUNCTION, Y_i

Either of the Road Test single-load equations now being derived can be expressed in the general form:

$$n_1 = X(L_1, D, g) \tag{14}$$

in which $X(L_1, D, g)$ is a function, X, of L_i, D and g and n_1 is the number of applications of the axle load, L_i, required to reduce the serviceability index of a pavement of design, D, from P_O to P. The function Y of L_i, D and g is defined as

$$Y(L_1, D, g) = \frac{\partial g}{\partial n_i} \tag{15}$$

in which L_i and D are regarded as constants. Then

$$Y(L_i, D, g) = \frac{1}{\frac{\partial X(L_i, D, g)}{\partial g}} \tag{16a}$$

or, in a briefer notation,

$$Y_i = 1 / \frac{\partial X_i}{\partial g} \tag{16b}$$

in which $Y_i = Y(L_i, D, g)$ and $X_i = X(L_i, D, g)$.

Thus the rate function, Y_i, appearing in the multiload equation (Eq. 13) may be readily obtained by differentiating the appropriate single-load equation with respect to g, and inverting the result, as indicated in Eq. 16b.

MULTILOAD EQUATION FOR SINGLE AND TANDEM AXLES

For a given pavement type (flexible or rigid) there will be two forms of the function X, say X' for single and X'' for tandem axles. Derived from these there will also be two forms of the function Y, say Y' for single and Y'' for tandem axles. In terms of Y' and Y'', Eq. 13 becomes

$$\hat{N} = \int_{k'}^{\quad} \frac{dg}{\sum_{1}^{k'} C_i Y'_i + \sum_{k'+1}^{k} C_i Y''_i} \tag{17}$$

in which the functions g, Y'_i and Y''_i are to be taken from the appropriate Road Test single-load equation.

AN APPLICATION

As an illustration the transformation procedure is applied to the hypothetical single-load equation for portland cement concrete pavement given in Part I and repeated here in a slightly different notation.

$$n_i = 10^{f_i} g \tag{18}$$

in which g is defined by Eq. 3 and n_1 is the number of applications of an axle load, L_i, required to reduce the serviceability index of a pavement of thickness D from an initial value P_o to the value P. For single axles,

$$f_i = 7.0 + 0.5D - 0.8\sqrt{L_i} \tag{19a}$$

and for tandem axles,

$$f_i = 7.0 + 0.5D - 0.7\sqrt{L_i} \tag{19b}$$

L_i is expressed in kips, and D in inches. According to Eq. 16b and 18,

$$Y_i = 10^{-f_i} \tag{20}$$

It follows from the definition of Y' and Y'', and from the two forms of the function f, that

$$Y'_i = 10^{-(7.0 + 0.5D - 0.8\sqrt{L_i})} \tag{21}$$

and

$$Y''_i = 10^{-(7.0 + 0.5D - 0.7\sqrt{L_i})}. \tag{22}$$

Noting that Y'_i and Y''_i are here independent of the variable g, one arrives at

$$N = \int \frac{dg}{\sum_{1}^{k'} C_1 Y_1' + \sum_{k'+1}^{k} C_1 Y_1''} = \frac{g}{\sum_{1}^{k'} C_i Y_1' + \sum_{k'+1}^{k} C_1 Y_1''} \qquad (23)$$

by performing the integration indicated by the general multiload equation for single and tandem axles.

That the constant of integration is zero follows from the condition that N and g are both zero when $P = P_O$; for, when $P = P_O$, N is zero by definition and $g = \log_{10}(1 + P_O - P_O) = 0$.

When the expressions for Y_1' and Y_1'' given in Eqs. 21 and 22 are substituted in Eq. 23, the result is the multiload equation (Eq. 5) already given in Part I.

The task of finding the multiload transform of Eq. 18 was made easier by the fact that n_i was linear in the damage function, g; thus, the integration of the general multiload equation offered no difficulty. On the other hand, it seems possible at the present writing that the final form of the Road Test single-load equations may not be linear in the damage function. In this event it may be necessary to employ some numerical technique in the integration of the general multiload equation.

REFERENCES

1. Carey, W.N., Jr., and Irick, P.E., "The Pavement Serviceability-Performance Concept." HRB Bull. 250 (1960).
2. "The AASHO Road Test: History and Description of Project." HRB Special Report 61A (1961).

Skid Studies at the AASHO Road Test

REX C. LEATHERS, Engineer of Special Assignments, AASHO Road Test, Highway Research Board, and R. IAN KINGHAM, Official Observer (AASHO Road Test) for the Canadian Good Roads Association

A series of six studies conducted periodically throughout the traffic testing period on the AASHO Road Test offered the opportunity to relate the effect of a number of variables on skidding resistance. The design of the skid resistance experiment and the controlled features of the test road made possible the isolation of these variables.

Various plots, diagrams and charts show the effect on the coefficients of friction of number of load applications, magnitude of load, number and spacing of axles, pavement design, and speed of the testing equipment. Certain seasonal or weather effects are also indicated.

● STUDIES of the resistance to skidding of wet and dry flexible-and rigid-type pavements of known design and traffic treatment were conducted at the AASHO Road Test in connection with the primary research.

The five traffic loops, each carrying a selected single- and tandem-axle load in the inner and outer lanes, respectively, were made up of test sections of variable design thicknesses for both the flexible and rigid pavements.

Design variables for the flexible pavement sections were subbase thickness, base base thickness, and surfacing thickness; those for the rigid pavement sections were subbase thickness, surfacing thickness, and surfacing reinforcement. All materials, mix designs, and construction procedures were identical for all test sections.

The uniformly constructed test facility and the controlled test traffic operations offered a unique opportunity to observe the effects of the axle load and arrangement (single or tandem), axle load applications, pavement design and skid test vehicle speed on the skid resistance of the pavement surface.

The experiment included 80 test sections of different design. Sixteen sections, eight in each traffic lane, were selected from each of the five test loops. Six series of tests are reported in this paper. The first was completed prior to any traffic operations and the sixth after more than 1,000,000 loaded axle applications.

The main part of this report is a general discussion of the experiment and the observations. The details of the experiment are included in the appendix. The test data may be obtained in tabular form from the Highway Resarch Board at the cost of reproduction (AASHO Road Test Data System 4340).

THE EXPERIMENT

Five controlled variables were selected for evaluation in this experiment. They were pavement design, axle load and arrangement (Tables 1 and 2), speed of the skid test equipment, pavement surface condition, and load applications. An outline of the first three variables is given in Tables 1 and 2.

In addition to the main experiment, a partial study of the effect of the condition of the pavement surface (wet or dry) was included. All of the sections noted in Tables 1 and 2 were tested in the wet surface study, but only selected sections were included in the dry surface study.

TABLE 1

OUTLINE OF SKID STUDY[a], FLEXIBLE PAVEMENTS

Axle Load[b] (kips)	Subbase (in.)	2-Inch Surface		3-Inch Surface		4-Inch Surface			5-Inch Surface			6-Inch Surface		
		3-In. Base	6-In. Base	3-In. Base	6-In. Base	3-In Base	6-In. Base	9-In Base	3-In. Base	6-In Base	9-In. Base	3-In. Base	6-In. Base	9-In Base
2KS	0	x	x	x	x	-	-	-	-	-	-	-	-	-
	4	x	x	x	x	-	-	-	-	-	-	-	-	-
6KS	0	x	x	x	x	-	-	-	-	-	-	-	-	-
	4	x	x	x	x	-	-	-	-	-	-	-	-	-
12KS	4	-	-	x	x	x	x	-	-	-	-	-	-	-
	8	-	-	x	x	x	x	-	-	-	-	-	-	-
24KT	4	-	-	x	x	x	x	-	-	-	-	-	-	-
	8	-	-	x	x	x	x	-	-	-	-	-	-	-
18KS	8	-	-	-	-	x	x	-	x	x	-	-	-	-
	12	-	-	-	-	x	x	-	x	x	-	-	-	-
32KT	8	-	-	-	-	x	x	-	x	x	-	-	-	-
	12	-	-	-	-	x	x	-	x	x	-	-	-	-
22.4KS	8	-	-	-	-	-	x	x	-	x	x	-	-	-
	12	-	-	-	-	-	x	x	-	x	x	-	-	-
40KT	8	-	-	-	-	-	x	x	-	x	x	-	-	-
	12	-	-	-	-	-	x	x	-	x	x	-	-	-
30KS	12	-	-	-	-	-	-	-	-	x	x	-	x	x
	16	-	-	-	-	-	-	-	-	x	x	-	x	x
48KT	12	-	-	-	-	-	-	-	-	x	x	-	x	x
	16	-	-	-	-	-	-	-	-	x	x	-	x	x

[a] All sections tested at 30 mph, underline sections at 10, 30, and 50 mph.

[b] S = single axle, T = tandem axle.

TABLE 2

OUTLINE OF SKID STUDY[a], RIGID PAVEMENTS

Axle Load[b] (kips)	Subbase (in.)	3.5-In Surface		5.0-In. Surface		6.5-In Surface		8.0-In. Surface		9.5-In. Surface		11.0-In. Surface	
		Non-Reinf.	Reinf	Non-Reinf	Reinf.	Non-Reinf	Reinf.	Non-Reinf.	Reinf.	Non-Reinf.	Reinf.	Non-Reinf.	Reinf.
2KS	3	x	x	x	x	-	-	-	-	-	-	-	-
	6	x	x	x	x	-	-	-	-	-	-	-	-
6KS	3	x	x	x	x	-	-	-	-	-	-	-	-
	6	x	x	x	x	-	-	-	-	-	-	-	-
12KS	3	-	-	x	x	x	x	-	-	-	-	-	-
	6	-	-	x	x	x	x	-	-	-	-	-	-
24KT	3	-	-	x	x	x	x	-	-	-	-	-	-
	6	-	-	x	x	x	x	-	-	-	-	-	-
18KS	3	-	-	-	-	x	x	x	x	-	-	-	-
	6	-	-	-	-	x	x	x	x	-	-	-	-
32KT	3	-	-	-	-	x	x	x	x	-	-	-	-
	6	-	-	-	-	x	x	x	x	-	-	-	-
22.4KS	3	-	-	-	-	-	-	x	x	x	x		
	6	-	-	-	-	-	-	x	x	x	x	-	-
40KT	3	-	-	-	-	-	-	x	x	x	x	-	-
	6	-	-	-	-	-	-	x	x	x	x	-	-
30KS	3	-	-	-	-	-	-	-	-	x	x	x	x
	6	-	-	-	-	-	-	-	-	x	x	x	x
48KT	3	-	-	-	-	-	-	-	-	x	x	x	x
	6	-	-	-	-	-	-	-	-	x	x	x	x

[a] All sections tested at 30 mph, underlined sections at 10, 30, and 50 mph.

[b] S = single axle, T = tandem axle.

Design variables for the rigid pavement sections included two levels of surfacing and subbase thickness for each axle load and arrangement. To insure a reasonably balanced experiment for the duration of the Road Test the higher levels of design for each axle load were selected for study. The possible effect of the joint spacing was observed by the inclusion of both reinforced and plain concrete sections. Transverse contraction joints, formed by sawing, were spaced at 40 ft in reinforced sections and 15 ft in nonreinforced sections.

Similarly, the design variables for the flexible pavement sections included two highest levels of surfacing, base and subbase thickness for each axle load and arrangement.

The possible effect of the speed of the skid test vehicle was investigated in a partial study. All sections given in Tables 1 and 2 were included in the main experiment at 30 mph. In addition, those underlined were tested at 10 and 50 mph.

The most pronounced effect on the skid resistance coefficients was anticipated to be as a result of the accumulation of load applications. To determine this possible effect, the six series of tests were scheduled at fairly regular intervals during the test

traffic phase of the Road Test. The date of each series and the accumulated axle applications are given in Table 3.

TABLE 3

HISTORY OF AXLE APPLICATIONS

Series	Date	Accum. Axle Applications
1	Fall 1958	0
2	Spring 1959	108,000
3	Summer 1959	232,000
4	Spring 1960	586,000
5	Summer 1960	851,000
6	Fall 1960	1,101,000

A total of 6 single- and four tandem-axle loads was selected. The pavement designs for the single-axle loads of 2, 6, 12, 18, 22.4 and 30 kips and for the tandem-axle loads of 24, 32, 40 and 48 kips are given in Tables 1 and 2.

Other variables in the test could be classified as uncontrolled. Of these the most important appeared to be the environmental conditions. Among the environmental conditions measured independently were the air temperature, pavement temperature, and the rainfall preceding the test series. Air temperature varied between 36 and 94 F, pavement temperature between 37 and 123 F, and the two-week rainfall prior to the test series varied from 0.36 to 1.77 in.

The dry surface studies were run in three series of tests. The sections selected for this study were those chosen for the special speed study and were in traffic lanes carrying vehicles with axle loads of 22.4 kips single and 40 kips tandem.

The mix designs, method of placement and finishing techniques of the surfacing courses, either asphaltic or portland cement concrete, were essentially the same throughout the Road Test. Figure 1 is a typical example of the surface texture of the two pavement types at the start of test traffic.

The General Motors skid trailer (Fig. 2) was used in all test series of the skid study. The skid resistance is described by the coefficient of friction and is computed from the known characteristics of the testing equipment and the measured force required to pull the trailer with the wheels locked (1).

TEST RESULTS

Despite rigid inspection of the finishing operations for both types of pavements, substantial differences were noted in the coefficients of friction before the start of test traffic. Values of the coefficients of friction for the flexible pavement sections ranged from 0.76 for those designed for the 2- and 6-kip single-axle loads to 0.67 for those designed for the 40-kip tandem-axle loads. For the rigid pavement sections the range was from 0.70 for those designed for the 2- and 6-kip single-axle loads to 0.60 for those designed for the 22.4- and 30-kip single-axle loads. Thus, the initial coefficients of friction for both rigid and flexible pavements were higher for those sections designed for the 2- and 6-kip single-axle load sections. An explanation of this might be in the lighter roller weights used on the thinner designs for the flexible sections and in the stiffness of the mix required for the rigid sections.

Standard deviations of the mean coefficients of friction for the first series were 0.030 for all flexible pavement sections and 0.050 for all rigid pavement sections. The initial variations between the pavements for each load were observed throughout the testing period. However, variations within sections for the same load were reduced considerably with each series of tests. Standard deviations for the last series of tests were 0.020 for all flexible pavement sections and 0.025 for all rigid pavement sections. The test indicated the replication error of the testing equipment was within 0.020 units.

Effect of Pavement Design

The design variable was investigated because of the belief that the increasing roughness of the thinner pavement designs might introduce an increase in the coefficients of friction. With reference to Tables 1 and 2, the range of design thicknesses incorporated within this experiment is from 5 to 31 inches for the flexible pavement sections and from 6.5 to 17.0 inches for the rigid pavement sections.

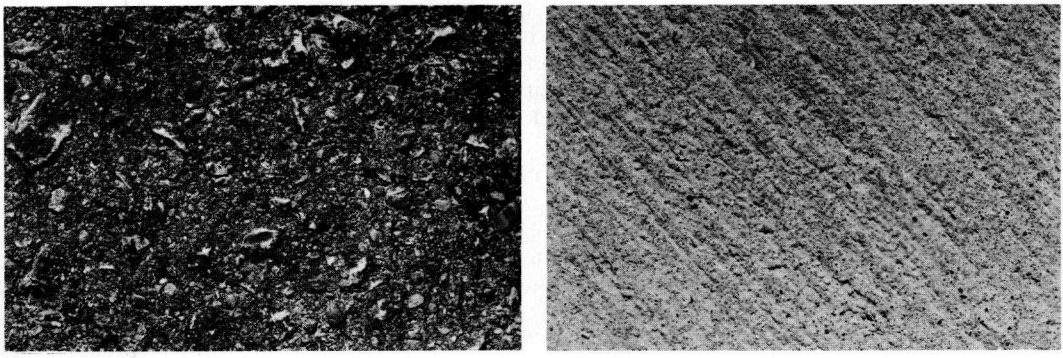

Figure 1. Typical example of surface texture of (left) asphaltic concrete and (right) portland cement concrete at start of test traffic.

Table 4 allows comparison of mean coefficients of friction for wet pavements across the various design levels. Comparisons can be made to examine the effect of surfacing, base and subbase thicknesses and the effect of joint spacing in the portland cement concrete on the coefficients of friction. Results from the six test series were combined to develop these means.

For example, the greatest difference between the coefficients for the effect of the concrete reinforcement or joint spacing is 0.01 units. This difference, occurring in all loops, is well within the replication error of the experiment and cannot be considered significant.

Similar comparisons of the effect of the design variables on the coefficients of friction indicated quite clearly that, within the limits of the study, pavement design has no significant effect on the resistance to skid.

Effect of Axle Load and Arrangement

The effect of axle load and axle arrangement (single or tandem) on the pavement surface wear is shown in Figures 3 and 4. The reduction of the coefficient of friction is plotted against wheel load with the reduction plotted upwards, indicating a decrease in the coefficient. Each plotted point is the mean of 48 tests, six series on the eight sections for each load. There appears to be a clear distinction between the single-axle loads and tandem-axle loads, the tandem-axle loads causing a greater reduction in the coefficients of friction.

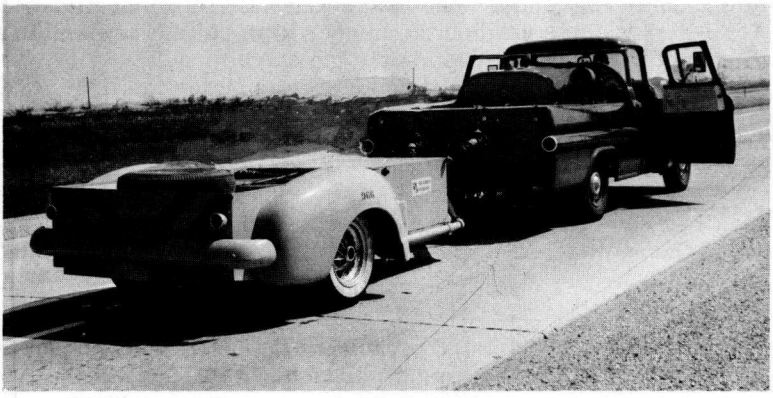

Figure 2. General Motors skid trailer.

There is little indication of any over-all trend that would suggest a reduction of the coefficient of friction due to an increase in load in the lighter axle loadings. However, there is a slight indication that this may be true for the heavier axle loadings. For both the flexible and rigid pavements a greater reduction of the coefficient of friction was experienced with the 30-kip single- and 48-kip tandem-axle loads than for the 22.4-kip single- and 40-kip tandem-axle loads.

The high reduction in the coefficient of friction for test sections designed for the 3-kip wheel load suggests a possible effect of the front axle. The only axle loads counted as axle load applications were those with the selected load. To keep the rate of selected load applications the same for pick-up trucks and tractor-trailer combinations, it was necessary to have double the number of vehicle trips carrying the 3-kip wheel load. The greater number of uncounted steering axles may account for the high reduction in the coefficient of friction.

Effect of Test Vehicle Speed

Figures 5 and 6 show the effect of the speed of the testing vehicle on the coefficient of friction measured on wet pavements. In each figure, the curves show, along with the mean relationships for all series of tests, the relationships when the test sections were newly constructed and at the end of the traffic testing period.

For each test series the results of the measurements on the 2-kip and 6-kip single-axle load sections were deleted because of incomplete data. Thus a point on the curve is the mean of 32 tests—four tests for each of the remaining loads. A point on the curve for all test series is the mean of 192 tests—four tests for each of the remaining loads for each series.

For all tests on wet pavements the measured coefficient of friction was substantially reduced with an increase in speed of 20 mph. The relationship appears to be curvilinear within the range of the test data. For tests on dry pavements the speed of the testing equipment had very little effect.

Dillard and Allen (2) have shown that for an excellent pavement the coefficient of friction was only slightly affected by the speed of the testing equipment, whereas for a poor pavement there was a substantial reduction. The curves for test series 1 and 6 (Fig. 5 and 6) clearly indicate that the condition of the pavements on the Road Test had little effect on the influence of the speed of the test vehicle.

Effect of Pavement Surface Condition

Figures 7 and 8 for the rigid and flexible pavement surfaces, respectively, show the effect of pavement surface conditions (wet or dry) on the coefficient of friction. Each point is the mean of four coefficients of friction of four test sections.

Dry tests show to a marked degree an increase in the coefficient for both pavement types. The over-all trend of the dry surface coefficient of friction is a decrease with the increasing load applications. Differences between axle loads and axle arrangements do not appear to influence the coefficient within the range of the tests. Also the seasonal variations do not appear to have any significant effect on the dry surface condition coefficients.

Effect of Axle Load Applications

With a range of loaded axle applications from 0 to 1,100,000 for all loads, the influence of the number of applications on the coefficient of friction was expected to be the most significant finding of this experiment.

As mentioned previously (see Table 3), the six test series were conducted as nearly as possible at regular intervals throughout the test traffic phase of the Road Test.

A typical set of data representing the change in coefficient of friction at 30 mph with increasing load applications for the 22.4-kip single-axle load is shown in Figure 9.

The over-all trend of the data is a decrease in the coefficient of friction with an in-

crease in axle applications. However, the coefficients show an increase for two periods: from the summer 1959 test series to the spring 1960 test series, and from the summer 1960 to the fall 1960 test series.

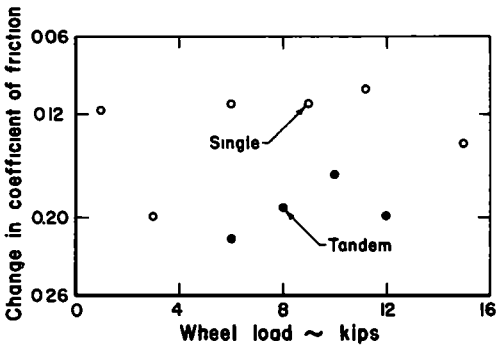

Figure 3. Influence of wheel load on rigid pavement coefficient of friction.

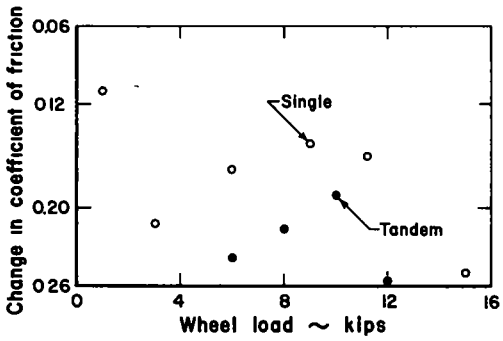

Figure 4. Influence of wheel load on flexible pavement coefficient of friction.

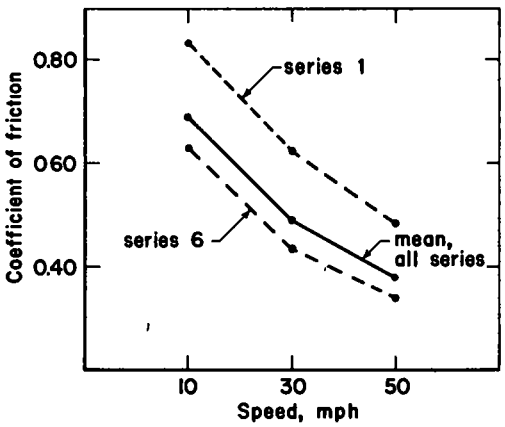

Figure 5. Influence of test vehicle speed on rigid pavement coefficient of friction.

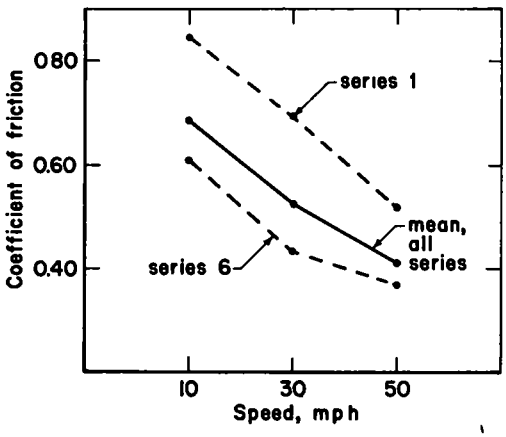

Figure 6. Influence of test vehicle speed on flexible pavement coefficient of friction.

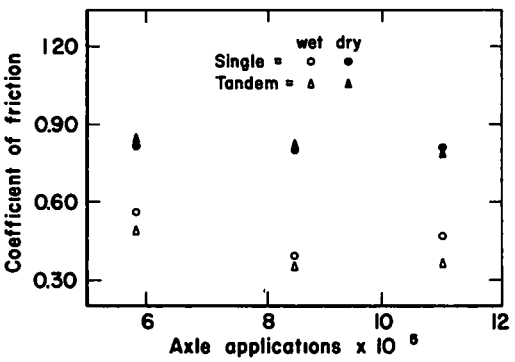

Figure 7. Influence of pavement surface conditions on rigid pavement coefficient of friction.

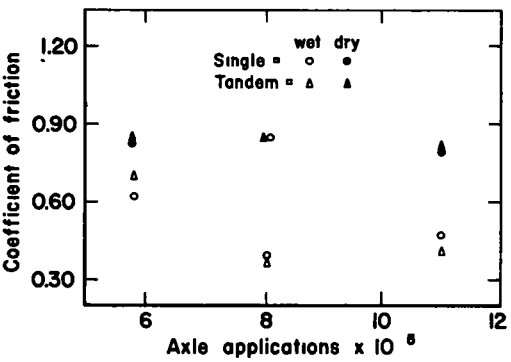

Figure 8. Influence of pavement surface conditions on flexible pavement coefficient of friction.

The first increase may be attributed to the influence of the freeze-and-thaw cycles and the scouring of the pavement surface by heavy rainfall immediately prior to the tests. The second increase could be associated with rainfall before the latter test series, which reduced the accumulation of dust and oil slicks on the pavement surface. Furthermore, the heavy rainfall prior to the summer 1959 tests may have reduced the dust and oil slick on the pavement surface, resulting in a higher coefficient of friction than one would normally expect. The scouring effect of heavy rainfall would appear, therefore, to have a significant effect on the coefficient of friction. Table 5 gives the rainfall accumulation for the two-week period preceding each test series.

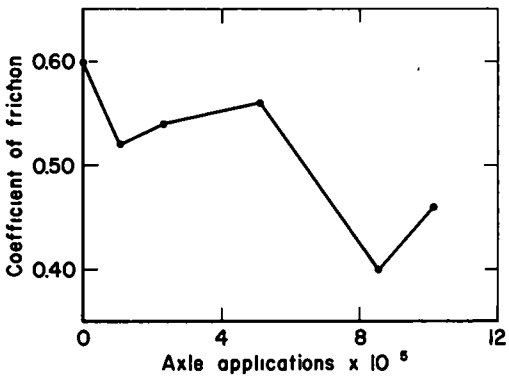

Figure 9. Influence of axle applications on coefficient of friction.

Other weather phenomena recorded during the test series are also given in Table 5. No apparent effect of these phenomena was observed, but further investigation of possible interactions may show some influence on the coefficient of friction.

TABLE 4

MEAN COEFFICIENT OF FRICTION FOR VARIOUS COMBINATIONS[a] OF PAVEMENT DESIGN AND LOAD[b]

Design Feature	Axle Load				
	2-6KS	12KS 24KT	18KS 32KT	22.4KS 40KT	30KS 48KT
Rigid pavement:					
Reinforced	0.57	0.50	0.52	0.50	0.46
Nonreinforced	0.56	0.49	0.53	0.50	0.47
Surface thickness:					
Second level	0.57	0.49	0.53	0.50	0.46
Third level	0.57	0.51	0.52	0.50	0.47
Subbase thickness:					
3 in.	0.57	0.51	0.53	0.49	0.47
6 in.	0.57	0.49	0.52	0.50	0.46
Flexible pavement:					
Surface thickness:					
First level	0.62	0.56	0.56	0.54	0.50
Second level	0.62	0.53	0.55	0.54	0.47
Base thickness:					
First level	0.62	0.53	0.56	0.54	0.49
Second level	0.62	0.56	0.56	0.55	0.48

[a] Flexible subbase values not shown—incomplete study.

[b] All values are the mean of six series of tests except those for the 12-kip single- and 24-kip tandem-axle loads, which were the mean of four series.

TABLE 5

RECORDED WEATHER PHENOMENA

Series	Rainfall, Two Weeks Preceding (in.)	Temperature Range (°F)		
		Air	Rigid Pvt.	Flexible Pvt.
1	1.22	80-47	84-55	73-91
2	1.77	86-45	102-45	107-46
3	1.63	94-73	113-78	123-84
4	0.53	63-36	63-37	65-37
5	0.36	88-65	119-80	117-81
6	0.79	60-37	62-40	67-39

SUMMARY

In the research investigation reported here, the unique characteristics of the design, construction and treatment of the test sections on the AASHO Road Test presented an opportunity to evaluate certain controlled variables fully.

From the observations made previously in this report, the following briefly summarizes the effect of the variables on the coefficient of friction:

1. The coefficients of friction remained reasonably constant throughout the entire range of design thicknesses selected for study. However, this observation is limited, because the pavements selected for skid testing represented the thicker designs in each loop.
2. The coefficients of friction of pavement sections exposed to tandem-axle loads were considerably less than those for pavement sections exposed to single-axle loads. There appeared to be little effect of axle load on the coefficients of friction, except possibly for the increases observed with the heavier loads in the experiment.
3. A pronounced effect of the test vehicle speed on the coefficients of friction measured on wet pavements was noted in all test series. Pavement conditions from very good to fair did not appear to influence the relationship.
4. The findings of the surface condition study were as predicted. The coefficients of friction for the wet surface condition were in all instances considerably lower than the coefficients for the dry surface conditions.

The influence of axle load, axle arrangement, test vehicle speed and pavement design was not significant in the dry surface study; however, a general downward trend in the coefficients of friction was noted when related to the number of axle applications.

5. The most pronounced influence on the coefficients of friction was noted when viewed with the number of axle applications. This relationship, however, is affected by certain environmental factors. Careful observation of the phenomena contributing to the seasonal vairations allows for an explanation of the deviations from the downward trend.

ACKNOWLEDGMENTS

The authors wish to express their appreciation to the General Motors Corporation for the use of the skid test equipment and for the assistance of thier personnel in preparing the data for analysis.

Indebtedness also is acknowledged to the staff members of the AASHO Road Test for thier assistance in the design of the experiment and in the interpretation of the test results.

REFERENCES

1. Skeels, P.C., "Measurements of Pavement Skidding Resistance by Means of a Simple Two-Wheel Trailer." HRB Bull. 186 (1958).

2. Dillard, J.H., and Allen, T.M., "Comparison of Several Methods of Measuring Road Surface Friction." HRB Bull. 219 (1959).

Appendix

DETAILS OF THE EXPERIMENT

Measurement of Coefficient of Friction

The coefficient of friction is defined in this report as the ratio of the horizontal force required to pull the trailer at a constant speed with the wheels locked to the vertical reaction at the wheels. The vertical reaction is determined by subtracting from the static weight on the trailer wheels the force exerted by a couple produced by the force in the drawbar and the wheel friction. Thus, by measuring the drawbar force the coefficient of friction may be determined. The General Motors skid trailer is designed to measure this force.

Materials Specification and Finishing Techniques

Portland Cement Concrete. Two coarse aggregates and one sand were blended together for the portland cement concrete. Both the coarse aggregate and the sand were obtained near the project site: the aggregate was predominantly dolomite and the sand was mostly siliceous.

The two coarse aggregates had maximum sizes of 2½ in. and 1½ in. and the sand had a fineness modulus of 2.90. The sieve analysis for the coarse aggregates and sand are given in Table 6; the lithological analysis for the coarse aggregates, in Table 7. Type 1 portland cement was supplied by one manufacturer from one continuous grinding and burning operation.

The design characteristics of the portland cement concrete are given in Table 8. Mean 14-day compressive strengths for concrete containing the 2½ in. and 1½ in. maximum size aggregates were 3,966 and 4,004 psi, respectively. Mean 14-day flexural strengths for concrete containing the 2½ in. and 1½ in. maximum size aggregates are 636 and 668 psi, the means of 394 and 67 tests, respectively.

The portland cement concrete was finished by the non-vibratory method. After the concrete had been deposited and spread between the forms, it was accurately struck off, screeded and consolidated with at least two passes of a non-vibrating finishing machine. It was further smoothed and consolidated by a mechanical longitudinal float. The floating operation was continued until the surface of the concrete was smooth, and at the proper crown and grade.

The surface was checked with a 10-ft straightedge; when most of the water sheen had disappeared, it was belted with one application of a mechanical belt. This was followed by edging, and final finish was obtained with two passes of a double thickness burlap drag.

Immediately after the finished concrete had attained sufficient set it was covered with two layers of burlap, which was saturated with water and kept wet until moved. The morning following the placement of the concrete, the forms and burlap were removed and the surface and edges of the pavement were covered with a layer of clean straw. The straw was then saturated with water, attaining a wet thickness of approximately 8-in., and was kept wet for the first three days. It was thoroughly wet down on the morning of the fourth day and remained in place until after test beams indicated that the concrete had attained a flexural strength of at least 500 psi.

Asphaltic Concrete, Surface Course. The coarse aggregate was predominantly crushed dolomitic limestone from near the project site. The maximum size for the surfacing course was ¾ in. Two sands, coarse and fine, were blended together for the fine aggregate to a specified fineness modulus of 2.35. The grain size analysis and percent of asphalt for the 96 extraction tests on surface course material is given in Table 9.

TABLE 6

SUMMARY OF GRADATION TESTS ON PCC AGGREGATES

Sieve Size	Gradation Formula Tolerances	Mean Percent of Material Passing	Standard Deviation
(a) Coarse Aggregate Size A (170 Tests)			
2½ in.	100	100	-
2 in.	90-100	96.3	3.45
1½ in.	62±7	63.5	6.11
1 in.	10±5	10.6	3.18
½ in.	0-5	3.8	2.14
(b) Coarse Aggregate Size B (171 Tests)			
1½ in.	100	100	-
1 in.	90-100	94.1	1.30
½ in.	38±5	37.9	1.65
No. 4	0-10	1.5	0.78
(c) PCC Sand (80 Tests)			
⅜ in.	100	100	-
No. 4	95-100	99.0	0.97
No. 8	85±5	84.1	1.55
No. 16	67±4	67.0	1.83
No. 30	46±4	45.4	1.51
No. 50	13±3	12.3	0.73
No. 100	3±2	2.7	0.46

TABLE 7

LITHOLOGICAL ANALYSIS OF PCC COARSE AGGREGATES

Rock Type	Percent Passing, by Weight					
	2 - 1½	1½ - 1	1 - ¾	¾ - ½	½ - ⅜	⅜ - No. 4
Dolomite	38	47	38	64	59	59
Argillaceous limestone	28	27	23	9	12	14
Soft sandstone	15	12	11	8	11	11
Hard sandstone	0	5	6	4	5	3
Chert	13	4	18	8	7	7
Diabase	4	0	0	2	2	2
Granite	2	2	2	3	3	4
Quartz	0	3	2	2	1	0

Other characteristics of the surface material are: Marshall stability, 2,000 lb; flow, 0.11 in.; voids by volume, 3.6 percent; and voids filled with asphalt, 77.9 percent.

Bituminous construction was performed in lane widths. Two spreading and finishing machines were used, one for each lane. While construction operations were being performed in one lane, the other machine was being positioned in the opposite lane so that the crew could move back and immediately start spreading in that lane. Sufficient material was kept on hand at all times to insure a continuous spreading operation throughout a test section. Delays in operation were confined to transition areas, except on rare occasions due to equipment failure.

TABLE 8

DESIGN CHARACTERISTICS PORTLAND CEMENT CONCRETE

Item	Surface Thickness	
	5 In. and Greater	2.5-3.5 Inches
Cement content (bags/cu yd)	6.0	6.0
Water-cement ratio (gal/bag)	4.8	4.9
Volume of sand (% total agg. vol.)	32.1	34.1
Air content (%)	3-6	3-6
Slump (in.)	1.5-2.5	1.5-2.5
Maximum aggregate size (in.)	2.5	1.5

TABLE 9

SUMMARY OF EXTRACTION TEST RESULTS[a]

Sieve Size	Mix Design	Mean Value	Standard Deviation
¾ in.	100	100	-
½ in.	90±5	92	2.43
⅜ in.	80±5	81	3.17
No. 4	64±5	63	4.06
No. 10	45±4	46	2.99
No. 20	31±4	34	1.66
No. 40	20±4	22	2.06
No. 80	11±3	13	1.07
No. 200	5±1	5.9	1.16
Asphalt[b] (%)	5.4±0.3	5.2	0.18

[a]Ninety-six tests on surface course mixture.

[b]Percent asphalt by total weight of mix. Control tests have shown that the extraction tests underestimated asphalt by 0.1 to 0.2 percentage points.

TABLE 10

ROLLING WEIGHTS AND TEMPERATURES FOR BITUMINOUS CONCRETE CONSTRUCTION

Roller Set	Roller Weights (lb/in. width)			Section Thickness[b] (in.)
	Three Wheel[a]	Pneumatic Tired	Tandem	
Heavy	300	300	250	15 (also all 9" base sections)
Intermediate	214	250	190	8 to 15
Light	180	200	120	8 or less

Mat Rolling Temperatures (°F)		
Three Wheel	Pneumatic Tired	Tandem
250 - 275	190 - 220	-[c]

[a]Based on 9-in. tire tread, inflation pressure 75 psi.

[b]Subbase plus base.

[c]While mat was still workable but had cooled sufficiently to prevent shoving.

TABLE 11

TIRE SIZES AND PRESSURES

Axle Load (kips)	Tandem or Single Axle	Tire Size	Tire Pressure (psi)
2	S	6:70x15	24
6	S	7:00x16	45
12	S	7:50x20	75
24	T	7:50x20	75
18	S	10:00x20	75
32	T	9:00x20	70
22.4	S	11:00x20	75
40	T	11:00x20	75
30	S	12:00x24	80
48	T	12:00x20	80

Compaction of each layer of bituminous mixture required the use of a three-wheel roller followed by a self-propelled pneumatic-tired roller, with final rolling by a tandem roller. Pneumatic-tired rollers were not being used extensively for compacting bituminous concrete, but experimental work indicated that the attained level of density more nearly corresponded to that produced by traffic on existing highways. The other requirements pertaining to the time of rolling and the speed and procedure for compacting the bituminous concrete courses were in line with normal construction practice.

The thickness of the subbase plus base was used as a guide in selecting the proper set of rollers for each structural section. At any indication that a section was being damaged or might be damaged, the set of rollers being used was immediately removed and replaced with the next lighter set of rollers or the number of passes of the rollers was reduced. Roller weights and mat temperatures used are given in Table 10.

Usually one pass of the three-wheel roller followed by eight passes of the pneumatic-tired roller was sufficient to obtain the required density on the layer being compacted. The tandem roller was considered only as a finish roller to remove the roller marks of the three-wheel and pneumatic-tired rollers, and sufficient number of passes were made over a layer to accomplish this. Experimental work indicated that little, if any, additional increase in density was obtained with the tandem roller.

A steel bristle broom drag was placed behind the spreading and finishing machine for the placement of the surface course to correct any slight tearing that might occur.

Tire Sizes and Pressures

Table 11 gives details of tire sizes and pressures for each load. Numerous makes of new tires and types of recaps were used in the operation and no attempt has been made to associate any make with a particular axle load. The pressure shown should be considered as nominal cold measurement.

Cooperative Materials Testing Program at the AASHO Road Test

J. F. SHOOK and H. Y. FANG, respectively, Materials Engineer and Soils Engineer, AASHO Road Test, Highway Research Board

During the construction of the AASHO Road Test in 1957 and 1958, samples of embankment soil, subbase material, and base material were sent to more than 60 interested agencies as part of a cooperative materials testing program. Returns from 61 State highway, university, Canadian provinicial, and other laboratories are summarized in this report.

The primary purpose of the program was to provide for the interested agencies a first-hand knowledge of the Road Test materials, to be used in applying Road Test findings to their areas. A second purpose was to secure information and test data not available through normal facilities at the Road Test site.

Because each laboratory was free to select its own test procedures, there was considerable variation in both procedures and test values. This report summarizes the data by type of test, gives pertinent information on test variables and procedures, and allows comparisons of values where possible. Discussion of the data and comparisons among laboratories are included.

● THE AASHO Road Test was primarily a scientific study of the performance of highway pavements of various designs when subjected to repeated applications of known loads. The test facility, located near Ottawa, Ill., in an area where climate and soils are typical of many areas of the nation, was constructed of one type soil, subbase, and base material considered typical of national practice. Both flexible and rigid pavements of various design thicknesses were included.

Analyses of data from the AASHO Road Test will provide engineering information which will be of value to highway administrators and engineers. However, it should be noted that the findings will relate specifically to the soils and materials actually used in constructing the test pavements. Information on the history and background of the project, design, construction, properties of materials, and other features is given in other Highway Research Board publications (1, 2).

Preparation of specifications and construction of the test facilities were directly under the supervision of engineers from the Illinois Division of Highways. General guidance in choice of test methods and construction procedures was given by committees of the American Association of State Highway Officials. Of necessity, only a limited variety of tests could be included in the specifications, and most of these followed practices of a majority of State highway departments as determined in a 1953 national survey.

A summary (2) of physical test data, properties of materials, and construction control test data obtained during the construction phase of the AASHO Road Test summarizes, for the most part, tests which apply directly to the specifications.

Additional information on the properties of materials was obtained by the Materials Branch of the Road Test staff, by Illinois and other State highway department laboratories, by the Bureau of Public Roads, and by other agencies. Nevertheless, it was not possible to cover completely the range of interest. Therefore, it was decided

early during the construction phase of the Road Test that interested agencies should be given an opportunity to secure an intimate knowledge of the basic materials of construction using their own test methods. Such information would be of value to them in applying the Road Test findings to their areas. At the same time it would provide an opportunity to secure data not otherwise available.

As a result, a program for cooperative tests of AASHO Road Test materials was planned. More than 60 State highway, university, Canadian provincial, and other laboratories participated in the study. Large stocks of the soil, subbase material, and base material were secured and made available to the participating agencies for testing by them using their own test methods and procedures. Test results from most of those who received samples are reported herein.

This paper has been prepared with several purposes in mind. As previously indicated, there are many different tests and methods used in the United States for evaluating soils, subbase, and bases for potential use in highway substructures. The cooperative program resulted in collection of much information of this type of materials used at the AASHO Road Test, where performance has been well documented. Many of the participating agencies have indicated an interest in using the information in making a tie-in with their own experiences and in comparing their test data with those reported by the other laboratories. Additional requests for data such as obtained in the triaxial test and for comparative data such as between the Hveem stabilometer and the California Bearing Ratio test have made publication of the results of the cooperative program desirable.

Most of the data are presented in tabular and graphical form. Some discussion and interpretation of the methods used are given, but it is usually assumed that the reader is familiar with the various test procedures. A brief discussion and summary of the indicated physical properties and some indications of laboratory-to-laboratory variations are made. However, the data are presented for the use of the reader, and no inferences are intended as to the relationship of indicated physical properties of the material to the performance of the Road Test pavements.

It is possible, using data from this report, to make trial pavement thickness designs using published procedures. However, no attempt was made to do this in the report. It is suggested that conclusions based on such designs be tempered by the knowledge that a complete understanding of the various factors involved cannot be had until all Road Test data are in and published.

Limited comparisons between laboratories are possible from the data given. The materials were obtained at one source and, though of large quantity, were carefully prepared and divided into individual samples. Because of the randomizing which was done, there should be no systematic bias among laboratories. There was, no doubt, some sample-to-sample variability. Singling out one laboratory for special discussion is not valid, however, because each laboratory tested only one sample. General discussion of variability is valid.

A major source of variation in reported test values arises from the freedom with which each laboratory was allowed to select its own test procedures. Because of this fact, care will have to be taken in assessing some of the reported data. For the same reason indiscriminate application of the reported data to evaluation of Road Test results will also be dangerous.

NOMENCLATURE

The terms and symbols used throughout this report conform generally to "Tentative Definitions of Terms and Symbols Relating to Soil Mechanics" (ASTM Designation D 653-58T), as follows:

Symbol	Definition
abs.	= Absorption;
C	= Cohesion;
C_v	= Coefficient of consolidation;
CA	= Coarse aggregate;

CBR = California Bearing Ratio;
D_{max} = Maximum dry density;
e = Void ratio
e_o = Initial void ratio; and
e_f = Final void ratio.
FA = Fine aggregate;
G_a = Specific gravity (apparent);
G_m = Specific gravity (bulk);
G_m(SSD) = Specific gravity (bulk, surface saturated dry);
G_s = Specific gravity (soil solids);
K = Coefficient of permeability;
P_h = Transmitted horizontal pressure (Hveem stab.);
P_v = Applied vertical pressure (Hveem stab.);
PI = Plasticity index;
PL = Plastic limit;
R-value = Resistance value (Hveem stab.);
r = Primary consolidation ratio;
W = Moisture content;
W_o = Optimum moisture content;
σ_1 = Major principal stress;
σ_3 = Minor principal stress;
ϕ = Angle of internal friction;

SCOPE OF PROGRAM

The cooperative program for testing Road Test materials included only the embankment soil, the crushed stone base material, and the subbase material. The embankment soil and subbase were common to both rigid and flexible pavements. The crushed stone base was part of the flexible pavement only.

All State highway departments and representatives on the National Advisory Committee for the AASHO Road Test, representing universities, State highway departments, and other organizations, were invited to participate in the cooperative materials testing program. In addition, many Canadian provincial highway departments and other groups asked to be included and were supplied material as were one private testing laboratory and four agencies of the Federal Government. All groups which returned test data included in this report are named in Table 1 with the abbreviations used in the tabulations of test data.

Each agency was free to select the tests and test methods it wished to perform. No effort was made to control the conditions of the tests which each laboratory chose. A standard report form was provided in an attempt to get some uniformity, but in each case the agency was free to report as much or as little as it wished. Specifically, each was requested to report the following:

1. Grading, results of sieve analysis or hydrometer analysis.
2. Liquid and plastic limits, with method of preparing sample and running tests.
3. Specific gravity and method of test.
4. Moisture-density relationship, specifically at optimum condition, and method of test.
5. Results of California Bearing Ratio, Hveem stabilometer, and triaxial tests with test details.
6. Other tests and comments.

Other data reported included field moisture equivalent, shrinkage factors, consolidation, direct shear, permeability, frost susceptibility, soundness, abrasion, and petrographic analyses.

Almost all agencies reported results of sieve analyses, tests for moisture-density relationship, and Atterberg limits. Such tests as California Bearing Ratio, Hveem stabilometer, and the triaxial were reported by 10 to 30 laboratories in varying detail. One agency reported complete CBR curves on all three materials; others reported tests on only one set of conditions. Many other tests were made by only one or two laboratories.

TABLE 1

AGENCIES PARTICIPATING IN COOPERATIVE MATERIALS TESTING PROGRAM

Name of Agency	Abbrev	Address
AASHO Road Test	Rd Test	Ottawa, Ill
Arctic Construction and Frost Effects Laboratory, U S Army	ACFEL	Waltham, Mass
Alabama Highway Department	Ala	Montgomery, Ala
Alberta Department of Highways	Alta	Edmonton, Alta , Canada
Arizona Highway Department	Ariz	Phoenix, Ariz
Arkansas Highway Department	Ark	Little Rock, Ark
The Asphalt Institute	AI	College Park, Md
Banff Materials Testing Laboratory, Dept of Public Works of Canada	Banff	Banff, Alta., Canada
British Columbia Dept of Hwys	BC	Victoria, B C , Canada
Bureau of Public Roads	BPR	Washington, D C
California Division of Hwys	Calif	Sacramento, Calif
Delaware State Highway Dept	Del	Dover, Del
Federal Aviation Agency (formerly CAA)	FAA	Indianapolis, Ind
State Road Dept of Florida	Fla	Gainesville, Fla
State Hwy Dept of Georgia	Ga	Atlanta, Ga
Hawaii Highway Department	Hawaii	Honolulu, Hawaii
Idaho Dept of Highways	Idaho	Boise, Idaho
Illinois Division of Hwys	Ill	Springfield, Ill
State Hwy Dept of Indiana	Ind	Indianapolis, Ind
State Hwy Commission of Kansas	Kan	Topeka, Kan
Kentucky Dept of Highways	Ky	Frankfort, Ky
Louisiana Dept of Highways	La	Baton Rouge, La
Maine State Hwy Commission	Me	Maine Technology Experimental Station, University of Maine, Orono, Me
Manitoba Highways Branch, Province of Manitoba	Man	Winnipeg, Man , Canada
Maryland State Roads Commission	Md	Baltimore, Md
Massachusetts Dept of Public Works	Mass	Wellesley Hills, Mass
Michigan State Hwy Dept	Mich	Lansing, Mich
Mississippi State Hwy Dept	Miss	Jackson, Miss
Missouri State Hwy Commission	Mo	Jefferson City, Mo
National Research Council of Canada	NRC	Ottawa, Ont , Canada
Nebraska Dept of Roads	Neb	Lincoln, Neb
Nevada Dept of Highways	Nev	Carson City, Nev
New Brunswick Dept of Public Works	NB	Fredericton, N B , Canada
Newfoundland Dept of Hwys	Newf	St John's, Newf , Canada
New Jersey State Hwy Dept	NJ	Trenton, N J
New Mexico State Hwy Dept	NM	Santa Fe, N Mex
New York Dept of Public Works	NY	Albany, N Y
North Carolina State Hwy Comm	NC	Raleigh, N C
North Dakota State Hwy Dept	N Dak	Bismarck, N Dak
Ohio Dept of Highways	Ohio	Ohio State Univ , Columbus, Ohio
Oklahoma State Hwy Comm	Okla	Oklahoma City, Okla
Omaha Testing Laboratories	Omaha	Omaha, Nebr
Ontario Dept of Highways	Ont	Toronto, Ont , Canada
Oregon State Highway Dept	Ore	Salem, Ore
Portland Cement Association	PCA	Skokie, Ill
Pennsylvania Dept of Hwys	Penn	Harrisburg, Pa
Puerto Rico Dept of Public Works	PR	Santurce, P R
Quebec Department of Roads	Que	Quebec City, Que , Canada
Rhode Island Dept of Public Works	RI	Providence, R I
Saskatchewan Dept of Hwys and Transportation	Sask	Regina, Sask , Canada
South Carolina State Hwy Dept	SC	Columbia, S C
Texas Highway Department	Tex	Austin, Tex
University of Minnesota	U Minn	Minneapolis, Minn
State Road Commission of Utah	Utah	Salt Lake City, Utah
Virginia Dept of Highways	Va	Charlottesville, Va.
Washington State Hwy Comm	Wash	Olympia, Wash
Waterways Experiment Station, U S Army	WES	Vicksburg, Miss
State Road Comm of W Virginia	W Va	Charleston, W Va
State Hwy Comm of Wisconsin	Wis	Madison, Wis
Wyoming State Highway Dept	Wyo	Cheyenne, Wyo

Most of the test data received are included. When convenient, they are presented in tabular and graphical form. To simplify the rather extensive explanatory notes, these have been collected in Appendix A.

Text has been confined primarily to explanatory information in the first part of the paper. Some data are included in this form, however. Following the presentation of the data, some discussion of the indicated physical properties of the materials is given. Summaries are also included here. Finally, comparisons are made among laboratories where valid and meaningful comparisons can be made.

PREPARATION OF ORIGINAL MATERIALS

All materials for this program were prepared from samples selected to represent the average material used during construction. The embankment soil was removed in the spring of 1957 from embankment constructed late in 1956. It was secured by coring with a 12-in. diameter auger. Each loop was divided into ten blocks and individual borings were located by random selection within each block. They were, however, restricted to areas not immediately under a test section.

Material from each core hole was deposited on a large concrete slab for drying, pulverizing and mixing. The soil was pulverized by rolling with a lawn roller on the concrete slab. It was then mixed thoroughly by blending samples of each quarter of the total sample in a concrete mixer until the entire supply had been processed several times. Individual bags of mixed material were then filled with portions again obtained successively from each quarter of the entire pile. About 10,000 lb was prepared in this way.

Subbase and base were taken, respectively, from material produced in 1957 and 1958. In each case a truck load of the material which had previously been proportioned by weight and mixed in a concrete paving mixer was secured to form the basic stock. This was then placed in individual bags by sampling from successive portions of the stock sample.

Prior to shipping the soil samples, individual bags were selected at random for basic tests (moisture-density relationships, liquid and plastic limits, grain size analysis, and specific gravity) as a check on the uniformity of the sample and the efficiency of the mixing operation. An analysis of variance of the test data indicated no significant differences between the individual bags, compared to within-bag variability.

Due to the pressure of construction activities in 1957 and 1958 no similar tests were run on the subbase or base. A few samples of subbase and base material were lost in shipment and were replaced from a stockpile of material obtained about the same time. Wherever possible the particular data involved have been checked and consideration taken in evaluating the test results.

EMBANKMENT SOIL TEST DATA

Description of Soil

The embankment soil used on the AASHO Road Test was a yellow-brown clay having characteristics of the A-6 classification used by the American Association of State Highway Officials (3). It was a C-horizon material available on the Road Test site. The soil was quite uniform, although there were small pockets of sand located within the borrow material. A few pebbles and small boulders were also found.

Only two of the laboratories reported results of tests for identification of clay minerals. New Mexico reported that "results of nitro-benzene qualitative analysis indicate this material contains no bentonite." The Bureau of Public Roads reported that "the clay fractions are predominantly illite (about 60 percent) with about 30 percent chlorite and 5 to 10 percent montmorillonite."

Test Data

The method used in preparing the embankment soil samples for testing and the results of mechanical analyses on the samples are given in Table 2. Figure 1 is a plot of the mean results from mechanical analyses on the soil, with upper and lower limits shown to indicate the range in test values. Liquid and plastic limits, specific gravity, maximum density, and optimum moisture content are given in Table 3. Most laboratories reported using AASHO method T-87[2], dry preparation, for preparing the samples for these tests. A few indicated only air drying or oven drying followed by pulverizing to break up the lumps. There was variation in technique for breaking up lumps, but because this information was not generally available no specific methods are given.

Also given in Table 3 are the AASHO classifications with corresponding group indexes of the soils according to AASHO Specification M 145-49. Maximum densities

TABLE 2

MECHANICAL ANALYSIS OF EMBANKMENT SOIL SAMPLES*

Agency	Method of Prep	Percent Finer Than[1] No 4	No 40	No 200	0 05 mm	0 02 mm	0 005 mm	0 002 mm
Rd Test	T 87[2]	98 1	90 3	78 2	74 2	61 1	35 5	21 5
ACFEL	-	95 0	87 5	74 5	70 0	58 0	-	-
Ala	Oven dry	99 4	85 0	73 2	-	69 6	47 6	33 8
Alta	Dry	96 0	89 0	76 0	-	66.0	42 0	30 0
Ariz	-	95 0	88 0	76 0	72 0	60 0	35 0	21 0
Ark	T 87	96 9	89 9	77 0	-	-	-	-
AI	T 87	96 9	94 4	79.9	77 0	67 0	44 0	34 0
Banff	D 421[2]	100	94 1	81 0	77 0	66 0	41 0	18 0
BC	D 421	95 6	88 4	75 1	74 5	67 6	44 5	30 0
BPR	T 87	97 0	90 0	77 0	74 0	60 0	40 0	28 0
Calif	T 87	99 0	90 0	77 0	73 0	63 0	40 0	28 0
Del.	T 87	88 2	69 1	59 7	-	-	-	-
FAA	-	97 0	89 0	75 0	73 0	58 0	36 0	21 0
Fla	T 87	98 0	94 0	80 0	74 0	65 0	43 0	22 0
Ga	T 87	95 0	85 0	74 0	73 0	59 0	36 0	22 0
Hawaii	T 87	97 0	88 0	73 0	72 0	67 0	50 0	42 0
Ida	T 87	96 0	88 0	75 0	72 0	62 0	46 0	32 0
Ill.	T 87	96 4	88 7	74 7	73 0	64 0	40 0	-
Ind	T 87	91 4	83 4	71 5	69 4	-	36 4	-
Kan	Oven dry	100	94 0	80 0	77 0	64 0	38 0	25 0
Ky	D 421	-	93 6	75 2	-	-	47 5	-
La	T 87	94 0	86 0	72 0	68 0	61 0	37 0	25 0
Me	-	97 3	90 3	78 4	76 4	65 1	44 2	30 2
Man	D 421	100	89 0	76 0	-	-	37 0	-
Md	T 87	93 4	86 2	73 8	-	-	41 0	-
Mass	T 87	97 1	88 6	75 2	-	-	-	-
Mich	T 87	96 0	-	77 8	76 0	74 0	51 0	39 0
Miss	T 87	100	94 0	79 0	73 0	58 0	33 0	23 0
Mo	-	95 0	89 1	76 0	69 0	-	37 0	-
NRC	Air dry	98 5	92 0	80 0	76 5	66 0	44 0	31 5
Nebr	T 87	100	91 0	77 0	73 0	63 0	41 0	29 0
Nev	T 87	95 7	88 0	74 7	-	-	-	-
NB	-	96 0	82 8	75 3	71 0	63 0	50 0	41 0
Newf.	T 87	97 0	90 0	77 0	-	-	-	-
NJ	T 87	97 0	88 0	76 0	73 0	-	49 0	-
NM	-	95 3	85 8	73 8	-	-	-	-
NY	Air dry	96 6	88 0	74 7	-	48 9	-	23 0
NC	Air dry	94 0	82 0	70 0	68 0	-	26 0	-
N Dak	T 87	100	-	-	61 0	53 0	33 0	25 0
Ohio	D 421	97 0	91 0	78 0	73 0	61 0	41 0	28 0
Okla	T 87	99 0	94 0	80 0	75 0	61 0	38 0	26 0
Omaha	-	95 0	88 0	74 5	73 0	65 0	42 0	30 0
Ont.	-	96 0	89 0	76 0	73 0	62 0	42 0	30 0
Oreg	T 87	96 8	88 4	74 4	73 5	63 0	42 7	21 5
PCA	-	96 4	86 0	76 0	72 0	64 0	43 0	31 0
Penn	T 87	92 0	86 0	74 0	72 0	57 0	40 0	32 0
PR	T 87	95 0	86 0	74 0	-	-	-	-
Que	D 421	96 8	94 3	70 5	58 3	44 0	28 8	24 2
Sask	T 87	100	91 0	75 0	72 0	62 0	42 0	27 0
SC	Air dry	97 0	89 0	76 0	-	-	-	-
Tex	T 146[3]	96 0	88 0	73 0	72 0	63 0	40 0	28 0
U Minn	-	96 8	89 2	76 1	72 4	61 1	41 3	30 6
Ut	-	97 4	92 1	78 0	-	-	-	-
Va.	T 87	96 1	87 7	75 3	70 5	60 0	38 5	27 9
Wash	T 87	96 0	88 0	75 0	73 0	61 0	29 0	10 8
WES	-	95 5	88 1	75 6	-	-	-	-
W Va	T 87	97 0	89 6	78 4	76 7	63 2	41 5	33 0
Wis	D 421	96 0	88 0	75 0	72 0	63 0	40 0	29 0
Wyo	T 87	100	89 0	75 0	-	62 0	37 0	21 0
No of tests		58	57	58	42	42	47	40
Mean		96 6	88 6	75 5	72 3	61 9	40 3	27 6
Std dev		2 25	3 90	3 16	3 58	5 07	5 40	6 08

*For footnote explanations see Appendix A

reported included both the standard and modified AASHO procedures, plus a few local variants.

Table 4 gives the field moisture equivalent, shrinkage factors, dust ratio, and sand equivalent values for the embankment soil.

Data for California Bearing Ratio tests on the soil samples are given in Table 5. There were two generally different test methods used by the different laboratories. Seven laboratories used the procedure suggested by Stanton[31] in which the specimen is molded at a static pressure of 2,000 psi and no correction is made for curvature in the load-deformation curve. Nineteen used variations of the drop-hammer compacting technique, following procedures suggested by the Corps of Engineers[30]. Two laboratories reported different techniques.

Some agencies reported data for only one moisture and density condition, while one reported a complete set of moisture-density-compactive effort curves. Others conducted their tests for a range in density at about optimum moisture and reported CBR values for 95 or 100 percent of maximum density. For the most part, 10-lb surcharge weights and 4-day soaking periods were used.

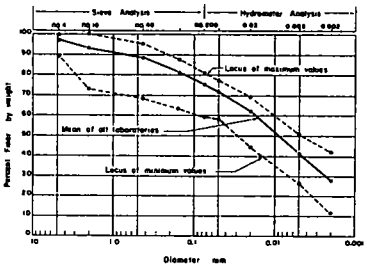

Figure 1. Grain-size distribution curve for embankment soil.

TABLE 3

ATTERBERG LIMITS, SPECIFIC GRAVITY, AND MOISTURE-DENSITY RELATIONSHIPS OF EMBANKMENT SOIL*

Agency	AASHO Classification**	Atterberg Limits			Specific Gravity		Moisture-Density Relationship		
		LL	PL	PI	Method	G_s	Method	W_o	D_{max}
Rd Test	A-6(10)	29 5	15 8	13 7	T 100[8]	2 77	T 99[16]	13 9	117 5
ACFEL	A-6(9)	27 3	15 4	11 9	T 100	2 74	-	-	-
Ala	A-6(8)	29 2	17 4	11 8	T 100	2 75	T 99	14 6	116 7
							T 180[17]	10 9	128 0
Alta	A-6(10)	29 7	15 2	14 5	T 100	2 74	T 99	13 2	119 7
Ariz	A-6(10)	29 0	13 0	16 0	T 133[9]	2 63	T 99	9 5	119 0
Ark	A-6(9)	27 3	14 8	12 5	T 100	2 75	T 99	12 8	122 7
AI	A-4(8)	27 3	17 0	10 3	T 100	2 73	-	-	-
Banff	A-6(9)	26 9	14 1	12 8	D 854[8]	2 69	T 99	13 5	120 3
BC	A-6(9)	26 4	14 7	11 7	D 854	2 68	T 99	13 6	120 4
BPR	A-6(9)	29 0	17 0	12 0	T 100	2 72	T 99	13 0	122 0
Calif	A-6(10)	29 0	15 0	14 0	C 208-B[10]	2 69	C 216-C[18]	12 0	129 0
Del	A-6(6)	26 1	14 9	11 2	-	-	T 180	11 5	126 0
FAA	A-6(10)	27 0	13 0	14 0	T 100	2 78	T 99	13 5	121 0
							T 180	10 7	129 0
Fla	A-6(11)	31 0	15 0	16 0	-	-	-	-	-
Ga	A-6(9)	24 6	13 2	11 4	T 100	2 72	T 99	12 3	119 0
Hawaii	A-6(9)	26 0	13 0	13 0	T 100	2 74	-[23]	9 5	132 3
Ida	A-6(8)	25 8	14 5	11 3	T 100	2 78	T 99	12 5	122 1
Ill	A-6(8)	27 0	16 0	11 0	-	-	T 99	13 3	121 8
Ind	A-6(8)	28 0	15 1	12 9	T 100	2 73	T 99	14 1	116 5
Kan	A-6(10)	29 0	15 0	14 0	C 188[9]	2 70	-[25]	13 0	119 0
Ky	A-6(9)	26 5	14 9	11 6	D 854	2 76	T 99	12 8	120 2
La	A-6(7)	22 5	15 1	10 4	T 100	2 77	T 99	13 8	118 6
Me	A-6(9)	27 0	16 4	10 6	T 100	2 77	T 99	14 6	117 5
Man	A-6(9)	28 0	16 0	12 0	-	2 70	T 99	12 9	119 5
Md	A-6(8)	29 7	16 8	12 9	-	-	T 99	13 4	118 4
Mass	A-6(10)	25 0	10 3	14 7	-	-	T 180	9 7	132 0
Mich	A-6(10)	28 2	14 4	13 8	T 100	2 66	T 99	14 5	116 2
Miss	A-6(10)	29 0	15 5	13 5	T 100	2 67	T 99	14 5	118 1
							-[26]	13 0	119 0
Mo	A-6(10)	29 0	13 0	16 0	T 100	2 72	T 99	14 0	117 0
NRC	A-6(9)	29 3	15 8	13 5	D 854	2 78	T 99	12 8	118 0
Nebr	A-6(8)	28 0	17 0	11 0	T 100	2 75	T 99	14 0	119 2
Nev	A-6(9)	26 6	13 4	13 2	T 100	2 63	C 216-C	10 0	128 3
NB	A-6(10)	27 0	13 0	14 0	T 100	2 67	T 134[20]	13 5	119 0
Newf	A-6(9)	28 2	15 7	12 5	T 100	2 75	T 180	10 5	129 0
NJ	A-6(9)	26 7	14 1	12 6	T 100	2 60	T 99	13 5	119 4
NM	A-6(8)	26 9	15 3	11 6	D 854	2 72	T 99	15 2	114 7
NY	A-6(10)	27 5	13 4	14 1	T 100	2 74	T 99	13 5	121 0
NC	A-6(9)	29 0	15 0	14 0	-[13]	2 70	T 99	12 4	119 0
N Dak.	-	25 0	14 0	11 0	-[14]	2 65	T 99	13 0	121 0
Ohio	A-6(9)	27 0	15 0	12 0	D 854	2 72	D 698[16]	12 5	120 0
Okla	A-6(10)	32 0	18 0	14 0	T 100	2 77	T 99	15 0	117 1
Omaha	A-6(9)	26 6	15 5	11 5	T 100	2 75	T 99	13 3	121 1
Ont	A-6(9)	27 2	14 2	13 0	T 100	2 70	T 99	14 0	118 4
Oreg	A-4(8)	26 0	16 0	10 0	C 188	2 72	-[21]	13 5	120 8
PCA	A-6(11)	30 0	14 0	16 0	T 100	2 68	D 698	15 5	114 0
Penn	A-6(9)	27 0	15 0	12 0	T 100	2 76	T 99	12 3	121 2
PR	A-6(8)	26 2	15 0	11 2	-	-	T 180	8 5	127 6
Que	A-4(7)	26 9	17 4	9 5	D 854	2 73	T 99	14 4	116 1
Sask	A-4(8)	27 7	17 0	10 7	T 100	2 73	T 99	13 5	119 5
SC	A-6(10)	29 0	14 0	15 0	T 100	2 73	T 99	13 4	119 4
Tex	A-6(11)	34 0	16 0	18 0	T 100	2 70	T 99	13 7	116 1
U Minn	A-6(8)	27 2	17 0	10 2	T 100	2 76	T 99	14 2	119 1
							T 180	12 0	126 0
Ut	A-6(8)	25 6	14 6	11 0	D 854	2 73	T 99	15 0	117 7
Va	A-6(10)	27 0	15 0	12 0	T 100	2 72	T 99	13 0	121 0
Wash	A-6(10)	31 3	16 8	14 5	D 854	2 74	T 99	14 1	119 5
WES	A-6(9)	28 0	15 0	13 0	D 854	2 75	T 180	9 4	132 5
W Va	A-6(9)	26 1	13 9	12 2	D 854	2 74	THD 83[22]	13 2	120 1
Wis	A-6(9)	26 8	15 2	11 6	D 854	2 74	T 99	11 9	125 1
Wyo	A-6(10)	30 4	15 9	15 0	T 100	2 65	T 99	13 0	121 2
No of tests	54	59	59	59	-	53	-	44	44
Mean	A-6(9)	27 7	15 1	12 6	-	2 72	T 99	13 5	119 2
Std dev	-	1 91	1 40	1 77	-	0 042	-	1 0	2 2

*For footnote explanations see Appendix A

**According to AASHO Specification M 145-49; numbers in parentheses refer to group index

TABLE 4

FIELD MOISTURE EQUIVALENT, SHRINKAGE FACTORS, DUST RATIO AND SAND EQUIVALENT FOR EMBANKMENT SOIL*

Agency	Field Moisture Equivalent[30]	Shrinkage Factors of Soils[28]				Dust Ratio[32]	Sand Equivalent[31]
		Shrinkage Limit	Shrinkage Ratio	Volumetric Change	Lineal Shrinkage		
Rd. Test	19.7	12.7	2.02	14.1	4.5	-	-
Calif.	-	-	-	-	-	-	6
Ida.	18.2	-	-	-	4 8	-	-
Ind.	22 8	13.6	1.90	17.5	5.2	-	-
Ky.	17.3	13.9	1.99	6 8	-	-	-
Man.	-	13 7	1.96	-	-	-	-
Mich.	20.4	-	-	-	-	-	-
Miss.	22 0	13.0	1.89	13.0	-	84.3	-
NB	-	12.3	1 86	22.3	7.0	-	-
NY	-	11 9	2.09	9.8	8.2[29]	-	-
N. Dak.	16.0	13.0	1.98	5.0	-	-	-
Okla.	27.0	14 3	1.93	24.1	-	-	-
Va.	-	11.0	1.90	-	-	-	-
No. of tests	8	10	10	8	5	-	-
Mean	20.4	12.9	1.95	14.1	5.9	84.3	6
Std dev.	3 51	1.0	0.07	6.88	1.59	-	-

*For footnote explanations see Appendix A.

Most of the data received from the different laboratories have been included in Table 5. Data from four agencies were too extensive for Table 5 and are given in separate tables. Table 6 and Figure 2 show tests conducted at several surcharge weights over a range in densities. Table 7 includes tests at several moisture-density conditions. Table 8 and Figure 3 show data for a complete set of CBR curves for a different molding densities, water contents, and number of blows of the drop hammer. Both soaked and unsoaked CBR values are also included.

Results of Hveem stabilometer tests on the soil were reported by eight laboratories. Details are shown in Table 9 and plots of R-values versus exudation pressure in Figure 4. Variations in compaction procedure, indicated in the footnotes, were involved in three cases. The other five made use of AASHO method T 173-56[40]. R-values are shown for 400 psi exudation pressure. Values at other exudation pressures may be selected from Figure 4. Some data on swell were also included. Those reported as pressures are given in Table 9. A few agencies indicated design thicknesses or equilibrium R-values, but since these involved using estimated thicknesses and densities of overlying courses, they are not included in this report.

North Dakota reported a value of 140 psi for their cone bearing test on laboratory specimens compacted at 120 pcf and 13.4 percent moisture. They added, however, that they have never been able to correlate results of soil bearing tests in the field with tests on laboratory molded specimens.

Data from the 15 laboratories reporting triaxial tests of embankment soil are given in Table 10. Figure 5 shows shear stresses plotted against principal stresses, with Mohr envelopes for stresses at failure. It will be observed that static and dynamic (using drop hammer) methods predominated as methods for preparing the samples, and that most samples were tested unsaturated. Presumably, all

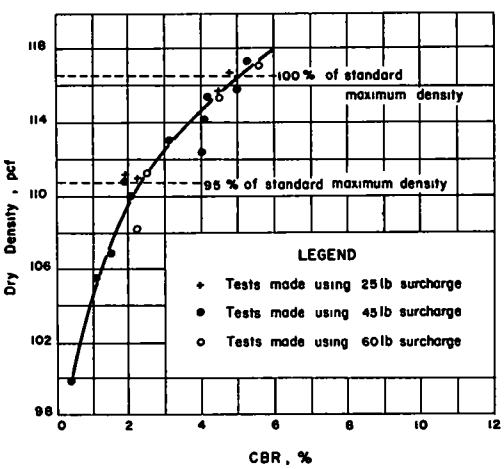

Figure 2. Effect of surcharge weight on CBR of embankment soil (Indiana).

TABLE 5
CALIFORNIA BEARING RATIO TEST DATA FOR EMBANKMENT SOIL*

Details of Test	Agency: Ala	Alta 1	Alta 2	BPR 1	BPR 2	BPR 3	Hawaii	Ill	Ind 1	Ind 2	Ky	Md	Miss 1	Miss 2	Miss 3	Mo	N J	N C	Ohio	Okla	Ont
Compaction method																					
Dynamic[23]		x			x		x[23]		x			x		x				x	x		x
Wt of hammer, lb		5 5			5 5[27]				5 5			5 5		10				5 5	5 5		10
Drop, in		12			12				12					18				12	12		18
No layers		3			4				3			3		4				5	5		5
No blows per layer		55		25	30	35			Variable			55	10	25	55			52	56		55
Static, 2000 psi[24]	x							x			x					x	x			x	
Other																					
Testing conditions																					
Surcharge weight, lb	10	10			10		10	10	Variable		17 5	10		10		10		13	22	10	45
Soaking period, days	7	1	4		4		7	4	3		7	4		4		1	4	4	4	4 5	4
Molding conditions																					
Dry density, pcf	133 3	117 1	119 2	115	118	120	128 1	126 2	Variable		120 2	119 5	112 5	124 8	126 4	105 3	119 4	121 1	119 4	132 3	133 4
Moisture content (%)	9 6	13 6	13 5	13 0	13 0	13 5	7 6	13 3	Optimum		12 8	13 2	13 6	13 2	13 0	14	13 5	12 4	13 4	10 9	11 0
Optimum conditions (Table 3)																					
Max dry den (T 99)		119 7			122			121 6	116 5		120 2	118 4				117 0	119 4	119 0	120 0	117 1	
Max dry den (T 180)	128 0																				135 7
Max dry den (Other)							132 3[25]							119 0[25]							
Opt moisture content	10 9	13 2			13		9 5	13 3	14 1		12 8	13 4		13 0		14	13 5	12 4	12 5	15	10 9
Test results.																					
Final moisture content	16 1	15 4	14 4	17 3	16 7	14 7	11 7	13 9				14 0	15 1	14 2	13 9	24 3		13 5	13 9		11 9
Swell (%)	5 0	0 5	0 5	0 9	0 8	0 3	0 8	1 0				0 5	1 0	0 6	0 9	2 8	3 0	0 6	0 2	5 5	1 4
CBR at 0 1-in pen (soaked)		7 2	10 1			8 1	25		2 4 at 95% Max Dens	5 1 at 100% Max Dens	7 6 at 0 5-in pen	5 1	1	7	9	0 8	1 7		6 7	6 0	
CBR at 0 2-in pen (soaked)	45			3 5	4 2			4 0										8 0	7 6 at 0 5 in		22
Remarks				CBR, 4 at 95% T 99 max density					See Table 6 Fig 2							Design CBR, 7 90% Max Dens					

Details of Test	Agency: Pa	PCA	P R.	Que	Sask	S C 1	S C 2	S C 3	U Minn 1	U Minn 2	Utah	Va	WES	W Va	Wis 1	Wis 2	Wis 3	Wyo
Compaction method																		
Dynamic[23]	x	x	x	x	x		x		x	x		x	x			x		
Wt of hammer, lb	10	5 5	10	10	5 5		10		5 5	10		5 5	10			10		
Drop, in	18	12	18	18	12		18		12	18		12	18			18		
No layers	5	3	5	5			5		3	6		5	5			5		
No blows per layer	55	55	55	55		10	25	55	56	56		45	Variable		10	25	55	
Static, 2000 psi[24]											x							
Other														x				x[28]
Testing conditions																		
Surcharge weight, lb	10	15	10	30	20		10			10	12	10	20			10		10
Soaking period, days	4	4	0	5	4		4			4	5	4	4	0		4		4
Molding conditions																		
Dry density, pcf	129 3	114	127 6	127 4	119 5	110 1	121 9	128 5	Variable		125 3	123		Variable	116 7	124 1	130 4	121 2
Moisture content (%)	10 1	15 5	8 5	9 5	13 5	10 8	10 3	10 7			13 8	13		Variable		9 5		12 5
Optimum conditions (Table 3)																		
Max dry den (T 99)	121 2	114			119 5				119 1		117 7	121						121 2
Max dry den (T 180)			127 6	129 5			128 4			126 0			132 5			132		
Max dry den (Other)														120 1[25]				
Opt moisture content	12 3	15 5	8 5	9 0	13 5		10 3		14 0	12 0	15 0	13	9 4	13 2		9 5		13 0
Test results																		
Final moisture content	13 0			10 5	14 7	16,9	13 3	11 2			14 5	14			17 3	13 2	12 5	14 3
Swell (%)	0 4			1 8	0 3	1 9	1 7	0 6			2 3	0 2			3 3	3 3	2 1	1 6
CBR at 0 1-in pen (soaked)	13	5		7 2	6 0	2 2	5 1	17			5 0	7 1		4 0[25]				6 7
CBR at 0 2-in pen (soaked)	16	pen not given	82	11 at 0 15 in		1 9	6 3	21						Design CBR	2	5	24	
Remarks			Not soaked						See Table 7				See Table 8 Fig 3					

[a] For footnote explanations see Appendix A

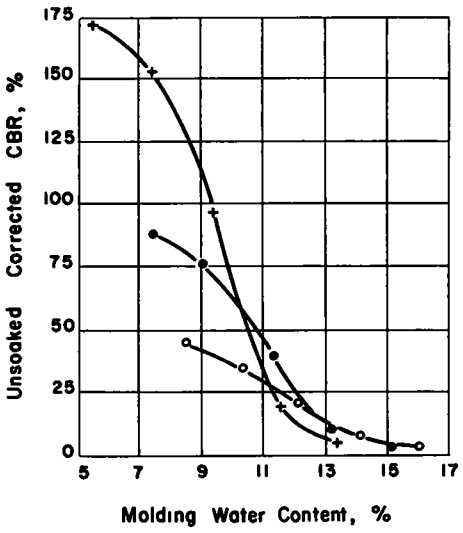

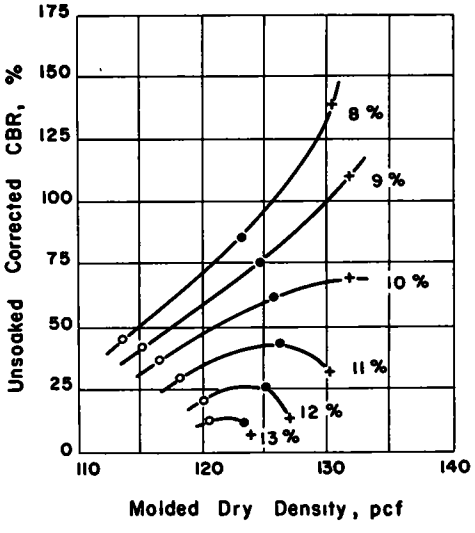

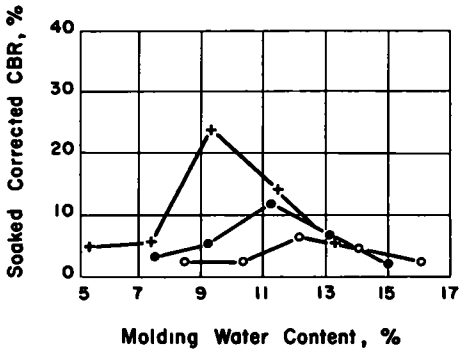

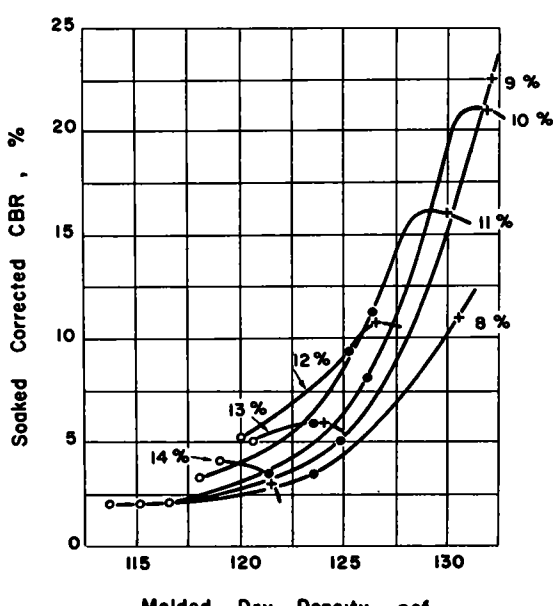

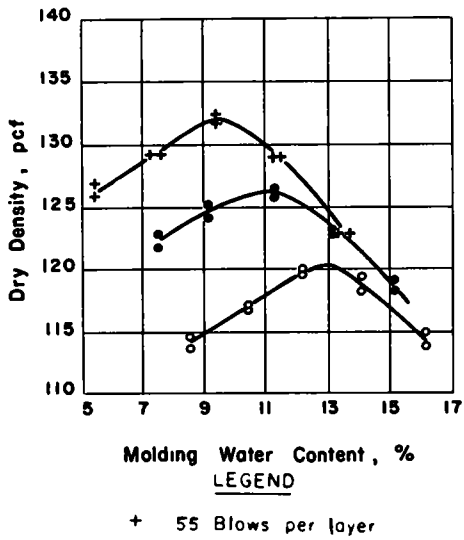

LEGEND

+ 55 Blows per layer

● 26 Blows per layer

○ 12 Blows per layer

NOTES

1 Figure beside curve is molding water content

2 Surcharge equal 20 lb soaking and penetration

3 All samples soaked 4 days

4 All samples compacted in 5 layers, 10 lb hammer, 18-inch drop in CBR mold

Figure 3. CBR tests on embankment soil (Waterways Experiment Station).

were tested unconsolidated and undrained (quick). Two laboratories tested 6- by 12-in. specimens, one 6- by 8-in. specimens. Values for ϕ and c are given, either as reported or as determined by the authors.

Kansas reported on tests which were not tested to failure. Inasmuch as this test is involved in the Kansas method of design, Figure 6 has been prepared to show the stress-strain curve developed. No other stress-strain curves are shown, but strains at failure are given in Table 10.

Results of the standard triaxial test of Texas are reported for two density conditions according to their classification system. The data are plotted in Figure 5.

Unconfined compression, direct shear and consolidation tests on the embankment soil were run by the Ohio Department of Highways. Results of their tests are given in Table 11 and Figure 7. Permeability tests by four agencies are summarized in Table 12.

Results of a study of frost susceptibility of the soil by the Arctic Construction and Frost Effects Laboratory of the U.S. Army Engineer Division, New England, have been included as Appendix B.

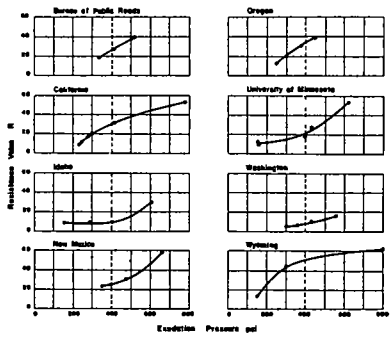

Figure 4. Resistance value vs exudation pressure, embankment soil.

TABLE 6
EFFECT OF SURCHARGE WEIGHT ON CBR OF EMBANKMENT SOIL (INDIANA)

Specimen No	Moist Cont (%)	Dry Dens (pcf)	Moist Cont After Soaking (%)	Swell (%)	Surcharge (lb)	CBR (%) At 0.1-In Pen	CBR (%) At 0.2-In Pen
1	14.2	110.9	16.9	0.38	25	1.8	2.2
2	14.1	111.0	16.9	0.42	25	1.5	1.9
3	14.5	115.7	18.4	0.16	25	4.2	4.5
4	14.5	116.7	15.9	0.18	25	4.3	4.6
5	14.3	99.7	22.4	-1.04	45	0.4	0.4
6	14.6	105.5	19.3	0.02	45	1.1	1.1
7	13.6	108.7	18.3	0.04	45	1.5	1.4
8	14.3	110.0	17.4	0.16	45	2.0	2.1
9	13.8	110.8	16.0	0.24	45	1.8	1.9
10	14.4	112.3	16.3	0.12	45	4.0	3.9
11	14.4	113.0	16.4	0.24	45	2.9	3.1
12	14.6	114.1	16.0	0.14	45	4.1	3.9
13	14.1	115.3	15.3	0.10	45	4.1	4.2
14	13.7	115.7	15.0	0.16	45	4.8	5.0
15	14.5	117.3	15.3	-0.02	45	4.9	5.3
16	14.4	108.1	18.0	0.02	80	2.2	2.1
17	14.4	111.2	16.6	0.08	80	2.4	2.5
18	14.5	115.3	15.4	-0.04	80	4.3	4.5
19	14.8	117.1	15.2	-0.02	80	5.2	5.6

SUBBASE MATERIAL TEST DATA

Description of Material

The subbase material used on the AASHO Road Test was a natural sand-gravel material modified by washing and additions of fine silica sand in the minus No. 40 sieve range and a small amount of binder soil. Its mineral composition is given in Table 13.

Mississippi reported the results of a petrographic analysis of the coarse fraction (retained on No. 4 sieve), about 26 percent of the entire sample. The Bureau of Public Roads reported the composition of the minus 2-micron fraction. None of the analyses reported reflect directly the approximately 18 percent silica sand (99 percent SiO_2) additive.

Test Data

Results of sieve analyses of the subbase material samples are given in Table 14 and Figure 8. Four laboratories reported results of hydrometer analyses, which are shown at the bottom of the table.

Also shown in Table 14 are the methods used in preparing the samples for classification tests. Plasticity indices of the minus No. 40 sieve fraction, specific gravities, maximum densities, and optimum moisture contents are given in Table 15. Specific gravities of the minus No. 4 sieve fraction of the subbase are listed together as G_s or G_a according to the test method used. Where available, bulk specific gravities and absorptions for the coarse fraction are also given.

Optimum moisture content and maximum density were determined by AASHO methods T 99 (using 5.5-lb hammer, 12-in. drop, 25 blows on each of 3 layers) and T 180

TABLE 7

CBR TEST DATA FOR EMBANKMENT SOIL (UNIVERSITY OF MINNESOTA)

Details of Test	Test Data						
Compaction method:							
Dynamic							
Wt. of hammer (lb)	5.5	5.5	5.5	5.5	10	10	10
Drop (in)	12	12	12	12	18	18	18
Layers	3	3	3	3	5	5	5
Blows per layer	56	56	56	56	10	25	56
Testing condition:							
Surcharge weight (lb)	10	10	10	10	10	10	10
Soaking period (days)	4	4	4	4	4	4	4
Molding conditions:							
Dry density (pcf)	116.5	112.5	118.5	119.0	112.2	123.5	128.0
Moisture content (%)	15.6	16.4	13.8	13.9	12.4	11.9	11.6
Optimum conditions: (Table 3)							
Max. dry dens. (T 99)	119.1	-	-	-	-	-	-
Max. dry dens. (T 180)	-	-	-	-	-	-	126.0
Test results:	14.0	-	-	-	-	-	12.0
Final moisture content	15.9	16.2	14.8	14.5	16.1	13.4	12.7
Swell (%)	0.8	0.6	0.3	0.5	3.0	2.7	1.5
CBR at 0.1-in. pen. (soaked)	2.8	2.6	3.7	3.8	1.5	4.5	7.2
CBR at 0.2-in. pen. (soaked)	2.8	2.4	4.0	4.1	1.7	6.4	10.2

TABLE 8

RESULTS OF CBR TESTS ON EMBANKMENT SOIL (WATERWAYS EXPERIMENT STATION) — Tabulation of test data

Before Soaking			After Soaking			
Moisture Content (%)	Density (pcf)	CBR	Moisture Content (%)	Density (pcf)	CBR	Swell (%)
(a) 12 Blows						
8 4	114 8	44	18 0	111 6	2	2 86
10 3	117 0	34	16 6	114 6	2	2 07
12 1	120 0	19	14 7	118 9	6	0 91
14 0	119 5	6	15 1	119 4	4	0 09
16 0	113 8	2	16 9	113 6	2	-0 02
(b) 26 Blows						
7 4	123 1	89	15 5	118 5	3	3 84
9 0	125 4	77	14 6	121 4	5	3 26
11 2	126 8	39	13 1	125 1	12	1 38
13 1	123 3	8	13 8	122 9	5	0 29
15 0	119 2	2	15 4	119 3	2	0 07
(c) 55 Blows						
5 4	127 2	173	14 7	121 5	4	4 66
7 3	129 5	154	13 9	123 9	5	4 48
9 3	132 7	98	11 6	130 1	24	1 98
11 4	129 1	18	12 1	128 8	14	0 24
13 3	123 1	3	13 5	122 9	5	0 18

(using 10-lb hammer, 18-in. drop, 56 blows on each of 5 layers) in most cases. There was, however, variation in the maximum size of material included. In a few cases mathematical corrections for plus No. 4 material were made where only minus No. 4 material was used in the test. Where such information was available, it is given in the table.

Table 16 gives the reported sulfate soundness, Los Angeles abrasion, and sand equivalent test data. Not all laboratories reported the number of cycles or type of sulfate solution used.

California Bearing Ratio test data are given in Table 17. General comments are much the same as for the embankment soil. Again, data for a complete set of CBR curves by the Waterways Experiment Station are reported separately in Table 18 and Figure 9.

Hveem stabilometer test data are given in Table 19. Here the variations in compaction procedures should be noted. Some of the data are plotted in Figure 10.

Table 20 gives test data from triaxial compression tests on the subbase. Plots of deviator stress versus principal stresses are included in Figure 11. Again stress-strain curves reported by Kansas are shown separately. Some agencies did not report values for ϕ and c. Where possible, these were computed by the authors.

Results of permeability tests are given in Table 21.

TABLE 9

HVEEM STABILOMETER TEST DATA FOR EMBANKMENT SOIL*

Agency	Method of Compaction	Molding Moisture Content (%)	Molded Dry Density (pcf)	P_h at p_v = 160 psi	Displacement (turns)	R-Value[44]	Exudation Pressure (psi)	R-Value at 400 psi	Swell Pressure (psi)
	AASHO[42]	11 7	128 0	97	2 70	38	517		2 4
BPR	T 173-56	11 9	127 0	117	2 56	26	401	26	1 9
		11 9	126 0	128	2 84	18	333		0 4
		10 9	130 0	73	2 60	53	780		
		12 0	127 0	110	2 60	30	410		
Calif	AASHO	12 8	126 0	120	3 10	21	300	28	
	T 173-56	13 0	125 0	128	3 00	17	280		
		14 0	122 0	138	3 40	10	240		
		15 0	119 0	142	3 75	8	230		
		11 4	128 0	100	2 55	30	688 5		
		13 1	121 2	130	4 09	9	288 5		
Idaho	-[46]	12 9	121 7	138	3 14	8	405 9	8	
		15 0	115 2	140	4 21	8	159 2		
		10 9	128 0	60	3 02	59	656		
New Mexico	AASHO	11 8	127 0	103	3 15	31	480	26	
	T 173-56	12 4	126 0	107	3 54	26	400		
		12 7	125 0	111	3 56	24	356		
		12 3	124 5	95	2 83	38	350		3 7
Oregon	AASHO	12 6	126 0	105	3 05	30	374	32	2 4
	T 173-56	13 5	124 3	134	3 20	13	255		0 6
		12 1	124 9	75	2 44	53 7	621		0 6
		11 8	118 0	115	2 65	26 9	438		0
Univ of Minn	-[47]	12 3	114 0	130	2 96	16 3	398	21	0
		13 1	117 5	138	3 24	10 9	159		0 2
		14 2	117 9	144	3 16	8 1	167		0
		13 3	121 4	130	2 85	16	560		
Washington	-[48]	13 8	119 7	140	2 95	10	430	9	
		14 3	118 4	145	3 05	7	360		
		15 3	116 2	148	3 65	5	300		
		11 5	127 0	55	2 75	63	800		154
Wyoming	AASHO	12 4	127 0	89	2 50	44	300	50	62
	T 173-56	14 7	120 0	132	3 40	13	150		3

*For footnote explanations see Appendix A

BASE MATERIAL TEST DATA

Description of Material

The base material used on the AASHO Road Test was a crushed dolomitic limestone produced by blending various sizes from the same quarry. Mineral composition, as reported by four agencies, is given in Table 22.

Test Data

Results of sieve analyses and hydrometer analyses are reported in Table 23, as are the methods used for preparing samples for classification tests. Plasticity indices, optimum moistures, and maximum densities are given in Table 24. Both standard (5.5-lb hammer, 12-in. drop, 25 blows on each of 3 layers) and modified (10-lb hammer, 18-in. drop, 56 blows on each of 5 layers) procedures were used. Maximum size aggregate used varied as indicated in the table.

Table 25 gives specific gravities and absorptions. Soundness, Los Angeles abrasion, Deval abrasion, and sand equivalent results are given in Table 26.

Fairly complete California Bearing Ratio test data are given in Table 27. Results of a complete set of CBR curves by the Waterways Experiment Station are reported in Table 28 and Figure 14.

Hveem stabilometer test data are given in Table 29 and plots of R-value versus exudation pressure in Figure 15.

Results of triaxial tests are reported in Table 30 and plots of deviator stress versus principal stresses in Figure 16. The Kansas stress-strain data are shown in Figure 17. It should be noted that Saskatchewan used a closed-system triaxial cell. Some laboratories did not report values for ϕ and c. These were computed by the authors where possible.

Permeabilities are given in Table 31.

DISCUSSION

In previous sections, values reported by the participating agencies have been pre-

TABLE 10

TRIAXIAL TEST DATA FOR EMBANKMENT SOIL

Details of Tests	Agency																																							
	Alabama		Alberta			BPR (A)			BPR (B)			California		FAA			Kansas[a]			Manitoba			Missouri			New Brunswick			North Carolina				Ohio			Oregon			Texas (A)[a]			
	1	1	2	3	1	2	3	1	2	3	1	2	1	2	3	1	2	3	1	2	3	1	2	3	1	2	3	1	2	3	4	1	2	3	1	2	3	1	2	3
Method of compaction																																								
Dynamic	x		x					x															x			x													
Static					x	Double plunger			Double plunger								x	Double plunger				x																		
Kneading											x																														
Initial condition																																								
Molding moisture (%)	14 4		13 2		13 0	13 0	13 0	13 0	13 0	13 0	13 3	13 6		10 6	10 9	10 8	15 5	15 6	15 1		13 0			14 4			13 5	14 2	13 3											
Dry density (pcf)	118 0		119 7		122 0	122 0	122 0	116 0	116 0	116 0	119 0	122 0		128 6	127 6	128 2	119 8	119 6	120 4	123 9	123 9	122 9	105 3			116 5	121 5	122 0											
Initial void ratio, e_o	0 454											0 399					0 45	0 45	0 44	0 359	0 359	0 363	0 612			0 362	0 380	0 357											
Deg of sat (%)																																								
Saturated sample																																								
Yes																	x																							
No	x		x			x			x			x									x			x			x												
Moisture content after sat																																								
Dry density after sat																	16 8	16 6	16 2																					
Deg of sat																																								
Failure condition																																								
Moisture content	15 6		13 1											10 7	10 6	10 8	15 2	15 5	15 2	12 8	12 1	12 1	14 4																	
Void ratio, e_f	0 429																0 41	0 41	0 40							0 269	0 271	0 267											
Confining pres , σ_3 (psi)	10	14 2	28 4	42 7	0	13 9	27 8	0	13 9	27 8	1 73	20 83	0	3	10			20		15	30	45	10	20	40	0	15	30											
Deviator stress, ($\sigma_1 - \sigma_3$)	25 7	49 1	62 3	77 8	62 5	88 0	92 4	40 5	66 6	79 0	29 17	30 28	112	128	159					100	112	122	38 1	55 4	76 1	23 0	34 0	40 4											
Strain (%)	10 3	20 5	13 7	21 6	6	12	14	4	20	18	3 25	6 25	4 4	5 8	6 1					3 5	3 6	3 4	19 6	21 2	20 6														
Type of test						Quick			Quick			Quick																												
Rate of loading (in per min)	0 035					0 08			0 08			0 05		0 05				0 005			0 055			0 1			0 5											
Specimen dimen (in)	1 4 x 2 8		1 48 x 3 6			2 x 4			2 x 4			2 x 4		6 x 12				2 8 x 6			1 38 x 2 99			2 57 x 4 85			2 8 x 5 6											
Reported values*																																								
Angle of friction, ϕ			(19)			(21)			(23)			0									15			(22)			14											
Cohesion, c (psi)			(13)			(24)			(14)			15									35			(8)			9											
Remarks						100 % T 99 Max dens			95 % T 99 Max dens					*avg of 4 tests			*Not tested to failure See Fig 6						*90 % T 99 Max Dens															
*Values in parentheses determined from Fig 5 by authors														*Values in parentheses determined from Fig 5 by authors																									

Details of Tests	Agency																																							
	Texas (A)[a]						Texas (B)[a]						Utah	WES																										
	1	2	3	4	5	6	1	2	3	4	5	6	1	1	2	3																									
Method of compaction																																								
Dynamic				[a]						[a]			x		x																									
Static																																								
Kneading																																								
Initial condition.																																								
Molding moisture (%)	14 5	14 6	14 4	14 5	14 4	14 5	10 3	11 6	10 2	10 7	10 3	10 7	13 5	9 0	9 2	8 8																									
Dry density (pcf)	114 3	114 5	114 5	114 6	114 4	124 3	124 3	125 1	124 7	125 2	125 4	103 5	124 5	127 4	125 4																											
Initial void ratio, e_o														0 379	0 347	0 369																									
Deg of sat (%)														65 5	72 7	65 8																									
Saturated sample																																								
Yes															x																									
No													x																												
Moisture content after sat		16 7	17 0	16 8	16 4	16 5								14 6	15 3	15 2																									
Dry density after sat							15 3	13 9	14 8	14 8	15 1	14 5		120 6	122 8	120 0																									
Deg of sat														94 8	100	96 8																									
Failure condition																																								
Moisture content														14 6	15 3	15 2																									
Void ratio, e_f													0 369	0 423	0 399	0 431																									
Confining pres , σ_3 (psi)	0	3 7	5 9	10 8	15 9	20 9	10	6 95	13 89	27 78																															
Deviator stress, ($\sigma_1 - \sigma_3$)	10 8	37 9	25 8	35 0	35 4	49 4	100	29 72	24 72	25 56																															
Strain (%)	4 38	7 85	7 55	7 70	7 53	7 61	20	12	13	16																															
Type of test															Quick																									
Rate of loading (in per min)													0 5																											
Specimen dimen (in)			6 x 8					6 x8					2 x 4		5 6 x 12																									
Reported values*																																								
Angle of friction, ϕ															0																									
Cohesion, c (psi)			Texas classification = 5 6					Texas classification = 4 7							13																									
Remarks			Compactive effort = 3 66 pcf *THD 83					Compactive effort = 13 26 pcf * THD 83																																	
*Values in parentheses determined from Fig 5 by authors																																								

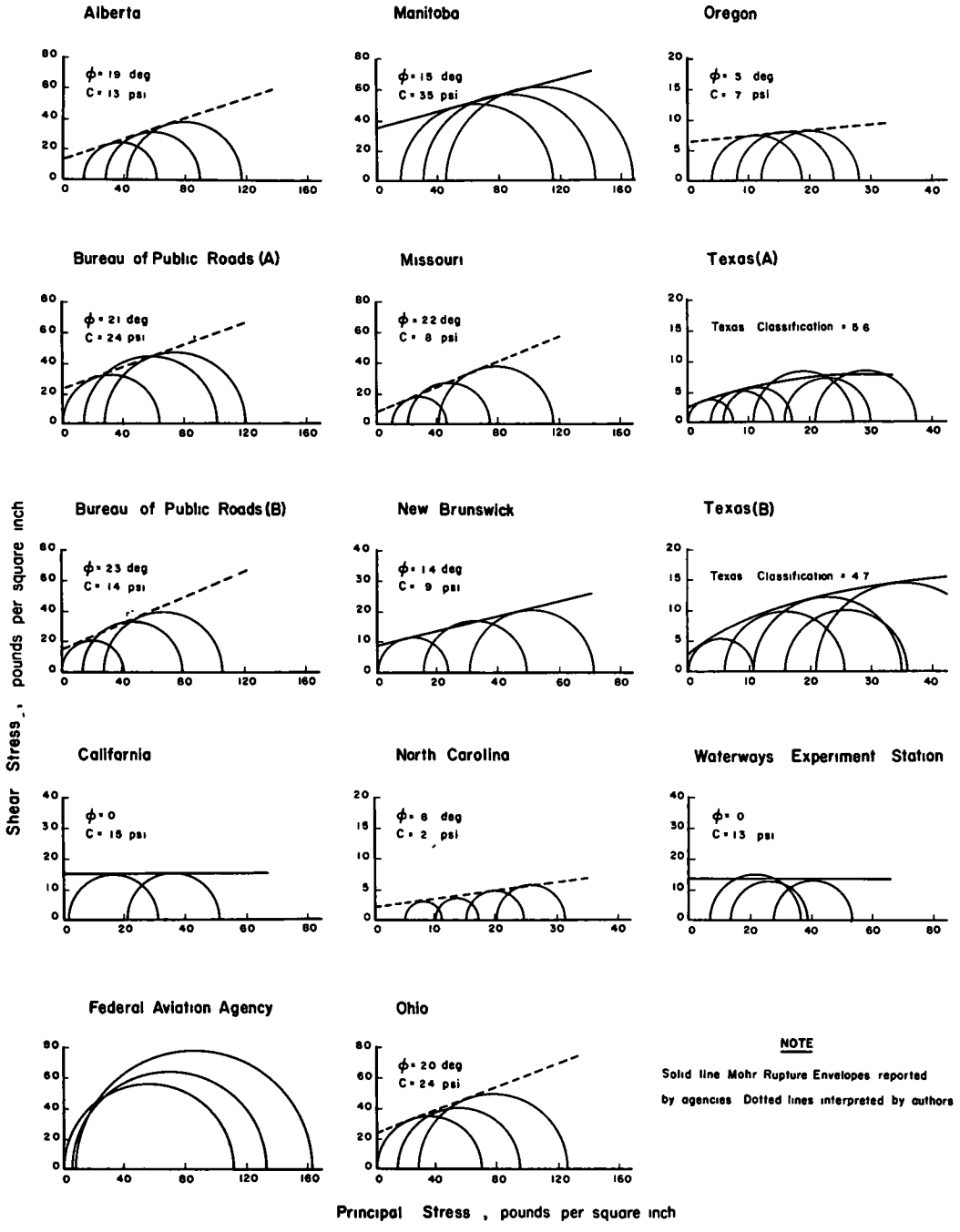

Figure 5. Mohr rupture envelopes for embankment soil.

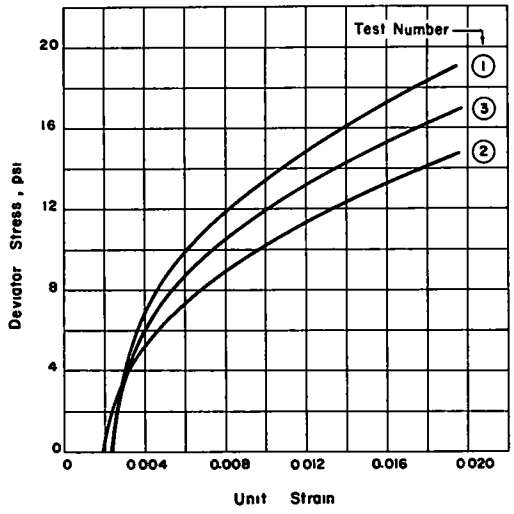

Figure 6. Stress-strain curves for triaxial tests on embankment soil (Kansas).

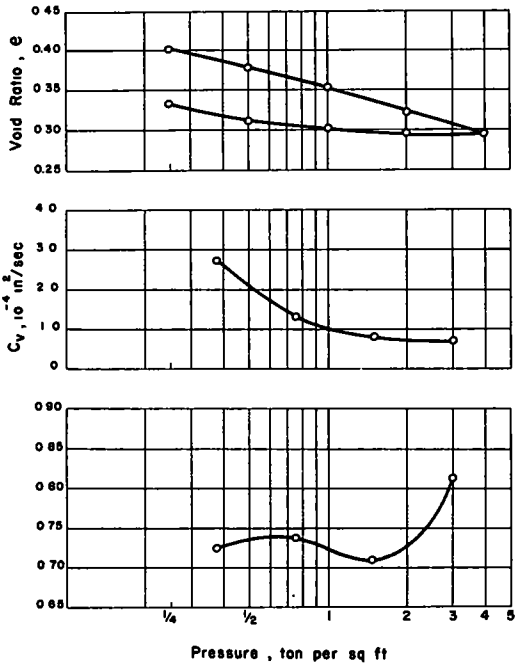

Figure 7. Consolidation test on embankment soil (Ohio).

TABLE 11

UNCONFINED COMPRESSION, DIRECT SHEAR, AND CONSOLIDATING TESTS ON EMBANKMENT SOIL (OHIO)

Item	Unconfined Comp.	Direct Shear	Consolidation (See Fig. 7)					
Compaction Method	ASTM	D 698-57 T[16]						
Moisture content (%)	12.5	12.2						
Dry density (pcf)	117.6	118.5						
Size of sample:								
Diameter (in.)	1.75	2.5						
Height (in)	4.5	1.0						
Loading Rate (in. per min)		0.02						
Comp. Str. (psi)	42.0							
ϕ (deg)		24						
C (psi)		10.4						
Vertical load (psi)			0	3.5	6.9	13.9	27.8	55.5
Void ratio			0.369	0.404	0.379	0.352	0 321	0.294
Vertical load (psi)			27.8	13.9	6 9	3.5	0	
Void ratio			0.296	0.301	0.312	0.335	0.340	
Vertical load (psi)			5.2	10.4	20 8	41.7		
C_v (in² per sec)			2.7×10^{-4}	1.3	0.8	0.7		
r			0.72	0.74	0.71	0.81		

TABLE 12

PERMEABILITY TESTS ON EMBANKMENT SOIL

Item	ACFEL			NB		Oregon				PCA
Type of test	Falling head, de-aired water, saturated specimens, 10° C			Constant head		20° C				-
Dry density (pcf)	-			117 5		-				114 0
Moisture content (%)	-			13 5		-				15 5
Void ratio, e	0 484	0 568	0 616	0 42	0 417	0 467	0 512	0 557	0 595	0 47
Permeability, K (cm per sec)	0.62 x 10^{-6}	3 1 x 10^{-6}	6 6 x 10^{-6}	4 1 x 10^{-6}	0 073 x 10^{-7}	0 108 x 10^{-7}	0 138 x 10^{-7}	0 188 x 10^{-7}	0 250 x 10^{-7}	6 3 x 10^{-7}

TABLE 13

MINERAL COMPOSITION* OF SUBBASE MATERIAL

Constituent	BPR	Mass.	Miss.	Nebr.
Size examined	minus 2 micron	-	1½"-No. 4	-
Shale	-	-	3	-
Dolomite	-	-	84	-
Chert	-	-	6	-
Miscellaneous	-	-	7	-
Kaolinite and vermiculite	10 - 15	-	-	-
Illite	40 - 50	-	-	-
Montmorillate	30 - 35	-	-	-
Quartz	10	-	-	-
Organic (loss on ignition)	-	6.1	-	-
Silt**	-	-	6	6
Clay	-	-	4	2
Colloid	-	-	2	1

*Approximate percentages.
**Criteria for size classification not reported.

sented generally as received and with a minimum of interpretation. In some cases reasonable agreement was noted between the different laboratories. In others there was considerable difference in values reported for the same test. Some test data also were reported incompletely. It is assumed, therefore, that readers may wish to interpret the information included in these sections for themselves. To facilitate this, much otherwise extraneous information has been included in the tabulations.

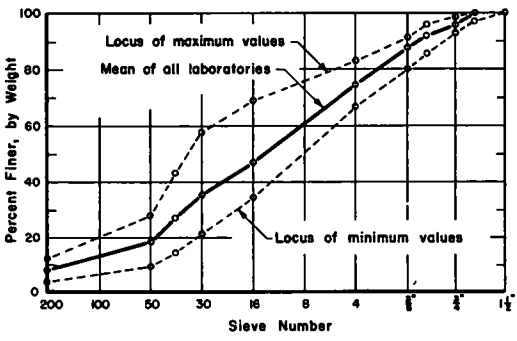

Figure 8. Grading curve for subbase.

In the following paragraphs the authors have made selections from the information available and summarized them to indicate the main characteristics of the materials. Exclusions were made for a variety of reasons, including great variability in either method or results, incompleteness, or lack of general applicability. Some discussion of the variability in reported values for the selected tests is included.

Mineral composition of the three materials was not reported upon generally; however, for the few reports received, there was little disagreement. Taken together they present a reasonable picture consistent with other information available on the parent material.

TABLE 14

MECHANICAL ANALYSES OF SUBBASE MATERIAL*

Agency	Method of Prep	Percent Finer Than[4]											
		1½"	1"	3/4"	1/2"	3/8"	No 4	No 16	No 30	No 40	No 50	No 200[5]	No 200**
Rd Test	T 87[2]	100	100	98 3	91 8	90 2	73 8	-	-	22 8	-	7 4	8 0
Ala	-	100	99 1	95 9	92 1	86 8	72 7	46 9	38 3	30 2	19 5	8 0	8 1
Alta	T 146[2]	100	100	97	91	87	72	42	33	25	17	7 4	7 4
Ariz	T 87	100	100	98	93	88	73	42	33	25	16	-	7
AI	T 87	100	100	98	93	88	76	46	37	-	18	7	8
Banff	T 87	100	98 2	97 9	93 1	89 0	74 0	44 0	31 5	24 5	19 0	-	7 0
BPR	T 87	100	100	98	93	89	75	47	35	29	21	-	8
Calif	T 87	100	100	97	92	88	74	46	37	25	19	-	8
Del	-	100	100	93 3	87 7	81 8	-	-	-	-	-	-	-
FAA	T 87	100	100	96	93	90	80	51	35	29	20	-	8
Fla	-	100	100	97	92	86	83	48	38	28	18	7 9	8 3
Ga	T 87	100	99 0	97 0	90 0	83 0	76 0	54 7	41 4	29 9	18 6	11 9	-
Hawaii	T 146	100	99	97	94	88	73	48	37	30	25	9	-
Ida	T 87	100	100	97	92	-	71	-	36	27	17	-	8
Ill	T 146	100	100	98	94	89	76	45	35	27	18	-	5 9
Kan	-[53]	100	100	98	-	89	76	47	37	31	18	-	8 2
Ky	D 421[2]	100	99 2	96 7	91 0	85 4	70 0	37 0	21 3	14 8	9 8	6 0	6 1
La	T 87	100	99	98	93	88	80	54	44	29	22	8	9
Me	-	-	-	-	94	90	76	44	31	25	17	6 8	6 8
Md	T 87	100	99 5	97 8	92 7	87 2	73 7	54 0	29 7	22 0	11 3	-	4 0
Mass	T 146	100	100	97 5	93 4	88 5	77 0	50 4	40 7	31 0	22 3	7 1	8 7
Mich	T 146	100	100	95 7	91 3	88 9	80 2	53 6	43 0	33 1	21 8	-	11 6
Miss	-	100	99 5	96 6	-	88 3	78 1	51 5	41 4	32 8	20 6	-	10 0
Mo	T 87	100	99 6	97 1	90 5	83 9	66 9	-	-	20 7	-	-	5 8
Nebr	T 87	100	100	97	96	90	78	47	37	28	18	8	8
Nev	T 87	100	98 5	94 6	90 7	86 0	71 6	44 3	34 8	24 1	16 5	7 7	7 7
NB	T 87	100	100	94 1	88 4	85 3	71 6	43 0	33 8	23 0	15 8	7 6	7 6
NJ	T 87	100	99	98	92	88	75	46	37	29	20	11 2	11 5
NM	T 87	100	100	97 9	93 0	88 5	73 5	45 0	34 5	27 9	20 8	-	7 0
NY	T 87	100	99 4	95 4	91 8	86 0	76 0	-	-	31 3	-	-	8 8
NC	T 87	100	100	97 7	93 1	89 0	72 5	44 4	35 2	26 8	17 5	7 3	8 0
N Dak	T 87	100	99 6	97 6	94 2	90 4	79 2	34 4	26 4	18 9	11 2	3 7	8 0
Ohio	T 87	100	99	96	92	86	70	40	31	23	14	6	-
Okla	T 87	100	100	96	93	88	71	42	33	26	17	8 3	8 9
Omaha	-	100	100	95 8	90 0	87 0	73 0	40 0	27 0	21 0	17 0	7 0	-
Ont	T 87	100	100	96	90	86	72	46	35	26	15	5 7	6 0
Oreg	T 87	100	99 4	97 8	93 6	88 9	75 0	44 6	35 3	27 6	18 1	-	7 8
PCA	-	100	-	98	95	-	75	-	-	30	-	7 5	-
Pa	T 87	100	99	94	89	84	69	60	49	39	27	12 5	13 2
PR	T 87	100	99	97	92	87	71	69	58	43	28	12	-
Sask	T 146	100	-	95	-	-	70	40	27	23	-	-	13
Tex	T 146	100	98	96	90	86	72	45	32	25	19	7	-
U Minn	-	100	97 9	94 4	85 9	79 9	71 3	42 2	33 7	26 0	16 5	7 1	7 2
Utah	T 87	100	99 5	97 4	92 6	87 8	74 8	39 0	32 8	24 7	15 9	7 1	7 1
Va	T 87	100	99	97	91	86	70	41	29	25	19	-	7
Wash	T 87	100	100	95	89	85	71	53	36	28	19	-	9
WES	-	100	99 7	98 1	93 7	89 3	75 4	50 4	40 5	30 7	20 9	9 2	10 0
Wis	T 146	100	100	97	92	88	73	44	35	26	16	-	7 5
Wyo	T 87	100	99 4	96 3	91 5	86 7	73 1	49 1	38.6	30 7	19 5	8 3	9 1
No of tests		35	46	48	46	46	48	43	44	47	43	29	41
Mean		100	99 5	96 7	91 9	87 2	74 0	46 5	35 6	27 1	18 4	7 9	8 2
Std dev		0	0 6	1 3	1 9	2 2	3 3	6 2	6 1	4 7	3 6	1 9	1 8

	0 05 mm	0 02 mm	0 005 mm	0 002 mm
	Hydrometer analyses			
Hawaii	5	3	2	1
Me	6	4	2	1
PCA	7	6	4	2
Texas	6	4	2	1
Average	6	4	2	1

*For footnote explanations see Appendix A
**Includes additional dry sieving after washing over No. 200 sieve

TABLE 15

PLASTICITY INDEX, SPECIFIC GRAVITY, AND MOISTURE-DENSITY RELATIONSHIP OF SUBBASE MATERIAL*

Agency	Plasticity Index, PI [7]	Specific Gravity F A Method	F A G_s / G_a	C A Method	C A G_m	C A G_a / G_s	C A Abs	Moisture-Density Relationship Method	Max Size	W_o	D_{max}
Rd Test	N P	T 84[11]	2 73	T 85[12]	2 55	2 76	3 0	T 99[26]	½"	7 9	137
Ala	1 0	T 100[6]	2 64	T 100	-	2 54	-	T 180[17]	-	7 1	137 4
Alta	N P	T 100	2 81	T 85	-	2 74	-	D 698-D[16]	¾"	7 0	142 1
Ariz	N P	T 84	2 74	T 85	-	2 67	-	T 99	-	5 5	135 5
Al	N P	T 84	2 72	T 85	-	2 76	-	T 99[27]	-	7 5	132 4
Banff	N P	T 100	2 63	T 100	-	2 69	-	T 99	No 4	7 4	131 8
BPR	N P	T 100	2 72	-	-	-	-	T 99-A	No 4	9	133
Calif	N P	T 133[9]	2 71	T 85	2 54	-	-	C 216-C[15]	¾ in	6 0	145
Del	N P	-	-	-	-	-	-	T 180	-	7 8	135 9
FAA	N P	T 100	2 70	T 85	-	2 78	-	T 180	-	8 0	133
Fla	N P	-	-	-	-	-	-	T 99	-	6 8	128 0
Ga	N P.	T 100	2 83	T 85	2 55	2 75	3 1	T 99	-	8	130
Hawaii	3 0	T 84	2 70	T 85	2 52	-	-	-[23]	-	6 2	142 0
Ida	N P	T 84	2 70	-	-	-	-	-	-	-	-
Ill	N P	-	-	-	-	-	-	T 99[26]	½"	7 5	136 9
Kan	1 0	-	-	T 85	2 55	-	2 9	-[28]	¾"	7	136
Ky	0 6	T 100	2 67	T 100	-	2 72	-	T 99	-	5 8	140 3
La	N P	T 100	2 76	T 100	-	2 78	-	T 99	-	6 6	129 9
Me	N P	T 100	2 70	-	-	-	-	T 180-A	No 4	7 5	138 7
Md	N P	-	-	T 85	-	2 62	-	T 99	¾"	8 7	130 5
Mass	-	T 100	2 82	T 100	-	2 74	-	T 99	-	7 3	136 5
Mich	N P	T 100	2 70	T 85	2 46	2 63	2 7	T 99	-	8 2	132 3
Miss	N P	-	2 70	-	-	2 63	-	-[29]	-	6 2	136 4
Mo	N P	T 100	2 71	T 100	-	2 59	2 6	T 99	all	6 6	138 7
								T 99	No 4	8 6	129 6
Nebr	N P	T 100	2 75	T 100	-	2 76	-	T 99	-	8 2	132 9
Nev	N P	T 100	Composite Sample		-	2 67	-	C 216-C	¾"	6	140 7
N B	N P	T 100	2.69	T 85	-	2 58	-	T 99	No 4	10 5	130
									corr ***		138 5
N J	N P	T 100	2 63	-	-	-	-	T 99	-	10	130
N M.	N P	T 84	2 67	T 85	-	2 73	-	T 99	-	7 2	136 6
								T 180	-	6 6	139 4
N Y	N P	T 100	2 72	T 85	(2 62 - 88 D)			T 99	¾"	7 0	135 7
								T 99	½"	8 0	133 5
								T 180	¾"	7 5	139 3
N C	N P	-	2 69	T 85	-	2 77	-	T 99	-	6 5	135 8
N Dak	3 4	T 84	2 72	T 85	-	2 75	-	T 99	-	7 8	127 8
Ohio	N P	C 128[11]	2 67	T 14	-	2 62	-	D 698	-	7 0	134 8
Okla	1 0	T 100	2 77	T 85	-	2 64	-	T 99	No 4	7 8	131 2
									corr +		139 5
Omaha	N P	-	-	-	-	-	-	T 99	-	7 5	136 1
Ont	N P	T 100	2 74	T 85	-	2.67	-	T 99	No 4	8 0	129 0
								T 99	all	7 4	133 5
Oreg	N P	T 133	2 73	T 133	-	2 81	-	-[21]	No 4	10 7	131 2
PCA	N P	-	-	-	-	-	-	T 99	-	7 0	136.5
Pa	1 0	T 100	2 77	T 85	-	2 60	-	T 99	-	8 7	131 6
P R.	N P	D 854[9]	2 67	D 854	-	2 64	-	T 180	¾"	6 5	135 1
Sask.	N P	-	-	-	-	-	-	T 99	-	6 8	137 5
Tex	0 2	T 100	2 69	-	-	-	-	THD 83[22]	-	6 9	135 8
U Minn	N P	T 128	2 64	T 127[13]	-	2 65	-	T 99	-	7 2	135 0
								T 180	-	7 0	139 0
Utah	N P.	T 100	2.62	T 85	-	2 66	-	T 99	No 4	8 4	130 6
Va	N P	T 100	2 71	T 100	-	2 76	-	T 99	-	8 6	130 0
Wash	N P	D 854	2 68	C 127	-	2 74	-	T 99	No 4	8 5	129
								-[28]		8 5	136
WES	**	C 128	2 74	C 127	-	2 73	-	T 180	-	7 0	139 0
Wis	N P	T 84	2 61	T 85	-	2 53	-	T 180	-	6 3	139 4
Wyo	N P	-	2 64	-	-	2 67	-	T 99	-	8 3	134 0
No of Test			40			34				35	35
Mean			2 70			2.69		T 99		7 7	133 1
Std Dev			0 05			0 07				1 0	3 3

*For footnote explanations see Appendix A.
**Reported minus 1.0.
***Corrected for plus No. 4 material.

TABLE 16

SOUNDNESS, ABRASION, AND SAND EQUIVALENT OF SUBBASE MATERIAL*

Agency	Soundness[38] Type of Solution	No of Cycles	Loss (%) C.A.	Loss (%) F A	Loss (%) Total	Abrasion[40] Grading	Abrasion[40] Wear** (%)	Sand[31] Equiv
Ariz.								51
Calif								47
FAA							33	
Ida.								40
Kan						C	29 4	
Md.			14 2	2.2			32.7	43
N M	$MgSO_4$				8.0	B	28.0	
N.Y	$MgSO_4$	4	16 8					
		10	39 2					
N.Dak.			3.8	3 3				
Ont	$MgSO_4$	5	6 3	15 3		C	25 0	
Oreg.	Na_2SO_4				0.2	B	35 4	
Wash.								73
Average							31	51

*For footnote explanations see Appendix A
**500 revolutions.

Selected classification and quality tests are summarized in Table 32. Included are the Atterberg limits, moisture-density relationships at optimum conditions, apparent specific gravities, selected sizes from mechanical analyses, and results of sand equivalent, Los Angeles abrasion, and 5-cycle sodium sulfate soundness tests.

It will be noted from Table 3 that most laboratories classified the embankment soil in the A-6 category, with variations in group index values. Variations in group index largely reflected differences in liquid and plastic limits. Of the 59 agencies reporting, one reported a plasticity index below 10 and one above 16. The average PI was 12.6, with a standard deviation of 1.8. Coefficients of variation (standard deviation times 100 divided by the mean) were 6.9, 9.3, and 14.0, respectively, for LL, PL and PI.

Most of the agencies reporting classified the minus No. 40 fraction of the subbase and base as non-plastic. However, of those reporting, 17 percent gave PI values from 0.2 to 3.4 for the subbase and 29 percent from 0 to 4.3 for the base. In both cases one reported a minus PI.

Methods for determining specific gravity varied somewhat for each material and between materials. Nevertheless, most of those reporting gave a value which might be considered the apparent specific gravity. The average standard deviation associated with mean apparent specific gravity values from Tables 3, 15 or 25 was 0.05. This means that approximately 68 percent of the laboratories deviated from the mean values in Table 32 by as much as $\pm$ 0.05. The total range was, of course, greater. It is difficult to say what part differences among samples, methods of test, and laboratory techniques had in this variation; but the effects on computed degrees of saturation, for instance, are obvious.

Average values for selected sizes in the grain-size distribution curve are given in Table 32. Means and standard deviations for all sizes are given in Tables 2, 14 and 23. While distributions of tests on sizes on the ends of grain-size curves are not usually normal, the standard deviations do give an idea of the dispersion of the tests. Standard deviations for middle sizes (30 to 60 percent passing) were about 15 percent of the mean or less for the base material, up to 25 percent for the subbase material, and, except for the 0.002-mm fraction, less than 15 percent for the soil.

These and similar computations for each size may be compared to the following extracted from HRB Special Report 61 B (2). From 170 tests made during the production of the 33,700 tons of base material used in constructing the flexible pavements, these values were obtained:

TABLE 17

CALIFORNIA BEARING RATIO TEST DATA FOR SUBBASE MATERIAL*

Details of Test	Ala	Alta	Al	BPR 1	BPR 2	BPR 3	Hawaii	Ill	Ky	Md	Mass	Miss 1	Miss 2	Miss 3	Mo	N J	N Y
Compaction method.																	
Dynamic[82]		x	x[27]		x		x[28]			x	x		x[19]				x
Wt of hammer (lb)		5 5	10		5 9[27]					5 5	5 5						5 5
Drop (in.)		12	18		12					12	12						12
No layers		3	5		4					3	3						3
No blows per layer		55	12	15	25	45				55	55	10	25	55			56
Static, 3,000 psi[24]	x							x	x						x To desired density	x	
Testing conditions																	
Surcharge, weight, (lb)	10	10	10		10		10	10	17 4	10	10		10		10	12 5	10
Soaking period (days)	4	4	4		4		11	4	7	4			4		1	4	4
Molding conditions																	
Dry density (pcf)	134 0	141 4	131 8	126 6	133 6	134 2	135 0	133 3	140 3	134 1	136 5	135 1	137 0	138 9	116 6	130	131 5
Moisture content, (%)	6 3	7 0	7 5	8 7	7 4	7 8	5 5	7 5	5 8	7 5	7 4	6 6	6 3	6 0	8 8	10	7 6
Optimum conditions																	
(Table 15)																	
Max dry den (T 99)			132 4		133 0			136 9[24]	140 3	130 5	136 5		136 4[19]		129 6*	130	138
Max dry den (T 180)	137 4	142 1					142 2[23]										
Opt moisture content	7 1	7 0	7 5		9 0		6 2	7 5	5 8	8 7	7 3		6 2		8.6	10	7 0
Test results																	
Final moisture content	8 7	7 4	7 6				11 7	8 1	7 3	7 3		6 8	6 7	6 3	12 0		8 0
Swell, (%)	0 2	0 0	0 0	0 0	0 0	0 0	0 2	0 0	0 0	0 0		0 0	0 0	0 0	0 0		0 0
CBR at 0 1 in penetration (soaked)		100+					45		20 at 0 5 in		27	66	96	116	7 0 at 90%*	53 pen not given	28
CBR at 0 2 in penetration (soaked)	4 9		54	18	32	76		33		62	62	penetration not given					47
Remarks															*Minus No 4 only		

* For footnote explanations see Appendix A

Details of Test	N C.	Ohio	Okla.	PCA	Pa.	PR	Sask	U Minn 1	U Minn 2	Utah	Va.	WES	Wis 1	Wis 2	Wis 3	Wyo
Compaction method.																
Dynamic[83]	x	x		x	x	x	x	x	x		x	x				
Wt of hammer (lb)	5 5	5 5		5 5	10	10	5 5	5 5	10		5 5	10		10		
Drop (in)	12	12		12	18	18	12	12	18		12	18		18		
No layers	3	3		3	5	5	3	3	3		5	5		5		
No blows per layer	56	56		55	55	55	56	56	56		45	Variable	10	25	55	
Static, 3,000 psi[82]			x							x						x[82]
Testing conditions																
Surcharge, weight, (lb)	10	21 2	10	15	10	10	20	10	10	12	10	20				10
Soaking period (days)	4	4	4	4	4	4	4	4	4	4	4	4				4
Molding conditions																
Dry density (pcf)	134 5	134 7	136 5	136 5	136 8	137 9	137 5	132 2	134 2	136 7	137 6		131 1	133 8	138 0	129 3
Moisture content, (%)	7 5	5 2	5 7	7 0	7 0	5 8	6 8	7 1	6 8	7 3	7 7		6 3	6 3	6 3	7.2
Optimum conditions																
(Table 15)																
Max dry den (T 99)	135 8	134 8	139 5	136 5	131 6		137 5	135 0		130 6	130 0					134 0
Max dry den (T 180)						135 1						139 0		139 4		
Opt moisture content	8 5	7 0		7 0	8 7	6 5	6 8	7 2		8 4	8 6	7 0		6 3		8 3
Test results																
Final moisture content	7 5	5 7		8 3	7 2			7 9	7 4		8 2		7 7	7 2	6 7	8 3
Swell, (%)	0 0	0 0	0 0	0 0	0 0			0 0	0 0		0 0		0 0	0 0	0 0	0 0
CBR at 0 1 in penetration (soaked)		16	77	37	40		99	42	47	144	95 at 0 3 in					41
CBR at 0 2 in penetration (soaked)	80			pen not given	65	100		53	62				65	86	163	
Remarks												See Table 16, Fig 9				

* For footnote explanations see

TABLE 18

RESULTS OF CBR TESTS ON SUBBASE MATERIAL (WATERWAYS EXPERIMENT STATION)

Before Soaking			After Soaking			
Moisture Content (%)	Density (pcf)	CBR	Moisture Content (%)	Density (pcf)	CBR	Swell (%)
(a) 12 Blows						
0.3	128.9	57	8.9	129.2	29	-0.24
2.6	127.0	38	9.6	127.2	11	-0.18
5.5	130.4	58	8.8	130.4	40	0
8.0	130.6	80	8.6	130.7	68	-0.04
10.2	132.0	54	10.4	132.0	53	0.02
(b) 26 Blows						
0.3	130.8	58	8.8	131.2	22	-0.31
2.5	127.9	36	9.3	128.6	33	-0.53
5.3	132.4	64	8.5	132.7	76	-0.22
7.6	135.9	79	8.2	136.0	28	-0.04
9.4	134.2	27	9.1	135.5	8	-0.49
(c) 55 Blows						
0.3	136.2	178	7.7	136.2	75	-0.04
2.1	133.4	111	8.3	133.6	39	-0.13
4.0	136.3	157	7.8	136.5	100	-0.13
5.8	138.3	190	7.0	138.5	123	-0.18
7.7	139.1	102	7.7	139.3	100	-0.13

TABLE 19

HVEEM STABILOMETER TEST DATA FOR SUBBASE MATERIAL*

Agency	Method of Compaction	Molding Moisture Content (%)	Molded Dry Density (pcf)	P_h at p_v = 160 psi	Displacement	R-Value[45]	Exudation Pressure (psi)	Avg. R-value at 400 psi
AI	Kneading, 36 tamps at 200 psi ft pressure	5.5	133.4	32	3.25	76		
		6.5	133 5	26	3.47	79		
		7.5	134 6	28	3.78	76		77
BPR	AASHO T 173-56[42]	7.0		24**	3.94	78 5		
		6.5		22	4.05	79.5		
		6 9		19	4.08	82.0		80
Calif.	AASHO T 173-56	7.0	135.0	15	3.50	85	790 0	
		7.4	136 0	14	3 60	88	430 0	
		7.8	136 0	23	3.40	81	160.0	84
		8.2	135.0	20	3.60	83	70.0	
		8 7	136 0	21	3.25	80	60 0	
Idaho	—[46]	5 6	135 6	28	4.20	70	461 6	
		5 1	135 0	29	3.95	70	580 9	
		6.5	136.1	29	3.79	71	278.5	69
		7.5	136 8	31	5.54	60	198 9	
New Mexico	California kneading	7 3	127 0	19	3.72	83	764.0	
		7 7	134.0	20	3 79	83	384 0	
		8 0	133 0	22	3 80	82	400 0	81
		8 2	133 0	23	3.83	82	208 0	
Oregon		6.9	137.3	30	3 61	75	191 0	
		6.5	139.5	27	3.79	77	235.0	78
		6.2	137.9	23	3 58	81	700.0	
U. Minn.	—[47]	7 0	132 5	20	4 48	80	636.6	
		7 1	130 1	27	3 79	76	270.6	78
		6.5	126 0	26	5 02	72	206.9	
Wash	—[45]	6.9	132.9	27	3.61	77	460	
		7.0	131.4	29	3.56	76	300	76
		7.2	133.0	29	3 75	75	220	
Wyoming	AASHO T 173-56	6.6	130.1	19	4.20	83	800	
		7.2	133.0	24	4 15	80	400	80
		7.8	134.5	33	4 30	72	100	

* For footnote explanations see Appendix A.

** P_v = 167 psi.

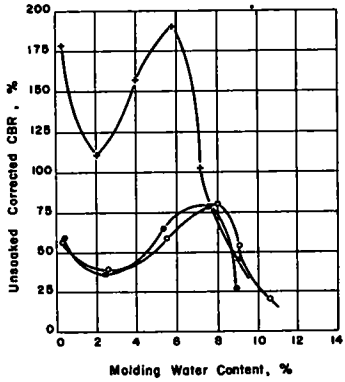

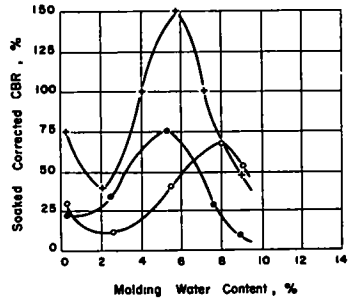

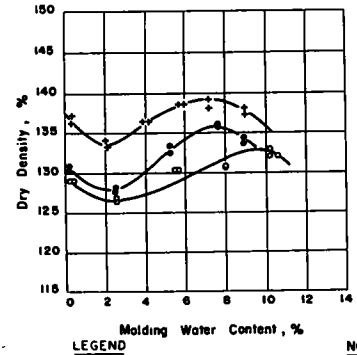

LEGEND

\+ 55 Blows per layer
• 26 Blows per layer
o 12 Blows per layer

NOTES

1. Figure beside curve is molding water content
2. Surcharge equal 20lb soaking and penetration
3. All samples soaked 4 days
4. All samples compacted in 5 layers, 10lb hammer, 18-inch drop in CBR mold

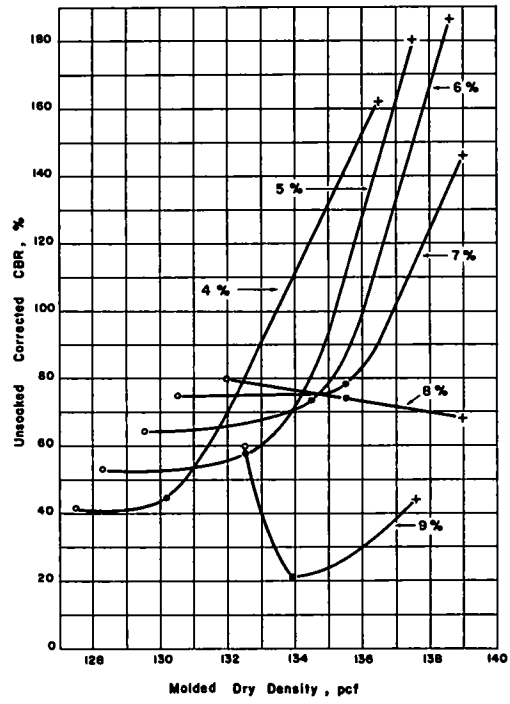

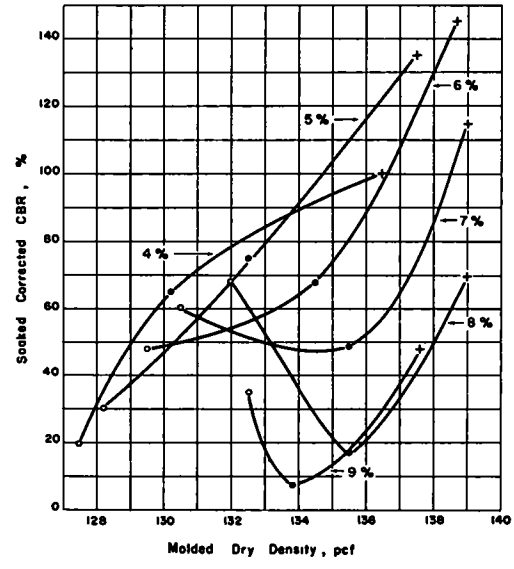

Figure 9. CBR tests on subbase, (Waterways Experiment Station).

TABLE 20

TRIAXIAL COMPRESSION TEST DATE FOR SUBBASE MATERIAL*

Details of Test	Agency																							
	Alberta			FAA			Kansas		Missouri			PCA	Saskatchewan	Texas						Utah			WES		
	1	2	3	1	2	3	1	2	1	2	3			1	2	3	4	5	6	1	2	3	1	2	3
Method of compaction.																									
Dynamic		x**			x					x		x	x			x**					x			x	
Static							x**																		
Portion of sample tested		-¾"					Dbl Plunger Total			-No 4											-No 4				
Initial condition.																									
Molding moisture (%)		6.7		6.7	6.9	6.9	7.3	7.0		8.6		7.0	6.8			6.9					8.4		6.9	7.0	6.8
Dry density (pcf)		142.0		140.6	140.1	140.8	132.2	132.7		118.6		136.5	137.5			135.9					126.0		132.1	131.5	132.1
Initial void ratio, e_o							0.29	0.30		0.407											0.325		0.295	0.301	0.295
Deg. of saturation (%)																							63.8	63.7	62.7
Saturated sample																									
Yes													x	x Capillary Moisture										x	
No		x					x					x									x				
Moisture content after sat							10.7	11.1															7.7	7.6	7.6
Deg. of sat																							71.4	69.4	70.8
Failure condition.							*																		
Moisture content							8.3	8.5	9.9	10.3	9.1										6.2		7.7	7.6	7.6
Void ratio							34	25															0.298	0.301	0.295
Confining pressure σ_3 (psi)	4	8	12	0	3	10	20	20	10	20	40	5 10, 15		0.0	3.7	5.7	10.7	15.7	20.7	13.9	25.0	40.0	7.0	13.9	27.8
Deviator stress $\sigma_1 - \sigma_3$ (psi)	61	86	140	6.8	27.1	62.4			45.6	72.6	117.0			9.7	29.6	43.8	73.3	114.3	128.6	0.94	1.22	1.06	44.3	73.3	115.6
Strain (%)	4.1	4.4	3.1	0.50	0.35	0.31			3.5	13.5	5.3			0.6	1.8	2.2	2.7	2.6	3.1		5.0				
Type of test																									
Rate of load app. (in. per min)		100 lb per min			0.05		0.1			0.1											0.05			0.08	
Specimen dimen. (in.)		6 x 14.5			6 x 12		4 x 8			2.87 x 4.85			4 x 8			6 x8					1.94 x 4.0			5.6 x 12.0	
Reported values:**																									
Angle of friction, ϕ°		(37)			(47)					(33)		45	40								1			40	
Cohesion, C, psi		(1)			(2)					(6)		1	2			Texas Classification = 3.7					0.3			5	
Remarks							*Not tested to failure, see Fig. 12						*See Fig. 11 Closed system triaxial test			Compactive effort = 13.26 ft-lb per cu in.									

* For footnote explanations see Appendix A.
** Values in parentheses determined from Fig. 11 by authors.

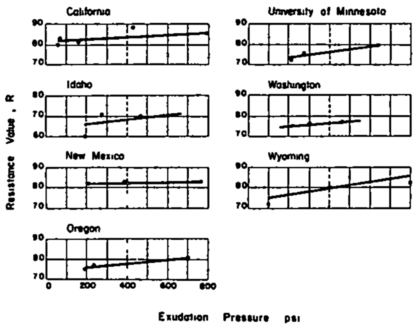

Figure 10. Resistance value vs exudation pressure, subbase.

Sieve Size	Mean	Std. Deviation Value	Percent of Mean
½ in.	68	3.5	5
No. 4	48	2.2	5
No. 40	20	0.9	4
No. 200	10	0.6	6

Only one agency reported a sand equivalent value for the soil. Values ranging from 40 to 73 were reported for the subbase, and 41 to 54 for the base sample. Averages for the sand equivalent, sodium sulfate, and Los Angeles abrasion tests are included in Table 32.

Considerable variations in procedure were noted for the methods used to determine maximum density and optimum moisture content. Table 32 includes the mean values for those tests reportedly run according to AASHO Method T 99 (5.5-lb hammer, 12-in. drop, 3 layers, 25 blows per layer in a 4-in. mold) or the equivalent ASTM Method D 698. Also included are means for AASHO Method T 180 (10-lb, hammer, 18-in. drop, 5 layers, 56 blows per layer in a 4-in. mold). Variations from the basic method, where known, are reported in Tables 3, 15 and 24, along with means and standard deviations for the T 99 test procedure.

Variant procedures, not always noted but which may have had an influence on the reported values, included re-use of the sample, maximum size of the subbase or base aggregate used, and size of mold. In arriving at the means for Table 32, no distinction was made between

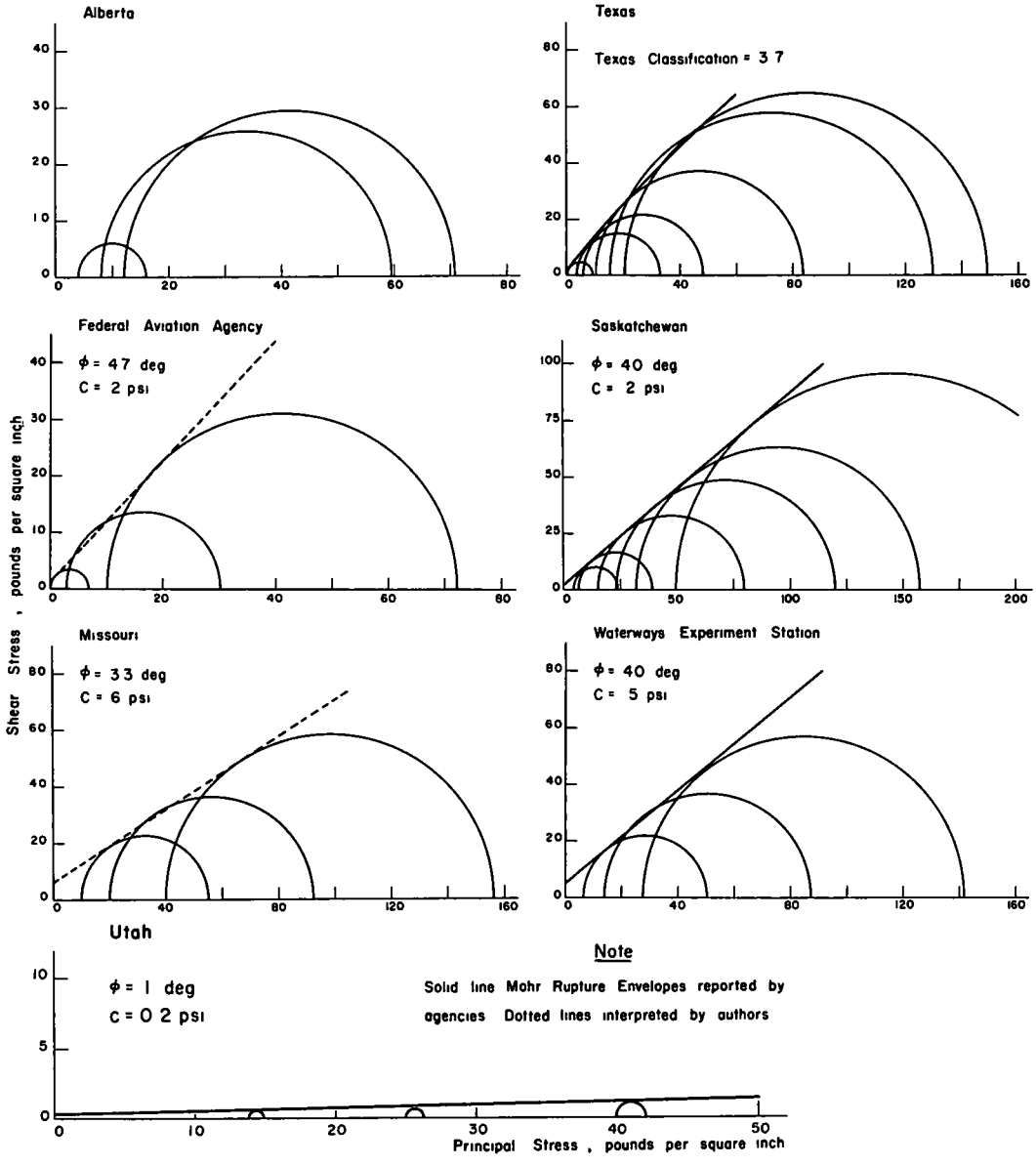

Figure 11. Mohr rupture envelopes for subbase.

TABLE 21

RESULTS OF PERMEABILITY TESTS ON SUBBASE MATERIAL*

Item	Georgia	Idaho	Mass.	N.B.	N.J.	Oregon
Method	—[41]	**	—	Constant head	—[41]	—
Dry density	138.0	135 to 137	—	—	—	—
K at 20°C, cm/sec	7.1×10^{4}	1×10^{-3} to 2×10^{-4}	1.9×10^{-4}	3.3×10^{-4}	1.0×10^{-5}	2.8×10^{-3}
Permeability rating	—	Medium	—	Low	—	—

* For footnote explanations see Appendix A.

**Hveem stabilometer specimens used.

TABLE 22

MINERAL COMPOSITION OF BASE MATERIAL

Constituent	Approximate Percentage			
	Banff	Kan.	Miss.	N. Mex.
Dolomitic limestone	100.0	-	*	-
Silica, SiO_2	-	4.0	-	3.7
Iron, Fe_2O_3	-	-	-	0.5
Alumina, Al_2O_3	-	-	-	1.0
Lime, CaO	-	-	-	28.8
Magnesia, MgO	-	-	-	19.6
Loss on ignition	-	-	-	46.4
Carbon dioxide, CO_2	-	-	-	(43.1)
Calcium carbonate, $CaCO_3$	-	51.5	-	51.4
Magnesium carbonate, $MgCO_3$	-	42.1	-	41.0
Water, H_2O	-	-	-	2.4
Undetermined	-	2.4	-	-
Insoluble in HCl	-	-	12.7	-

*Described as a dense, fine-grained to a very fine-grained crystalline dolomitic limestone.

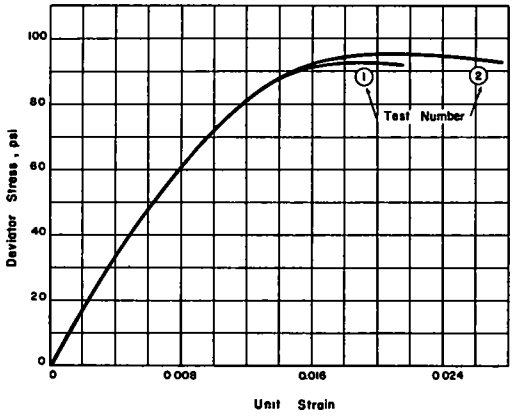

Figure 12. Stress-strain curves for triaxial tests on subbase (Kansas).

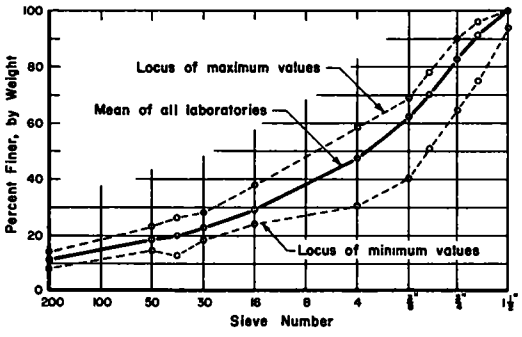

Figure 13. Grading curve for base.

TABLE 23

MECHANICAL ANALYSES OF BASE MATERIAL*

Agency	Method of Prep	Percent Finer Than[4] 1½"	1"	¾"	½"	⅜"	No. 4	No. 16	No. 30	No. 40	No. 50	No. 200[5]	No. 200**
Ala.	T 87[2]	100	93.6	86.4	76.7	69.0	55.8	33.4	25 5	23 1	20.4	11.7	13.6
Alta.	T 146[3]	100	94	87	75	68	52	28	23	21	19	11.5	11.7
Ariz.	T 87	100	95	87	73	66	49	29	23	21	19	-	11
B.C.	-	100	90.3	81.6	68.7	61 1	46.5	27 9	21.6	19 0	17.3	10 3	10.7
BPR	T 87	100	87	74	-	52	47	-	-	20	-	-	12
Calif.	T 87	100	91	83	69	62	48	30	23	21	19	-	12
Del	T 87	100	93.0	87.0	75.0	67.0	52.3	29 3	22.2	19.9	17.6	8.0	-
FAA	T 87	100	94	84	73	65	51	30	24	22	20	13	13
Fla.	T 87	100	95	84	73	-	46	-	-	18	-	9	-
Ga.	T 87	100	96	90	75	68	-	-	-	-	-	-	-
Hawaii	T 146	100	87.7	64.8	50.9	40.4	30.2	-	-	12.7	-	7.2	-
Idaho	T 87	100	88	80	65	57	43	-	19	17	16	-	9
Ill.	T 87	100	88 4	80.1	69.9	63.0	48 9	29.2	-	20.6	18.6	10.6	-
Kansas	-[53]	100	95	87	78	69	56	34	27	24	21	-	13
Ky.	D 421[2]	100	91.8	83.9	70.9	63.5	46.5	26.8	20.4	18.6	16.9	9.8	-
La.	-	100	89.8	79 6	65.8	59.4	58.6	32.4	23 8	20.3	18 8	-	10.9
Maine	T 87	100	91.0	82.0	69.0	62.0	46.0	28.0	22.0	19.0	17 0	-	-
Md	T 87	100	92.4	84.8	72.7	64 8	48 3	28.8	22.6	20.3	18.0	8.8	-
Mass.	-	100	94.8	84.2	72.6	65.3	46 1	28.0	22.3	20.9	19.0	12.4	-
Mich.	-	100	92.6	80.0	67 7	59 4	45.4	27.6	21.9	19.8	18.2	-	11.1
Miss.	T 87	100	91.2	83.1	71 7	63.5	45 2	26.0	21 0	17.9	17.0	-	8.7
Mo.	-	100	89.8	79.2	65.6	58.0	42.8	-	-	18 3	-	-	10.0
Nebr.	-	100	96	87	76	67	52	29	23	20	18	11	11
Nev.	T 87	100	90.4	79.9	68 6	58.4	43.6	25 0	19 0	17.1	15 5	-	8.4
N.J.	T 87	100	93	82	71	63	49	28	22	21	19	-	11
N.M	T 87	100	92	86	73	65	49	-	-	20	-	11	-
N.Y.	T 87	100	93.8	84.0	71.4	65 0	49.7	-	-	20.4	-	-	11.2
Ohio	T 87	100	87	79	64	56	43	28	22	20	18	10	-
Okla.	T 87	100	93	81	68	59	45	32	22	20	18	10.5	11.0
Omaha	T 87	100	93.8	87 1	71.8	63.3	48.8	-	-	20.3	-	-	10.7
Ont.	T 87	-	95.9	87 1	74 2	65.5	48.8	27 2	21 2	-	-	9 5	9.7
Oreg.	T 87	100	94.7	87 4	76.1	68.1	51.1	30.6	24.2	21.8	19 7	-	11.7
Pa.	T 87	100	87	84	74	66	50	29	22	20	18	11	11
Que.	-	100	87.6	75.8	62.4	55.4	43.0	-	-	-	-	9 7	-
R.I.	-	100	91.3	84.4	71.9	64 7	51.4	27.7	22.8	20.9	18.5	8.5	10.5
Sask	T 146	100	75.0	66.4	56.0	51.0	41 8	-	-	19 5	-	10.7	-
Texas	T 146	94	85	76	64	56	43	26	22	20	18	-	11
U. Minn.	T 87	100	90.5	82.7	68 8	61 0	48 7	28.4	22.2	19 6	18.6	8.7	10.3
Utah	T 87	100	92.3	83 9	69.7	61.5	46.7	24.0	18.4	16.7	15 1	8.8	8.8
Va.	D 421	100	93	86	72	64	52	29	22	20	18	-	11
Wash.	T 87	100	93	84	71	64	48	38	28	26	23	-	14
WES	-	100	93.0	85 6	73 5	65.6	50.5	32.2	25 5	23.1	21.3	13.2	13.4
Wis	T 146	100	93	87	74	67	50	30	23	21	19	-	11.0
No. of tests		42	43	43	42	42	42	32	32	40	32	23	30
Mean		99.9	91.4	82.5	70.2	62.1	47.9	29.1	22.6	20.0	18.5	10.2	11.1
Std. dev.		0.9	3.8	5.1	5.3	6.9	4.7	2.8	2.0	2.2	1.6	1.6	1.4

	0.05 mm	0.02 mm	0.005 mm	0.002 mm
	Hydrometer analyses			
Hawaii	7	4	2	1
N.J.	10	6	4	2
N.Y.	-	5	3	2
Texas	9	6	3	2
Average	9	5	3	2

*For footnote explanations see Appendix A.
**Includes additional dry sieving after washing over No. 200 sieve.

TABLE 24

PLASTICITY INDEX AND MOISTURE-DENSITY RELATIONSHIP OF BASE MATERIAL*

Agency	Plasticity Index PI[7]	Moisture-Density Relationship			
		Method	Max. Size	W_o	D_{max}
Ala.	N. P.	T 180[17]		6.6	139.2
Alta.	N. P.	D 698-D[18]	¾ in.	7.0	142.1
Ariz.	N. P.	T 99[16]		7.4	139.0
Banff	2.6	T 99		7.2	143.3
BC	0	T 99-D		7.3	141.2
BPR	N. P.	T 99-C	¾ in.	7	143
Calif.	N. P.	C 216-C[18]	¾ in.	5.0	152
Del.	N. P.	T 180		5.8	140
FAA	N. P.	T 180		6.9	140
Ga.	N. P.	T 99		7.8	131.0
Hawaii	4.3	-[23]		6.5	147.0
Ill.	N. P.	T 99[24]	½ in.	8.2	139
Kan.	1	-[25]	¾ in.	6.5	140
Ky.	2.9	T 99		4.5	151.8
Md.	1.6	T 99-A	No. 4	8.3	134.6
Mass.	3.7	T 180		6.5	140.0
Mich.	N. P.	T 99		7.6	135.6
Miss.	N. P.	-[18]		6.4	142.9
Mo.	N. P.	T 99-A	No. 4	8.6	135.2
Nebr.	N. P.	T 99-C	¾ in.	8.0	135.4
Nev.	N. P.	C 216-C	¾ in.	6.0	145.9
N. J.	N. P.	T 99		9.8	135.5
N. M.	N. P.	T 99		8.9	134.4
		T 99	No. 4	9.0	136.5
N. Y.	N. P.	T 99	¾ in.	7.3	141.0
		T 180	¾ in.	7.3	143.3
Ohio	N. P.	D 698		8.7	138.4
Okla.	N. P.	T 99	No. 4	8.4	136.5
Omaha	1+	D 698	¾ in.	5.7	142.0
Ont.	N. P.	T 99	No. 4	7.6	135.0
Oreg.	0	-[21]	No. 4	8.9	138.7
Pa.	0.1	T 99		8.4	138.0
P. R.	N. P.	T 180		6.5	143.5
R. I.	N. P.	T 99		8.1	135.9
Sask.	0.0	T 99		5.5	142.5
Texas	3.9	THD 83[22]		6.3	145.4
U. Minn.	N. P.	T 99		7.2	135.0
Utah	N. P.	T 99-A	No. 4	8.8	134.8
Va.	N. P.	D 698	No. 4	8.0	134.0
Wash.	N. P.	-[26]	No. 4	4.8	143.0
WES	**	T 180	¾ in.	6.8	145.8
Wis.	N. P.	T 180	¾ in.	6.5	144.6
No. of tests				27	27
Mean		T 99		7.7	137.9
Std. dev.				1.2	4.3

* For footnote explanations see Appendix A.

**Reported minus 4.

TABLE 25

SPECIFIC GRAVITY OF BASE MATERIAL*

	Specific Gravity								
	F.A.				C.A.				
Agency	Method	G_m	G_m (SSD)	G_a G_s	Method	G_m	G_m (SSD)	G_a G_s	Abs.
Ala.	T 84[11]	2.72			T 85[12]	2.60			1.3
Alta.	T 100[9]			2.69	T 85			2.74	
Ariz.	T 84			2.81	T 85			2.74	
Banff				2.73				2.76	
B.C.				2.83				2.78	
BPR	T 100			2.85	T 85	2.63	2.67	2.73	
Calif.	T 133[9]			2.79	T 85			2.62	
FAA	T 100			2.86	T 85			2.76	
Fla.	T 84	2.73	2.74	2.77	T 85	2.67	2.69	2.77	
Ga.	T 100			2.87					
Hawaii	T 84			2.83	T 85			2.64	
Kan.					T 85	2.62	2.66		1.7
Ky.				2.85				2.72	
La.					T 85			2.65	
Maine					T 85			2.67	
Md.	T 84			2.75	T 85			2.70	
Mass.	T 84			2.70				2.66	
Mich.	T 100			2.81	T 85	2.60	2.65	2.74	2.0
Miss.	T 100			2.77	T 100			2.67	
Mo.	T 100			2.80				2.63	1.5
Nebr.	T 84			2.80	T 85			2.74	
Nev.				2.79				2.64	
N.J.	T 100			2.88	T 85			2.68	
N.M.				2.82				2.78	
N.Y.				2.81				2.65	
Ohio	C 128[11]			2.76	T 14			2.65	
Okla.	T 100			2.74	T 85			2.67	
Omaha	T 100			2.82	T 85	2.68		2.77	1.7
Ont.				2.82				2.74	
Oreg.				2.81				2.81	
Pa.	T 100			2.81	T 85			2.65	
P.R.				2.78				2.69	
Que.	-[15]			2.77	-[15]			2.72	
R.I.	T 100			2.73	T 85			2.69	
Texas	THD 73			2.81					
Utah	T 100			2.72	T 85			2.68	
Va.	D 854			2.67				2.67	
Wash.	D 854			2.76	C 127[12]			2.77	
WES	D 854			2.84	C 127			2.75	
Wis.	T 84			2.70	T 85			2.62	
Summary:									
No. of tests				37				37	
Mean				2.78				2.70	
Std. Dev.				0.05				0.05	

*For footnote explanations see Appendix A.

TABLE 26

SOUNDNESS, ABRASION, AND SAND EQUIVALENT OF BASE MATERIAL*

Agency	Soundness[38] Type of Solution	No. of Cycles	% Loss C. A.	% Loss F. A.	% Loss Total	Abrasion[40] Grading	Rev.	% Wear	Sand[31] Equiv.
Ariz.	Na_2SO_4	5			6.0**	C	100	8.0	
							500	28.0	
Calif.									41
F. A. A.								30	
Idaho						B		27	42
Kan.						B		26.9	
La.								27.8	
Maine								28.1	
Md.			8.3	6.3				27.2	54
Miss.							500	28.3	
Nebr.	Na_2SO_4	5			2.3**	A		29.0	
		10			4.0				
N. M.								30.0	42
N. Y.	$MgSO_4$	4			8.3				
		10			16.5				
Ohio	Na_2SO_4				3.4**	B	(Deval)	9.2[39]	
Ont.								23.2	
Oreg.	Na_2SO_4				0.7**	A		29.0	
Pa.	Na_2SO_4	5	1.5	1.3	2.8**	A	100	5.5	
						A	500	26.5	
						B	100	5.5	
							500	23.9	
							100	6.3	
						C	500	24.3	
P. R.	$MgSO_4$	5			1.7			30.0	
Que.								28.0	
Utah		5	3.2	2.5		A		24.0	
Wash.									49
No. of tests					5			18+	5
Mean					3.0			27.3	46
Std. dev.								2.2	

*For footnote explanations see Appendix A.

**Indicates tests included in mean.

+The 9.2 value obtained from deval test and results of Los Angeles test at 100 rev. not included.

TABLE 27

CALIFORNIA BEARING RATIO TEST DATA FOR BASE MATERIAL*

Details of Test	Ala	Alta	B C	BPR 1	BPR 2	BPR 3	BPR 4	Fla	Hawaii	Ill	Md	Mass	Agency Miss 1	Agency Miss 2	Agency Miss 3	Missouri
Compaction method.																
Dynamic[23]		x	x		x			x	x[23]		x	x		x[28]		
Wt of hammer, lb		5 5	5 5		5 9[27]			10			5 5	10				
Drop, in		12	12		12			18			12	18				
No layers		3	3		4			5			3	5				
No blows per layer		55	60					55			55	25	10	25	55	
Static, 2,000 psi[24]	x									x						x (to desired den)
Testing conditions																
Surcharge weight, lb	10	10	10		10			10	10	10	10	10		10		10
Soaking period, days	4	4	0		4			4	3	4	4	1		4		1
Molding conditions																
Dry density, pcf	138 7	137	139 9	146	138	134	120	144 6	140 7	129 0	141 0	137 0	139	141	144	121 7
Moisture content, %	5 9	7 0	6 7	6 8	7 6	7 0	7 1	5 5	5 1	6 5(H)	5 0	6 3	7 2	6 0	5 6	8 6
Max aggregate size		¾"	¾"		¾"					½"						No 4
Optimum conditions																
(Table 24)																
Max dry dens (T 99)		138 4	141 2		143					139[26]	134 6			142 9[28]		135 2
Max dry dens (T 180)	139 2								142 2[25]			140 0				
Opt moisture content	6 6	6 1	7 3		7				6 5	8 2	8 3	6 5		6.4		8 6
Test results																
Final moisture content	7	7 7		5 9	6 7	6 5	6 9	6 1	6 8	6 7	5 4	6 6	7 9	6 6	5 8	12 5
Swell, %	0 0	0 0		0 0	0 0	0 0	0 0			0 0	0 0	0 0	0 0	0 0	0 0	0 0
CBR at 0 1 in pen (soaked)			72					170	120	225		80				3 0
CBR at 0 2 in pen (soaked)	145	100+	100	163	111	63	17			202	186	100+	83	135	149	
Remarks																

*For footnote explanations see Appendix A

Details of Test	N J	N Y	Ohio	Okla	Pa	P R	Sask	U Minn	Utah	Va	WES	Wis 1	Wis 2	Wis 3
Compaction method														
Dynamic[23]	x	x	x		x	x	x	x		x	x		x	
Wt of hammer, lb		5 5	5 5		10	10	5 5	5 5		5 5	10		10	
Drop, in		12	12		18	18	12	12		12	18		18	
No layers		3	3		5	5	3	5		5	5		5	
No blows per layer		56	56		55	55	56	56		45	Variable	10	25	55
Static, 2,000 psi[24]				x					x					
Testing conditions														
Surcharge weight, lb	12 5	10	21 2	10	10		20	10	12	10	10		10	
Soaking period, days	4	4	4	4	4	0	4	4	4	4	4		4	
Molding conditions														
Dry density, pcf	133 8	136	138 5	137 4	148 0	143 5	143 2	134 8	137 7	127 5		136 1	140 5	141 8
Moisture content, %	9 8	8 0	7 1	6 3	6 0	6 5	5 7	7 6	6 1	4 5		6 5	6 5	6 5
Max aggregate size		**					¾'							
Optimum conditions														
(Table 24)														
Max dry dens (T 99)	135 5	141	138 4	136 5	138 0	143 5	142 5	135 0	134 8	134 0				
Max dry dens (T 180)											145 8		144 6	
Opt moisture content	9 8	7 3	8 7	8 4	8 4	6 5	5 5	7 2	8 8	8 0	6 8		6 5	
Test results														
Final moisture content	10 0		7 4		6 3			6 8	7 8			6 7	6 2	6 1
Swell, %	0 0	0 0	0 9	0 0	0 0					0 0				
CBR at 0 1 in pen (soaked)	92	34	23 at 0 5"	200	93		190	87	180	53				
CBR at 0 2 in pen (soaked)	145	64			114	139		116			See Table 27	113	268	233

**Avg tests on -¾ and -No 4

Fig 14

TABLE 28

RESULTS OF CBR TESTS ON BASE MATERIAL
(WATERWAYS EXPERIMENT STATION)

Before Soaking			After Soaking			
Moisture Content (%)	Density (pcf)	CBR	Moisture Content (%)	Density (pcf)	CBR	Swell (%)
(a) 12 Blows						
0.2	138.5	161	7.2	138.5	100	0
2.5	130.7	57	8.8	130.8	24	-0.04
4.6	131.6	89	7.4	131.6	80	-0.02
7.2	139.4	138	7.3	139.5	128	-0.04
9.2	138.1	61	7.9	139.3	44	-0.84
(b) 26 Blows						
0.3	141.6	247	6.9	141.6	169	-0.02
1.9	136.7	139	8.1	136.7	70	0
3.9	137.4	159	7.6	137.4	91	-0.02
5.7	140.3	211	6.5	140.5	193	-0.13
7.9	142.4	158	6.9	142.4	168	0
9.0	139.8	128	7.5	139.9	133	-0.04
(c) 55 Blows						
0.2	144.2	418	6.3	144.2	249	0
2.9	140.1	266	7.0	140.2	129	-0.06
5.7	144.5	336	6.3	144.8	882	-0.04
8.4	142.7	94	6.8	142.7	120	-0.02

those who reported the variant procedures and those who did not. However, values corrected mathematically for plus No. 4 material were not included, nor were values determined with different sizes and weights of hammer or number of blows.

Part of the problem, and possibly confusion, of the variations in test procedure arose from the fact that during the time in which these studies were being made, both AASHO and ASTM were rewriting their methods for determining the moisture-density relationships of soils. In any event, it is interesting to compare the means and standard deviations of the test values reported for the standard T 99 test:

	Mean	Std. Deviation	
		Value	Percent of Mean
		(a) Maximum Density	
Soil	119.2	2.2	1.8
Subbase	133.1	3.3	2.5
Base	137.9	4.2	3.0
		(b) Optimum Moisture	
Soil	13.5	1.0	7.4
Subbase	7.7	1.0	13
Base	7.6	1.2	16

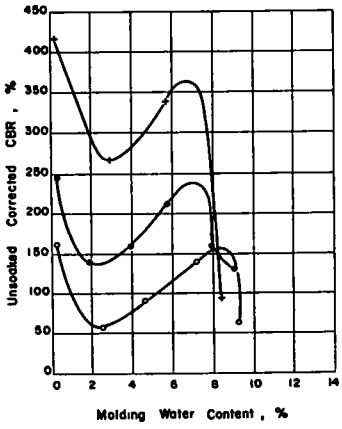

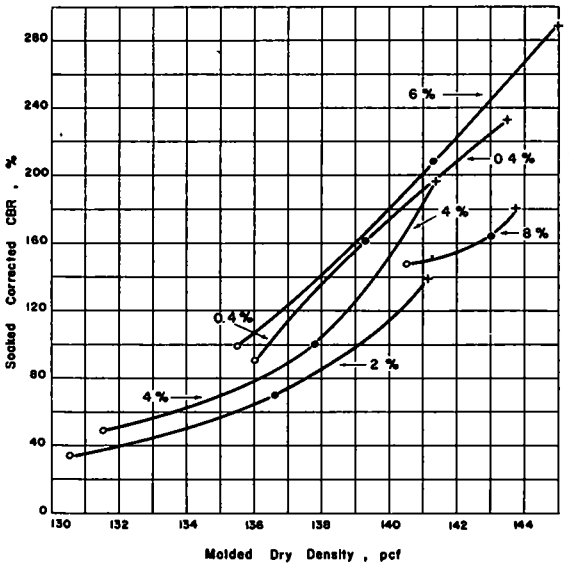

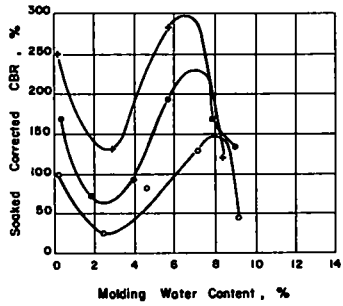

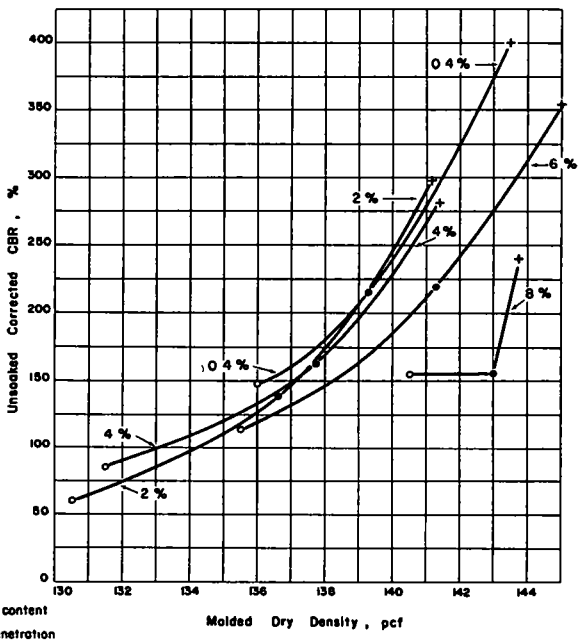

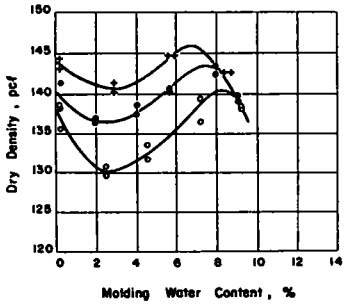

LEGEND

+ 55 Blows per layer
● 26 Blows per layer
○ 12 Blows per layer

NOTES

1 Figure beside curve is molding water content
2 Surcharge equal 20 lb soaking and penetration
3. All samples soaked 4 days
4 All samples compacted in 5 layers, 10 lb hammer, 18-inch drop in CBR mold

Figure 14. CBR tests on base (Waterways Experiment Station).

TABLE 29

HVEEM STABILOMETER TEST DATA FOR BASE MATERIAL*

Agency	Method of Compaction	Molding Moisture Content (%)	Molded Dry Density (pcf)	P_h at P_v = 160 psi	Displacement	R-Value[45]	Exudation Press (psi)	Avg R-value at 400psi
		6.0	142.0	14	3.22	89	652	
BPR	AASHO	6.3	142.0	17	3.63	86	247	86
	T 173-56[42]	6.6	142.0	18	3.77	84	446	
		4.3	134.0	9	4 25	84	660	
Calif.	AASHO	5 1	134.0	10	4.35	84	600	84
	T 173-56	5.9	133 0	9	4 70	85	420	
		7 2	135 0	9	4.85	84	240	
		3.3	135 0	24	4 74	75		
Idaho	AASHO	4 2	135 1	20	5.03	77		75
	T 173-56	5 1	135.4	24	4 62	75		
		6.4	129.0	12	5.14	86		
N M.	Kneading	6 8	130 0	10	4.58	85		81
	Compactor	7 3	130 0	18	5 70	78		
		8.2	129.0	22	5.61	74		
		7.1	140 1	14	4.08	87	239	
Oregon		6 7	139 1	13	4.06	87	382	87
		6.3	138.7	14	4.08	87	796	
		7 2	133 0	19	4.65	85	195	
Univ of	-[47]	6 7	138.8	15	4.73	84.5	310	82
Minn		6 7	134.5	14	4 73	80	470	
		5 9	130.4	12	4 96	86		
Wash.	-[45]	5.4	129.1	14	4.96	84	400	84
		5 6	128.6	13	6 30	81		
		5 2	128.1	12	6.25	83		

*For footnote explanations see Appendix A.

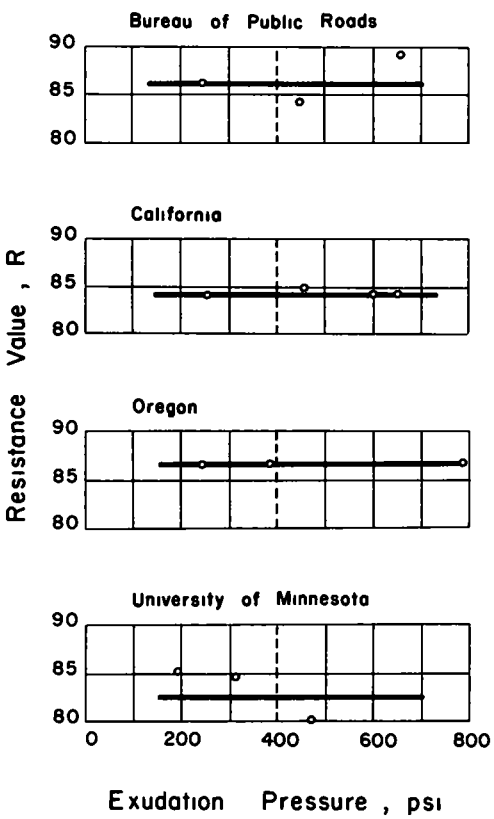

Figure 15. Resistance value vs exudation pressure, base.

Although the standard deviations are not large, there is still a considerable number of test values varying from the average by two or more pounds per cubic foot. Because of the lack of proper experimental evidence, it is difficult to say whether or not this is due to specific differences in techniques, or it is a random error associated with the sample or operators. Tests by New York, Missouri, and Ontario reported in Tables 15 and 24 indicate that the exclusion of the plus No. 4 material reduced the maximum density of the granular materials by about 4 percent.

Most pavement design methods presume, in some fashion, to take into consideration the conditions of soil placement, i.e., its moisture and density. This report includes, in addition to the maximum densities and optimum moisture contents previously discussed and summarized in Table 32, other information which could be used to make trial pavement designs. In view of the possibility

TABLE 30

TRIAXIAL COMPRESSION TEST DATA FOR BASE MATERIAL*

Details of Test	Agency																	
	Alberta		Kansas				Oregon			Sask	FAA							
Method of compaction.																		
Dynamic	x[21]						x			x								
Static			x[20] Dbl plunger															
Kneading																		
Portion of sample tested	-¾"		Total				-1½"			-¾"	x[19]							
Initial Condition																		
Molding moisture content, %	6 5		6 5		6 2	5 4	5 5		5 1		5 9		5 6		5 6			
Dry density, pcf	137 1		138 9		139 9	140 3	143 8		141 7	143	141 3		140 3		139 8			
Initial void ratio, e_o			27		24													
Deg of saturation, %	78 0																	
Saturated sample																		
Yes			x							x								
No																		
Moisture content after sat			10 1		8 9													
Dry density after sat																		
Deg of sat.																		
Failure condition.																		
Moisture content			7 4		6 8						5 9		5 6		5 6			
Void ratio			21		22													
Confining press , σ_3, psi	4	8	12		20		5		10	20			0		3		10	
Deviator stress, $\sigma_1 - \sigma_3$, psi	12	52	59				84 9		113 0	185 9			22 0		65 0		140 1	
Strain, %	1 0	1 7	1 1		**		1 49		3 62	3 42			0 89		1 35		1 35	
Type of test																		
Rate of load app in per min	100 lb per min				0 1				0 1		10 psi per mean							
Specimen dimen in	6 x 14 5				4 x 8				12 x 21		4 x 8				6 x 12			
Reported values ***																		
Angle of friction, $\phi°$									(50)		84				(55)			
Cohesion C psi									(9)		0 9				(9)			
Remarks																		
*For footnote explanations see Appendix A											closed system triaxial test							
**Values in parentheses determined from Fig 16 by authors			**Not tested to failure See Fig 17															

Details of Test	Agency																	
	Texas								Utah		WES							
Method of compaction.																		
Dynamic	x[20]								x				x					
Static																		
Kneading																		
Portion of sample tested	Total								-No 4		-¾"							
Initial Condition																		
Molding moisture content, %	6 3	6 3	6 2	6 2	6 3	6 3			8 0		5 9		7 0		6 9			
Dry density pcf	145 2	145 3	145 3	145 6	144 9	145 5			128 0		138 3		138 2		138 5			
Initial void ratio e_o									353		247		265		263			
Deg of saturation, %											77 3		73.6		73 3			
Saturated sample																		
Yes	Capillary Absorption												x					
No																		
Moisture content after sat	5 1	5 0	5 0	5 0	5 1	5 0			x		7 2		8 9		10 0			
Dry density after sat																		
Deg of sat.											81 5		94 6		100			
Failure condition.																		
Moisture content									7 5		7 2		8 9		10 0			
Void ratio																		
Confining press σ_3, psi	0	3 7	5 7	10 7	15 7	20 7	13 9		25 0	40 0	6 9		13 9		27 6			
Deviator stress, $\sigma_1 - \sigma_3$, psi	46 7	147 5	165 5	229 2	277 1	367 6	4 1		5 6	9 1	67 4		123 3		81 4			
Strain, %	2 19	3 26	3 10	3 24	3 99	4 32	2 0		2 3	1 9								
Type of test											Quick							
Rate of load app , in per min	0 15								0 05		0 06							
Specimen dimen in	6 2 x 8								1 94 x 4 0		5 6 x 12							
Reported values ***																		
Angle of friction, $\phi°$									8		See Fig 16							
Cohesion, C, psi									0 7									
Remarks:	Texas classification = 1 0																	
*For footnote explanations see Appendix A	Compactive effort = 13 26 ft-lb/cu in																	
***Values in parentheses determined from Fig. 16 by authors																		

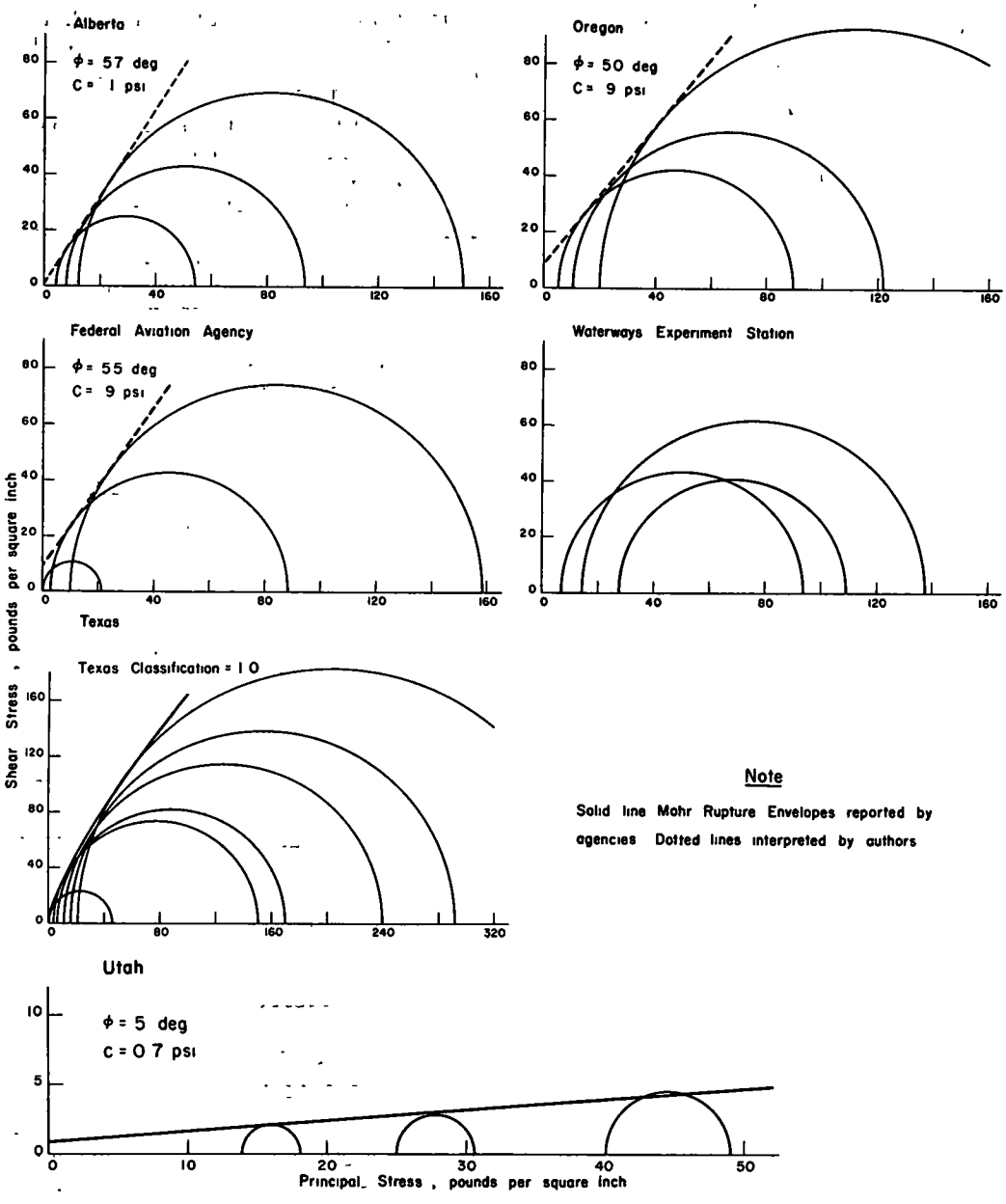

Figure 16. Mohr rupture envelopes for base.

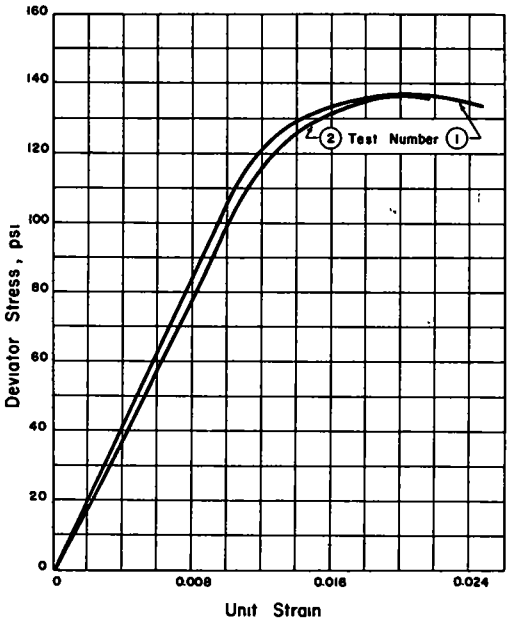

Figure 17. Stress-strain curves for triaxial tests on base (Kansas).

TABLE 31

RESULTS OF PERMEABILITY TESTS ON BASE MATERIAL*

Agency	N J	N. Y	Ohio
Method	-[41]		-[41]
Max. size	Whole	¼"	
Density (pcf)	-**	-**	130 (Wet)
K at 20°C (cm/sec)	2 08 x 10^{-6}	5 04 x 10^{-3}	4 94 x 10^{-2}
(ft/day)		14 3	140.0

*For footnote explanations see Appendix A.
**Not reported.

TABLE 32

SUMMARY OF CHARACTERISTICS OF MATERIALS*

Items	Soil	Subbase	Base
Liquid limit	28		
Plastic limit	15		
Plasticity index	13	N P	N P
AASHO classification (group index)	A-6 (9)	A-1 (0)	
Optimum moisture (%) AASHO T 99	13	8	8
AASHO T 180	10	7	7
Maximum density (pcf) AASHO T 99	119	133	138
AASHO T 180	129	138	142
Specific gravity, apparent	2 72	2 70	2 74
Mechanical analysis			
Maximum size		1 in	1½ in
Percent finer than			
No 4 sieve	97	74	49
No 40 (0 42 mm) sieve	89	27	20
No 200 (0 074 mm) sieve	76	8	10
0 02 mm	62	4	5
0 005 mm	40	2	3
Sand equivalent	6	51	46
Sodium sulfate soundness loss, 5 cycles (%)			3 0
Los Angeles abrasion loss, 500 rev (%)		31	27

*See text, appropriate tables, and notes for specific details and test methods

that such designs may be used to compare the design procedures with Road Test performance information, it appears to the authors that additional discussion is necessary. At the same time, they reiterate the remark made earlier that no such designs or comparisons are necessarily implied.

Table 33 has been prepared to show, in juxtaposition, what may be considered design properties of the soil, subbase and base material. Included are factors from CBR, Hveem stability (R-values), Kansas triaxial (modulus of deformation), and Texas triaxial (classification number) tests. Also indicated are the number of reports included and the range in values of those included. Selections from those available were made by the authors from the entire group available. Other than personal judgment, the prime criterion for selection was that the molding moisture and density condition be close to the reported average for the standard (T 99) or modified (T 180) conditions and that no extreme value be included.

Of the 28 reports showing California Bearing Ratio data for the embankment soil, 14 were included in three categories in Table 32. Twelve of 26 subbase reports and 11 of 24 base reports were included. Mention was made earlier of the variations in basic test procedure. The factors which made selection most difficult were the variations in molding moisture and density. Figures 3, 9, and 14 make it clear that molding conditions are important. Reported CBR (soaked only) values showed these total ranges: soil, 2 to 45; subbase, 5 to greater than 100; base, 3 to greater than 200. In many cases there appeared to be little relationship between the molding condition and the reported optimum condition, although it may be presumed that this was considered in the individual application of the CBR values. However, indiscriminate application of published design charts to the various reported CBR values would certainly yield a surprising variety of designs. Whether or not this would apply to the application of the design charts of certain individual States to their own CBR values was not ascertained.

Hveem stabilometer test data for the embankment soil also varied appreciably from agency to agency. There was more uniformity for the granular materials. In

TABLE 33

SELECTED PROPERTIES FOR DESIGN*

Item	Soil			Subbase			Base		
	No.	Mean	Range	No.	Mean	Range	No.	Mean	Range
Property at approximately T 99 optimum conditions:									
CBR (soaked), Corps of Engineers procedure	8	5.0	4.0 to 6.7	5	58	32 to 86	5	100+	83 to 140
CBR (soaked), static method	1	1.7		2		5 to 33	3	200+	145 to 200
Hveem stability, R-value	3	21**		9	78	69 to 84	7	83	81 to 86
Kansas triaxial, modulus of deformation (psi)		1,300			8,000			10,000	
Texas classification		5.6 (96% max. dens.)			3.7 (102% max. dens.)				
Property at approximately T 180 optimum conditions:									
CBR (soaked), Corps of Engineers procedure	5	18	10 to 24	5	100+	86 to 163	3	186	135 to 233
CBR (soaked), static method					1	20			
Texas classification		4.7 (97% max. dens.)						1.0 (102% max. dens.)	

*See appropriate tables and notes for references to test methods.
**Determined at 300-psi exudation pressure.

Table 32 averages or reported values at 400-psi exudation pressure were used to obtain the subbase and base R-values. For the soil, only the R-values for California, New Mexico, and Oregon were used, and these were taken from Figure 4 at 300-psi exudation pressure. The 300-psi exudation pressure was used after considering a plot of moisture content versus exudation pressure for those three agencies. It must be emphasized here that no implication of the insufficiency of the combination of a test value and a design method for a given agency is meant.

Several agencies reported the results of triaxial tests, a few reporting data for all three materials. Inasmuch as only two, Kansas and Texas, reported explicitly on design tests, they alone have been included in Table 32. The Texas classifications were reported by that agency, the Kansas moduli were determined by the authors.

In the interest of clarification and to make it possible to extend the use of the material previously discussed, further mention of the moisture and density condition

of the AASHO Road Test is in order. Table 34 has been prepared from data presented in HRB Special Report 61 B (2) to show how the average maximum densities and optimum moisture contents given in Table 32 compare with initial, as-constructed conditions. The optimums as obtained on the original materials are given. The conditions corresponding to P_{20} and P_{50} were obtained from distribution curves of all tests made during construction and are the 20th or 50th percentiles of these distributions. In the case of density, P_{20} is the density below which 20 percent of the tests fell. For moisture content it is the value above which 20 percent of the tests lay, both being in order of descending stability (in general terms).

A question of the philosophy of design is involved here. Will design be for optimum conditions, expected mean conditions, or some condition below either of these? Certainly such factors should be considered if stability (again in general terms) is a function of molding or compacting conditions and if constructed conditions vary. An illustration can readily be given using data from the Waterways Experiment Station (CBR) and California (R-value):

Soil Molding Condition	CBR	R-value
P_{20}	2	less than 8
P_{50}	2.5	less than 8
T 99	5	21
T 180	17	-

TABLE 34

CONSTRUCTION DENSITY INFORMATION FROM AASHO ROAD TEST*

	Soil		Subbase		Base	
Basis for Selection	Dry Density (pcf)	Moisture Content (%)	Dry Density (pcf)	Moisture Content (%)	Dry Density (pcf)	Moisture Content (%)
P_{20}** (construction)	112	17.1	133***	7	141	7
P_{50}** (construction)	114	16.2	136***	7	141	7
Optimum (construction)	117	15	137	7	139	7
T 99 (Table 32)	119	13	133	8	138	8
T 180 (Table 32)	129	10	138	7	142	7

*See text for explanation of items in table.

**P_{20}: 20th percentile, or density below which 20 percent of tests lie, or moisture content above which 20 percent lie.

P_{50}: 50th percentile

***Before paving, initial density was higher.

SUMMARY

Tabulations of test data collected on soil, subbase, and base material from the AASHO Road Test as part of a cooperative materials testing program have been presented. Primary reasons for conducting the tests were to allow each participating agency to develop information about the materials using its own methods and procedures, and to develop information not obtainable with facilities available at the Road Test.

Indicated characteristics, design properties, and variability of reported test data were discussed and summarized in Tables 32 and 33.

ACKNOWLEDGMENT

Acknowledgment is made to William N. Carey, Jr., Chief Engineer for Research, and A. C. Benkelman, Flexible Pavement Research Engineer, AASHO Road Test, for conception and supervision of much of this project. The authors take responsibility, however, for compiling the data and having made such interpretations as were deemed necessary.

Acknowledgment also is made of the participating agencies and their permission to use the data in this report.

REFERENCES

1. "The AASHO Road Test: History and Description of Project." HRB Special Report 61A (1961).
2. "The AASHO Road Test: Materials and Construction." HRB Special Report 61 B (1962).
3. "Classification of Soils and Soil-Aggregate Mixture for Highway Construction Purposes (AASHO Designation: M 145-49)." Standard Specs. for Highway Materials, Part I. American Assn. of State Highway Officials (1955).

Appendix A

REFERENCES AND EXPLANATORY NOTES

Abbreviations

T 000 refers to the standard designation for methods of test of the American Association of State Highway Officials.
D 000 and C 000 refers to the standard designation for methods of test of the American Society for Testing Materials.
C 000 refers to the standard designation for methods of test of the Division of Highways, State of California.
THD 000 refers to the standard designation for methods of test of the Highway Department, State of Texas.
AASHO American Association of State Highway Officials.
ASTM American Society for Testing Materials.
HRB Highway Research Board.

General References

"Standard Specifications for Highway Materials and Methods of Sampling and Testing, Parts I, II and III." American Society for Testing Materials, Philadel-Washington, D. C. (1955, 1958).
"ASTM Standards, Part 4." American Society for Testing Materials, Philadelphia, Pa. (1958).
"Procedures for Testing Soils." American Society for Testing Materials, Philadelphia, Pa. (1958).
Lambe, T. W., "Soil Testing for Engineers." Wiley, New York (1951).

Specific References and Explanatory Notes

Numbers correspond to superscript numbers in the tables.

1. AASHO T 88-54 or ASTM D 422-54, "Mechanical Analysis of Soils."
2. AASHO T 87-49, "Dry Preparation of Disturbed Soil Samples for Test;" or ASTM D 421-58, "Dry Preparation of Soil Samples for Grain-Size Analysis and Determination of Soil Constants."
3. AASHO T 146-49, "Wet Preparation of Disturbed Soil Samples for Test."
4. AASHO T 27-46 or ASTM C 136-46, "Sieve Analysis of Fine and Coarse Aggregates."

5. AASHO T 11-49 or ASTM C 117-49, "Amount of Material Finer Than No. 200 Sieve in Aggregate."
6. AASHO T 89-54, "Determining the Liquid Limit of Soils;" or ASTM D 423-54T, "Liquid Limit of Soils."
7. AASHO T 90-54, "Determining the Plastic Limit of Soils;" or AASHO T 91-54, "Calculating the Plasticity Index of Soils;" or ASTM D 424-54T, "Plastic Limit and Plasticity Index of Soils."
8. AASHO T 100-54 or ASTM D 854-52, "Specific Gravity of Soils."
9. AASHO T 133-45 or ASTM C 188-44, "Specific Gravity of Hydraulic Cement."
10. Division of Highways, State of California, C 208-B, "Materials Manual," Vol. 1 (1956), "Method of Test for Apparent Specific Gravity of Fine Aggregates."
11. AASHO T 84-57 or ASTM C 128-57, "Specific Gravity and Absorption of Fine Aggregates."
12. AASHO T 85-45 or ASTM C 127-42, "Specific Gravity and Absorption of Coarse Aggregates."
13. Jackson method for determination of specific gravity of soils. See Agg, T.R., "Construction of Roads and Pavements," McGraw-Hill (1936). This method uses kerosene and a special burette, calibrated to read specific gravity directly.
14. "Hogentogler" Method for determination of specific gravity of soils, computed from

$$\text{Specific Gravity} = \frac{1}{\frac{1}{R_S} - \frac{W_S}{100}}$$

where R_S = shrinkage ratio and W_S = shrinkage limit.

15. Using Chapman flask.
16. AASHO T 99-57 or ASTM D 698-58T, "Moisture-Density Relations of Soils Using a 5.5-lb Rammer and a 12-in. Drop." Where information was available, letter indicates method used.
17. AASHO T 180-57 or ASTM D 1557-58T, "Moisture-Density Relations of Soils Using a 10-lb Rammer and an 18-in. Drop." Where information was available, letter indicates method used.
18. Division of Highways, State of California, C 216-C, Materials Manual, Vol. 1 (1956), "Method of Test for Relative Compaction of Untreated and Treated Soils and Aggregates."
19. Method of Compaction: 10-lb hammer, 25 blows, 4 layers in 4-in. mold.
20. AASHO T 134-57 or ASTM D 558-57, "Moisture Density Relations of Soil-Cement Mixtures."
21. Wilson, S.D., "Suggested Method of Test for Moisture-Density Relations of Soils Using Harvard Compaction Apparatus." Procedures for Testing Soils, ASTM, 1958.
22. THD 83, "General Laboratory Compaction Test for Moisture-Density Relations for Soils," Texas Highway Department, 1953 (revised).
23. Hawaii method of compaction: 1/10-cu ft mold, 10-lb rammer, 18-in. drop, 5 layers, 55 blows per layer.
24. Plus ½-in. material removed and replaced with an equal weight of ½ to No. 4 material.
25. Kansas method of compaction 1/10-cu ft mold, 5.5-lb rammer, 12-in. drop, 4 layers, 56 blows per layer. Samples are not reused. Details of method are given in "Soil and Base Course Manual," State Highway Comm. of Kansas (1959).
26. Static-vibration method of compaction. See Humphres, H.W., "A Method for Controlling Compaction of Granular Materials." HRB Bull. 159 (1958).
27. Using modified Vicksburg hammer (weighing 5.9 lb) which compacts soils to densities similar to those attained with 5.5-lb standard hammer having a 12-in. drop.
28. AASHO T 92-54, "Determining the Shrinkage Factors of Soils;" or ASTM D 427-39, "Shrinkage Factors of Soils."

29. Determined in "bar shrinkage limit mold" for rapid determination of shrinkage by direct measurement of specimen dimensions. The individual specimen molds are approximately $\frac{5}{8}$ by $\frac{3}{4}$ by 5 in. long.
30. AASHO T 93-54, "Determining the Field Moisture Equivalent of Soils;" or ASTM 426-39, "Field Moisture Equivalent of Soils."
31. AASHO T 176-56, "Plastic Fines in Graded Aggregates and Soils by Use of the Sand Equivalent Test."
32. "Dust ratio" is defined as the percentage of material finer than No. 40 sieve passing No. 200 sieve.
33. Determination of CBR by dynamic compaction. See "Suggested Method of Test for Moisture-Density Relationships and California Bearing Ratio of Soils," submitted by U.S. Army, "Procedures for Testing Soils," ASTM, 1958. Except where variants in compaction procedure are noted, it is presumed all generally follow this method.
34. Determination of CBR by static loading. See Stanton, T.E., "Suggested Method fo Test for Bearing Ratio and Expansion of Soils," "Procedures for Testing Soils," ASTM, 1955. This procedure specifies 2,000-psi compression pressure. In a few cases other pressures were used for static compaction but were not incidated. It is assumed specimens were compressed to desired density.
35. Recommendations based on methods described in paper prepared for presentation at 36th Annual WASHO Conference on June 13, 1957, by Chester McDowell, Senior Soils Engineer, Texas Highway Department.
36. Wyoming Modified CBR Method. See Russell, I.E., and Olinger, D.J., Wyoming Method of Flexible Pavement Design," Proc. HRB, Vol. 27 (1957). Specimen is compressed to 100 percent T 99 maximum density at optimum water content in testing machine.
37. Equivalent to Standard AASHO, using 6-in. mold, 10-lb hammer, 18-in. drop, 5 layers, 12 blows per layer.
38. AASHO T 104-57 or ASTM C 88-56T, "Soundness of Aggregates by Use of Sodium Sulfate or Magnesium Sulfate."
39. AASHO T 3-35, "Abrasion of Stone and Slag by Use of the Deval Machine."
40. AASHO T 96-56 or ASTM C 131-55, "Abrasion of Coarse Aggregate by Use of the Los Angeles Machine."
41. "Suggested Method of Test for Permeability of Granular and Semi-granular Soils," by Ohio State Highway Testing and Research Laboratory, Procedures for Testing Soils, ASTM, 1958.
42. AASHO T 173-56, "Compaction of Soil and Soil Mixtures for the Expansion Pressure and Hveem Stabilometer Tests." Standard procedure using kneading compactor, 350-psi foot pressure.
43. AASHO T 174-56, "The Expansion Pressure of Soils."
44. AASHO T 175-56, "Resistance of Soils to Deformation Using the Hveem Stabilometer."
45. For Washington procedure see "Flexible Pavement Design Correlation Study." HRB Bull. 133, 1956. This kneading compaction procedure uses a foot pressure of 100 psi for 40 blows on soil and 250 psi for 40 blows on subbase and base materials.
46. For Idaho procedure see Erickson, L.F., "Flexible Pavement Design in Idaho," HRB Bull. 210, (1959). This kneading compaction procedure uses a foot pressure of 250 psi for 140 strokes.
47. Skok, E.L., Jr., "A Comparison of Methods of Flexible Pavement Design," University of Minnesota (1959). This procedure uses kneading compactor, 250-psi foot pressure applied 10 times on each of four layers followed by 100 blows on top of specimen.
48. Kansas Triaxial Compression Test Method. See "Design of Flexible Pavements Using Triaxial Compression Test," HRB Bull. 8, (1947).
49. Texas Triaxial Compression Test Method. See McDowell, C., "Triaxial Tests in Analysis of Flexible Pavements," HRB Research Report 16-B, (1954).

50. Boyd, K., "Suggested Method of Test for Bearing Power of Soil by Means of a Cone Machine," Procedures for Testing Soils, ASTM, 1959.
51. Compacted with 5.5-lb hammer, 12-in. drop, 55 blows for 3 layers, 60 blows for 4 layers.
52. Compaction with kneading compactor as follows: 8 layers, 60-deg. table turn, 1-sec. dwell time, 130-psi foot pressure.
53. See "Soils and Base Course Manual," State Highway Commission of Kansas, p. 110. This is wet preparation method using 230 F drying temperature.

Appendix B

FROST SUSCEPTIBILITY STUDY OF EMBANKMENT SOIL

As part of this cooperative study, the Arctic Construction and Frost Effects Laboratory of the U.S. Army Engineer Division, New England, ran a series of studies of the frost susceptibility of the soil. Included in the study were determinations of the effect of dry unit weight and pressure using ACFEL standard freezing tests, the effect of initial degree of saturation in a closed system test, and the initial freezing point of the soil moisture. Brief summaries are presented in this report.

In the open system test normally used by ACFEL, tapered specimens 5.75 to 5.50 in. in diameter by 6 in. high were frozen from the top down at a rate of ¼ to ½ in. per day. The bottom ends of the specimens were connected to a free water source. Cabinet temperatures and heave measurements were made daily. This procedure was used for the studies of the effect of unit weight and pressure. Pressure was applied to the tops of the specimens with weights. The closed system test differed in that no water was allowed to enter the specimens during freezing.

The data from the open system tests are given in Table 35; closed system tests, in Table 36.

Initial freezing temperature was determined on two samples compacted in thin-walled copper tubes 3½ in. long by ¾ in. in diameter, sealed to prevent desiccation. The specimens were compacted to 106.7-pcf density at 19.9 percent moisture and 122.9-pcf density at 13.8 percent moisture. Thermocouple measurements were made at the center of the specimen as it was placed suddenly from room temperature to an air bath at -12 F. The freezing point of the soil moisture was reported as 31.7 F.

TABLE 35

TEST FOR EFFECT OF DRY UNIT WEIGHT AND PRESSURE*

ACFEL Specimen No.	Surcharge Pressure (psi)	Molded Dry Unit Wt (pcf)	Degree of Saturation (%)	Void Ratio, e	Permeability, k, at 10 C (cm/sec)	Water Content (%) Before Test	Water Content (%) After Test	Total Heave** (%)	Average Rate of Heave (mm/day)
(a) Effect of Unit Weight									
ART-1	0 5	110.1	100	0 553	2.150×10^{-6}	20.3	90.2	156 8	7.2
ART-2	0 5	116.6	100	0 467	$0\ 417 \times 10^{-6}$	17 2	26 4	28.4	2 3
ART-15	0.5	118 6	100	0 442	$0\ 300 \times 10^{-6}$	16.3	26.2	27 0	2 8
ART-3	0.5	120.4	100	0.420	$0\ 200 \times 10^{-6}$	15 5	20.2	17.1	1 3
ART-4	0 5	125 1	100	0 367	$0\ 075 \times 10^{-6}$	13.5	18 6	13.9	1 1
ART-16	0 5	125 7	100	0.360	$0\ 067 \times 10^{-6}$	13 3	18 0	10.1	1 2
(b) Effect of Pressure									
ART-7	0	116	100	0.480	0.592×10^{-6}	17 6	31 2	34.9	3.1
ART-8	2	117	100	0.464	$0\ 451 \times 10^{-6}$	17.6	32.3	54.6	2 8
ART-6	4	117	100	0.468	$0\ 475 \times 10^{-6}$	17 2	36.6	44 8	2.7
ART-5	6	117	100	0.462	0.434×10^{-6}	17.0	30.6	34.5	2.3

*Open system test, ART-1 through 8 frozen at rate of 1/4 in. per day; ART-15 and 16 frozen at rate of 1/2 in. per day.
**Based on original height of frozen portion.

TABLE 36

CLOSED SYSTEM TESTS, EFFECT OF INITIAL DEGREE OF SATURATION*

ACFEL Specimen No.	Molded Dry Unit Wt. ** (pcf)	Void Ratio, e	Degree of Saturation (%)	Water Content (%) Before Test	Water Content (%) After Test	Total Heave** (%)
ART-9	114	.500	58.8	10.7	9.9	0
ART-10	114	.499	71.7	13.0	10.5	0
ART-11	114	.502	85.5	15.6	14.4	1.7
ART-12	114	.501	100	18.2	16.8	5.4

*Rate of freezing, 1/4 in. per day; load intensity on specimen, 0.5 psi.
**Based on original height of frozen portion.

Determination of the frost susceptibility classification was made on the basis of the open system tests. No classification was actually made, but the following quotation is pertinent:

"The freezing tests performed on these specimens, where free water was available at the base of each specimen (open system), simulate extremely severe field conditions in which an unlimited supply of water is available to the soil during the freezing process. Such condition is seldom present in a well-designed roadway where adequate drainage has been provided. Therefore, the test results obtained in the laboratory during freezing are unlikely to be duplicated in severity under most normal field conditions. The following scale for classification of the degree of frost susceptibility of soil tested by this procedure, based on average rate of heave, has been adopted for rates of freezing between 1/4 and 3/4 in. per day.

Average Rate of Heave (mm/day)	Frost Susceptibility Classification
0 - 0.5	Negligible
0.5 - 1.0	Very low
1.0 - 2.0	Low
2.0 - 4.0	Medium
4.0 - 8.0	High
Greater than 8.0	Very high

Creep and Shrinkage of Concrete in Outdoor Exposure and Relaxation of Prestressing Steel

R. I. KINGHAM, Observer for the Canadian Good Roads Association;
J. W. FISHER, Assistant Bridge Research Engineer; and
I. M. VIEST, Bridge Research Engineer, AASHO Road Test, Highway Research Board

A study of the long-time behavior of prestressed concrete beams requires the determination of stress losses caused by creep and shrinkage of concrete and by relaxation of prestressing steel. Losses can be calculated accurately only if creep, shrinkage and relaxation are determined for the materials actually used in the beams. Furthermore, if the creep and shrinkage characteristics of concrete are determined by tests, the environmental conditions in such tests must approximate those to which the prestressed beams are exposed.

Outdoor creep and shrinkage tests of 24 concrete cylinders, and indoor relaxation tests of 20 samples of prestressing wire and strand are reported. The test data are described by mathematical equations obtained with the same basic model expressing shrinkage strain, creep strain or relaxation loss as a function of time. Numerical coefficients in the equations are evaluated by multiple regression analyses.

The results of the tests are used in computations of long-time strains in six prestressed concrete bridge beams. The computed strains compare favorably with the results of strain measurements on the beams.

● Studies of creep and shrinkage of concrete and relaxation of prestressing wire and strand carried out at the AASHO Road Test were made in connection with research involving four one-lane, simple-span bridges each made of three precast prestressed concrete beams and a cast-in-place reinforced concrete slab (1). Objectives of this research made it necessary to know stresses in the beams during their entire life. However, it was not convenient to make measurements except during stressing of the steel and after erection of the beams. To estimate stress changes during the intervening period, two long-term experiments were carried out on samples of materials used in the beams.

The study of shrinkage and creep characteristics of concrete was made on 24 cylinders. Two cylinders were cast in conjunction with each of the twelve bridge beams made of concrete of essentially the same quality. The experiment was conducted outdoors near the site of the prestressed concrete bridges. Observations began a few days after casting the cylinders in the fall of 1957 and continued through 1960.

The relaxation tests were made on ten samples of each type of prestressing steel. Beams for two bridges were prestressed with cables made up of parallel wires 0.192 in. in diameter; beams for the other two were prestressed with 7-wire strands of 3/8-in. diameter. The minimum length of any test was 1,000 hr. Observations of one sample of wire and two samples of strand were continued more than 9,000 hr.

The main part of this report is a general discussion of the experiments and the results of the analyses of the test data. The details of the experiments and analytical studies are contained in three appendices. The test data may be obtained in tabular form (AASHO Road Test Data Systems 2414, 2423, 2424 and 2425) from the Highway Research Board at the cost of reproduction.

EXPERIMENTAL STUDY OF CREEP AND SHRINKAGE

The creep and shrinkage characteristics of concrete were evaluated by tests on pairs of 6- by 12-in. cylinders, as shown in Figure 1. The eight pairs in the foreground were kept under constant loads and observed for the combined effects of creep and shrinkage. The four pairs in the background were kept free and observed for the effects of shrinkage alone.

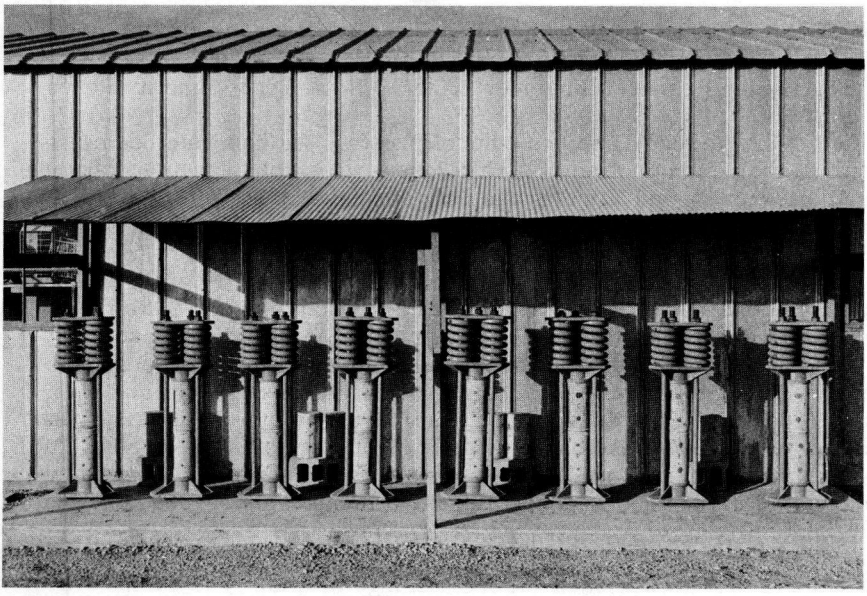

Figure 1. Creep and shrinkage tests.

The experiment included three controlled variables: the source of cylinders, the level of load, and time. An outline of the first two variables is given in Table 1.

TABLE 1

OUTLINE OF CREEP AND SHRINKAGE EXPERIMENT

Bridge	No Load		Load = 1,000 psi			Load = 2,000 psi		
	Beam	Age* (days)	Beam	Age* (days)	Strength* (psi)	Beam	Age* (days)	Strength* (psi)
5A	3	22	2	41	7,150	1	25	6,500
5B	2	18	3	40	7,100	3	33	6,820
6A	1	13	3	13	5,850	2	21	6,330
6B	1	17	2	15	6,020	3	14	5,950

*At beginning of test.

One pair of test cylinders was made in conjunction with each bridge beam and tested in the same loading frame. The test was designated by the combined bridge and beam designations given in Table 1; for example, the pair of cylinders made in conjunction with beam 2 of bridge 5B was observed unloaded and is referred to as test 5B2. (Because of early indications of large eccentricity of load, test 5B1 was discontinued

after a few days and replaced by a second set of cylinders from beam 3 of bridge 5A.)

Three levels of load were chosen: 0, 1,000, and 2,000 psi. Four tests were made at each level. The load for any particular pair of cylinders is given in Table 1.

The tests were begun shortly after stressing of the corresponding beams and continued for more than three years. The strain measurements on the creep cylinders were taken immediately before and after loading and at intervals of two days to 1 1/2 months thereafter. Each time measurements were made on creep cylinders, strains were measured on shrinkage cylinders from the same bridge.

The creep and shrinkage of concrete are affected by a number of factors other than the three controlled variables of this experiment. Kept as one-level factors were the aggregates, mix proportions and water-cement ratio, curing conditions and specimen size. Other variables could be classified as uncontrolled. Of these, the most important were the age and strength of concrete at the time of loading and the environmental conditions.

These three uncontrolled variables varied with some of the controlled variables. The age and strength of concrete at the time of loading varied with the source. The changes in environmental conditions were essentially the same for all specimens, as all were tested in the same place. However, the environment changed with time.

Differences in the uncontrolled variables were determined by independent measurements. The age at loading varied from 13 to 41 days and the corresponding strength of concrete from 5,850 to 7,150 psi (Table 1). Among the environmental conditions, the temperature and relative humidity were recorded. The temperature varied between -20 F and +100 F and the relative humidity between 11 and 100 percent.

Strains were measured with a mechanical gage on three 6-in. gage lines on the surface of each cylinder. All readings were corrected for temperature effects in the concrete cylinders. The corrected readings for the six gage lines on any one pair of cylinders were generally in good agreement except for small strains. For example, for a mean strain of 0.0006 one standard deviation, based on readings on individual gage lines, was approximately 0.0001. The standard deviation increased with increasing strain but considerably less than in direct proportion.

The temperature-corrected strains for the six gage lines were averaged and the means were used in the analyses. Two typical sets of data are shown in Figure 2: one for test 6A3 representing apparent creep (i.e., the combined creep and shrinkage) in cylinders loaded to 1,000 psi and the other for test 6A1 representing shrinkage of cylinders without load. The strains are plotted against time, with unit shortenings plotted upward and unit elongations plotted downward.

The tests shown in Figure 2 were started in October 1957. The over-all trend of both the shrinkage and the apparent creep data was a shortening of cylinders with time. However, the shrinkage data showed expansion immediately after the beginning of tests and again one and two years later. A similar effect was noted on the apparent creep curve one and two years after beginning the test. On the other hand, the difference between the apparent creep and the shrinkage, labeled as corrected creep, was largely independent of this cyclic effect.

It is believed that the cyclic effect was, at least in part, the result of cyclic variations in the environmental conditions. In fall and winter the humidity was relatively high and the temperature low: the cylinders absorbed moisture and expanded. In spring and summer the humidity decreased and the temperature increased: the cylinders dried and shrank.

It was apparent from the corrected creep curves that the creep strains in loaded cylinders increased rapidly at first. By 1,100 days the creep strains were increasing at a very slow rate, giving evidence that the creep might be approaching a finite value. Shrinkage was essentially completed, except for the seasonal variations, by the end of the first year.

The corrected creep data at any particular time showed marked differences from specimen to specimen. This is illustrated in Table 2, which includes creep strains that accumulated in 1,150 days. The specimens are listed in the order of decreasing age at loading, and the strains are given per psi of load. On the average, this unit

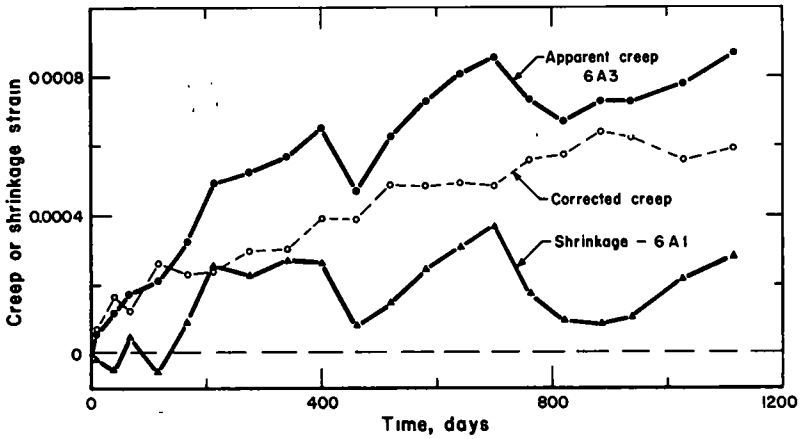

Figure 2. Typical creep and shrinkage data.

creep was about the same for the cylinders subjected to 1,000 psi and for those subjected to 2,000 psi, indicating that creep was proportional to load. A more detailed examination of the data suggested an increase in creep with decrease in the age of cylinders at loading.

TABLE 2

INSTANTANEOUS STRAINS AND CORRECTED CREEP STRAINS IN 1,150 DAYS

Load = 1,000 Psi				Load = 2,000 Psi			
Test	Strain per Psi*		Creep	Test	Strain per Psi*		Creep
	Initial	Creep	Initial		Initial	Creep	Initial
5A2	0.196	0.242	1.2	5B3	0.236	0.464	2.0
5A3	0.175	0.540	3.1	5A1	0.217	0.445	2.1
6B2	0.252	0.593	2.4	6A2	0.235	0.571	2.4
6A3	0.254	0.544	2.1	6B3	0.246	0.578	2.3
Mean	0.219	0.480	2.2	Mean	0.233	0.515	2.2

*Strain in micro-inches per inch divided by the magnitude of load.

Table 2 also includes initial strains per unit load caused by the application of load. The unit initial strains were larger for the greater loads and for younger specimens. The ratio of creep in 1,150 days to the initial strain was of the order of 2.2. Although further testing might have shown further increases in creep strains, it was apparent that to attain significant increases the period of observation would have had to be extended considerably.

EXPERIMENTAL STUDY OF RELAXATION

The relaxation characteristics of prestressing steel were evaluated by studies of 20 60-in. specimens of wire and strand tested in steel frames, as shown in Figures 3 and 4. Each specimen was stressed to the desired level and anchored at both ends. The distance between the anchorages, approximately 40 in., was constant throughout

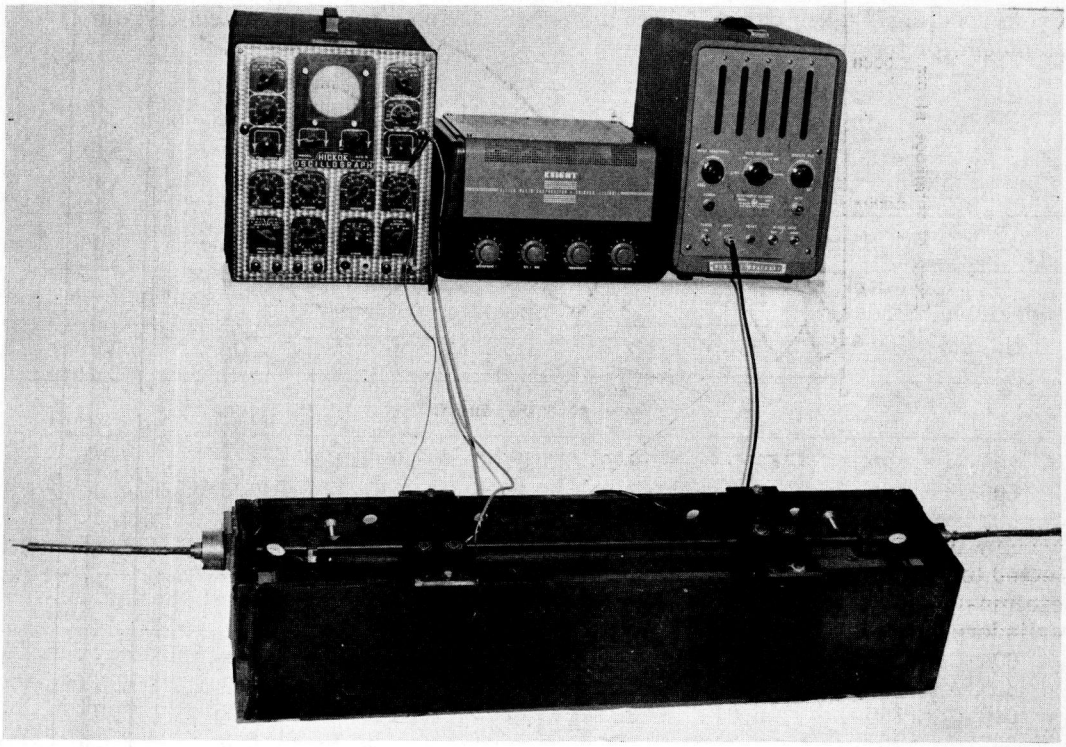

Figure 3. Relaxation test of wire.

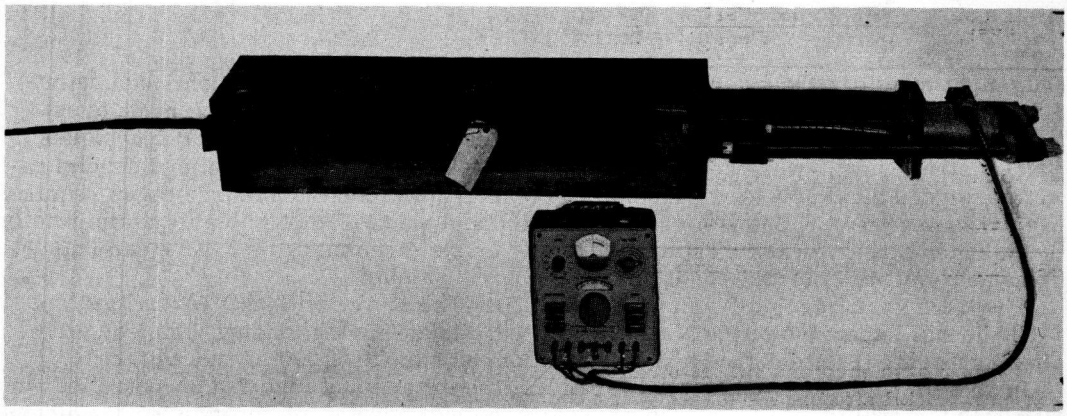

Figure 4. Relaxation test of strand.

the experiment. The changes in the stress level in the specimens were determined at intervals by measuring the changes in the fundamental frequency of the wire specimens (Fig. 3) and with the aid of a load cell in the strand specimens (Fig. 4).

The experiment included four controlled variables: the type and the source of prestressing steel, the level of initial stress, and time. The first three variables are listed in Table 3.

Two types of cold-drawn prestressing steel were used in the bridge beams: stress-relieved wire and stress-relieved strand. Each was furnished in two shipments.

From specimens taken during fabrication of the beams, five were selected from each shipment for the relaxation study.

TABLE 3

RELAXATION LOSSES IN 1,000 HOURS

Shipment A				Shipment B			
Specimen	Initial Stress, f_i, (ksi)	Relaxation loss		Specimen	Initial Stress, f_i, (ksi)	Relaxation loss	
		r, (ksi)	%			r, (ksi)	%
(a) 0.192-In. Wire*							
509	199.1	18.0	9.0	507	196.4	14.1	7.2
506	187.5	14.8	7.9	505	184.7	10.8	5.8
502	180.8	13.0	7.2	504	180.5	7.7	4.3
510	169.1	8.1	4.8	503	175.0	7.3	4.2
(b) 3/8-In. Strand+							
604	187.5	10.2	5.4	606	195.5	11.9	6.1
609	185.0	11.9	6.4	608	189.0	8.2	4.3
610	165.4	5.0	3.0	603	185.8	7.2	3.9
607	163.0	4.2	2.6	601	169.3	5.3	3.1
602	158.0	3.1	2.0	605	168.3	5.9	3.5

*Ultimate strength, f'_s = 257 ksi for both shipments.
+Ultimate strength, f'_s = 265 ksi for shipment A, 275 ksi for shipment B.

Only eight tests of wire are reported in this paper. One test was discontinued before 1,000 hr as a result of accidental movement of the testing frame, which made questionable a portion of the results; the other because of faulty experimental techniques.

Two stress levels were selected for both types of prestressing steel and specimens were assigned these levels at random. However, initial seating of anchorages required overstressing the specimens for a short period and made it impossible to attain exactly the selected stress levels. The initial stress levels given in Table 3 were determined by measurements immediately after anchoring the samples.

The tests were carried out in 1959 and 1960. The minimum length of any test was 1,000 hours. Readings of the stress levels were taken during loading, immediately after anchoring the steel, and at intervals from 90 sec. to 1,000 hr thereafter.

In addition to the four controlled variables, the experiment included uncontrolled variations in the quality of steel and in the environmental conditions. Control tests indicated that all steel in any one shipment had essentially the same mechanical properties and chemical composition. The variations in environmental conditions were not recorded but were believed to have been relatively small because the tests were carried out in a heated room.

Typical data from one relaxation test are shown in Figure 5. Strand specimen 609, selected for this figure, was stressed initially to 185 ksi. The relaxation loss in 1,000 hr was 11.9 ksi, or 6.4 percent of the initial stress. Observations beyond 1,000 hr showed substantial losses at later ages: e.g., at 5,000 hr the loss was 40 percent in excess of the 1,000-hr loss.

The rate of relaxation loss decreased with time. The log-log plot in the lower portion of Figure 5 illustrates that within the duration of these tests the relaxation losses followed closely a logarithmic straightline relationship. Thus the data gave no definite

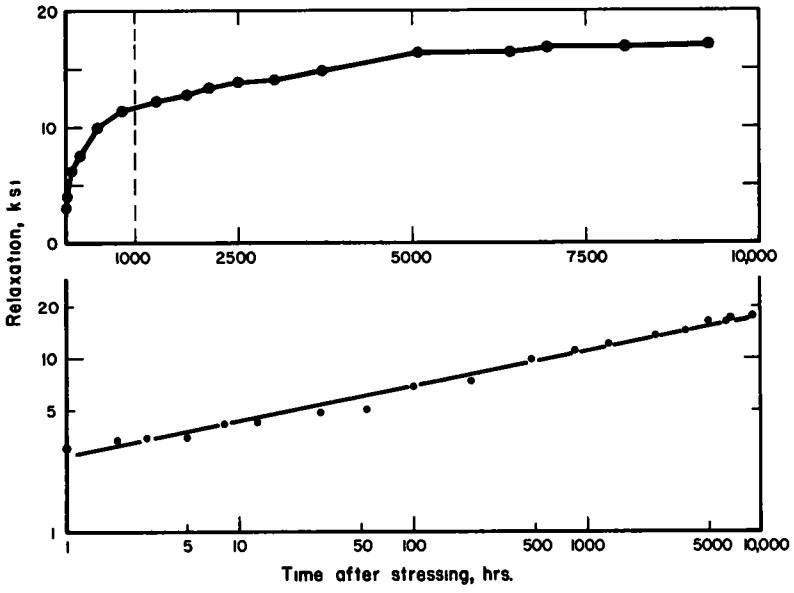

Figure 5. Typical relaxation data, specimen 609.

indication whether the relaxation loss would approach a finite limiting value at later ages.

The relaxation loss in 1,000 hr is given for all specimens in Table 3. It is apparent that the relaxation loss increased with increasing initial stress and was smaller for wire B than for wire A. The relaxation loss for strand B appeared to be somewhat lower than that for strand A.

ANALYSIS OF TEST DATA

The objective of this study was to develop a reliable basis for estimating the time-dependent losses in prestressed concrete beams. This objective could be met by statistical correlations of shrinkage and creep strain and relaxation stress with time. The correlations required first the selection of mathematical models suitable for regression analyses.

The primary criterion in the choice of the final model was the degree of correlation between observed test data and corresponding values calculated from the evaluated model. However, it was also considered desirable, although not essential for the objective of this study, for the model to satisfy the following three characteristics of creep, shrinkage (without the cyclic effects), and relaxation:

1. At time $t = 0$, the deformation (or stress loss) $\Delta = 0$.
2. At $0 < t < \infty$, Δ increases at a decreasing rate.
3. At $t = \infty$, Δ reaches a finite value Δ_∞.

Several models found in the literature were examined in the original as well as in various modified forms. Of these, the simple exponential model used by Shank (2)

$$\Delta = at^b \tag{1}$$

and the semilogarithmic model used by Raphael(3)

$$\Delta = a \ln(t + 1) \tag{2}$$

could be fitted satisfactorily only to limited ranges of the test data. Furthermore, they did not satisfy the third characteristic. A modification of the exponential Eq. 1, proposed by Stüssi(4), although satisfying all three characteristics, fitted satisfactorily

only the relaxation data.

Another simple model studied by several investigators (5, 6, 7) and satisfying all three desired characteristics may be written in the form

$$\Delta = \Delta_{\infty} (1 - e^{-t/a}) \tag{3}$$

which could not be fitted accurately to the full range of creep observations, indicating that the rate of creep did not follow the simple relationship on which the equation is based (that is, that the rate of creep is at all times proportional to the amount of potential creep remaining). McHenry (5) proposed a series of additive terms to correct for this discrepancy. A similar multiple-term model, proposed by Freudenthal and Roll (6), was found in excellent agreement with their test data.

Both McHenry's and Freudenthal and Roll's expressions are unsuitable for fitting through linear regression analysis. It was noted, however, that the rate of deformation increase indicated by Eq. 3 may be modified by the following adjustment:

$$\Delta = \Delta_{\infty}(1 - e^{-t/a})^{b} \tag{4}$$

in which

Δ = time deformation or stress loss at time t;
Δ_{∞} = total potential time deformation or stress loss;
t = time; and
a, b = empirical constants.

The general shape of Eq. 4 is shown in Figure 6. It will be noted that the model satisfies the three characteristics of time deformations. Furthermore, it may be linearized as

$$\log \Delta = \log \Delta_{\infty} + b \log (1 - e^{-t/a}) \tag{4a}$$

and is, therefore, suitable for linear regression analysis. (However, it is necessary to choose the constant a arbitrarily. Thus a series of analyses is needed to determine the best values of Δ_{∞}, b, and a).

It may be noted further that for small values of t/a, the term $(1 - e^{-t/a})$ approaches the value of t/a. In such case Eq. 4 is reduced to a simple exponential expression of the type used by Shank (2), and may be linearized as

$$\log \Delta = \log (\Delta_{\infty}/a^{b}) + b \log t \tag{4b}$$

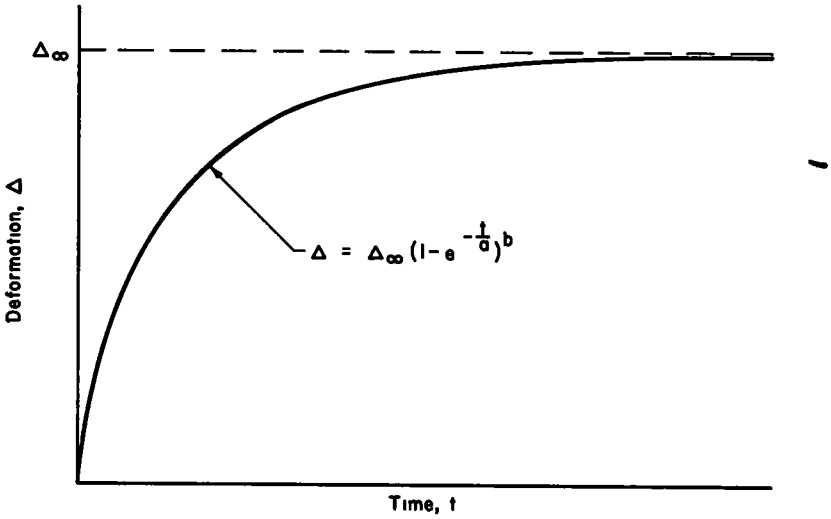

Figure 6. Time-deformation relationship.

The linearized Eq. 4a and 4b were fitted to the individual creep and relaxation tests and to the moving averages of all shrinkage data. (The moving averages rather than the original data were used in order to eliminate cyclic variations.) The ranges of the resulting coefficients of correlation (Table 4) indicate that Eq. 4 is an excellent representation of the time-deformation and time-stress loss relationships observed in this investigation.

TABLE 4

CORRELATION FOR INDIVIDUAL SPECIMENS

Type of Test	Number of Analyses	Range of r^{2*}
Creep	7+	0.86-0.98
Shrinkage	1	0.99
Wire	8	0.98-0.99
Strand	10	0.87-0.99

*r = coefficient or correlation.
+Analysis for test 5A2 not included.

The term Δ_∞ in Eq. 4 represents the total potential time-deformation or time-stress loss. If it is expressed in terms of the known variables of the tests, such as the load and the properties of the material, a generalized model is established for the multiple regression analysis of all data pertaining to one problem. This procedure was used in separate analyses of the creep, shrinkage and relaxation data, as shown in the following sections.

The test observations were continued even after the completion of analytical studies. Furthermore, the data obtained during early periods of tests were subject to large percentage errors, which were magnified by the logarithmic linearization. For these reasons, only certain portions of the test periods were utilized in the analytical studies, as is indicated in the following text.

Shrinkage Equation

The analysis of shrinkage was made in two steps: the first step determined the best fit to the test data without regard to the cyclic effects and the second step determined a correction factor accounting for the cyclic effect. The analyses utilized only data obtained between October 28, 1957, and December 19, 1959.

After eliminating the cyclic effects by the method of moving averages, a regression analysis of the shrinkage data made on the basis of Eq. 4a resulted in the following expression for the long-time trend:

$$\Delta'_s = 0.00028\,(1 - e^{-t/166})^{0.50} \qquad (5a)$$

in which t is the time in days from casting the concrete.

The residuals obtained as the difference between the shrinkage data and Δ'_s followed a cyclic trend with season. A regression analysis of the residuals based on the equation of a sine wave gave the following expression for the second term of the shrinkage equation:

$$\Delta''_s = 0.000087\,(1 - e^{-t/10})\sin\frac{\pi}{182}(t' + 60) \qquad (5b)$$

in which t' is time in days from January 1. (For example, t' for February 15 of any year would be 45 days.)

The complete equation representing the shrinkage data of this investigation is then:

$$\Delta_s = 0.000280\,(1 - e^{-t/166})^{0.50} - 0.000087\,(1 - e^{-t/10}) \sin \frac{\pi}{182}(t' + 60) \qquad (5)$$

in which

Δ_s = shrinkage strain at time t;
e = base of natural logarithm;
t = time from casting the cylinder, in days; and
t' = time from January 1, in days.

Eq. 5 is compared with the test data in Figure 7. The full lines represent the portions obtained by the analysis of the test data; the dashed lines represent extrapolations. The mean absolute residual strain for the data used in derivation of Eq. 5 is 0.000043.

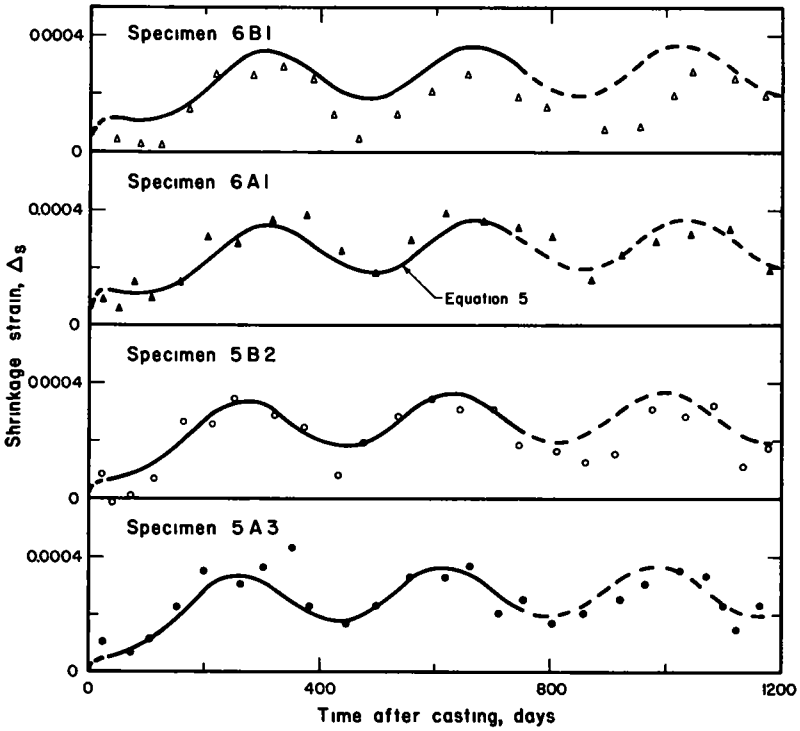

Figure 7. Correlation of shrinkage data.

Creep Equation

Earlier studies of creep have shown that the total potential creep is a function of the magnitude of load and of the age at the time of loading (5). More recent studies have indicated that the effect of this age may be accounted for by expressing the load as a percentage of the strength of concrete at the time of loading (7). Thus, the total potential creep may be expressed as

$$\Delta_\infty = c(f_c/f'_{c1})^d \qquad (6a)$$

in which c and d are empirical constants.

The data from six creep tests corrected for shrinkage were analyzed with multiple regression techniques on the basis of Eq. 4a combined with Eq. 6a. (Data from test 5A2 showed behavior radically different from that observed for the other specimens and were, therefore, excluded from the analysis. To avoid bias in relation to the load

level, data from test 5A1 were also omitted from the regression analysis.) Only observations made between 100 and 1,150 days after loading were included. The resulting creep equation was found to have the form:

$$\Delta_c = 0.00356\left(\frac{f_c}{f'_{ci}}\right)^{0.96}(1 - e^{-t/500})^{0.73} \qquad (6)$$

in which

Δ_c = creep strain at time t;
f_c = load per unit area of concrete;
f'_{ci} = strength of concrete at the time of loading;
e = base of natural logarithm; and
t = time from loading the concrete, in days.

Eq. 6 is compared with test data in Figure 8. It will be noted that the data for specimen 5A1, not included in the analysis, are in reasonable agreement with the theoretical line; but the data for 5A2, also excluded from the analysis, fall substantially below the regression line as well as below the range of all other test points. The mean absolute residual for the data included in the analysis is 0.000062.

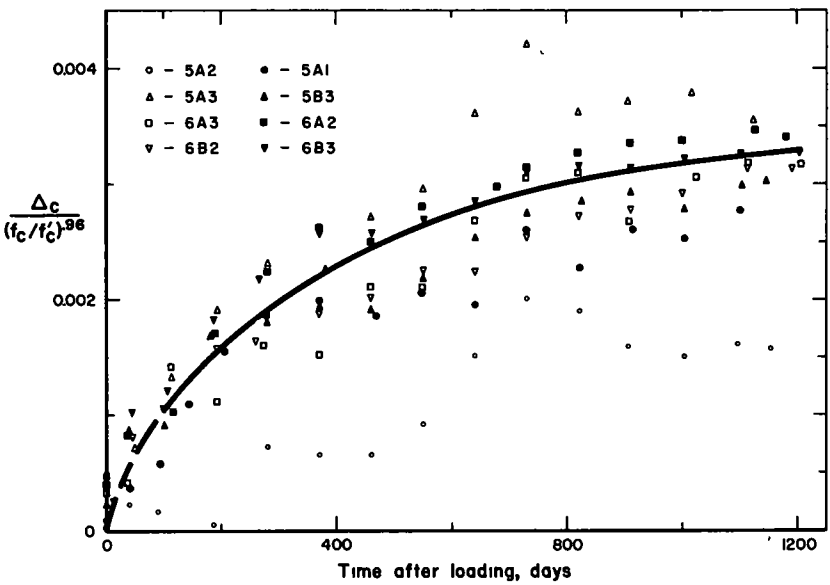

Figure 8. Correlation of creep data.

The measurements on creep cylinders determined the apparent creep, including both creep and shrinkage. This apparent creep was computed for the six tests utilized in the creep analysis as a sum of values given by Eq. 5 and 6 and is compared with the measurements in Figure 9. It will be noted that all data are located close to the line of equality. The mean absolute residual for the data shown is 0.000087.

In Figures 8 and 9, the data for specimens loaded to 1,000 psi are shown as open symbols and the data for specimens loaded to 2,000 psi are shown as full symbols. It will be noted that the equations appear to fit both sets of data equally well.

It has been pointed out in connection with the discussion of the creep experiment that the rate of increase of creep strains was very slow at 1,150 days, the terminal point of the analysis. The analytical studies indicated that equally good correlation with the test data could be obtained by the choice of several different sets of constants

greater than the set used in Eq. 6. However, constants significantly different from those used gave total potential creep substantially in excess of the creep observed at 1,150 days.

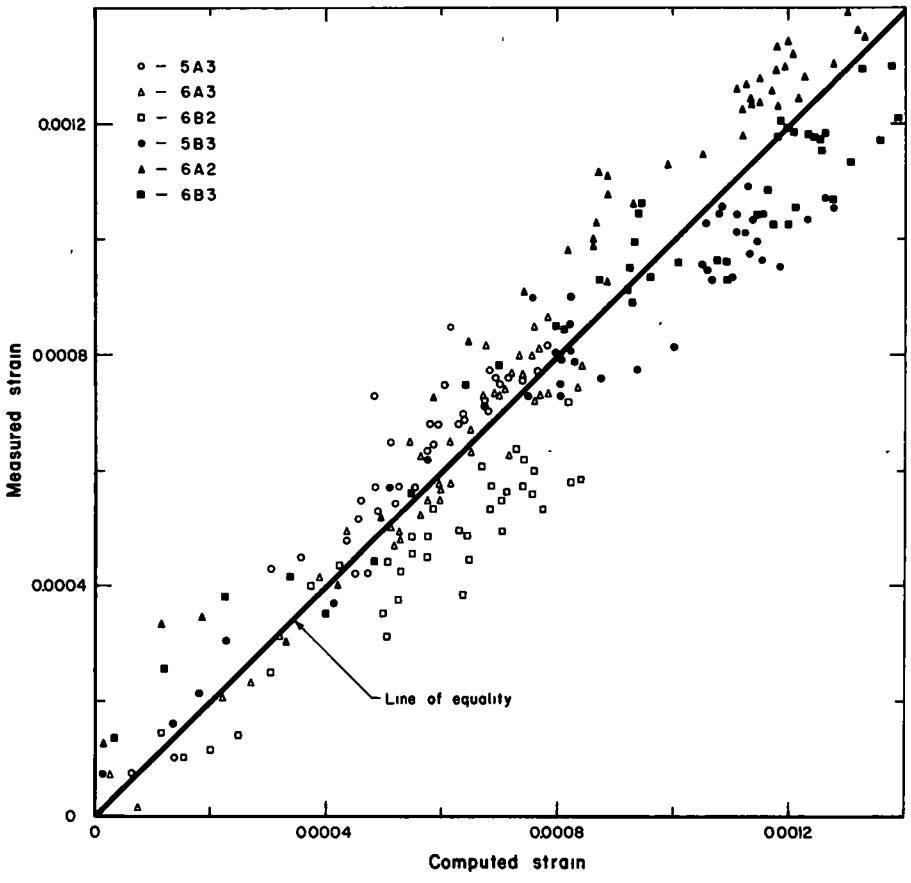

Figure 9. Comparison of computed and measured apparent creep strains.

Relaxation Equations

The relaxation data obtained in this investigation showed a logarithmic straight-line relationship and thus gave no indication concerning the total potential relaxation loss. Furthermore, the authors were unaware of any published data indicating directly either the probable magnitude of the potential loss or the variables which have influence on it. (Stüssi's study (4) suggested that several years of observations are needed even to reach one-half of the total potential loss; i.e., the half-life. Of the experimental data utilized by Stüssi only one test appeared to approach the half-life.) However, studies of the current relaxation tests of strand have shown that the correlation between the individual specimens may be improved if the potential stress loss is expressed as

$$\Delta_\infty = cf_i \, (f_i/f_s')^d \qquad (7a)$$

Thus, Eq. 4 may then be written in the form:

$$\Delta_r = cf_i \left(\frac{f_i}{f_s'}\right)^d (1 - e^{-t/a})^b \qquad (7b)$$

In view of the linear relationship between $\log \Delta_r$ and $\log t$, the term $(1 - e^{-t/a})$ in Eq. 7b may be replaced by the term t/a. Thus Eq. 7b may be given in the form:

$$\Delta_r = g\, f_1 \left(\frac{f_i}{f_s'}\right)^d t^b \qquad (7)$$

in which

Δ_r = relaxation stress loss at time t;
f_i = initial stress;
f_s' = ultimate strength of steel;
t = time from application of initial stress, in hours; and
g, d, b = empirical constants.

Eq. 7 does not indicate that the stress loss approaches a finite value. This is consistent with the trend shown by the test data. However, it is believed that the stress loss would have approached a finite value if the tests had been continued for a considerably longer period. In such case, Eq. 7b rather than Eq. 7 would have been better used for the regression analysis.

Using test data from 10 to 1,000 hr, the empirical constants of Eq. 7 were determined by multiple regression analysis based on Eq. 4b combined with Eq. 7a. Separate analyses were made for the strand, wire A and wire B. The results were as follows:

Type of Steel	g	b	d
Strand	0.0488	0.274	5.04
Wire A	0.1020	0.238	6.08
Wire B	0.0313	0.284	4.28

The correlation between Eq. 7, using these constants, and the test data is shown in Figures 10, 11, and 12. In all three figures open symbols are used for specimens subjected to lower initial stress levels. No definite bias with respect to the stress levels may be noted in any of the three figures.

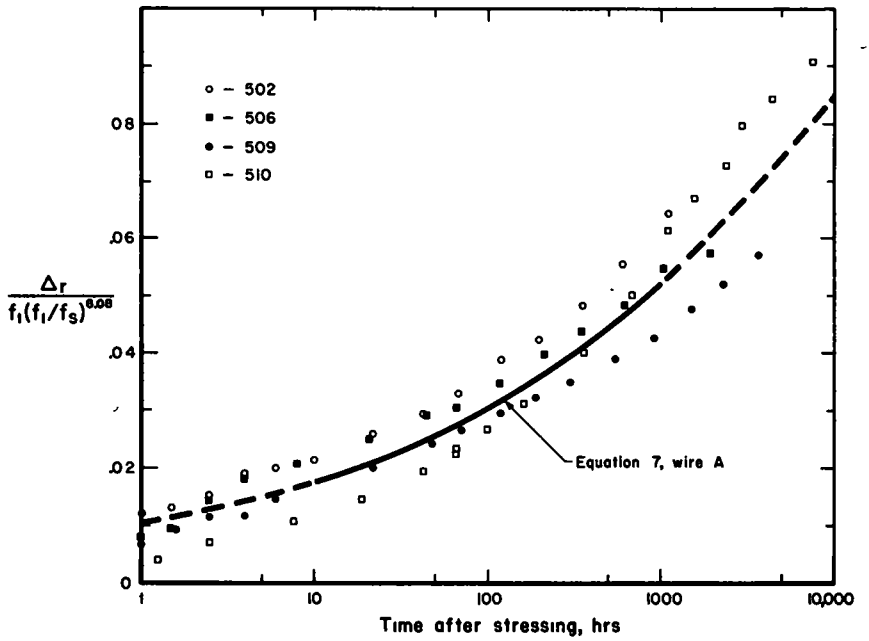

Figure 10. Correlation of relaxation data for wire A.

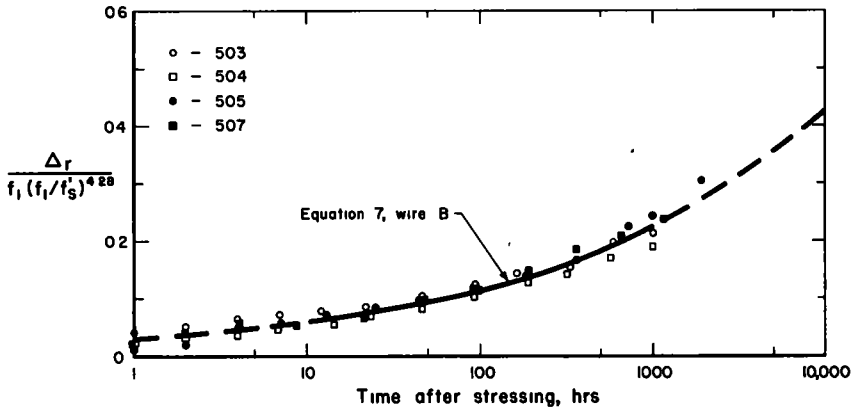

Figure 11. Correlation of relaxation data for wire B.

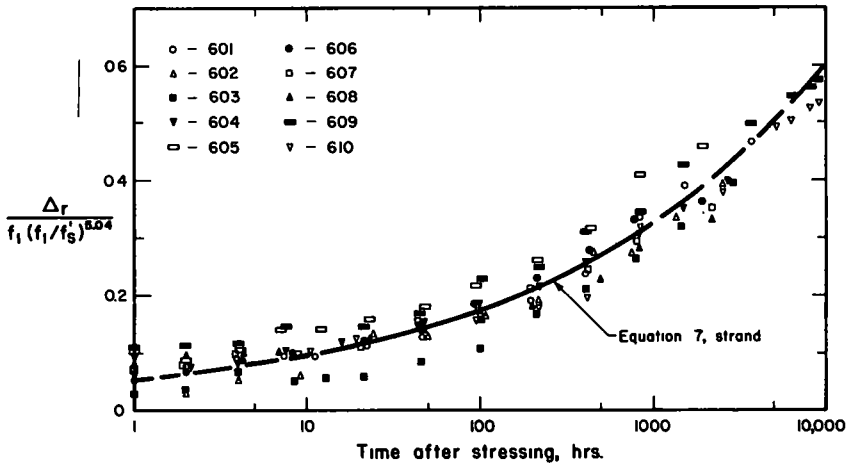

Figure 12. Correlation of relaxation data for strand.

Beyond 1,000 hr Eq. 7 is shown as a dashed line, because it represents an extrapolation. However, even the dashed lines are in reasonable agreement with the test data. The data are available up to 9,000 hr.

The mean absolute residuals for the data used in the analyses are 0.59, 1.12, and 0.38 ksi for the strand, wire A and wire B, respectively.

COMPARISON OF RESULTS WITH OTHER MEASUREMENTS

Relaxation Tests of Strand

The relaxation tests were made on short specimens of steel. Earlier experiments with wire indicated a good correlation between results of tests involving 100-ft specimens (8) and those involving 3-ft specimens (9). On the other hand, no data on the relaxation characteristics of strand were available. It was considered desirable, therefore, to check on the possible length effect by supplementary tests.

Two 100-ft specimens of the strand from shipment A, designated 631 and 632, were tested in the stressing bed described by Everling (8). The relaxation data for specimens 631 and 632 are plotted in Figure 13. Also included is the cure of Eq. 7 and the upper

and lower envelopes of the test data for short specimens of the strand.

The data for the 100-ft specimens follow the same general trend as Eq. 7 and fall within the range of the test data for the short specimens. It is further interesting to note by comparison with the data in Figure 12 that the results of specimens 605 and 631, having the same initial stress, showed practically identical relaxation losses; and specimens 607 and 632, also having the same initial stress, showed practically identical relaxation during the first 100 hr.

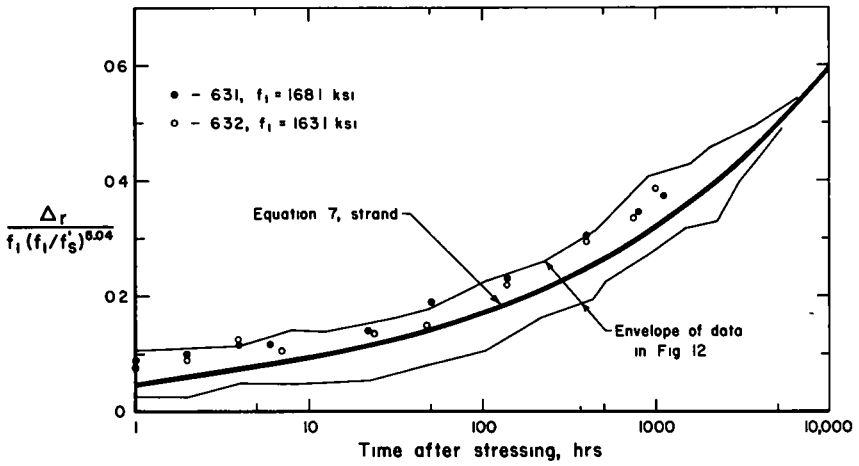

Figure 13. Relaxation tests of 100-ft strands.

Time Losses in Prestressed Concrete Beams

The six post-tensioned beams for the test bridges at the AASHO Road Test were erected four months before casting the slab (1). The change in the bottom flange strains during this period may be computed on the basis of the shrinkage, creep and relaxation characteristics represented by Eq. 5, 6, and 7, and compared with the measured change.

In a beam, the shrinkage and creep of concrete, and the relaxation of prestressing steel, are accompanied by decreases in the prestressing force. Thus, the time deformations in a prestressed concrete beam occur under a varying stress. Of the several methods accounting for this variation in stress (10), the rate of creep method was selected for this study. (The rate of creep method was compared on one beam with the superposition method. For the interval considered in this paper, there was no significant difference between the results of the two methods.) A numerical integration procedure, described elsewhere (11), was used on the basis of twelve intervals of nine to eleven days.

The computed strains are compared with measurements in Table 5. Although the measured strains were usually lower than the computed ones, the differences for beams 5A2, 5A3, 5B1 and 5B2 were within the accuracy of the measurements. For beams 5A1 and 5B3 the measured strains were considerably below the computed quantities. It should be noted, however, that the measured strains for these two beams are inconsistent with the trends indicated by measurements on the other four beams.

SUMMARY

1. Tests of 24 concrete cylinders and 20 samples of prestressing wire were made to determine the creep, shrinkage and relaxation characteristics for use in the interpretation of the tests of prestressed concrete bridges. The cylinders were tested for

TABLE 5

COMPARISON OF COMPUTED AND MEASURED LOSSES IN PRESTRESSED CONCRETE BEAMS*

Beam	Date of Casting	Age at Stressing (Days)	f'_c (psi)	Computed Partial Strains(x 10^6)				Total Strain(x 10^6)		Measured / Computed
				Δc	Δs	Δr	Δel	Computed	Measured	
5A1	509	3	4600	150	135	-61	-18	206	108	0 52
2	480	13	5850	106	113	-69	-12	138	129	0 93
3	508	5	5050	136	135	-86	-17	168	153	0 91
5B1	391	97	8100	154	72	-120	-19	87	97	1 11
2	496	4	4950	226	127	-133	-27	193	172	0 89
3	496	3	4600	257	127	-134	-30	220	94	0 43

*Losses between the dates 543 and 654 for bridge 5A and between the dates 533 and 654 for bridge 5B. Dates relate to consecutive numbering, with 391 = July 27, 1957.

more than three years in an outdoor exposure. The samples of steel were tested for at least 1,000 hr. The results were correlated by multiple regression analyses utilizing one basic model for all three phenomena.

2. The results of shrinkage tests are represented by Eq. 5, including the effects of age and of seasonal variations. Pronounced seasonal variations, believed to be the result of environmental changes, were observed in the tests of both shrinkage and creep cylinders.

3. The results of creep tests are represented by Eq. 6, indicating the existence of a maximum potential creep. The potential creep is expressed as a function of the ratio of the applied stress and the strength of concrete at loading.

4. The results of the relaxation tests are represented by Eq. 7, having different empirical constants for the strand, wire A, and wire B. The equation should not be applied beyond 9,000 hr, representing the upper limit of the test data.

5. Satisfactory comparisons with measurements made on the companion prestressed concrete beams indicated that the equations form a suitable basis for computing the stress losses in these beams.

ACKNOWLEDGMENTS

The study reported herein was carried out as a part of the bridge research at the AASHO Road Test. The authors wish to acknowledge the contributions of all those who were connected with various phases of the investigation and particularly the many helpful suggestions made by Dr. Paul Irick, Chief of Data Analysis, during the course of planning the experiment and of data analysis.

The relaxation tests of the 100-ft strands were made by the laboratories of the American Steel and Wire Division, United States Steel Corporation.

REFERENCES

1. Viest, I. M., "Bridge Research at the AASHO Road Test." HRB Spec. Rep. 38, pp. 24-43 (1958).
2. Shank, J. R., "The Plastic Flow of Concrete." Ohio State Univ. Eng. Exper. Sta., Bull. 91 (1935), 62 pp.
3. Raphael, J. M., "The Development of Stresses in Shasta Dam." Am. Trans. ASCE, 118: 289-309 (1953).
4. Stüssi, F., "On Relaxation of Steel." Intern. Ass. for Bridge and Struct. Eng. Publ., 19: 273-286 (1959).
5. McHenry, D., "A New Aspect of Creep in Concrete and Its Application to Design " Proc. ASTM, 43: 1069-1084 (1943).
6. Freudenthal, A. M., and Roll, F., "Creep and Creep Recovery of Concrete under High Compressive Stress." Am. Proc. Con. Inst., 54: 1111-1142 (1958).
7. Lyse, I., "Shrinkage and Creep of Concrete." Am. Proc. Con. Inst.,56: 775-782 (1960).

8. Everling, W. O., "Discussion of Steel Wire for Prestressed Concrete." Proc., First U. S. Conf. on Prestressed Concrete, Mass. Inst. of Technology, pp. 161-166 (1951).
9. McLean, G., and Siess, C. P., "Relaxation of High-Tensile-Strength Steel Wire for Use in Prestressed Concrete." ASTM, Bull. 211, pp. 46-52 (Jan. 1956).
10. Ross, A. D., "Creep of Concrete under Variable Stress."Am. Proc. Con. Inst.,54: 739-758 (1958).
11. Corley, W. G., Sozen, M. A., and Siess, C. P., "Time-Dependent Deflections of Prestressed Concrete Beams." HRB Bull. 307 (1962).

Appendix A

DETAILS OF CREEP AND SHRINKAGE EXPERIMENT

Specimens

The aggregates used in the 6- by 12-in. concrete cylinders were lake sand and crushed stone. The lake sand, mostly siliceous, had an average fineness modulus of 2.67; the coarse aggregate, with a maximum size of 1 in., was a crushed limestone. Sieve analyses for sand and gravel are given in Table 6.

TABLE 6

GRADATION OF AGGREGATES

Crushed Stone		Sand	
Sieve Size	Retained (%)	Sieve Size	Retained (%)
1 1/2	0.0	3/8	0.0
1	0.2	No. 4	3.2
3/4	19.8	No. 8	12.8
1/2	61.0	No. 16	26.1
3/8	81.9	No. 30	46 1
No. 4	97.3	No. 50	80.6
No. 8	98.0	No. 100	97.8
		No. 200	99.4

The concrete, made with type I portland cement furnished by one manufacturer, had the following characteristics: Cement content, 7.00 sacks per cubic yard; water content, 4.6 gal per sack; mix proportions by weight (cement: sand: crushed stone), 1:1.74: 2.86; air-entraining agent, approximately 3/4 oz per sack; average slump, 1 5/8 in.; and air content, 3.1 to 5.0 percent.

The amount of air-entraining agent was adjusted according to the control tests of air content. Concrete was compacted with internal vibrators and steam cured for 12 to 84 hr with a maximum temperature of 110 F. Concrete cylinders were delivered to the bridge site with their respective beams and kept with the beams until the start of testing.

In addition to those reserved for the creep and shrinkage experiment, several cylinders were prepared for compression tests. Results of the compression tests are shown in Figure 14. Cylinders were tested at the time of stressing the bridge beams, at 28 days, and at the beginning of test traffic. A mean strength value was found for each of the three groups and the curve shown in Figure 14 was fitted to the three means The strengths given in Table 1 were taken off the mean curve.

The coefficient of thermal expansion of the concrete was found to vary between 0.0000048 and 0.0000075 per ^{0}F when temperature varied between 37 and 100 F

Testing Apparatus and Instrumentation

The loading frame for creep tests consisted of a yoke made up of steel plates, tie bars and springs shown schematically in Figure 15. Two concrete cylinders were placed end on end and separated by a steel plate. The cylinders were capped with a high-strength gypsum plaster to insure uniform distribution of load. The load was applied by tightening the nuts on the tie bars to deflect the springs, which transmitted the load to the cylinders through the loading head.

Concrete cylinders for shrinkage tests were placed on end near the creep cylinders. They, of course, required no loading frame.

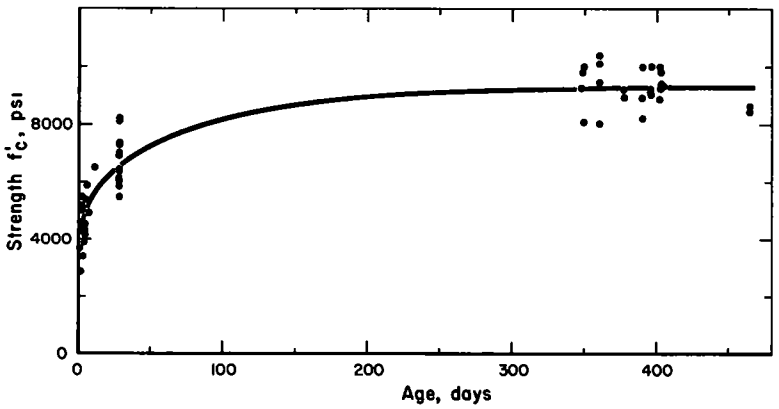

Figure 14. Cylinder strength of concrete.

The creep cylinders were instrumented for measurement of longitudinal strains on six equidistant gage lines spaced around the circumference on the surface. Electric resistance strain gages 6 in. long were placed on every other gage line. On each remaining gage line, two brass plugs spaced at 6 in. provided reference points for measurements with a mechanical gage. The plugs were fitted tightly into shallow holes drilled in the cylinders, and held by epoxy resin. The distance between two small holes in the brass plugs was measured with a Metzger gage. One division on the dial of the gage was equal to the strain of 0.0000149.

The shrinkage cylinders had only the three gage lines for measurements with the mechanical strain gage.

The load was determined from the deflection of the springs. Each spring had two reference holes approximately 10 in. apart when unloaded and was calibrated with several increments of load. The rate of spring deflection was approximately 0.0001 in. per lb. The deflections were measured with a caliper graduated to 0.01 in.

Testing Procedure

After the creep cylinders were assembled in the frame, initial readings were taken on all twelve gage lines. Then the load was applied in three increments After each increment, the electric strain gages were read to check the concentricity of the load. Differences in the strains on the three gages served as a basis for distribution of the following load increment to the three springs. After the total load was applied and distributed to the three springs so as to result in essentially equal strain on all electric gages, another set of readings was taken on all twelve gage lines. The time required for loading one set of cylinders varied from 1 to 5 hr.

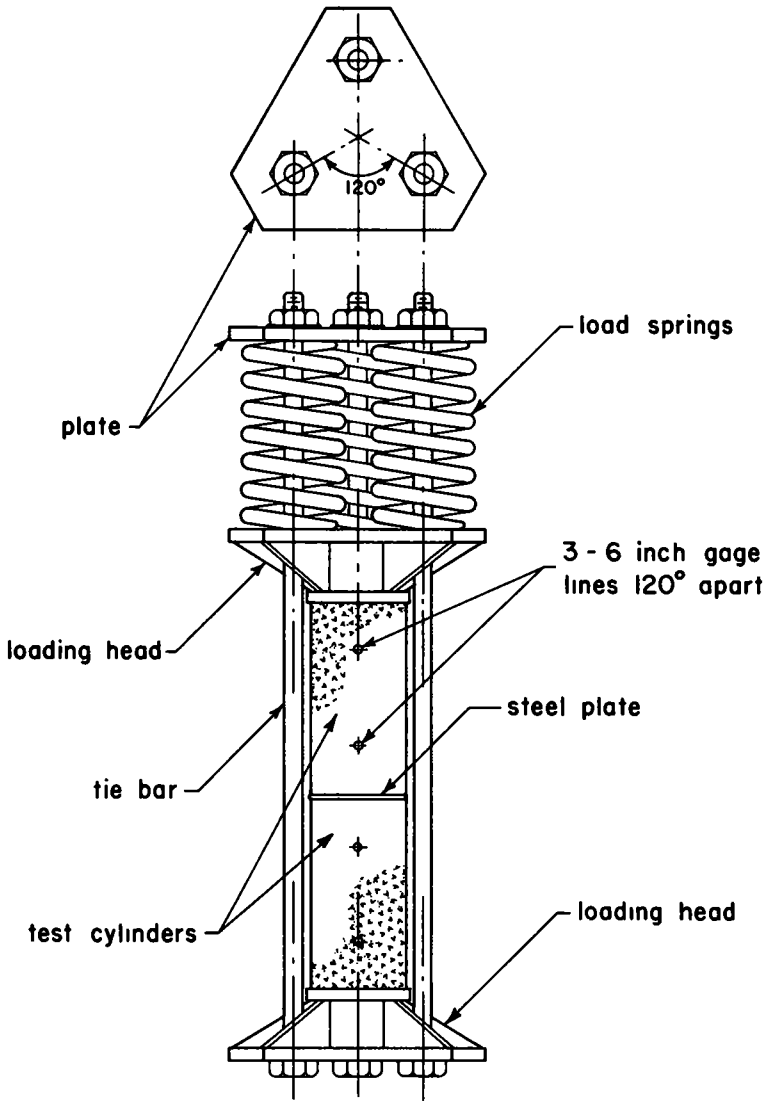

Figure 15. Loading frame for creep tests.

The mechanical strain measurements on creep cylinders were repeated every other day during the first week after loading, weekly during the following three weeks, every three weeks during the next seven months, monthly during the next two years, and every month and a half thereafter.

Each time readings were taken on a set of creep cylinders, several readings were made also on a standard bar, on shrinkage cylinders from the corresponding bridge, and on springs. Whenever the spring measurements indicated a deviation of more than 75 psi from the desired stress in the cylinders, the load was adjusted.

The air temperature was recorded near the test site every hour. The daily maxima and minima were averaged for every month (see Fig. 16).

The relative humidity data were obtained from the tables of Local Climatological Data of the U. S. Weather Bureau in Peoria, Ill. The daily maxima and minima were averaged for every month.

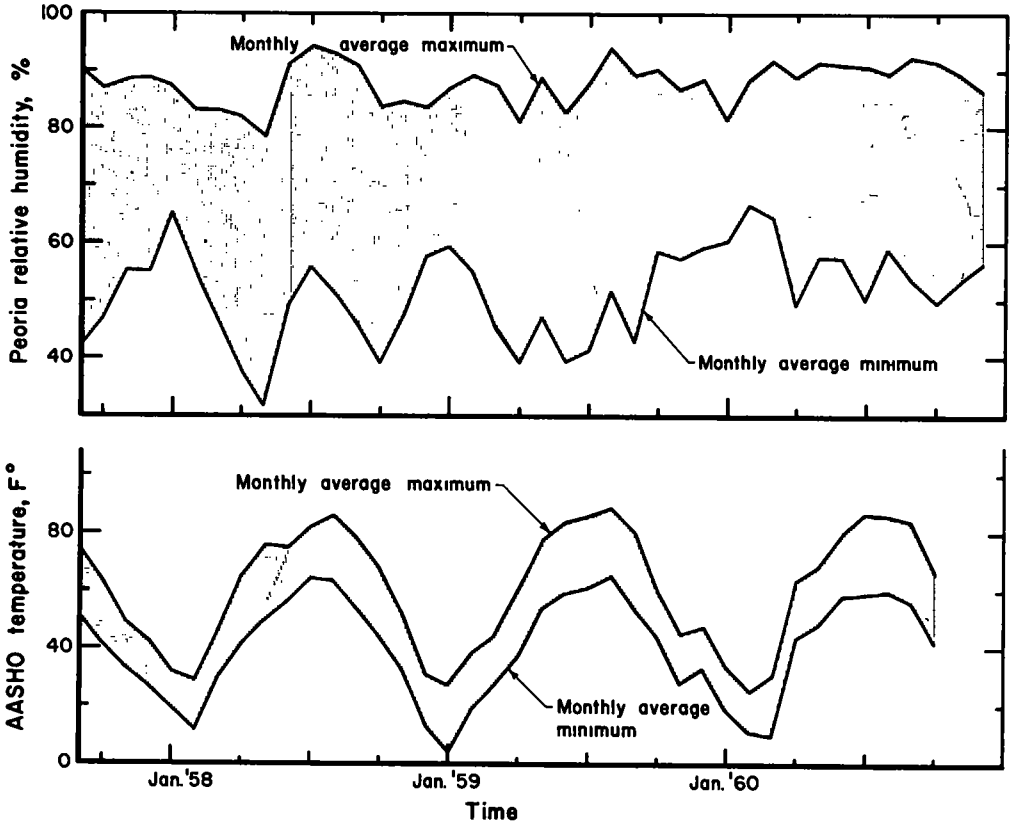

Figure 16. Relative humidity and air temperature history.

Appendix B

DETAILS OF RELAXATION EXPERIMENT

Specimens

The prestressing wire was cold-drawn and stress relieved with bright, smooth surface. The wire, produced by the John A. Roebling's Sons Corp., was delivered in approximately 55-ft lengths enclosed in flexible metal sheathing. One length of prestressing wire was taken from each shipment for relaxation tests.

The prestressing strand was made of seven cold-drawn bright wires and stress relieved. The strand, produced by the American Steel and Wire Division, United States Steel Corp., was delivered in two coils. After release of prestress, several pieces of strand of varying length were saved for relaxation and other tests.

Tensile tests were made on 90 coupons of wire and on 33 coupons of strand. Typical stress-strain diagrams are shown in Figure 17. The following mean ultimate strengths were found:

Wire, both shipments, ...257 ksi
Strand, shipment A, ...265 ksi
Strand, shipment B, ...275 ksi

The mean cross-sectional area of the wire was 0.0293 sq in.; that of the strand, 0.0806 sq. in.

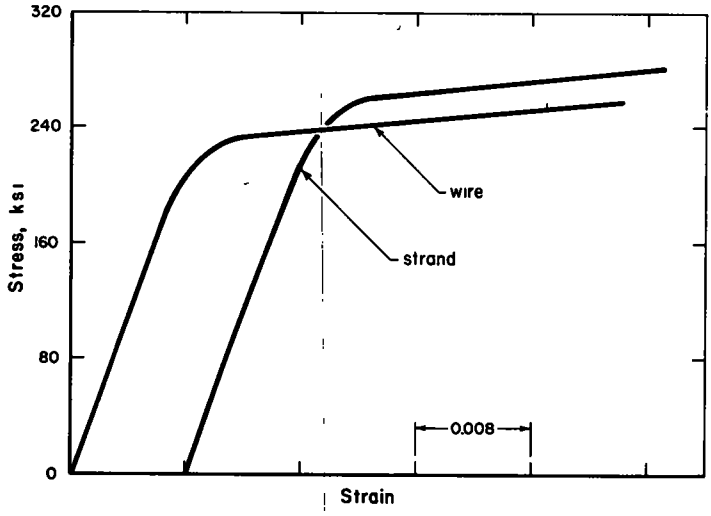

Figure 17. Typical stress-strain curves of prestressing steel.

The chemical composition of the steel was determined by analyses of three samples for each shipment. The averages are given in Table 7.

TABLE 7

CHEMICAL COMPOSITION (%) OF WIRE AND STRAND

Element	Wire		Strand	
	Shipment A	Shipment B	Shipment A	Shipment B
Carbon	0.80	0.80	0.72	0.73
Manganese	0.67	0.63	0.71	0.78
Phosphorus	0.016	0.016	0.015	0.017
Sulfur	0.040	0.037	0.034	0.040
Silicon	0.25	0.25	0.23	0.24

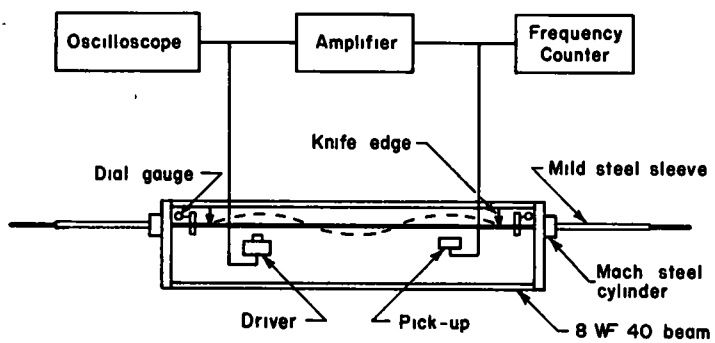

Figure 18. Testing apparatus for wire.

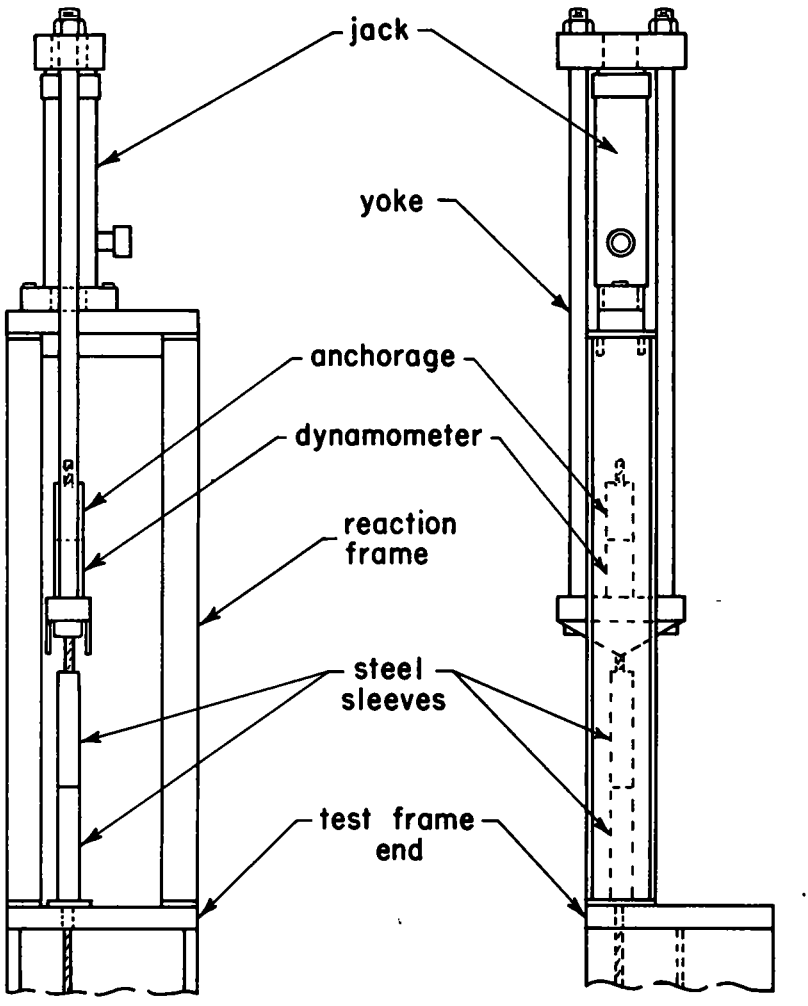

Figure 19. Jacking assembly for wire and strand.

Testing Apparatus and Instrumentation

Wire and strand specimens were tested in frames, shown schematically in Figure 18. The frames were made from 36-in. lengths of 8WF40 beam with plates welded on each end. The wire or strand was anchored with mild steel sleeves crimped on the specimen. For wire specimens the bearing area of the anchorage was increased with a steel cylinder into which the sleeve was press-fitted. The anchorage bore against steel shims which in turn bore against wedges.

The initial stress was applied with the jacking assembly shown in Figure 19. It consisted of a 10,000-psi hydraulic jack, a reaction frame, a yoke, a dynamometer, and a wedge-type grip anchorage.

The initial stress and the relaxation stress losses in strands were determined with a calibrated load cell placed in an assembly as shown in Figure 20. The cell was seated on a reaction frame bearing against the testing frame. A yoke transmitted the force from the strand to the load cell. The response of the load cell was monitored by a strain indicator with one division corresponding to 48 lb.

The initial stress in the wires was determined with a calibrated dynamometer made of an aluminum cylinder. The dynamometer was incorporated into the jacking assembly shown in Figure 19. The response of the dynamometer was monitored by a

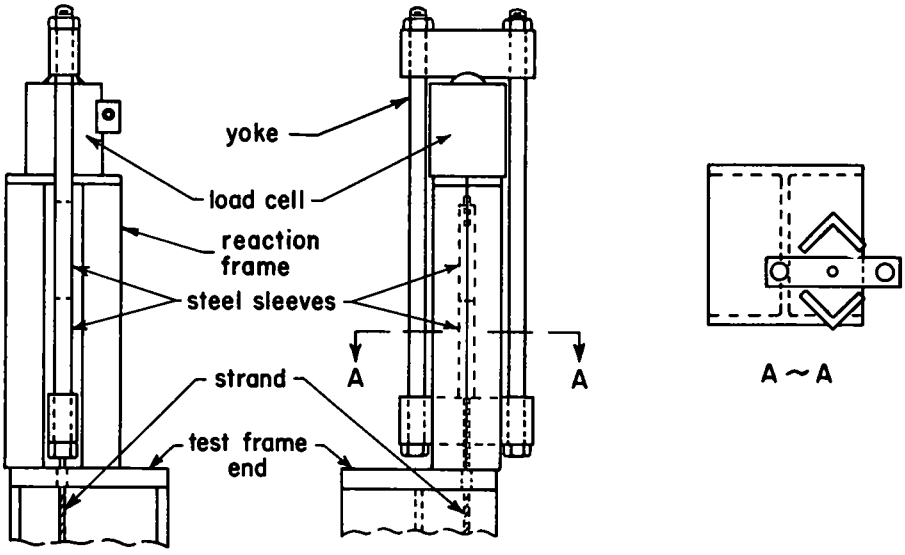

Figure 20. Load cell assembly for strand.

strain indicator with one division corresponding to 17 lb.

The relaxation stress losses in the wires were determined by measurements of the third mode of the fundamental frequency of lateral vibration of the wires. The fundamental frequency of lateral vibration of a wire depends essentially upon the tension in the wire and to a lesser degree upon the effect of the wire resting as a simply-supported beam (9). The relationship between the frequency and stress was obtained experimentally during initial loading of each specimen. Within the range of the test data, the stress was found to be a linear function of the frequency squared, but the calibration lines did not pass through the origin.

Measurements of the frequency required a pick-up, a five-digit frequency counter, an amplifier, a driver, and an oscilloscope, as shown schematically in Figure 18. The pick-up was of standard magnetic type used on musical instruments. The driver was built of a 500-ohm relay coil and a permanent magnet. A standard oscilloscope was inserted into the system to provide a check against excessive amplification of the wire vibration.

The wave length was determined by two knife edges supported from the test frame 28 in. apart. The driver and the pick-up were placed at the outer 1/6 points between the knife edges.

Slippage in the anchorages of both the wires and the strands was checked with two dial gages graduated to 0.0001 in. One gage was mounted near each end of the test frame and was resting on a collar attached to the specimen.

Loading and Testing Procedures

For the tests of strand, the specimen was stressed with the hydraulic jack 20,000 psi in excess of the desired level, the overstress being required to compensate for losses caused by seating of anchorages. Steel wedges were then inserted between the anchorage sleeve and the loading frame and the jack was released. The strand was overstressed for no longer than one minute.

Load cell readings were taken before and immediately after loading, and were continued at intervals to measure the loss of stress in the strand. Readings were taken on the basis of a logarithmic interval with approximately 10 readings per cycle taken between 1 1/2 min to 100 hr, and from 15 to 20 readings between 100 to 1,000 hr. On two specimens readings were also taken approximately every 1,000 hr to over 9,000 hr. The readings were believed accurate to about 100 psi.

While the initial readings were taken, the collars for the dial gages were attached to the strand and zero readings on the dial gages were recorded. Before every subsequent reading of the load cell, the dial gages were checked. There were no indications of anchorage slippage on any specimen throughout the testing period.

In the tests of wire, the initial loading procedure had to include the determination of the stress-frequency relationship. The load was applied to the wire in increments and the frequency, as well as the dynamometer response, was noted for each increment. An overstress of 19,000 to 24,000 psi was required to seat the wire at the desired stress level. The overstress was held for 20 to 30 sec, the time required to position wedges between the anchorage and the frame. If the desired stress level was not reached upon the release of the jack, the specimen was overstressed a second time, and a third time if necessary. The entire loading procedure took 5 min at the most.

After the wire was secured in the frame, the initial frequency reading was taken as quickly as possible. Subsequent readings were taken at the same time intervals as those chosen for the strand. One hour after loading, the collars were put on the wire and initial readings on the dial gages were taken.

The procedure for determining the stress loss in the wire was somewhat more complicated than for strand. After checking the dial gages for any movement in the time interval between readings, the collars attached to the wire had to be taken off as they would change the mass of the vibrating wire and thus also the frequency-stress relationship. The wire was excited by plucking. The position of the driver and pick-up coils produced the third mode of the fundamental frequency. (The third mode was chosen for two reasons. First, the change of frequency encountered in the wire was least affected by other influences, such as unknown and conditions and vibrations of the frame or instruments. Second, the change in stress due to relaxation losses was such that the third mode gave a range of frequency sufficient in relation to the sensitivity of the measuring system.) By adjusting the amplifier, the amplitude of the wire vibration could be controlled and an undistorted wave seen on the oscilloscope. The frequency, measured with a frequency counter, was read over a 10-sec interval to obtain a reading of one-tenth of a cycle or approximately 40 psi. However, the overall accuracy depended also on the calibration of the dynamometer and was estimated to be within 100 psi.

As in the case of strand, no indications were found of any anchorage slippage in the wire tests.

Appendix C

ANALYSIS OF TEST RESULTS

The time-dependent losses were assumed to be described by the mathematical model given as Eq. 4, which in its linearized state (Eq. 4a or 4b) can be written as

$$\Sigma X_1 = A + bX_2 + \text{residual}$$

The least squares normal equations that will minimize the sum of squared residuals are:

$$\Sigma X_1 = N\,A + b\ \Sigma X_2 \tag{8a}$$

$$\Sigma X_1 X_2 = A\ \Sigma X_2 + b\ \Sigma X_2^2 \tag{8b}$$

in which component parts X_1 and X_2 constituted measured test variables and N was the number of test data used in the analysis. The coefficients A and b were determined by simultaneous solution of Eq. 8a and 8b. This method was used to fit all shrinkage data, and creep and relaxation data for individual tests.

For relaxation stress losses and creep strains, the potential time-dependent loss Δ_∞ was expressed in terms of the initial load and ultimate strength (Eq. 6a and 7a).

The linearized equation that represents three variables has the form

$$X_1 = A + c\,X_2 + b\,X_3 + \text{residual}$$

Multiple regression analysis must now be used and the least squares normal equations that will minimize the sum of squared residuals for the linear series were

$$\Sigma X_1 = N\,A + c\;\Sigma X_2 + b\;\Sigma X_3 \tag{9a}$$

$$\Sigma X_1 X_2 = A\;\Sigma X_2^2 + b\;\Sigma X_2 X_3 \tag{9b}$$

$$\Sigma X_1 X_3 = A\;\Sigma X_3 + c\;\Sigma X_2 X_3 + b\;\Sigma X_3^2 \tag{9c}$$

in which the component parts X_1, X_2 and X_3 constituted the measured variables. These equations were solved simultaneously for the values of coefficients A, c and b.

The solutions of Eq. 8 and 9 were programed for the electronic computer used at the Road Test. Separate analyses were made for shrinkage, creep and relaxation with the component parts of the equations expressed as outlined in the following.

Shrinkage Analysis

The shrinkage data showed a well-defined seasonal variation, which appeared to be superimposed on a long-time trend. The method of moving averages was used to extract this long-time trend from the test data. The moving averages were established in the following manner:

1. The test period was divided into 25 monthly intervals.
2. It was observed that the seasonal effect was approximately one year in length; therefore, the data for the first twelve intervals was averaged, giving an average at the sixth period.
3. Next the data for the first 13 intervals minus the first interval was averaged giving the moving average at the seventh period. This was continued until the nineteenth period, giving a total of fourteen moving average points.

The moving averages for the four specimens were averaged ($\bar{\Delta}_S$) and then fitted with Eq. 4a. As shrinkage is not a function of load and all concrete was of the same quality, the total potential shrinkage contained no independent variable. Therefore, Eq. 8a and 8b were used to obtain the regression coefficients. The component parts were

$$X_1 = \log(\bar{\Delta}_S + Z) = \log \Delta'_S$$

$$X_2 = \log(1 - e^{-t/a})$$

and

$$A = \log \Delta_\infty$$

in which Z represents an estimate of shrinkage strain that occurred before the measurements were started. It was assumed in the analysis that Z corresponded to the shrinkage strain at t = 18 days.

The analysis was repeated for several chosen combinations of a and Z values. The best correlation corresponded to the following values of coefficients: Z = 0.0001; a = 166, Δ_∞ = 0.00028, and b = 0.50.

The differences between the shrinkage data, corrected by the term Z = 0.0001, and the strains computed from Eq. 5a were evaluated next. These residuals (Δ''_S) showed a seasonal variation following the trend of a sine wave. Attempts were made to correlate the residuals to the relative humidity. Although some correlation was found with the monthly average relative humidity in Peoria (Fig. 16), better results were obtained by correlation with the time of the year utilizing the equation of a sine wave having length equal to 364 days. Therefore, the equation of a sine wave was selected for the mathematical model. The sine term was modified by function ($1 - e^{-t/x}$) to

satisfy the boundary condition at time t = O.

The resulting model used for the regression analysis of the residuals was

$$\Delta_s'' = A + b(1 - e^{-t/x}) \sin \frac{\pi(t' + \phi)}{182} \qquad (10)$$

so that the component parts of Eq. 8a and 8b were

$$X_1 = \Delta_s''$$

$$X_2 = (1 - e^{-t/x}) \sin \frac{\pi(t' + \phi)}{182}$$

The constant 182 was selected on the basis of a one-year cycle. The constant x was selected so that the cyclic variation would have little influence on shrinkage before six days of age and full influence after thirty days. A value of x = 10 appeared to fulfill this condition. Analyses were then made with several chosen values of the phase angle ϕ and the following constants were found to give the best correlation: x = 10, ϕ = 60, A = 0.000000, and b = 0.000087.

Creep Analysis

The creep data were analyzed in two steps. The first entailed fitting Eq. 4a to the data of individual creep tests. The component parts of Eq. 8a and 8b were

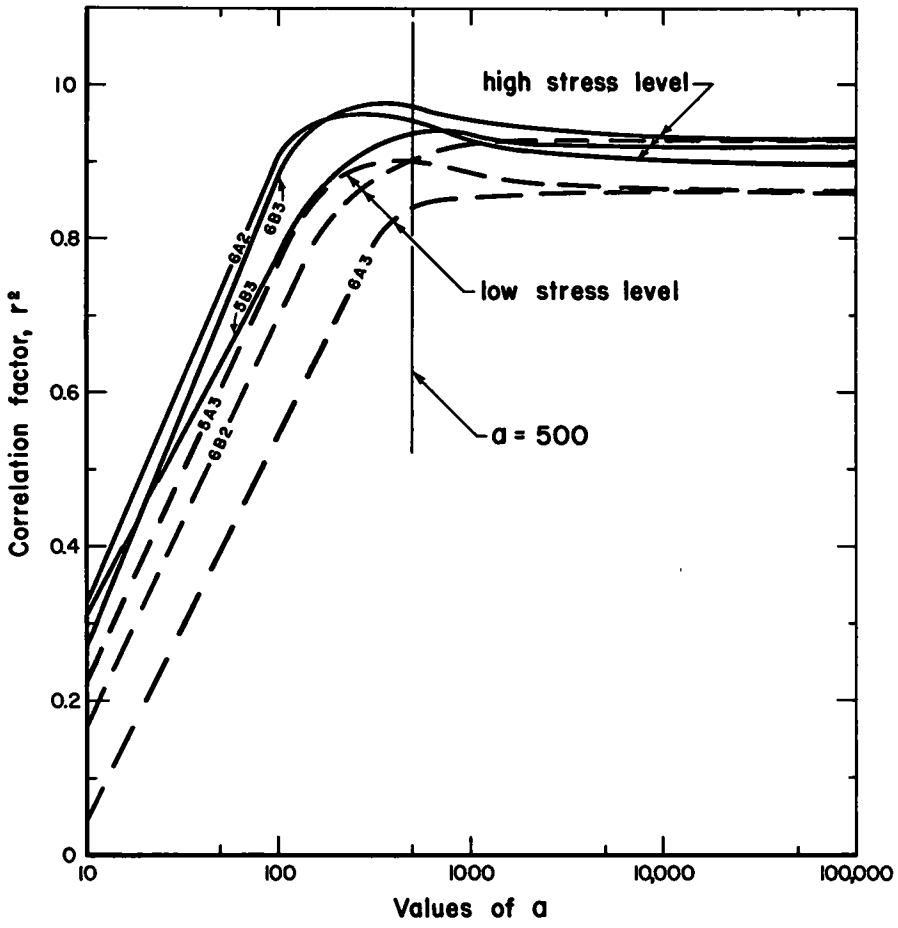

Figure 21. Variation in correlation with choice of a.

$$X_1 = \log \Delta_c$$

$$X_2 = \log (1 - e^{-t/a})$$

The results of fitting the individual creep tests assuming different values of a are shown in Figures 21 and 22. Figure 21 shows the variation in the correlation coefficient for different values of a. Figure 22 shows the change in total potential creep for each specimen as the coefficient a is changed. From studies of the test data and Figures 21 and 22, a choice of a = 500 appeared to give reasonable values of Δ_∞ corresponding to high correlation coefficients for each specimen.

Analyses using a = 500 are reported in Table 8. No large variation in coefficient b was noted.

The final step in analyzing the creep data was a combined regression analysis of tests 5A3, 5B3, 6A2, 6A3, 6B2 and 6B3, using the constant a = 500.

A combination of Eq. 4 and 6a, used for this purpose, resulted in the transformed form:

$$\log \Delta_c = \log A + c \log \frac{f_{c1}}{f'_{c1}} + b \log (1 - e^{-t/a}) \qquad (11)$$

Eq. 9a, 9b and 9c were used to obtain the regression coefficients. The component parts were

$$X_1 = \log \Delta_c$$

$$X_2 = \log \frac{f_{ci}}{f'_{c1}}$$

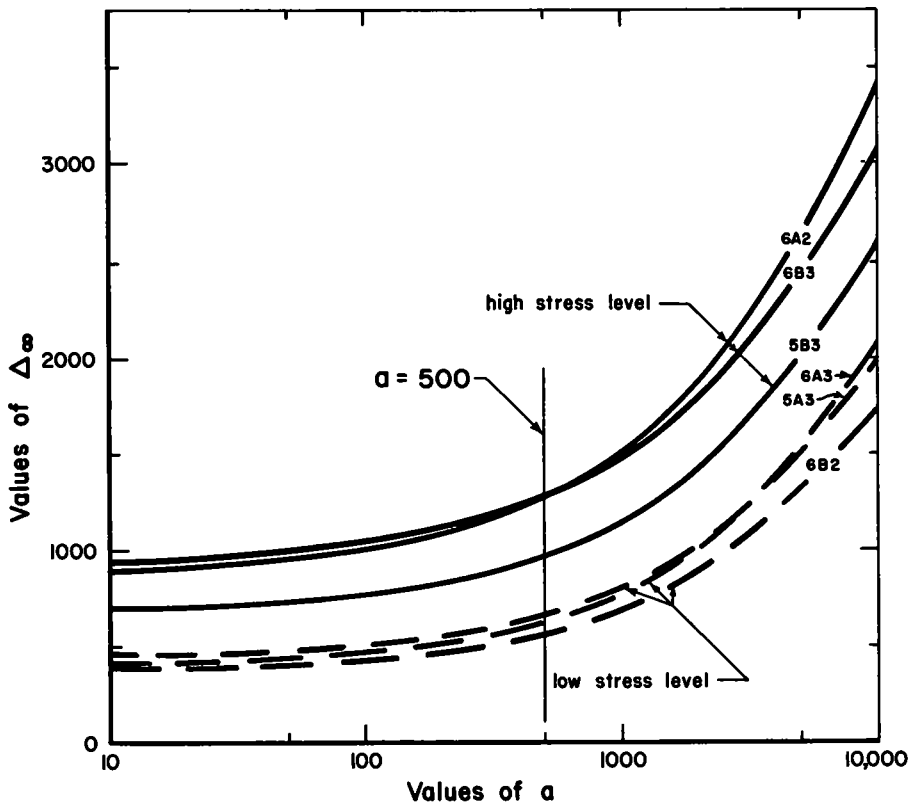

Figure 22. Variation of Δ_∞ with choice of a.

$$X_3 = \log (1 - e^{-t/500})$$

The combined regression analysis gave the coefficients: A = 0.00356, c = 0.96, and b = 0.73.

The value of c = 0.96 shows that the effect of f_{ci}/f'_{ci} was practically linear.

TABLE 8

REGRESSION COEFFICIENTS FOR INDIVIDUAL CREEP TESTS WHEN a = 500

Load = 1,000 psi				Load = 2,000 psi			
Test	Δ_{∞_1}	b	r^{2*}	Test	Δ_{∞_i}	b	r^{2*}
5A3	666	0.77	0.90	5B3	972	0.67	0.93
6A3	625	0.82	0.83	6A2	1261	0.72	0.95
6B2	574	0.75	0.91	6B3	1256	0.63	0.97

*r = coefficient of correlation.

Relaxation Analysis

The relaxation data also were analyzed in two steps. Each individual test was first fitted with Eq. 4b. The component parts of the equation were:

$$X_1 = \log \Delta_r$$

$$X_2 = \log t$$

The coefficients of regression for each individual specimen of wire and strand are given in Table 9. Coefficients b were reasonably uniform but the value of A decreased

TABLE 9

REGRESSION COEFFICIENTS FOR INDIVIDUAL WIRE AND STRAND TESTS

Specimen	Initial Stress, f_i, (ksi)	A	b	r^{2*}	Specimen	Initial Stress, f_i, (ksi)	A	b	r^{2*}
				(a) 3/8-In Strand					
604	187 5	1 970	0 240	0 993	606	195.5	1 810	0 274	0 996
609	185.0	2 050	0.251	0 985	608	189 0	1 535	0 238	0 978
610	165.4	0 830	0 243	0.945	603	185 8	0.445	0 409	0 991
607	163.0	0 727	0.259	0.948	601	169 3	0 609	0 303	0 967
602	158 0	0.469	0.304	0.870	605	168.3	0 935	0 262	0 971
				(b) 0 192-In Wire					
502	199.1	0.0205	0 192	0 989	507	196 4	0 0083	0 321	0 991
510	187 7	0.0043	0 338	0 997	505	184.7	0 0080	0 281	0 982
509	180 7	0 0235	0 199	0 996	504	181 0	0 0062	0 286	0 993
506	169.1	0.0150	0.231	0 994	503	175 0	0 0077	0 246	0 994

*r = coefficient of correlation.

with a decrease in initial stress level. Furthermore, the order of magnitude of A was different for the strand, for wire from shipment A, and for wire from shipment B.

Studies have shown that the differences in the order of magnitude of coefficient A could not be explained in terms of the known differences in the properties of the strand and wire. Therefore, three separate multiple regression analyses of the combined data were performed, one including all strand specimens, one including all wire A specimens and one including all wire B specimens.

Eq. 7 was the basic equation for the multiple regression analyses of relaxation data. In linearized form, it was

$$\log \frac{\Delta_r}{f_i} = \log g + d \log \frac{f_i}{f'_s} + b \log t \qquad (12)$$

so that the component parts of Eq. 9a, 9b and 9c were

$$X_1 = \log \frac{\Delta_r}{f_i}$$

$$X_2 = \log \frac{f_i}{f'_s}$$

$$X_3 = \log t$$

The solution of Eq. 9a, 9b and 9c gave one set of coefficients g, d and b for each of the three multiple regression analyses. The coefficients are listed in the preceding text under "Relaxation Equations."

Fatigue Tests of Bridge Materials Of the AASHO Road Test

J. W. FISHER, Assistant Bridge Research Engineer; and
I. M. VIEST, Bridge Research Engineer, AASHO Road Test, Highway Research Board

Analyses of the behavior under repeated applications of overstress of the test bridges at the AASHO Road Test required knowledge of the fatigue properties of reinforcing bars, prestressing wire and strand, and of steel beams with partial-length cover plates. Studies aimed to develop such knowledge are reported in this paper.

Included are fatigue tests of 20 specimens of No. 11 reinforcing bars, 18 specimens of prestressing strand, and 50 specimens of prestressing wire. In addition, tests of 10 beams with partial-length cover plates reported by other investigators are utilized in the study. The test data are described by mathematical equations which express the fatigue life as a function of the stress range and minimum stress. Numerical coefficients in the equations were evaluated by regression analyses.

● STUDIES of fatigue characteristics of structural metals were carried out at the AASHO Road Test, Ottawa, Ill., in connection with research on one-lane, simple-span bridges (1). One of the principal objectives of the bridge research was to study the behavior of the bridges under repeated applications of overstress. To correlate the observed behavior with simpler experimental laboratory studies, three fatigue experiments were carried out on samples of steel used in the beams of the reinforced and prestressed concrete bridges. Studies also were made of the fatigue strength of steel beams with partial-length cover plates utilizing data from experiments on materials similar to those used at the Road Test.

Fatigue tests of reinforcing bars were made on 20 specimens cut from No. 11 bars used as tension reinforcement in the reinforced concrete bridges. The bars were cast into short concrete beams and the beams were tested in bending at the Research and Development Laboratories, Portland Cement Association.

Fatigue tests of prestressing strand were made on 18 specimens of 7-wire strands of 3/8-in. diameter cut from excess lengths after stressing of beams for two prestressed concrete bridges. Tension specimens were prepared and tested at the Fritz Engineering Laboratory, Lehigh University.

Fatigue tests of prestressing wire were made on 50 specimens of 0.192-in. diameter wire cut from excess lengths of cables after tensioning of beams for two prestressed concrete bridges. Tension specimens were also prepared and tested at the Fritz Engineering Laboratory.

The study of the fatigue strength of steel beams with partial-length cover plates utilized the results of tests reported by Hall and Stallmeyer (2, 3). Bending tests were made on ten small built-up beams with partial-length cover plates having the same details as those used in seven steel bridges.

This report is a general discussion of the experiments and a presentation of the results of the analyses of the test data. The test data may be obtained in tabular form as data system 2145 from the Highway Research Board at the cost of reproduction. The details of the tests of beams with partial-length cover plates can be found elsewhere (2, 3).

EXPERIMENTAL STUDY OF REINFORCING BARS

The fatigue characteristics of intermediate-grade reinforcing bars were evaluated by tests on 20 No. 11 bars. (Altogether, 21 bars were tested. One failed in the weld and was omitted from this report.) Each bar was embedded near the top of a 12 by 14 by 80-in. concrete beam and the beam was tested in bending as shown in Figure 1.

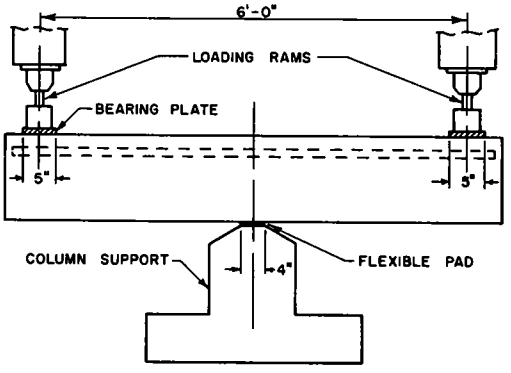

Figure 1. Arrangement for testing reinforcing bars.

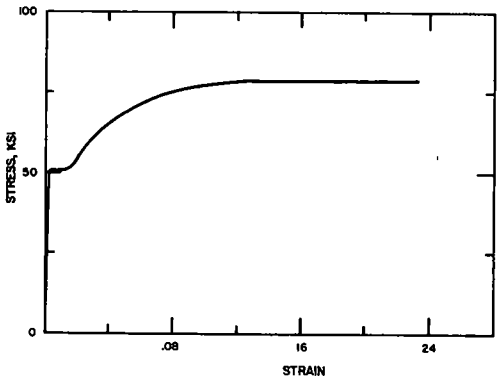

Figure 2. Typical stress-strain curve for reinforcing bars.

The bars were rolled from one heat and had diamond-shaped deformations conforming to ASTM designation A 305-56T. Fifteen additional coupons were tested in static tension. A typical stress-strain diagram of the bars in shown in Figure 2. The control tests (Table 1) indicated that all bars had essentially the same mechanical properties. The mean modulus of elasticity was 28.8 x 10^3 ksi and the mean cross-sectional area was 1.524 sq in. The chemical composition is given in Table 2.

TABLE 1

MECHANICAL PROPERTIES OF STEEL

Material	Yield Point or Yield Strength[a]			Ultimate Strength		
	No. Tests	Mean (ksi)	Std. Dev. (ksi)	No. Tests	Mean (ksi)	Std. Dev. (ksi)
No. 11 bars	15	49.5	0.77	15	81.0	1.72
3/8-in. strand	33	234.3	8.52	33	270.4	7.53
0.192-in. wire	90	227.2	1.93	90	257.5	2.29
3/16-in. plate	-	44.6	-	-	64.7	-
1/2-in. plate	-	36.1	-	-	61.0	-
3/4-in. plate	-	35.6	-	-	59.5	-

[a]The yield strength at 1% strain is applicable to the 3/8-in. strand and 0.192-in. diameter wire.

The details of the test beams are shown in Figure 3. The actual test coupon, obtained from the material used in the bridges, was 2 ft long; extensions were butt-welded

to both ends making the overall bar length 78 in. Two No. 4 splice bars were placed adjacent to the welds to prevent failure at those points.

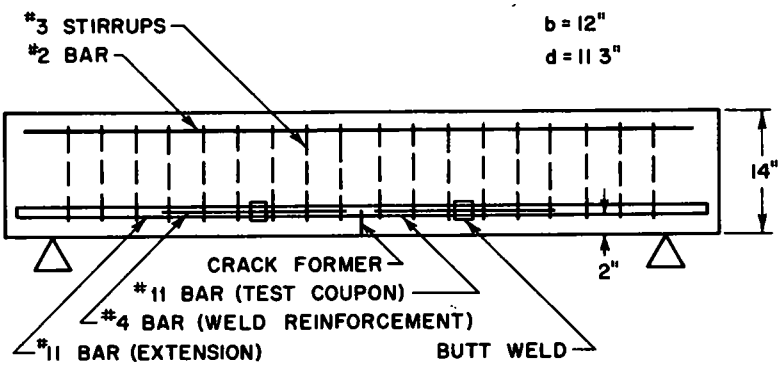

Figure 3. Details of beams for testing of reinforcing bars.

(The splice bars were not included in the first three specimens tested. One of the three specimens (Test No. 2) failed in the weld. No weld failures occurred in specimens with splice bars.) Stirrups were provided to prevent shear failure and longitudinal splitting. A metal strip was inserted in the beam at midspan to initiate a crack in the tension zone at the section of maximum moment.

TABLE 2

CHEMICAL COMPOSITION OF STEEL

Material	Chemical Content (%)				
	C	Mn	P	S	Si
No. 11 bars	0.37	0.60	0.023	0.03	0.07
3/8-in. strand	0.725	0.745	0.016	0.037	0.235
0.192-in. wire	0.800	0.670	0.016	0.040	0.250
3/16-in. plate	0.21	0.50	0.011	0.026	-
1-in. plate	0.25	0.46	0.010	0.024	-

The test beams were cast in groups of three. Four batches of concrete were distributed evenly through the three specimens. Nine cylinders were taken from the fourth batch representing concrete in the compression zone. Three cylinders were tested at the conclusion of the fatigue test of each beam. The mean compressive strength of all cylinders was 5,250 psi, with individual strengths varying between 4,200 to 5,890 psi.

The tests were made with an Amsler hydraulic pulsator, which induced sinusoidal stress cycles at the rate of 500 cycles per minute. The test beams were balanced on a center support and vertical downward loads were applied at each end (Fig. 1).

The tension caused in the bar by the load was computed on the basis of the cracked-section straight-line theory, assuming f'_c = 5,000 psi and E_c = 4,100,000 psi. In earlier studies, these procedures were found to result in close agreement between measured and computed stresses in similar specimens.

The hydraulically applied loads were read directly from an oil pressure gage calibrated to the ram area. In early stages of each test, periodic adjustments of the oil pressure had to be made to compensate for decreasing stiffness of the test beam and increasing temperature of the hydraulic fluid. The maximum variation observed was less than 1 percent and occurred only within the first 100,000 cycles. The repeated loads were applied continuously between the specified levels until failure occurred or 3,000,000 cycles of stress was exceeded.

The experiment included two controlled variables — the maximum stress level and the minimum stress level. An outline of these two variables and of specimens is given in Table 3.

TABLE 3

OUTLINE OF REINFORCING BAR EXPERIMENT

Specimen Designation for Test Block			Minimum Stress (ksi)	Maximum Stress (ksi)
1	2	3		
3111	3112	3113	5.0	34.0
3121	3122	3123	5.0	39.0
3131	3132	3133	5.0	44.0
3221	3222	3223	15.0	39.0
3231	3232	3233	15.0	44.0
3241	3242	3243	15.0	49.0

Four maximum stress levels and two minimum stress levels were selected on the basis of the stresses observed in the test bridges and of the expected endurance limit. Each minimum stress level was combined with three maximum stress levels in such a manner that two 2 by 2 factorial experiments were included: one to obtain data on the effect of the maximum and minimum stress (specimens 312, 313, 322 and 323) and the other to obtain data on the effect of stress range (specimens 311, 312, 323 and 324).

Stress levels were assigned to the test beams at random. One specimen from each maximum-minimum stress combination was assigned to a test block. There were three such test blocks, as indicated in Table 3.

Within each test block a random order of testing was followed to prevent variations caused by controlled variables from being confused with systematic variations due to uncontrolled variables.

The applied stresses and the numbers of cycles to the end of tests are given in Table 4 for each specimen, listed in order of testing. All bars tested to failure were ruptured completely; without exception the rupture occurred at the intersection of two diagonal ribs with a longitudinal rib. Figure 4 shows the rupture surfaces of two bars tested at different stress levels. All failures occurred within 2 in. of the beam center adjacent to a crack in the concrete.

EXPERIMENTAL STUDY OF PRESTRESSING STRAND

The fatigue characteristics of prestressing strand were evaluated by tension tests on 18 specimens of seven-wire, 3/8-in. diameter strand. The specimens were approximately 72 in. long and were tested in axial tension as shown in Figure 5.

The prestressing strand, made of seven cold-drawn bright wires, was stress relieved. The 18 specimens used in this study were selected from 24 pieces of strand, 6 to 15 ft long, taken from two spools used in construction of test bridges. Static tension

TABLE 4

TEST RESULTS OF REINFORCING BARS

Order of Testing	Specimen Designation	Stress (ksi)		No. of Cycles
		Min.	Max.	
1	3221	15.0	39.0	3,702,400[a]*
3	3121	5.0	39.0	515,300
4	3250	15.0	40.0	3,496,500[a]
5	3260	15.0	41.0	2,214,500
6	3241	15.0	49.0	441,000
7	3131	5.0	44.0	288,100
8	3111	5.0	34.0	864,500
9	3231	15.0	44.0	1,232,300
10	3242	15.0	49.0	406,600
11	3132	5.0	44.0	216,400
12	3112	5.0	34.0	626,000
13	3222	15.0	39.0	3,187,500[a]
14	3232	15.0	44.0	746,000
15	3122	5.0	39.0	356,800
16	3113	5.0	34.0	920,200
17	3233	15.0	44.0	971,900
18	3223	15.0	39.0	8,164,000[a]
19	3123	5.0	39.0	506,100
20	3133	5.0	44.0	315,600
21	3243	15.0	49.0	645,300

*[a]Specimen did not fail; all other specimens failed by fracture of the No. 11 bar.

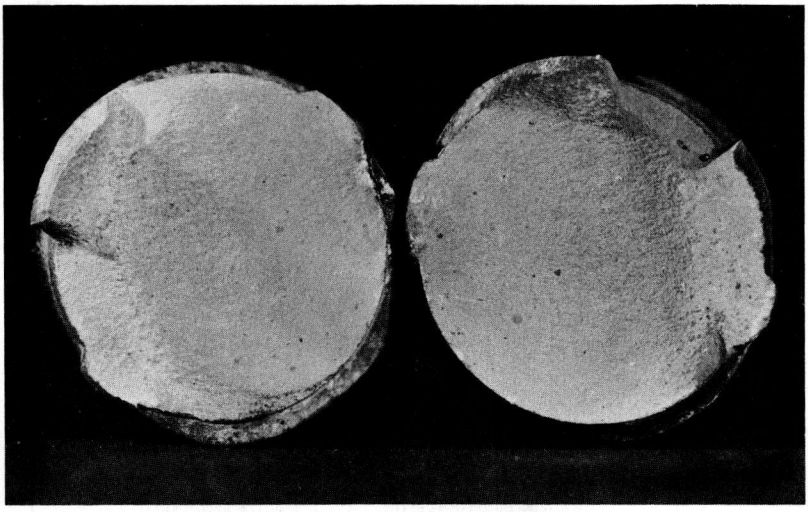

Figure 4. Fracture surface of reinforcing bar (specimen 3112).

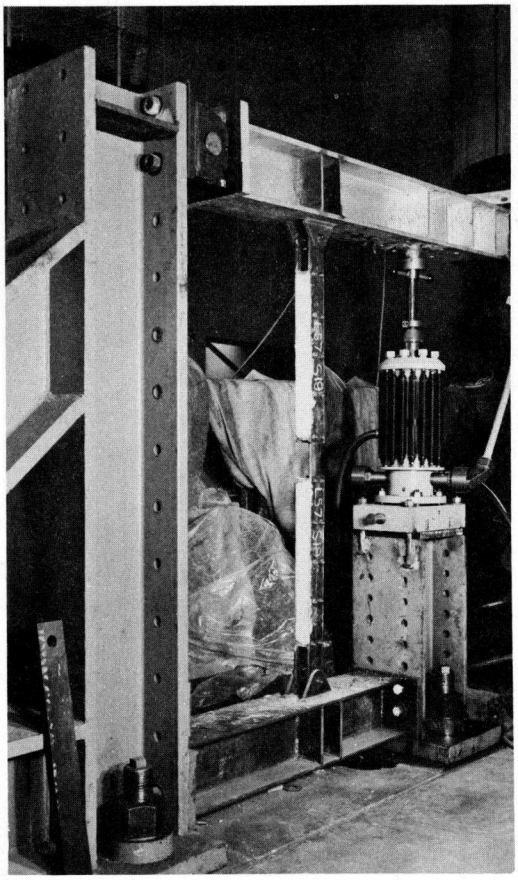

Figure 5. Strand fatigue test equipment.

tests on 33 coupons indicated that the two spools had only slightly different mechanical properties. A typical stress-strain diagram is shown in Figure 6; the mean yield and ultimate strengths are given in Table 1. The mean modulus of elasticity of the strand was 27.6×10^3 ksi and the mean cross-sectional area was 0.08065 sq in. Both spools had essentially the same chemical composition as given in Table 2.

The tests were performed in a steel frame (Fig. 5). The strand was connected to the frame through special end grips, shown schematically in Figure 7. Prior to placement in the testing frame, the strand was pretensioned to approximately 188 ksi and the end grips were attached to it with cement grout. After the grout had hardened, a spacer block was placed between the grips, the strand was released from the stressing bed and the specimen was transferred to the testing frame. A static load was then applied to the specimen, the spacer block removed and the load decreased to the minimum level for the fatigue tests.

The load was applied to the testing frame with a hydraulic jack (Fig. 5) operated from an Amsler pulsator. In the fatigue test the load fluctuated between the minimum and maximum levels at 500 cycles per minute. The test was discontinued when the strand failed or after 2,000,000 cycles of load were exceeded.

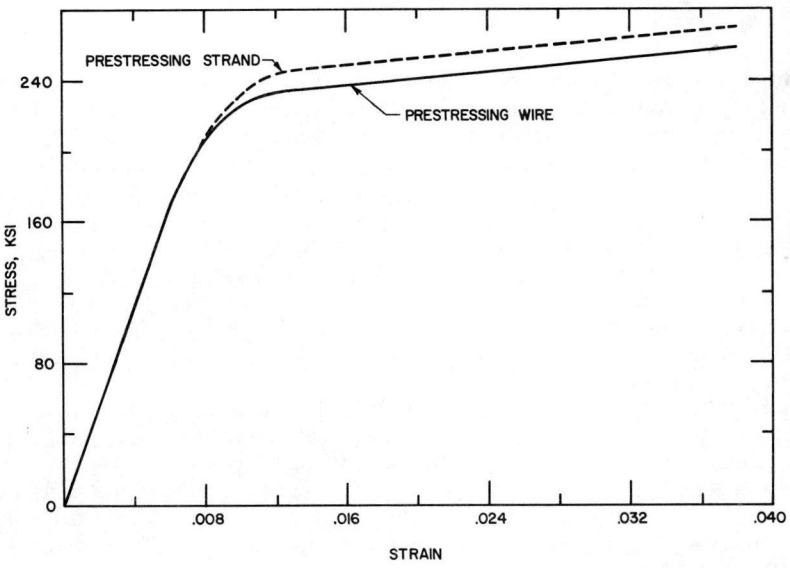

Figure 6. Typical stress-strain curve for prestressing steel.

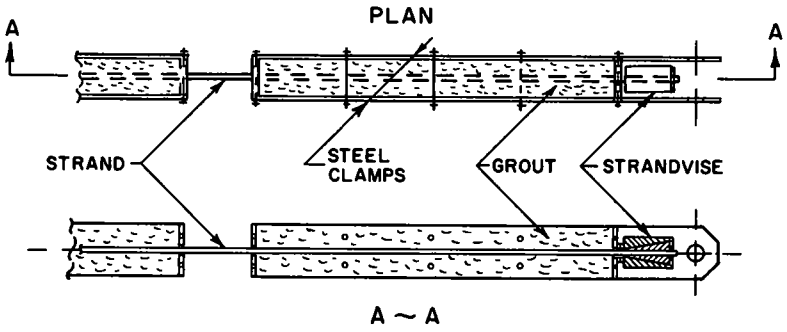

Figure 7. Gripping device for strand.

The experiment included two controlled variables — the maximum and minimum stress levels. The detailed outline of the strand experiment is given in Table 5.

TABLE 5

OUTLINE OF PRESTRESSING STRAND EXPERIMENT

Specimen Designation for Test Block			Minimum Stress (ksi)	Maximum Stress (ksi)
1	2	3		
1111	1112	1113	135.2	183.9
1121	1122	1123	135.2	197.4
1131	1132	1133	135.2	210.9
1221	1222	1223	162.5	197.4
1231	1232	1233	162.5	210.9
1241	1242	1243	162.5	224.4

Two minimum stress levels were used in combination with four maximum stress levels. The stress levels, chosen on the basis of stresses observed in the test bridges and of the expected endurance limit, were arranged into two 2 by 2 factorial experiments; one to obtain data on the effect of maximum and minimum stress levels (specimens 112, 113, 122 and 123), the other to provide data on the effect of stress range (specimens 111, 112, 123 and 124). The specimens were grouped into three test blocks with one specimen for each load combination tested in each block. The order of testing the specimens was randomized within each test block.

The stresses in the strand resulting from the applied loads were computed on the basis of the mean strand area. The applied stresses and the number of cycles to failure of one wire or, where the test was discontinued before failure, to the end of testing are given in Table 6.

All failures occurred by fracture of one or more wires at the following locations: (a) in the gap, (b) at the edge of the steel clamps adjacent to the gap, (c) inside the grout of the grip, and (d) at the strand vise anchorage.

In specimens tested to failure, generally three of the seven wires failed by fracture due to fatigue. The remaining wires failed by static tension. Some difficulty was encountered in locating the area of the first wire failure when the failure occurred inside the grout. Typical fractured surfaces are shown in Figure 8.

TABLE 6

TEST RESULTS OF PRESTRESSING STRAND

Order of Testing	Specimen Designation	Stress (ksi)		No. of Cycles	Location of Failure
		Min.	Max.		
1	1221	162.5	197.3	1,351,400	In grout
2	1131	135.2	210.9	68,100	In gap
3	1111	135.2	183.6	1,236,000	In grout
4	1241	162.5	224.6	213,400	Edge of clamp
5	1121	135.2	197.3	560,700	At strand vise
6	1231	162.5	210.9	512,800	In grout
7	1112	135.2	183.6	909,200	In grout
8	1222	162.5	197.3	2,190,000	Did not fail
9	1232	162.5	210.9	422,000	Edge of clamp
10	1132	135.2	210.9	48,700	Edge of clamp
11	1122	135.2	197.3	152,700	In gap
12	1242	162.5	224.6	90,600	At strand vise
13	1113	135.2	183.6	579,000	In grout
14	1123	135.2	197.3	174,000	In grout
15	1243	162.5	224.6	159,000	In grout
16	1223	162.5	197.3	2,489,300	Did not fail
17	1233	162.5	210.9	199,100	In grout and gap
18	1133	135.2	210.9	38,200	In gap and edge of clamp

EXPERIMENTAL STUDY OF PRESTRESSING WIRE

The fatigue characteristics of the prestressing wire were evaluated by tension tests of 50 short specimens of 0.192-in. diameter wire. The specimens were 12 in. long and were tested in axial tension as shown in Figure 9. (Altogether, 82 specimens were tested. Thirty-one failed where the specimen entered the grips. One other failed with the fracture following a crack existing in the specimen before testing. As these tests were repeated until failure occurred outside the grips, results for 32 specimens are not reported here.)

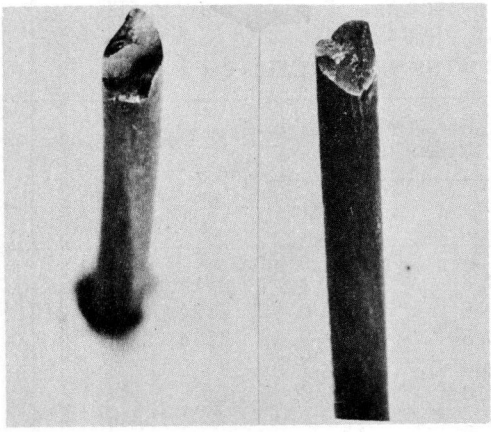

Figure 8. Typical fatigue failure of strand wire (specimen 1233).

The prestressing wire was cold-drawn and stress-relieved with bright, smooth surface. All specimens were taken from one shipment of wire. Static tensile tests on 90 coupons indicated that the material had uniform mechanical properties. Means of the yield and ultimate strengths are given in Table 1. The mean modulus of elasticity of the wire was 28.6×10^3 ksi and the mean cross-sectional area was 0.0293 in. The chemical composition of the wire was determined by analyses of three samples. The mean composition is given in Table 2.

The tests were performed in an Amsler high-frequency vibrophore shown in Figure 9. The wire was connected to the vibrophore through wedge jaws. To prevent

failure in the grips, the surface of the wire in contact with the grips was treated by cold rolling. The rolled surface extended a small distance beyond the grips. (The set of grips and the procedure for preparation of specimens was changed during the conduct of the tests in the second test block.)

At the beginning of a test, a static load equal to the mean of the desired minimum and maximum loads was applied to the wire. The dynamic load was then superimposed at the frequency of 5,000 cycles per minute. The test was continued until failure of the wire or until 2,000,000 cycles were exceeded.

The wire experiment included two controlled variables — the maximum and minimum stress levels. The outline of the wire experiment is given in Table 7.

Two minimum stress levels were used in combination with five maximum stress levels. The stress levels, chosen on the basis of the stresses observed in the test bridges and of the expected endurance limit, were arranged into a 2 by 4 factorial experiment to obtain data on the effect of the maximum and minimum stress levels (specimens 212, 213, 214, 215, 222, 223, 224 and 225), and into a 2 by 3 factorial experiment to obtain information on the effect of the stress range (specimens 211, 212, 213, 223, 224 and 225). The original experiment was arranged in an order that permitted the tests to be conducted in three test blocks, with each block containing a complete combination of minimum and maximum stress levels.

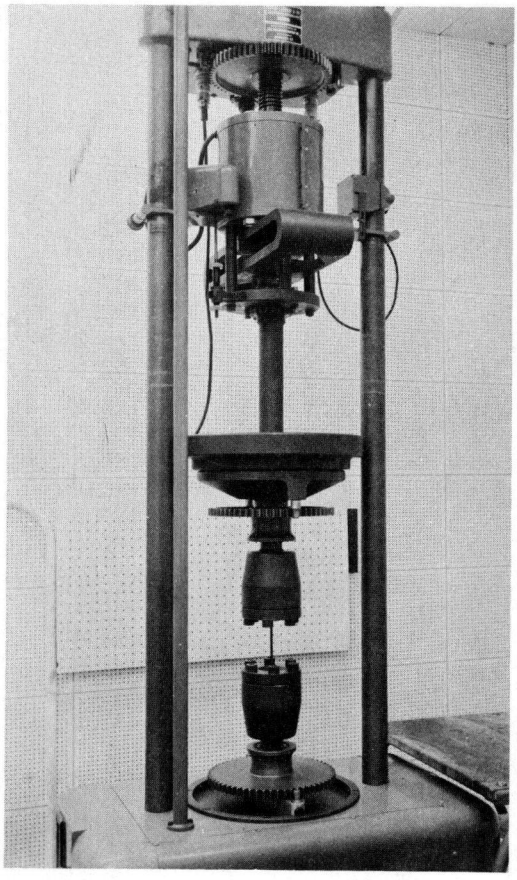

Figure 9. Wire fatigue test equipment.

TABLE 7

OUTLINE OF PRESTRESSING WIRE EXPERIMENT

Designation of Original Specimens Test Block			Stress (ksi)		Designation of Additional Specimens
1	2	3	Min.	Max.	
2111	2112	2113	128.8	175.1	2114, 2115
2121	2122	2123	128.8	188.0	2124 through 21212
2131	2132	2133	128.8	200.9	2134, 2315
2141	2142	2143	128.8	213.7	
2151	2152	2153	128.8	226.6	
2221	2222	2223	154.5	188.0	
2231	2232	2233	154.5	200.9	2234
2241	2242	2243	154.5	213.7	2244, 2245
2251	2252	2253	154.5	226.6	

TABLE 8

TEST RESULTS OF PRESTRESSING WIRE

Order of Testing	Specimen Designation	Stress (ksi)		No. of Cycles	Location of Failure
		Min.	Max.		
1	2221	154.5	188.0	7,539,000	Did not fail
2	2241	154.5	213.7	949,000	At center
3	2111	128.8	175.1	1,603,000	At center
6	2121	128.8	188.0	980,000	At center
7	2131-B	128.8	200.9	4,968,000	Did not fail
8	2231-B	154.5	200.9	3,358,000	Did not fail
10	2121-C	128.8	188.0	7,348,000	Did not fail
14	2251-C	154.5	226.6	285,000	In rolled surface
15	2141-B	128.8	213.7	324,000	In rolled surface
17	2141-C	128.8	213.7	378,000	In rolled surface
20	2251-G	154.5	226.6	360,000	At center
21	2141-D	128.8	213.7	207,000	At center
23	2151-B	128.8	226.6	140,000	At center
24	2232	154.5	200.9	2,505,000	Did not fail
29	2222	154.5	188.0	2,771,000	Did not fail
32	2112	128.8	175.1	5,617,000	Did not fail
33	2122	128.8	188.0	2,080,000	Did not fail
39	2252-L	154.5	226.6	502,000	At center
42	2152	128.8	226.6	146,000	In rolled surface
44	2142-B	128.8	213.7	241,000	At center
45	2132	128.8	200.9	578,000	In rolled surface
46	2132-B	128.8	200.9	1,034,000	At center
47	2242	154.5	213.7	5,310,000	Did not fail
48	2233	154.4	200.9	5,300,000	Did not fail
49	2123	128.8	188.0	3,098,000	Did not fail
51	2143-B	128.8	213.7	253,000	In rolled surface
52	2143-C	128.8	213.7	440,000	At center
54	2253-B	154.5	226.6	521,000	In rolled surface
57	2113	128.8	175.1	3,429,000	Did not fail
58	2223	154.5	188.0	5,646,000	Did not fail
59	2133	128.8	200.9	626,000	In rolled surface
60	2133-B	128.8	200.9	681,000	At center
61	2243	154.5	213.7	1,515,000	At center
63	2153-B	128.8	226.6	104,000	At center
64	2114	128.8	175.1	3,300,000	Did not fail
65	2244	154.5	213.7	778,000	At center
67	2124-B	128.8	188.0	444,000	At center
68	2234	154.5	200.9	6,800,000	Did not fail
69	2134	128.8	200.9	206,000	At center
70	2125	128.8	188.0	4,781,000	Did not fail
73	2245-C	154.5	213.7	404,000	At center
74	2135	128.8	200.9	272,000	At center
75	2115	128.8	175.1	3,029,000	Did not fail
76	2126	128.8	188.0	4,670,000	Did not fail
77	2127	128.8	188.0	3,522,000	Did not fail
78	2128	128.8	188.0	292,000	At center
79	2129	128.8	188.0	106,000	At center
80	21210	128.8	188.0	3,566,000	Did not fail
81	21211	128.8	188.0	370,000	At center
82	21212	128.8	188.0	250,000	At center

The original experiment design specified testing of three specimens at each maximum-minimum stress combination. However, because of the trends of test results, it was considered necessary to test additional specimens to establish median values for several maximum-minimum stress combinations. The additional specimens are also listed in Table 7.

The stresses in the wire specimens were computed on the basis of the mean area and the applied loads. The applied stresses, number of cycles to the end of test, and the location of failure, are given in Table 8, which lists the specimens in the order of testing.

Specimens failed by fracture in the center untreated portion between the grips or in the rolled surface near the grips. (When failure occurred in the grips the test was repeated within the same test block until failure occurred outside the grips. The additional specimens were identified by letters; e.g. 2131-B. A few tests with failure in the rolled surface were also repeated.) A typical wire failure is shown in Figure 10.

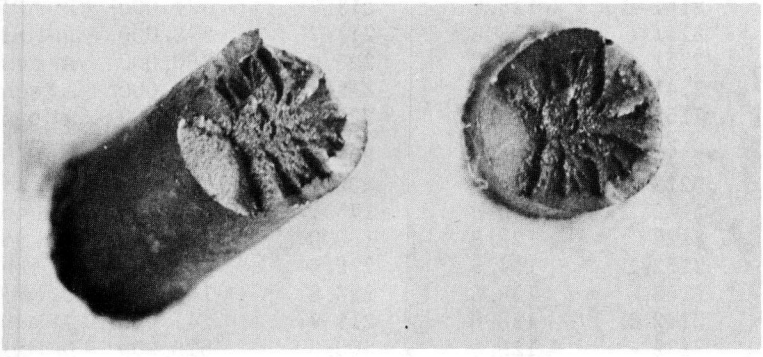

Figure 10. Typical fatigue failure of wire (specimen 2134).

Temperature measured on two specimens during the test indicated that the high frequency of loading had little, if any, effect on the temperature of the specimen.

STUDY OF BEAMS WITH PARTIAL-LENGTH COVER PLATES

The fatigue characteristics of steel beams with partial-length cover plates with no welds across the end were evaluated by studies of the results of flexural fatigue tests of ten small welded beams. Details of the experiments are given elsewhere (2, 3).

The beams were fabricated from A-373-54T plate steel. The mechanical properties, obtained by tests of coupons, are given in Table 1. The chemical compositions, given by mill reports, are given in Table 2. The beams of the Test Road bridges were rolled from steel of similar composition.

Six I-beam specimens were built up of two 3/4-in. thick flanges welded to a 3/16-in. web; 1/2-in. thick cover plates were attached to both the tension and the compression flanges. Four I-beam specimens were built up of two 3/8-in. thick flanges welded to a 1/4-in. web and a 1/4-in. thick cover plate attached to the tension flange. All welding was done manually with electrodes conforming to AWS Specification E-7016. The welds were continuous along the longtitudinal edges. The ends of the cover plates were cut off at right angle and there were no welds along the ends. All beams were 12 in. deep and 11 ft long.

The specimens were tested in flexure on a span of 8 ft 6 in. in a Wilson fatigue testing machine. The load was applied at a rate of 180 cycles per minute.

The experiment included two principal variables — the minimum and maximum stress levels. The stress level combinations were approximately as follows:

3 specimens, 0.4 to 13.6 ksi
3 specimens, 0.4 to 24.9 ksi
2 specimens, 15.5 to 27.9 ksi
2 specimens, 15.4 to 36.4 ksi

The results of the fatigue tests are given elsewhere (2,3) and are reproduced in Figure 14. (Figure 14 includes specimens CPDF-1, CPDG-1, CPCD-1, CPDF-2, CPAD-1 and CPCD-2 from Ref. 2; and specimens 1,2,3 and 4 from Ref. 3. Two symbols pertain to each specimen: a dot representing the number of cycles to failure and a triangle representing the number of cycles to last inspection prior to failure.) The number of cycles at which the crack became visible is not known; however, at the last inspection prior to failure three beams had small cracks 1/4 to 1 1/2 in. long.

Failure was defined as the number of cycles at which the deflection of the fractured beam exceeded the static deflection by 0.05 in. When this deflection occurred the beam activated a microswitch that shut off the testing machine. All failures were similar in nature. The cracks started at the tip of one of the longitudinal welds and propagated transversely and vertically through the flange cross-section. Generally, at the time of failure about one-quarter of the cross-sectional area of the tension flange was fractured.

ANALYSIS OF DATA

The objective of this study was to develop a reliable basis for estimating the fatigue life of the test bridges at the AASHO Road Test. To this end, statistical correlations were made of the stress levels with the number of cycles to failure observed in the tests described in the preceding sections.

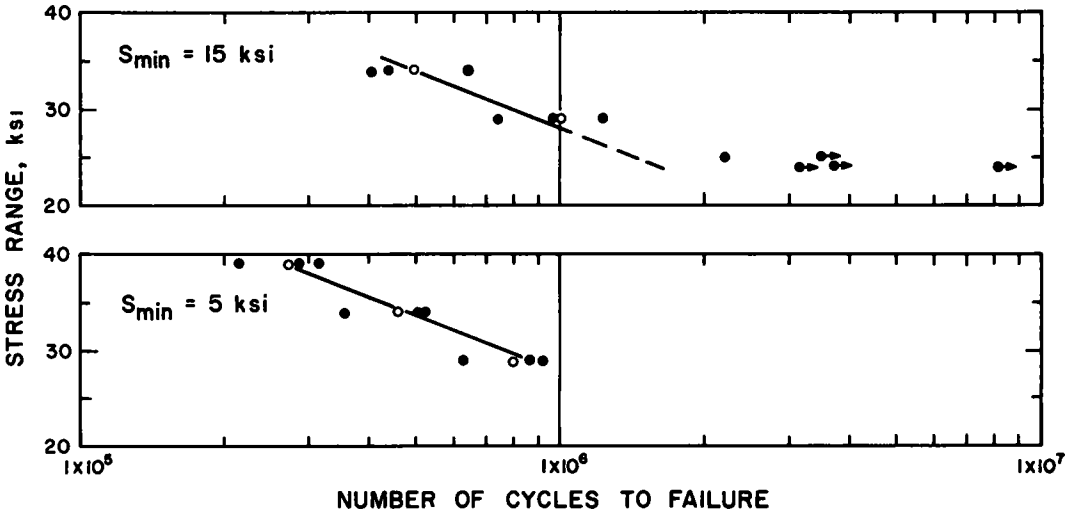

Figure 11. Test results for reinforcing bars.

The experimental data from Tables 4, 6 and 8 are plotted in Figures 11, 12 and 13, in which the stress range is given as a function of the logarithm of the number of cycles to failure. The experimental of Hall and Stallmeyer (2,3) are plotted in Figure 14. A separate plot is included for each minimum stress level. The test data are shown dots; an arrow attached to a dot indicates that the test was discontinued before failure. Where all specimens tested at the same maximum-minimum stress combination failed, the mean log N is shown as a circle. Where more than 50 percent of the specimens tested at the same maximum-minimum stress combination failed, the median log N is shown as a circle.

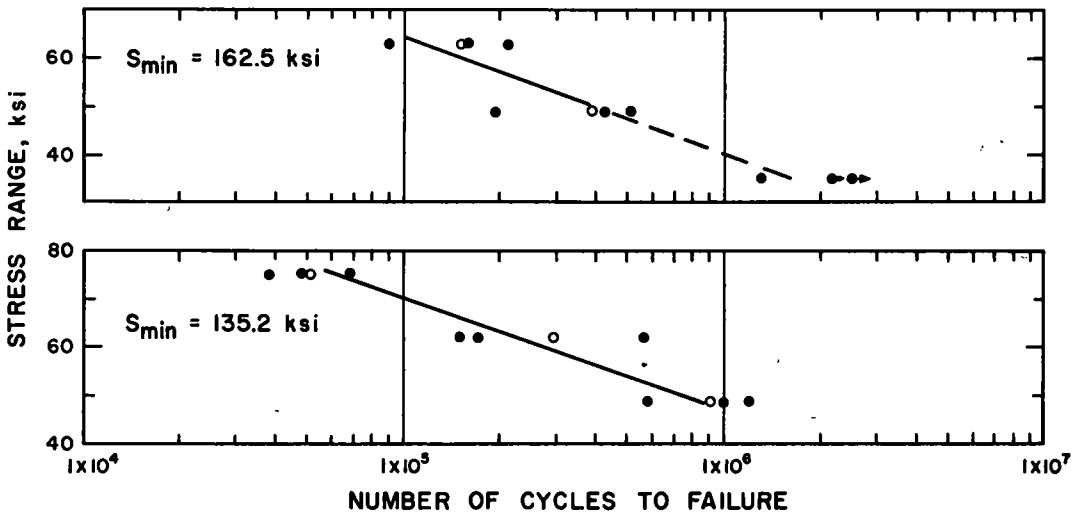

Figure 12. Test results for prestressing strand.

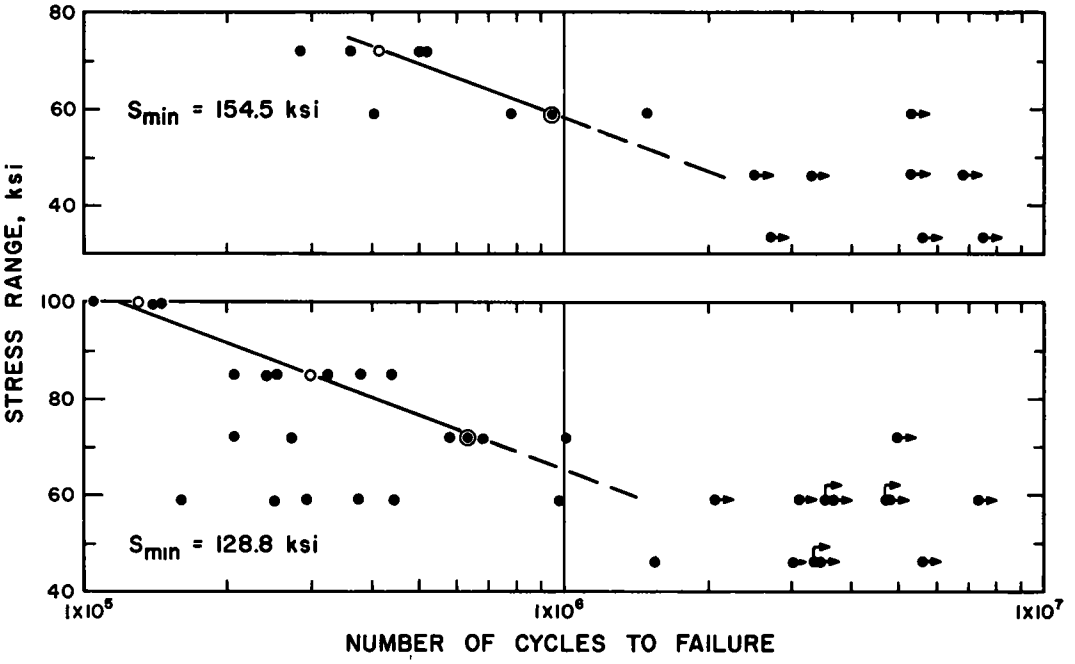

Figure 13. Test results for prestressing wire.

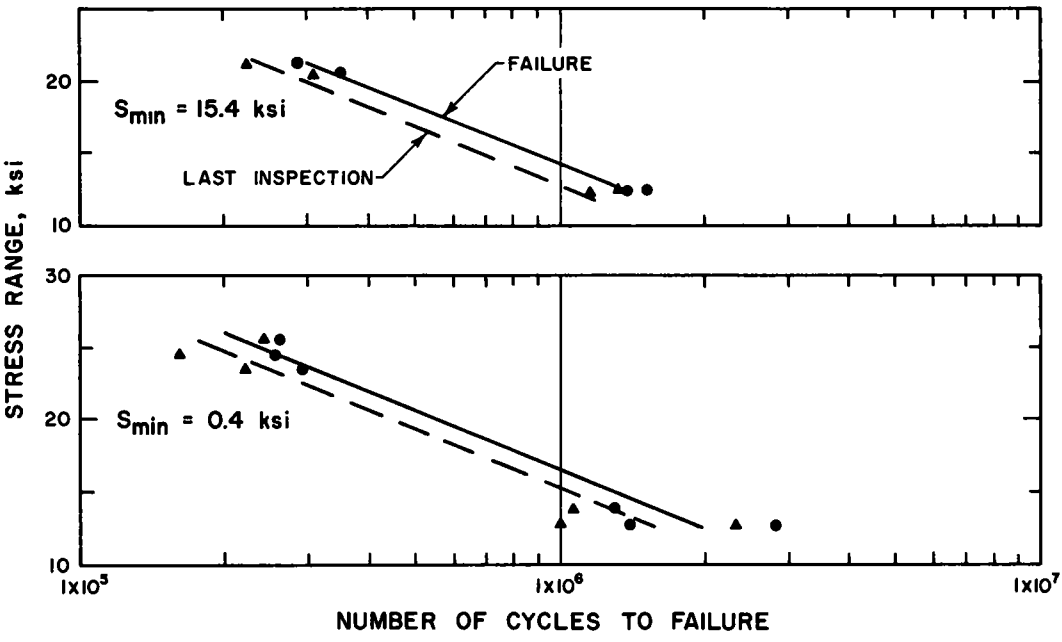

Figure 14. Test results for beams with partial-length cover plates and no end welds.

Examination of the means and medians in Figures 11, 12 and 13 shows that they follow essentially a straight line. Therefore, the following mathematical model was selected to represent the test data:

$$\log N = A + BS_r + CS_{min} \quad (1)$$

in which

S_r = range of stress, $S_{max} - S_{min}$;

S_{min} = minimum stress;

S_{max} = maximum stress;

N = number of cycles to failure; and

A, B, C = empirical constants.

Coefficients A, B and C of Eq. 1 were evaluated by a separate regression analysis for each material. For the reinforcing bars, prestressing strand, and prestressing wire the analyses were based on means or medians shown in Figures 11, 12 and 13 as circles. The following equations were obtained for the fatigue life:

Reinforcing bars:

$$\log N = 7.432 - 0.0515\, S_r \quad (2)$$

Prestressing strand:

$$\log N = 9.354 - 0.0423\, S_r - 0.0102\, S_{min} \quad (3)$$

Prestressing wire:

$$\log N = 8.722 - 0.0272\, S_r - 0.0074\, S_{min} \quad (4)$$

Two analyses were made for the beams with partial-length cover plates — one for the number of cycles to failure and the other for the number of cycles to the last

inspection before failure. The individual data were the basis for the analyses because of the absence of replication of maximum stress levels (Fig. 14). The following equations were obtained:

Failure:

$$\log N = 7.216 - 0.0729\, S_r - 0.0129\, S_{min} \quad (5)$$

Last inspection:

$$\log N = 7.136 - 0.0724\, S_r - 0.0102\, S_{min} \quad (6)$$

The coefficients of correlation and the standard errors of estimate for Eqs. 2 through 6 are given in Table 9. The goodness of fit may be judged also from Figures 11, 12, 13 and 14, where the relevant equations are shown as straight lines.

The factorial nature of the experiments with reinforcing bars, prestressing strands and prestressing wires made possible independent determinations of the relative significance of the effect of stress range and minimum stress level upon the fatigue life. Analyses of variance indicated that stress range alone accounted for most of the variation in the reinforcing bar experiment (the effect of S_{min} was not significant at the 10 percent level), whereas the minimum stress level accounted for a small, barely significant portion of the variation in the experiments with prestressing strands and wires (the effect of S_{min} was significant at the 10 percent level but not at the 5 percent level).

Eq. 1 applies only to the finite life portion of the S-N diagram. In tests reported herein, testing was discontinued when the material sustained between 2 and 8 million cycles of loading. The endurance limit was then presumed to be reached. The limited data available indicated the limits of endurance shown in the last column of Table 9. It is noteworthy that the endurance limit for wire was found to be a function of the minimum stress level. The endurance limit was encountered at both minimum stress levels only in tests of wire.

No endurance limit was found in the tests of beams with partial-length cover plates.

TABLE 9

ANALYSIS OF FATIGUE TEST DATA

Material	Eq.	Coeff. of Correl.	Standard Error of Estimate	Endurance Limit (ksi)
Bars	1	0.85	0.091	24
Strands	3	0.82	0.209	35
Wires	4	0.74	0.230	-[1]
Beams	5	0.96	0.094	-
Beams	6	0.94	0.128	-

[1] 124 ksi - 0.5 S_{min}.

SUMMARY

1. Tests of 20 reinforcing bars cast in concrete beams, and of 18 prestressing strands and 50 prestressing wires, were made to determine the fatigue characteristics of these materials. Also studied were the results of tests of 10 beams with partial-length cover plates having no end welds. The results of the fatigue tests of each of the four materials were correlated by regression analyses utilizing one basic mathematical model.

2. A mathematical model expressing the logarithm of the fatigue life as a linear function of stress range and minimum stress level was found to fit the test data. An analysis of variance indicated clearly that the stress range was by far the most important independent variable.

3. Within the limits of the experiments, the results of the fatigue tests of reinforcing bars, prestressing strand, prestressing wire and beams with partial-length cover plates are represented by Eqs. 2 through 6, correlating the number of cycles to failure or inspection prior to failure with the minimum stress level and the stress range. However, the equations are applicable only to the finite life portion of the S-N diagram.

ACKNOWLEDGMENTS

This study was carried out as a part of the bridge research at the AASHO Road Test. Paul Irick, Chief of Data Analysis, offered many helpful suggestions during the course of planning the experiments.

Tests of reinforcing bars were performed at the Structural Development Section, Research and Development Laboratories, Portland Cement Association. The tests were carried out and reported by J. F. Pfister, Assistant Development Engineer.

Tests of prestressing strand and wire were conducted at Fritz Engineering Laboratory, Lehigh University. The tests were carried out and reported by F. S. Ople and C. P. Pitts under the direction of C. L. Hulsbos.

The contributions of all those who were connected with various phases of the investigation are gratefully acknowledged. The authors are indebted also to Professors W. H. Munse and J. E. Stallmeyer of the University of Illinois for permission to use the material from the thus far unpublished reports (2, 3).

REFERENCES

1. VIEST, I. M., "Bridge Research at the AASHO Road Test." HRB Spec. Rpt. 38, pp. 24-43 (1958).
2. HALL, L. R., and STALLMEYER, J. E., "The Fatigue Strength of Flexural Members." Univ. of Illinois, Dept. of Civil Eng., Status Report to Fatigue Committee, Welding Research Council (1959).
3. HALL, L. R., "Fatigue Tests of Scale Model AASHO Road Test Bridges." Univ. of Illinois, Dept. of Civil Eng., Status Report to Fatigue Committee, Welding Research Council (1961).

THE NATIONAL ACADEMY OF SCIENCES—NATIONAL RESEARCH COUNCIL is a private, nonprofit organization of scientists, dedicated to the furtherance of science and to its use for the general welfare. The ACADEMY itself was established in 1863 under a congressional charter signed by President Lincoln. Empowered to provide for all activities appropriate to academies of science, it was also required by its charter to act as an adviser to the federal government in scientific matters. This provision accounts for the close ties that have always existed between the ACADEMY and the government, although the ACADEMY is not a governmental agency.

The NATIONAL RESEARCH COUNCIL was established by the ACADEMY in 1916, at the request of President Wilson, to enable scientists generally to associate their efforts with those of the limited membership of the ACADEMY in service to the nation, to society, and to science at home and abroad. Members of the NATIONAL RESEARCH COUNCIL receive their appointments from the president of the ACADEMY. They include representatives nominated by the major scientific and technical societies, representatives of the federal government, and a number of members at large. In addition, several thousand scientists and engineers take part in the activities of the research council through membership on its various boards and committees.

Receiving funds from both public and private sources, by contribution, grant, or contract, the ACADEMY and its RESEARCH COUNCIL thus work to stimulate research and its applications, to survey the broad possibilities of science, to promote effective utilization of the scientific and technical resources of the country, to serve the government, and to further the general interests of science.

The HIGHWAY RESEARCH BOARD was organized November 11, 1920, as an agency of the Division of Engineering and Industrial Research, one of the eight functional divisions of the NATIONAL RESEARCH COUNCIL. The BOARD is a cooperative organization of the highway technologists of America operating under the auspices of the ACADEMY–COUNCIL and with the support of the several highway departments, the Bureau of Public Roads, and many other organizations interested in the development of highway transportation. The purposes of the BOARD are to encourage research and to provide a national clearinghouse and correlation service for research activities and information on highway administration and technology.

HIGHWAY
RESEARCH
BOARD

SPECIAL
REPORTS
66-70,72